MINISTRY OF SCIENCE AND HIGHER EDUCATION
KAZAN NATIONAL RESEARCH TECHNOLOGICAL UNIVERSITY (KNRTU)

S.A. DOLGIKH
V.E. TKACHEVA
M.S. SUNTSOVA

CATHODIC PROTECTION OF OIL-WELL CASINGS

Study Guide

KAZAN
2019

UDC 620.193
LBC 34.66
D 70

Printed by the resolution of the Editorial Advisory Board of Kazan National Research Technological University.

Reviewers:
Doctor of Chemistry, Director General of OAO Tatneftekhiminvest-holding, Full member of the Academy of Sciences of the Republic of Tatarstan
Dr. R.S. Yarullin;
Doctor of Engineering, Dean of the Faculty of Engineering, Technology & Management and Full Professor at the Department of Chemical Engineering and Ecology, both at the Berezniki Branch of Perm National Research Polytechnic University
Dr. S.V. Lanovetsky

Dolgikh S.A.
D70 Cathodic Protection of Oil-Well Casings: a Study Guide / S.A. Dolgikh, V.E. Tkacheva, M.S. Suntsova. – Kazan: Publishing House of Kazan University, 2019. – 188 p.

ISBN 978-5-00130-272-8

This book considers the issues related to the corrosion resistance of oil-well casings and describes the schemes of protecting oil-well casings against corrosion. It also presents the methods of computing the electrochemical parameters of cathodic protection systems for oil-well casings, based on the experimental findings obtained in field conditions. The methods are considered for monitoring their corrosion condition.

This study guide is intended for students in master's program 18.04.01 – Chemical Engineering, full-time bachelor's program 03.21.01 "Oil and Gas Engineering", discipline "Development of oil and gas fields" and master's program 04.21.01 "Oil and Gas Engineering".

The book was developed and edited at the Department of Electrochemical Engineering in collaboration with the TatNIPIneft R&D Institute of PJSC Tatneft named after V.D. Shashin.

UDC 620.193
LBC 34.66

ISBN 978-5-00130-272-8

TABLE OF CONTENTS

INTRODUCTION

Oil wells are expensive capital facilities that serve for many decades, exceeding their design working life, and represent complex engineering structure. The most responsible part of a well is its casing that ensures cementing the well shaft and isolating various geologic beds.

An important condition of the efficient well operation is a reliable cement sheath on the outside surface of the casing pipe. However, for some geologic and engineering reasons, we do not always manage to ensure a quality cementation along the entire depth for the entire service life of the well, which may lead to anodic zones occurring at the points where metal contacts an aggressive medium and, therefore, to localizing corrosive processes.

For casing pipes, the characteristic types of corrosive damages in casings are pits, perforations, concentric-ring metal corrosion, and rill-shaped longitudinal pits.

Cathodic and anodic reactions can be distributed along the outside surfaces of casings for electrochemical protection that has been used since 1913 and is the only method of proactively protecting the casings against ground corrosion.

Cathodic protection efficiency evaluation based on the results of analyzing optimal parameters, particularly of the protection current value, and on the performance test of the findings in operation conditions evaluated by the nature of distributing the potential (current density) of the electric field applied along the surface of the structure to be protected, as well as the evaluation of the well flow string metal state, are sophisticated problems requiring a complex of methodological approaches.

Notations and Abbreviations

AB	Anode bed
APCS	Automated process control system
CPA	Cathodic protection assembly
FL	Flow line
GMS	Group Metering Station
DWPU	Deep-well pumping unit
BCS	Booster compressor station

CP	Cathodic protection
MOC	Metering Operation Center
CPS	Cluster pump station
WO	Workover of wells
PTS	Package transformer substation
CU	Cathodic unit
ETL	Electrical transmission line
CSRE	Copper-copper sulfate reference electrode
OGPD	Oil/Gas Production Division (field office)
MET	Mineral Extraction Tax
OWT	Oil-well tubing
WWO	Waiting for workover of a well
SP	Sacrificial protection
DWL	Distribution water line
CPS	Cathodic protection station
SMI	Scanning magnetic introscope
CS	Control station
C(S)PU	Cathodic (sacrificial) protection unit
DPUC	Deep-well pumping unit control
SWFR	Specific well failure rate
SCPS	Submersible Centrifugal Pump System
SRPU	Sucker-rod pumping unit
EMWD	Electromagnetic well detector
EIG	Electrically insulating gasket
FS	Flow string
ECP	Electrochemical protection
ElCP	Electric-centrifugal pump

Chapter 1. WELL CASING AND CORROSION PROBLEMS

1.1. Oil Production Process

Almost all oil produced globally is extracted using drilling wells cased with high-pressure steel pipes. The well has an enclosed system designed for working with pressures comparable with formation pressures.

The entire oil production process, starting from its influx through the formation to bottom holes and ending with the external delivery of commercial oil from the production field, is divided into three stages:

– Oil influx through the formation to the wells due to the artificially created pressure difference in the formation and at the bottom holes;

– Oil influx from the bottom holes to the hole tops on the surface; and

– Gathering oil and its accompanying gas and water on the surface, separating them, demineralizing the oil, processing the stratum water, and gathering the associated petroleum gas.

Oil is extracted from wells either due to natural flowing under the reservoir energy or by using one of several mechanized liquid-lifting techniques [1].

The oil production concept is shown in Fig. 1.1.

Production wells are tied in Group Metering Station (GMS) 2 (Figs. 1.1 and 1.2), on which a liquid meter is installed and in front of which isolation joint 3 is mounted. From the GMS, the gathering pipeline enters in booster compressor station 4 (Figs. 1.1 and 1.2), where a centrifugal pump is installed, which pumps the oil via oil pipeline under pressure 2-3 MPa to tank farm 13. In tank farm 13. the oil comes to process reservoirs 5. where the oil is settled. The top (lighter) part is pumped into oil tanks 7. while the bottom (heavier) part comes to water tanks 6. From water tanks 6. wastewater is fed under gravity to drainage system control room 9. from where it is pumped under a pressure of 2.5-3 MPa to cluster pump station (CPS) 10 (Figs. 1.1 and 1.2). From the CPS, the wastewater is fed via distribution water ducts 14 to water-injection wells under a pressure of12-16 MPa (sometimes, upon the request of geologists, the pressure may reach 18 MPa). Wastewater squeezes the oil from the reservoir, which oil comes to development wells. The oil is gathered from processing (5) and water (6) tanks to oil tanks 7. Widely used is the settling method where lighter oil is gathered on the top and the heavier water is gathered on the bottom. From oil tanks 7. the oil (finished stock) comes to the headworks of PJSC Transneft.

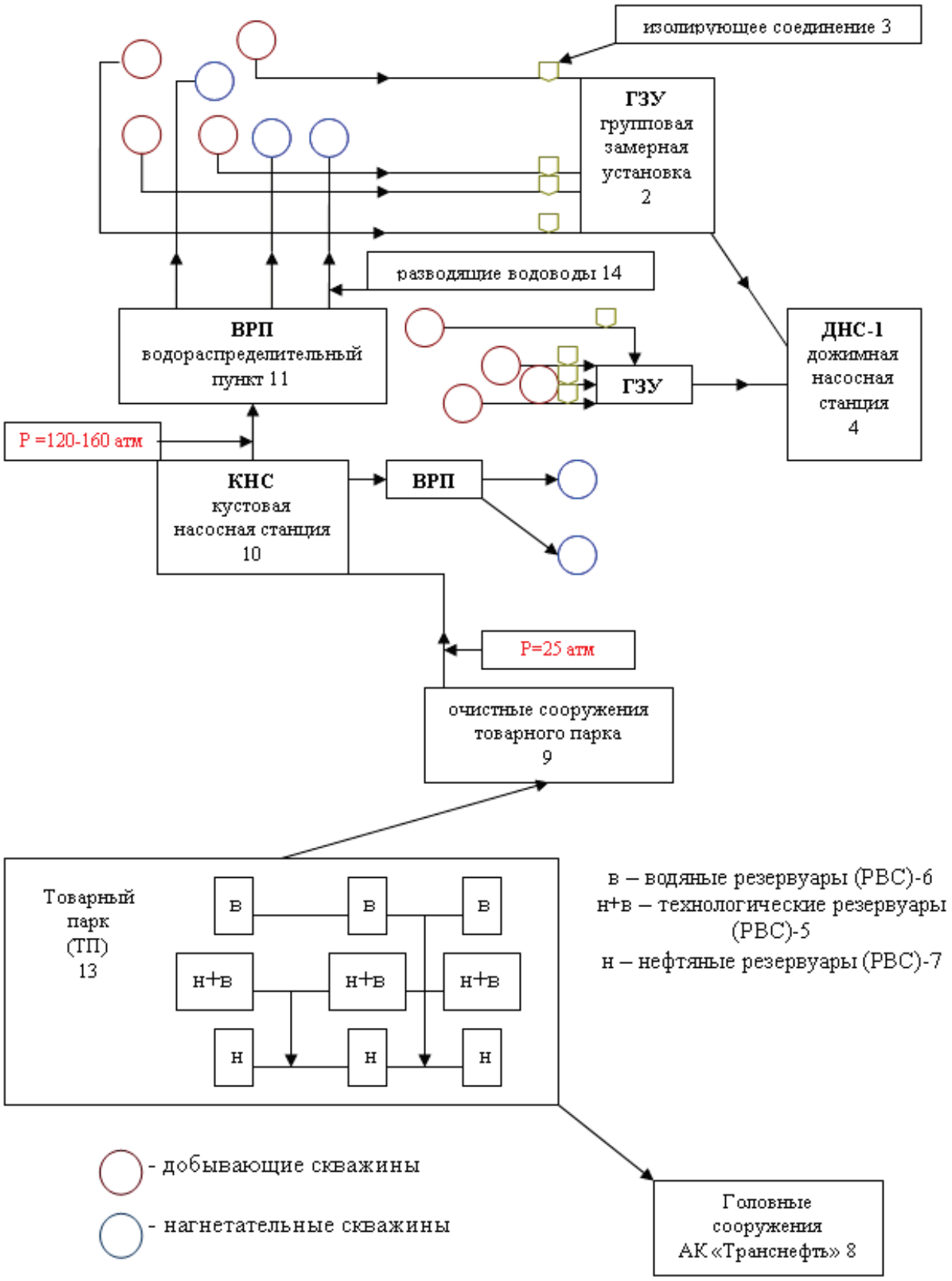

Fig. 1.1. Oil Production Concept at PJSC Tatneft

Appearance of the core components of Tatneft's oil production facilities is shown in Fig. 1.2 below.

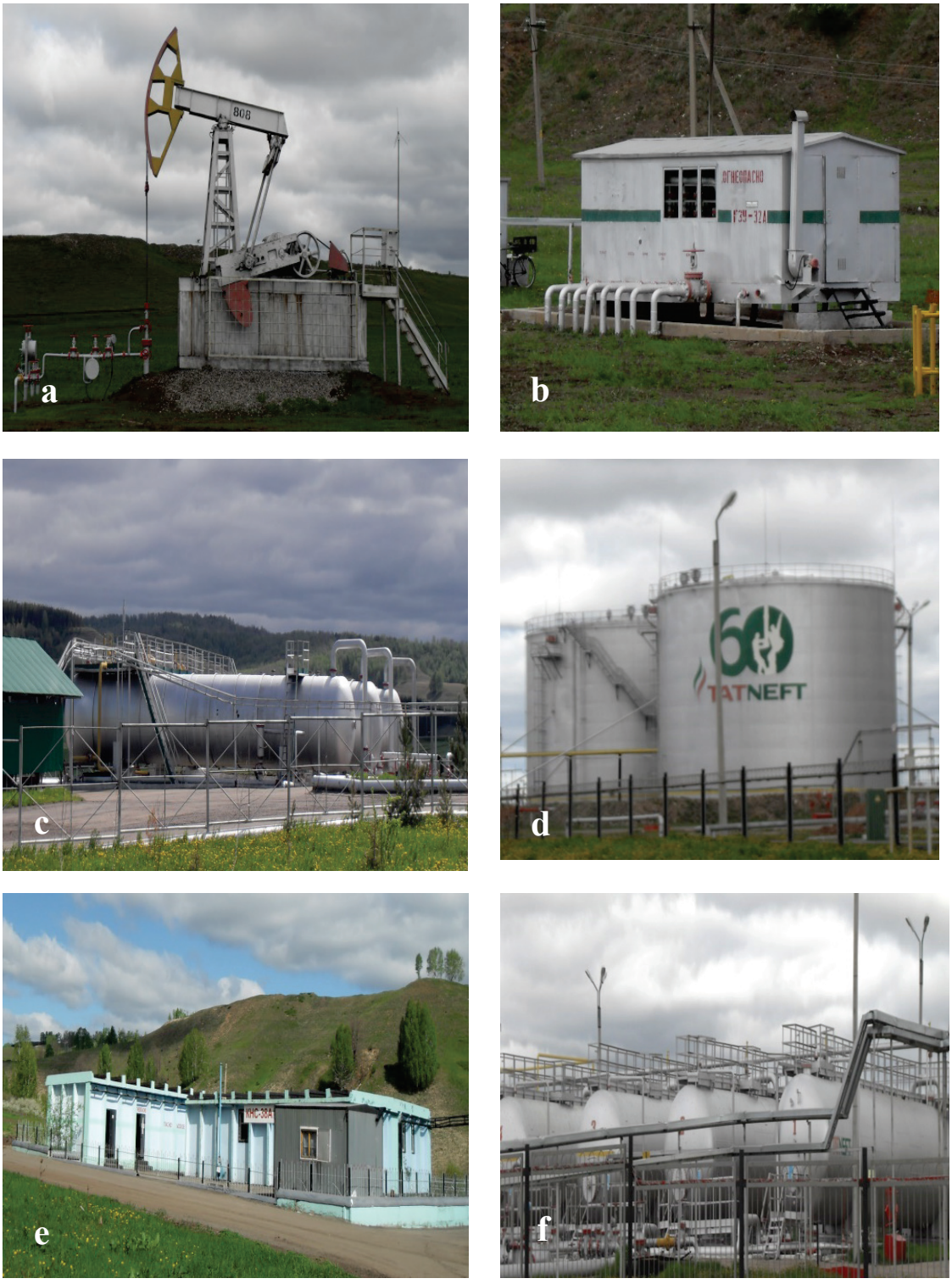

Fig. 1.2. Appearance of Core Components of Oil Production Facilities at PJSC Tatneft: a – Pumping unit; b – Group Metering Station; c – Booster compressor station; d – Preliminary wastewater discharge unit; e – Cluster pump station; f – Tank farm

Reservoir energy is renewed by injecting water. Currently, artificial water drive is created everywhere where geologic conditions allow that and where it is economically reasonable. In case of water drive of oil from

the formation, the oil deposit volume decreases continuously. Basically, only oil flows upstream of the waterfront, which is the reason for the effective permeability to oil remaining quite high. This produces a considerable waterflood displacement efficiency (70-80 %).

At PJSC Tatneft, over 80 % of oil is extracted from oilfields, in which formation pressure is supported using out-contour or contour flooding. Out-contour flooding is a process, in which water is pumped into reservoirs through water-injection wells located beyond the outer oil-water outline. Contour flooding is based on cutting the deposit with water-injection well sets into several separate areas [2-5].

1.2. Oil-Well Design

Casing, or well casing, is a pipe string that is run from the ground surface to assume the direction for the well bore (Fig. 1.3). Casing is usually cemented from outside either along its entire length or within range sufficiently long to ensure a secure mounting and stability of the bore section between the production horizon and the surface [6. 7].

Casing pipes allow:

– Preventing the liquid of overlying beds from penetrating;

– Withstanding the pressure of the surrounding geologic beds;

– Separating the inside surface of the well bore from the surrounding ground;

– Drilling ahead to the production horizon; and

– Running the pipe string from the surface down to the production horizon.

Within one well, two or more casings can be used, installed one inside the other:

– Surface casing: A casing running from the ground surface down to the sufficient depth to prevent the surface water or ground from penetrating into the well;

– Intermediate casing: A casing running from ground to the intermediate formation depth. This depth can be within the range between the ground surface and production horizon; and

– Production casing: A casing running from the ground surface down to the productive reservoir. The bottom part of the casing may be within the range between the top and the lowermost section of that reservoir.

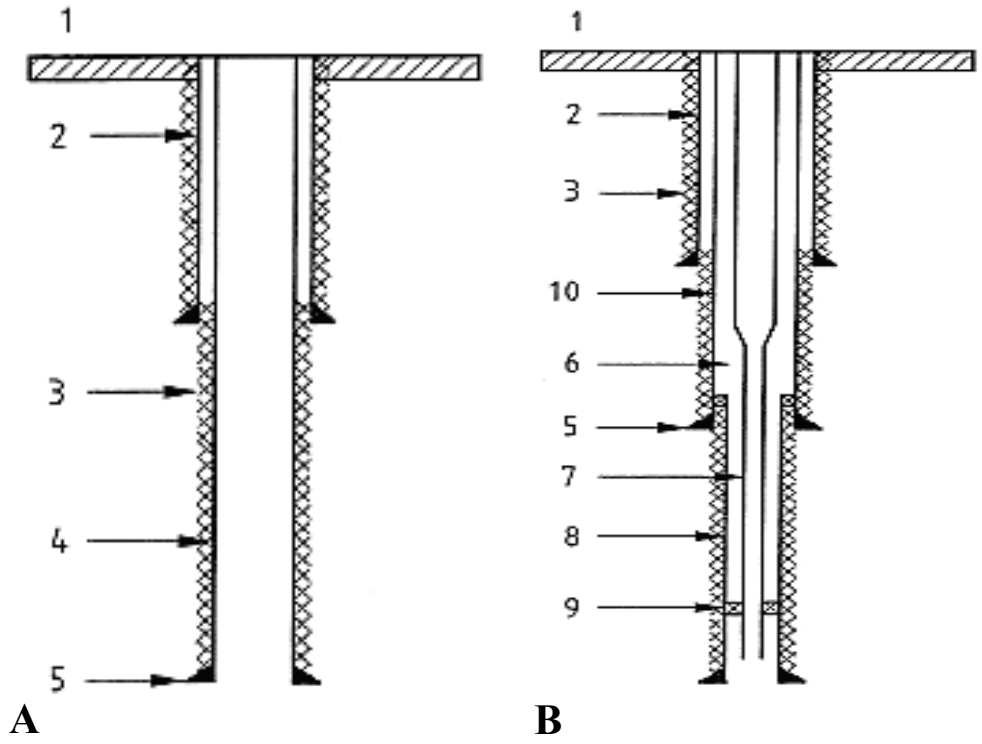

Fig. 1.3. Typical Design of an (a) Single-Casing or (b) Two-Casing Well: 1 – Ground surface; 2 – Surface casing; 3 – Cementation belt; 4 – Production casing; 5 – Pipe shoe; 6 – Tubing-casing annulus; 7 – Production casing; 8 – Production liner; 9 – Production packer; 10 – Intermediate casing

Liner is a pipe that executes the same function as that executed by intermediate or production casing, but it is suspended within the intermediate casing. Production packer is a concentric device designed for packing off tubing-casing annuluses between the intermediate casing and the liner or production casing. Pipe shoe is a cylindric element that is fastened to the bottom part of the pipe casing and allows placing the casing within the well (guide shoe) [6. 7].

The upper borehole sections are usually represented with recent sediments that are easy-washable by the circulating liquid flow during drilling. Therefore, they start drilling the well only after all necessary measures are taken against washing the formation under the wellsite substructure. For this purpose, before drilling a well, a shot hole is erected down to good ground (4-8 m), and then a pipe runs into it, with a window cut in its upper part. Space between the pipe and the shot hole wall is filled with quarry stones and cement mixture. As a result, the well head is well secured. A short metal trough is welded to the pipe window, and flush fluid is routed through this trough during drilling to the ditch system and to disposal facilities. The pipe installed within the shot hole is called *guide.* Upon installing a guide and performing some other activities, a rigging

availability report is prepared and well drilling starts. Having drilled through unstable, soft, fractured, and cavern grounds that complicate drilling (usually 50-400 m), they wall of and isolate those horizons, for which purpose, a collared joint steel casing runs into the well, while its annulus is cemented. The first casing is called *conductor*. After the conductor has run down, it is not always possible to drill the well down to the designed depth due to driving new complicating horizons or due to the necessity to overlap production formations that should not be operated by this well. In such cases, a need arises for running and then cementing the second casing that is called *intermediate casing*. At drilling deeper, some new horizons can appear that need isolation. Then the third casing is run and isolated, which is called the *second intermediate casing*. In this case, the previously run casing will be called the first intermediate casing. In complicated drilling conditions, there can be three or even four such intermediate casings. Having drilled to the designed depth, a *production casing* is run and cemented. After that, the quality of the cement sheath formed in the annulus is checked for the production casing, and all the casing strings at the well head are piped together with special equipment. After running the last production casing, the activities begin, performing which ensures oil influx from the formation into the production casing and commissioning of the well. Arranging casings, indicating their diameters, the depth of the transition from a larger well diameter to the smaller one, the running depths of casings, and their cementing ranges, forms the term of *well design* [8].

If, along with a guide and a conductor, only production casing is run in the well, then this design is called *single-casing design*. If, along a guide and a conductor, intermediate and production casings are run in the well, then it is a *two-casing* (in case of one intermediate casing) or *three-casing* (in case of two intermediate casings) *design*. Fig. 1.3 shows the single-casing (a) and two-casing (b) well design.

The oil-well design is chosen based on the characteristics of the geologic structure of the oil deposit, the well purpose, and other factors. Moreover, the design and equipment of production wells depend on the oil extraction method.

In the Field Office of PJSC Tatneft, the single-casing design is typically used, which, along with the guide and the conductor, is composed of a production casing only (Fig. 1.3a). Since the well head is located within the easy washable ground zone, it is strengthened using a guide up to 50 m long. Length of the conductor casing preventing from freshwater salination and from harmful substances penetrating in it from underlying formations,

reaches 500 m. Length of the production casing down to the production formation is about 2.000 m, and its diameter does not exceed 0.168 m.

In manufacturing a casing, threaded steel pipes are conventionally used (Fig. 1.4). Welding is used for joining the pipes less frequently, since the pipes joint with welded seams are corrodible and attackable at welding points, so that ground water may penetrate in the well shaft.

Fig. 1.4. Appearance of Casings

Oil casing dimensions are shown in the reference Appendix 1 [9].

1.3. Causes of Corrosion Hazards

The key reason for increase in the number of wells taken out of service due to technical factors is break of airtightness and, therefore, corrosion of casing strings, up to the occurrence of punctures (Fig. 1.5). Formation water aggressivity causes the high corrosion velocity of casings. Average velocity of the external casing metal corrosion ranges from 0.8 to 1.2 mm/year.

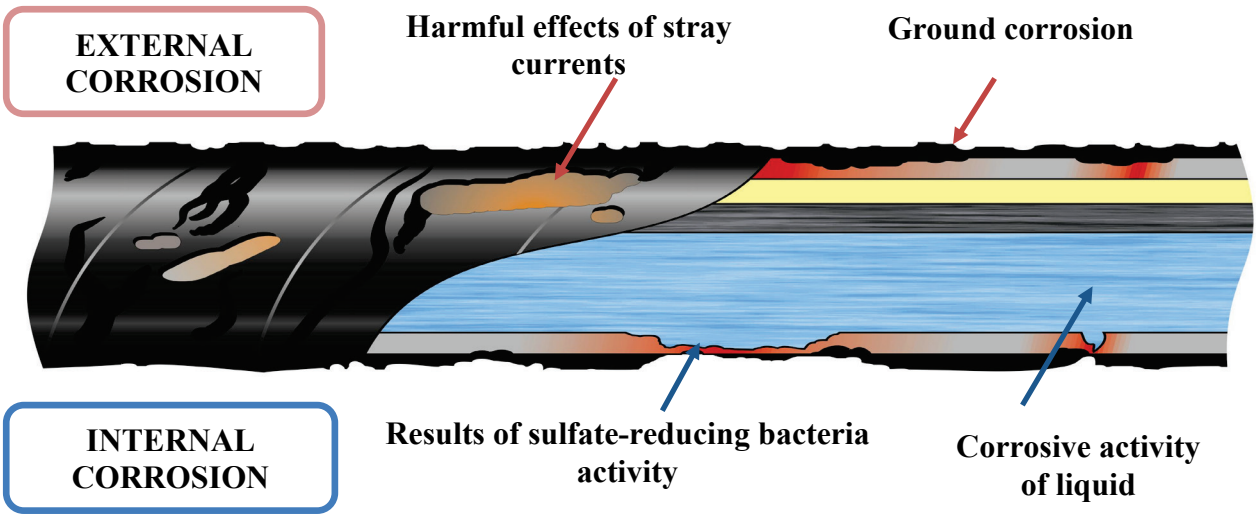

Fig. 1.5. Types of casing corrosion and its possible causes

Injection wells are under the largest load. The total value of external and internal corrosion in injection wells is 0.9-1.5 mm/year when injecting freshwater and 1.3-2.7 mm/year when injecting wastewater.

Main corrosive components in the formation water are hydrogen sulfide, carbonic acid, and oxygen (it occurs in phreatic aquifers). Sulfate-reducing bacteria activity is essential to intensifying corrosive processes.

Differences in the physicochemical parameters of formation water along the well log, such as temperatures, pH, and ionic or gas compositions, cause macrocorrosion couple currents flowing along the string, which reduces the corrosion velocity in cathodic zones and increases it in anodic zones, compared to the corrosion velocity at no macrocouple currents.

Inter-stratal flows in the casing-string annulus causes replenishing the corrosive medium, reduces the diffusion limitations of corrosion reactions and, therefore, increases the casing corrosion velocity.

Good-quality cementing considerably reduces the intensity of casing corrosion due to reducing the thermodynamic probability of corrosion, as a result of the high pH value, excluding the medium motion, and the significant diffusion limitation of corrosion reactions. A defective cement sheath has an insufficient protective efficiency: According to statistics, the specific failure rate of production casings is just 40-50% lower in cemented intervals than in the intervals without cement. As a rule, casing corrosion develops unevenly, especially in case of hydrogen-sulfide corrosion, and is usually of pitting nature, which causes perforations in pipes, often with the general corrosion being insignificant [10].

1.4. Typical Corrosion-Caused Damages

Corrosion-caused casing failure means its loss of tightness or integrity due to the corrosive wear of the pipe body [10].

Low-carbon steels, which oil-and-gas pipes are usually manufactured of, are exposed to general and local corrosion in aqueous production media and grounds. General corrosion develops on the entire surface of metal and causes the general pipe wall loss (Fig. 1.6). Local corrosion develops on the non-insulated surfaces of pipes in presence of general corrosion, while it also develops on insulated surfaces where there are insulation sheath defects, and causes forming the caverns relatively small in their areas and of different depths, up to full penetrations (Fig. 1.7).

Fig. 1.6. External corrosion of casings

Fig. 1.7. A penetration near the socket plus external corrosion

The general corrosion hazard consists in weakening the mechanical strength of the pipeline; in this case, ruptures are accompanied with longitudinal breaks of various lengths.

Typical corrosion-caused damages are:

– Single spots having dimensions comparable with the pipe wall thickness;

– Dense pitting, more frequently on the internal surfaces of pipes (Fig. 1.8);

– Single penetrations, more often on the external lamellar-structure surface of pipes (Fig. 1.9);

– Ring corrosion of the pipe metal near threaded junctions;

– Longitudinal flow-shaped damages on internal surfaces.

Fig. 1.8. Internal corrosion spots

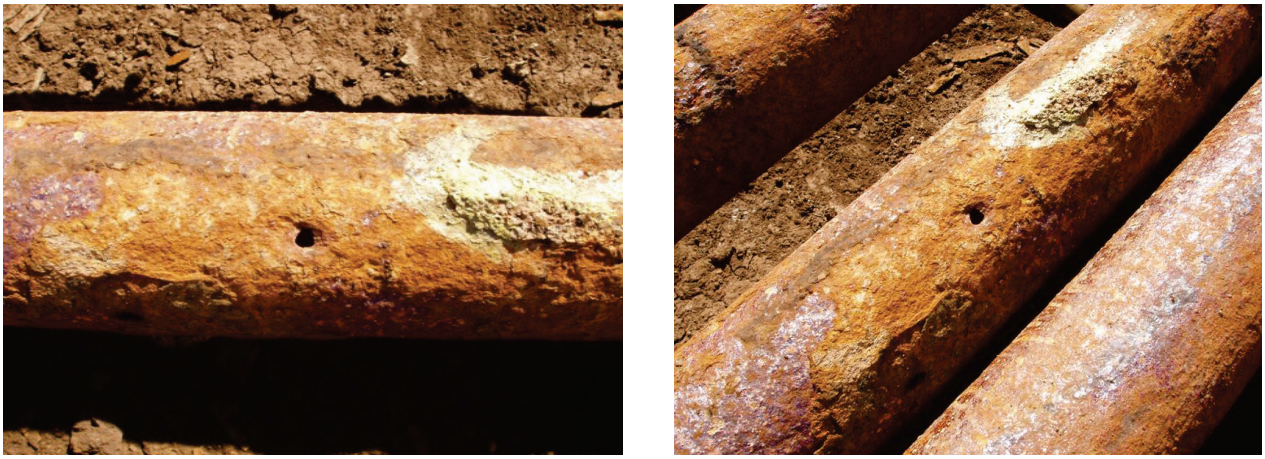

Fig. 1.9. External penetrating corrosion of casings

Caverns, depending on the diameter-to-depth ratio, are divided into spots (diameter exceeds depth), craters (diameter is comparable to depth), and pitting (depth exceeds diameter). Typical corrosion cavern types are shown in Fig. 1.10.

In case of penetrating, various types of corrosion cause the relevant corrosion holes in the pipe walls. Spot corrosion forms a hole in the pipe wall having low-sloped edges with the diameter (on the corroding surface) that significantly exceeds the wall thickness (Fig. 1.11.)

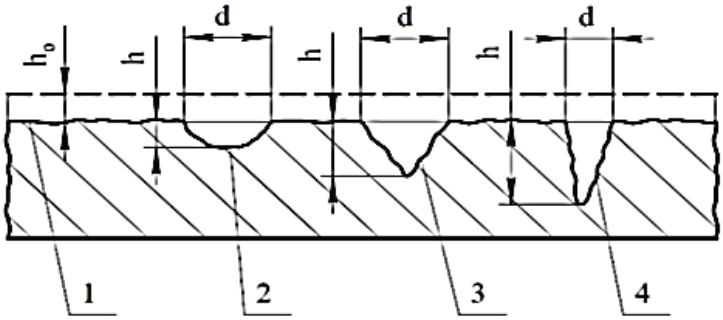

Fig. 1.10. Main types of corrosion caverns: 1 – general corrosion; 2 – spot; 3 – crater; 4 – pitting; h_0 – general corrosion penetration depth; h – cavern depth in presence of general corrosion; d – cavern diameter

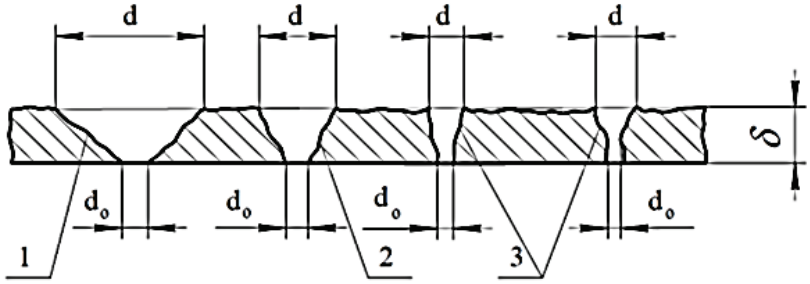

Fig. 1.11. Corrosion holes in the pipe wall at local corrosion: 1 – spotting; 2 – cratering; 3 – pitting; d – hole diameter at its opening; d_0 – hole diameter in the clear; δ – pipe wall thickness

Cratering corrosion causes a cone-shaped hole with high-sloped edges, the diameter of which hole is comparable to the wall thickness. In case of pitting corrosion, the hole is practically cylindrical, while the diameter is less than the wall thickness. A particular case of cratering is flowing corrosion, where multiple single craters develop into a single groove.

In some cases, the specific types of corrosion-caused damages are observed in the oil production practice, which are not basically related to dissolving metals, but to worsening their properties or structures. These are corrosion fatigue, corrosion (hydrogen sulfide and carbonate) cracking, and blistering of metals.

Corrosion fatigue occurs under cyclic stresses, such as changes in the pipeline pressure or vibrations, in combination with the corrosive action of the medium. Fatigue cracks are most frequently formed around stress raisers, such as welded seams, non-metal inclusions, scratches, scuffs, corrosion caverns, etc. While developing, fatigue cracks may lead to the leaks of the handled medium without pipe breakages (in case of high safety factor) or with pipe breaking along the generator line (in case of low safety factor).

Corrosion cracking happens where there are pulling stresses in pipes contacting the relevant media. Hydrogen-sulfide cracking is basically typical of high-resistance steels in aqueous or wet media with high hydrogen-sulfide content (over 100 mg/l). Carbonate cracking can be found in pipe steels in grounds under cathodic protection that increases the alkalinity (*pH*) of the pipe surface.

In aqueous media containing over 100 mg/l of hydrogen sulfide, structural-grade low-carbon steels may get hydrogen-charged, which causes blistering the metal surface due to the hydrogen penetration and accumulation in the microcavities of the surface layer [11].

1.5. Statistics on the Engineering Statuses and Failures of Production Casings [12–15]

Results of statistical analyses performed on the engineering statuses and failures of casings in the 1940s showed their low reliability, no economic efficiency, and endangering the environmental safety. Therefore, cathodic protection started to be used. We can observe how cathodic protection affects the situation, exemplified by operating the oil-well casings in the USA (Fig. 1.12. Table 1.1).

A similar situation was observed at PJSC Tatneft before the 1970s (Fig. 1.13). The main cause of casing failures was external corrosion in commercial wells and double-sided corrosion in injection wells [11].

The situation could be changed through using electrochemical protection in combination with special protective measures (Fig. 1.13). Prior to the ECP introduction, failures grew under a law that is close to the exponential one. As soon as they started implementing the ECP, that growth stopped due to low coverage – about 400-600 wells were enabled annually. Afterwards, with increasing the coverage, a sharp drop in failures began: In 1979–1995. the number of yearly corrosion-caused failures in PJSC Tatneft decreased by 5.5 times (the efficiency of 82 %, which is close to the average data for the USA). The efficiency of decrease in failures is found regarding the forecasted level that would have been reached in 1979-1995. if no ECP had been introduced.

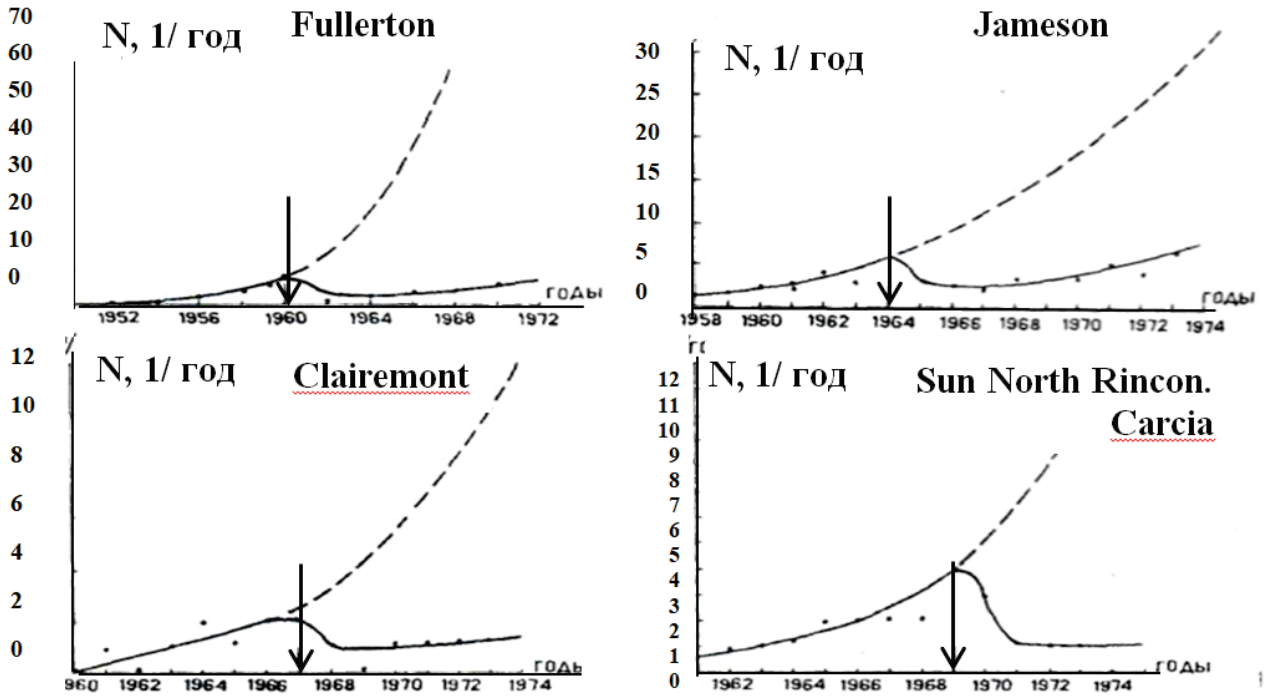

Fig. 1.12. Efficiency of using the electrochemical protection of oil-well casings at the US oil deposits: Solid line – the actual frequency of failures; dashed line – the forecasted frequency of failures; the arrow points at the year of introducing the protection

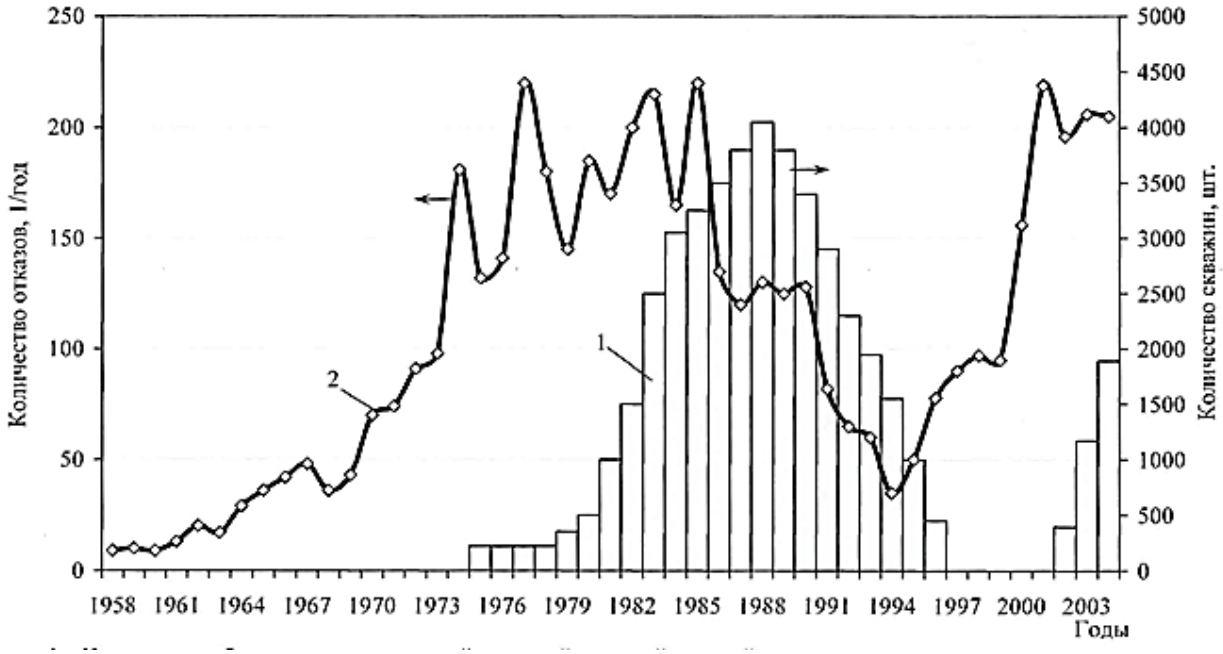

Fig. 1.13. Changes in the corrosion-caused failures of production well casings at PJSC Tatneft: 1 – number of production wells with active cathodic protection, 2 – number of the failures of production well casings

Table 1.1

Results of Introducing the Electrochemical Protection at Various Oil Deposits in the USA

Deposit	Number of Wells Protected	Depth of Damages, m	Protective Current, A	Type of Anodic Grounding	Efficiency of Reducing the Failures, %
Seeligson	251	300–400	3–6	Surficial	98
Sun North Rincon. Garcia	186	350–900	4–12	Deep	85
Jameson	172	350–1.400	6	Deep and surficial	70
Clairemont	55	400–1.650	6	Surficial	88
Nena Lucia	192	750–1.350	6–9	Surficial and deep	0
Ocho Juan	25	800–1.450	7	Deep	76
Boyd	53	850–1.700	9	Deep	100

Late in the 1980s and early in the 1990s, in the context of social and economic crisis, the number of the protected wells at PJSC Tatneft decreased sharply down to several dozens, which affected the number of failures – they increased rapidly. At the same time, the repeated growth of failures happened quicker than before, which was related to the ageing of well inventory. As long ago as in 2000. the level of failures was reached, which there was before introducing the ECP.

Early in this century, by the initiative of the PJSC Tatneft oil-and-gas departments that have noticed the endangering growth of failures, it was decided to start re-introducing the ECP from 2003.

As of 2009. an average of PJSC Tatneft, the CP coverage had made 17% for production wells and 12% for injection wells (Fig. 1.14).

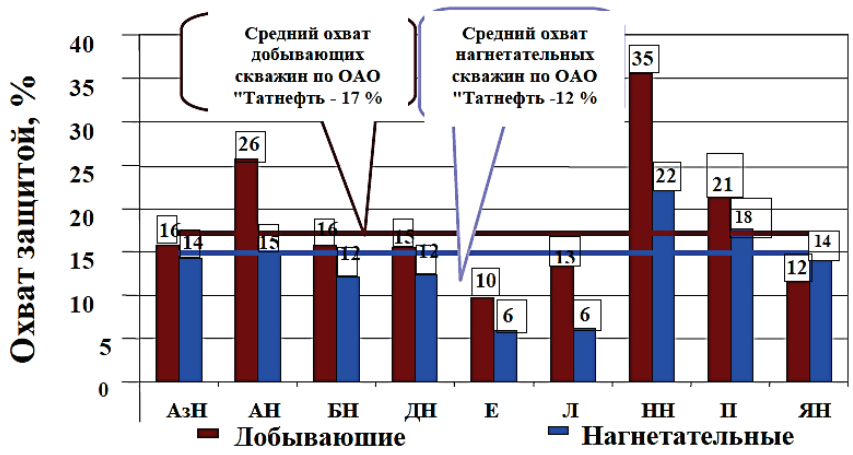

АзН – Азнакаевскнефть, АН – Альметьевнефть, БН – Бавлынефть, ДН – Джалильнефть, ЕН – Елховнефть, ЛН – Лениногорскнефть, НН - Нурлатнефть, ПН – Прикамнефть, ЯН - Ямашнефть

Fig. 1.14. CP coverage of oil-well casings at PJSC Tatneft in 2009

Using CP allowed reducing the frequency of casing failures in average by three times for both production and injection wells. This is found throughout all the years of introducing CP (2006-2008), Figs. 1.15-1.17.

In 2006. casing failures turned out to happen on the wells operated for over 26 years. For production wells, the frequency of failures made 0.026 pcs./well without CP and 0.019 pcs./well with CP; for injection wells, 0.030 pcs./well without CP and 0.011 pcs./well with CP. (Fig. 1.15).

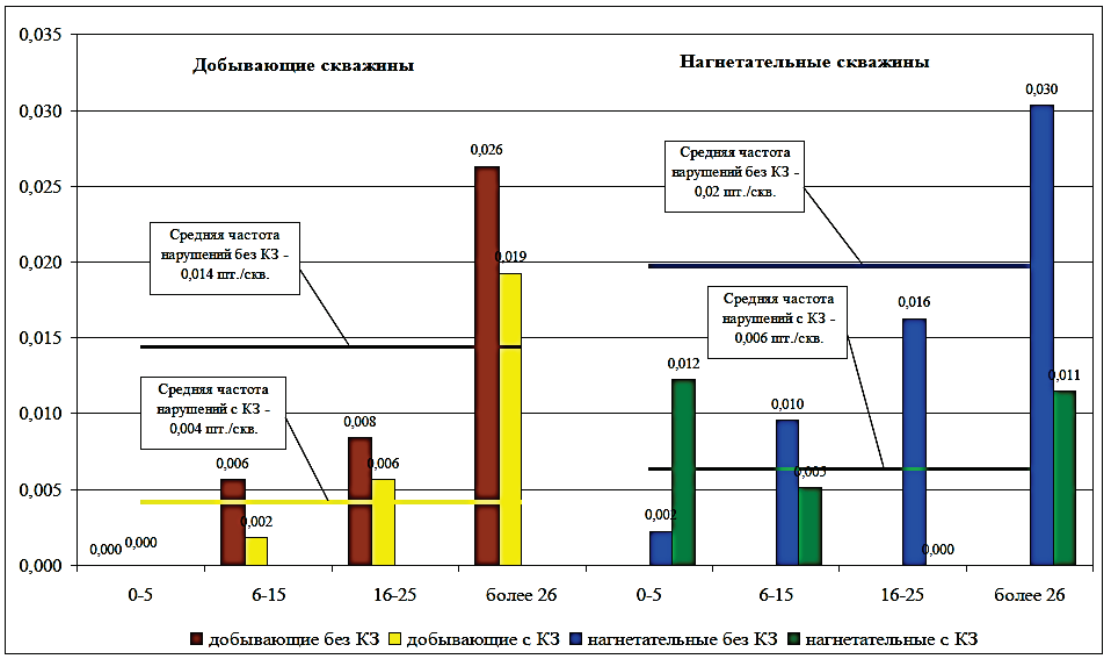

Fig. 1.15. Frequency of oil-well casing failures throughout PJSC Tatneft in 2006. by well ages

In 2007. at PJSC Tatneft, production wells aged over 26 years had the frequency of failures of 0.022 pcs./well without CP and 0.007 pcs./well

with CP, while injection wells had 0.030 pcs./well without CP and 0.014 pcs./well with CP (Fig. 1.16).

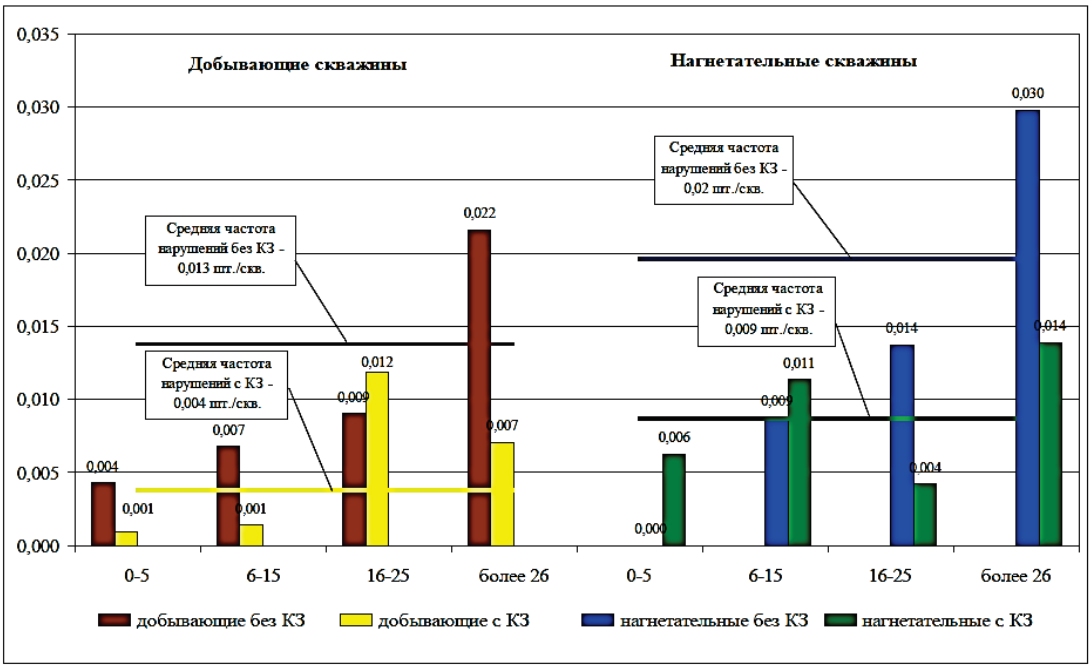

Fig. 1.16. Frequency of oil-well casing failures throughout PJSC Tatneft in 2007. by well ages

In 2008. at PJSC Tatneft, production wells aged over 26 years had the frequency of failures of 0.027 pcs./well without CP and 0.010 pcs./well with CP, while injection wells had 0.022 pcs./well without CP and 0.009 pcs./well with CP (Fig. 1.17).

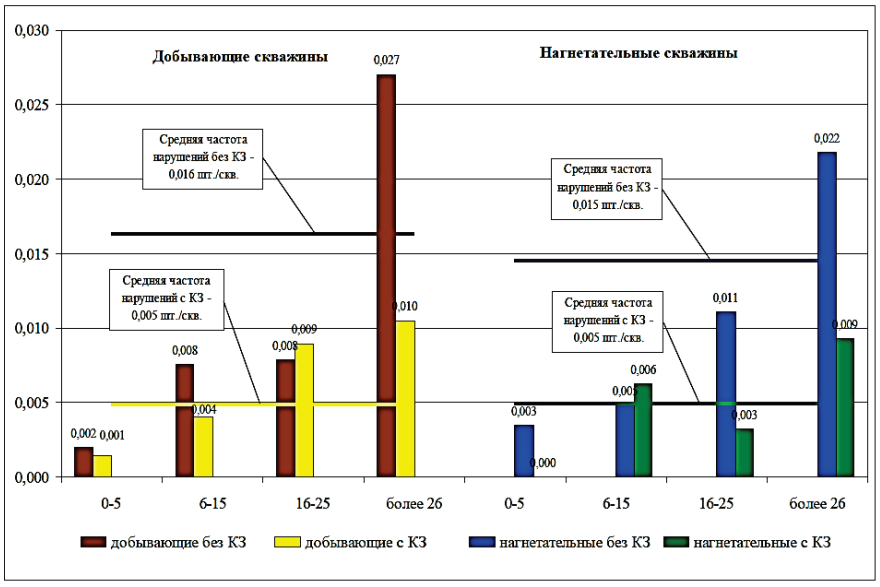

Fig. 1.17. Frequency of oil-well casing failures throughout PJSC Tatneft in 2007. by well ages

In Fig. 1.18. you can see the changes in the specific number of wells having the failures of production casings at PJSC Tatneft in 2007-2011.

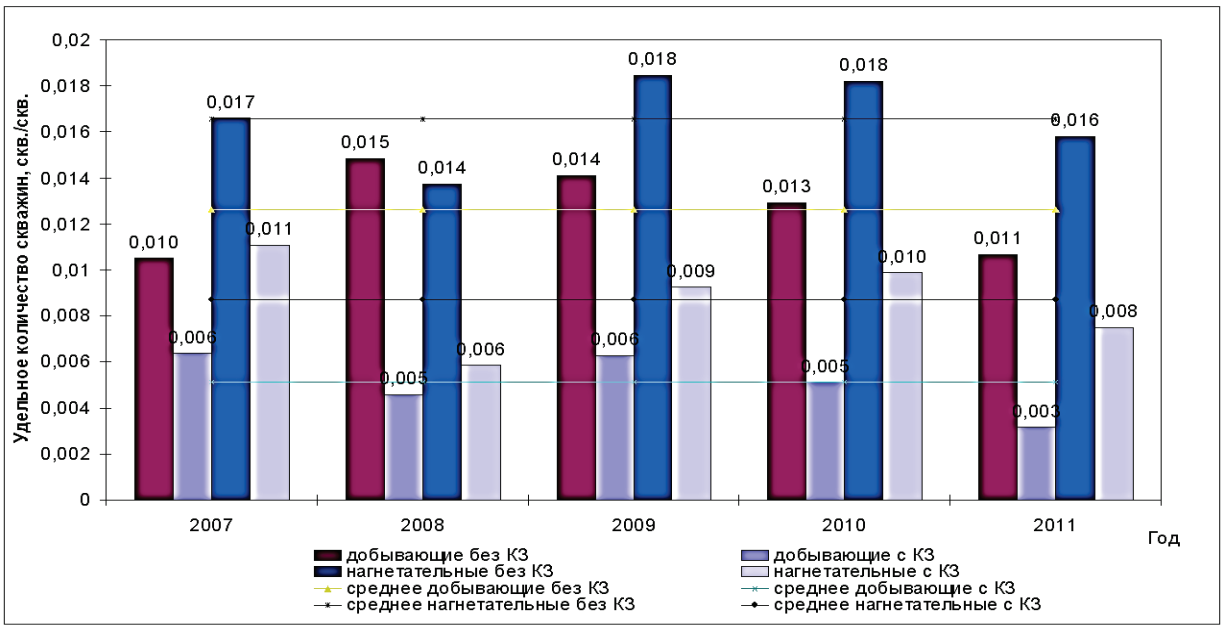

Fig. 1.18. Specific number of wells with the failures of production casings at PJSC Tatneft

Starting from 2003. in PJSC Tatneft, CP is introduced at all newly drilled wells and at the wells that had got in the area affected by CP. Annual growth rates of CPS are 600-700 wells per year.

As of 1/1/2012. the cathodic protection of oil-well casings had been introduced at 22 % of production wells and 19 % of injection wells. In Fig. 1.19. you can see the changes in introducing cathodic protection on the premises of PJSC Tatneft starting from the year 2000.

At the introduction of the cathodic protection, the frequency of failures decreased by 3 times at production wells and by 2.3 times at injection wells in average over the years 2007-2011.

Data collection form regarding the availability of the cathodic well-protection systems is given in Table 1.2.

Distribution of penetrating corrosive damages of casings in production well depths has changed over recent years. If, in the 1970s, about one half of all failures were within 600-1.000 m, at which depths the most aggressive water-bearing strata are located, then at current times, the distribution of failures has become more even along the entire string length, except for the range of 1.400-1.600 m where over 35% of failures are concentrated. This change in failures distribution is related to the fact that the largest part of casing strings is cemented, and the cement stone mitigates the differences in the aggressivity of surrounding strata to some extent. Increase in the occurrences of penetrating damages within the range of 1.400-1.600 m, which in many wells coincides with the level of deep well pump running, where a permanent deposit water column is formed in the high water-content conditions, is explained by the development of internal corrosion.

Table 1.2.

Form for collecting data on the usability of cathodic protection systems for wells, exemplified by OGPD Elkhovneft

№ п/п	Тип СКЗ	Номи-нальная мощность СКЗ,	Порядковый № СКЗ	№ скважины	Тип скважины	Тип АЗ	Количество АЗ, шт.	Глубина АЗ, м	Напряжение на выходе СКЗ, В				Ток на выходе СКЗ, А				Период простоя СКЗ	Причина простоя СКЗ
									при ПНР	Дата ПНР	последний замер	дата замера	при ПНР	дата ПНР	последний замер	Дата замера		
1	2	3	4	5	6	7	8	9	10	11	12	13	14	15	16	17	18	19
1	ПДЕ	1200	1	814	добыв.	ЭГТ-2500	2	20	6	31.10.03	28,5	18.03.10	4	31.10.2003	21,4	18.03.2010		
				2576	добыв.			20										
				2575	нагнет.													
2	ПДЕ	1200	2	2883	добыв.	ЭГТ-2500	2	20	6	31.10.03	21	18.03.10	6	31.10.2003	21,2	18.03.2010		
				2882	нагнет.			20										
				2884	нагнет.													
3	ПДЕ	600	3	719	нагнет.	ЭГТ-2500	1	41	6	30.10.03	15	07.07.2008	3,5	30.10.2003	6	07.07.2008		нет КТП (разобрано)
4	ПДЕ	1200	4	2986	нагнет.	ЭГТ-2500	1	41	13	30.10.03	28	18.03.2010	9	30.10.2003	0,2	18.03.2010		
				2980	добыв.													
5	ПДЕ	1200	5	750	добыв.	ЭГТ-2500	2	20	6	31.10.03	30	18.03.10	6	31.10.2003	7,1	18.03.2010		
				4384	нагнет.			20										
				2935	нагнет.													
6	ПДЕ	1200	6	2160	добыв.	ЭГТ-2500	1	41	15,1	28.11.03	30	08.04.2010	6,6	28.11.2003	6,9	08.04.2010		
				2161	нагнет.													
7	ПДЕ	1200	7	2167	нагнет.	ЭГТ-2500	1	41	15,1	28.11.03	30	08.04.2010	15,1	28.11.2003	4,2	08.04.2010		
				2168	нагнет.													
8	ПДЕ	1200	8	2908	добыв.	ЭГТ-2500	2	20	8,8	28.11.03	21	18.03.2010	7,7	28.11.2003	24	18.03.2010		
				2907	нагнет.			20										
				4479	нагнет.													
9	ПДЕ	1200	9	8306	добыв.	ЭГТ-2500	1	41	8	02.07.04	18	16.03.2010	4	02.08.2004	12,7	16.03.2010		
				8310	добыв.													
10	ПДЕ	1200	10	8308	добыв.	ЭГТ-2500	1	41	8	02.07.04	22	16.03.2010	4	02.08.2004	14,8	16.03.2010		
				8309	добыв.													
11	ПДЕ	1200	11	8334А	добыв.	ЭГТ-2500	1	41	8	02.07.04	19	16.03.2010	4	02.08.2004	13	16.03.2010		
				8311	нагнет.													
12	ПДЕ	1200	12	8392	добыв.	ЭГТ-2500	2	41	13	02.07.04	21	08.04.2010	11	02.07.2004	11,7	08.04.2010	1.01.10-02.02.1	ПРС (КРС)
				8393	добыв.			41										
13	ПДЕ	1200	13	8806	добыв.	ЭГТ-2500	2	41	13	02.07.04	21	08.04.2010	11	02.07.2004	11,9	08.04.2010	1.01.10-02.02.1	ПРС (КРС)
				8811	добыв.			41										
14	ПДЕ	1200	14	8326Г	добыв.	ЭГТ-2500	2	20	18	26.07.04	21	18.03.2010	17,4	26.07.2004	15	18.03.2010		
				8327	добыв.			20										
				8335	нагнет.												6.04.09-30.06.0	Обрыв дрен.провод
15	ПДЕ	1200	15	8318	добыв.	ЭГТ-2500	2	20	18	26.07.04	21	18.03.2010	6,9	26.07.2004	16	18.03.2010	6.06.09-30.06.0	Обрыв дрен.провод
				8319	добыв.			20										
				8320	добыв.													
16	ПДЕ	1200	16	2068	добыв.	ЭГТ-2500	2	41	18	02.08.04	27	08.04.2010	15	02.08.2004	16,6	08.04.2010		
				8357	добыв.			41										
				8358	добыв.													
17	ПДЕ	1200	17	8366	добыв.	ЭГТ-2500	2	41	18	02.08.04	26	08.04.10	15	02.08.2004	17,6	08.04.2010		
				8367	добыв.			41										
				4002	добыв.													
18	ПДЕ	1200	18	2063	добыв.	ЭГТ-2500	1	41	17	02.08.04	15	08.04.2010	12	02.08.2004	12,1	08.04.2010		
				2069	добыв.													
19	ПДЕ	1200	19	8355	нагнет.	ЭГТ-2500	1	41	12		24	08.04.2010	8	02.08.2004	12,3	08.04.2010		
				8369	нагнет.													
20	ПДЕ	1200	20	6865	добыв.	ЭГТ-2500	2	41	18	02.08.04	30	16.03.2010	10	02.08.2004	9,2	16.03.2010		
				6868	добыв.			41										

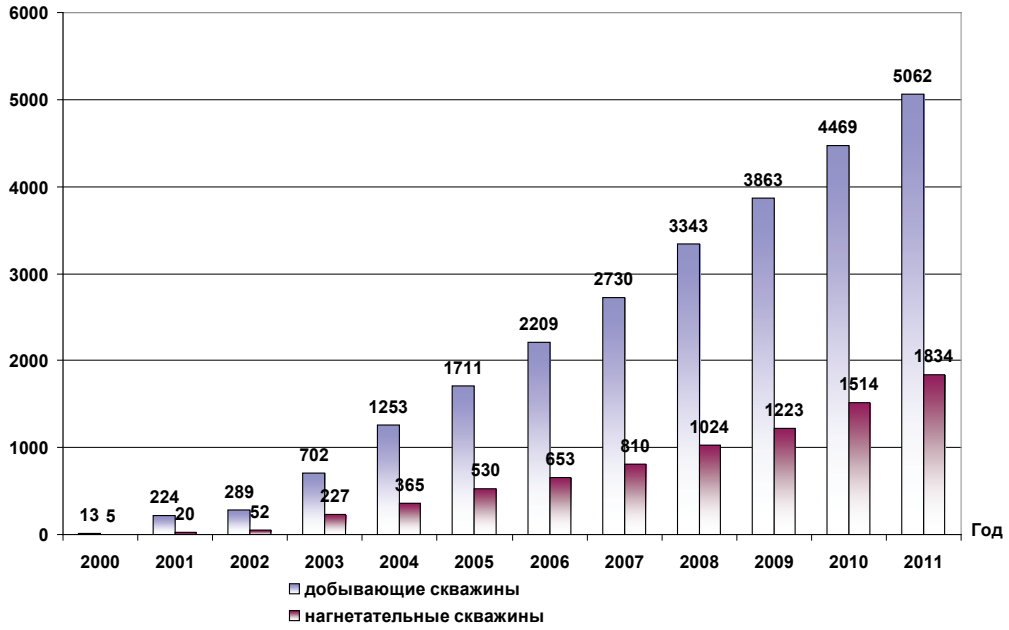

Fig. 1.19. Changes in the growth of wells with cathodic protection of casings on the premises of PJSC Tatneft

Recent statistics on the failures of casings indicates that the protective properties of cement stone decrease in the wells having service life for over 15-20 years, primarily within the areas of low-quality cementing. This is determined by at least three factors:

1) With the time, cement stone itself gets chemically destructed by aggressive formation fluids;

2) With cement getting destructed, the electrochemical corrosion of casings becomes more active at the cement stone defect locations, because high-quality sections of cement stone discontinue provide positive effects upon its defective sectors;

3) Cement stone with integrity defects creates additional galvanic inhomogeneity on the casing surface, which strengthens macrogalvanic corrosion due to occurrence of sectors having different electrode potentials.

Resulting from the above processes, the intensity of corrosion-caused failures (number of annual failures per 1 m of the string length) in cemented ranges is averagely just 40-50% lower than in the no-cement ranges. Hence, there also occurs a need for the electrochemical protection of wells, the casings of which are fully cemented; primarily, this concerns those having low-quality cementing ranges.

Studies are being performed now, aimed at solving the problem of the operating reliability of oil-well casings.

As of 1/1/2018. 39.4% of production wells and 29.2 % of injection wells at PJSC Tatneft were covered with cathodic protection. Changes in equipping the wells with cathodic protection over the years 2000-2018 are shown in Fig. 1.20.

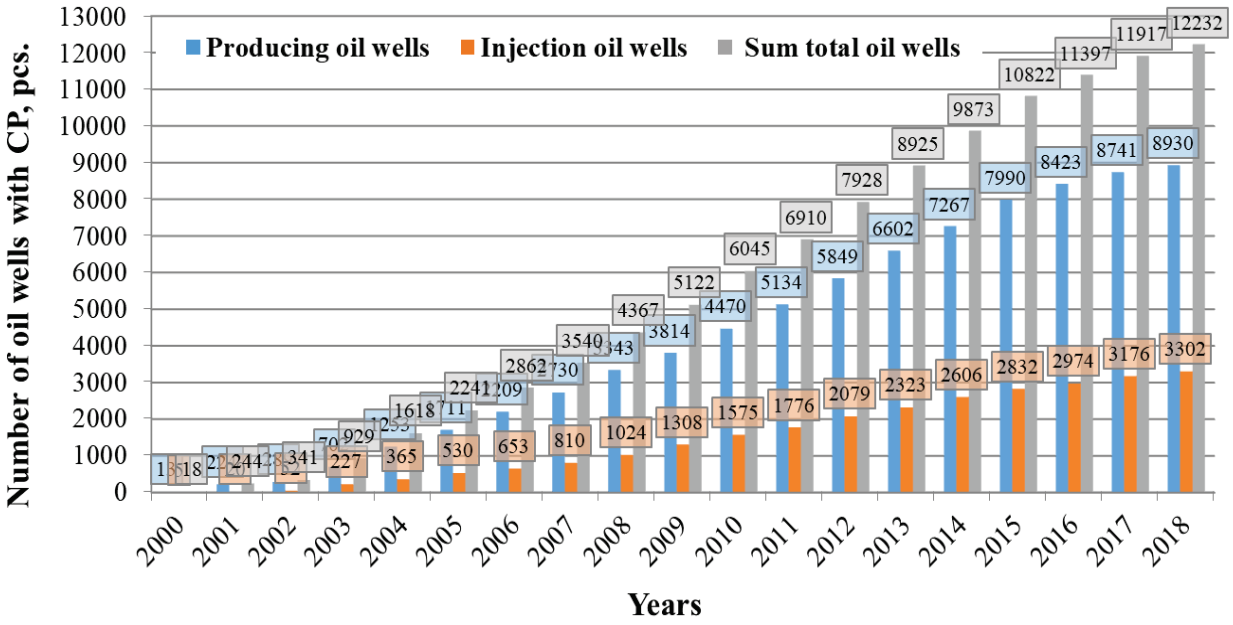

Fig. 1.20. Changes in equipping the wells with cathodic protection at PJSC Tatneft over the years 2000-2018

Collecting and systemizing the field data related to the number of wells operated, their ages, numbers of overhauls, and their failure frequencies (within the period of 2003-2015) have allowed us to evaluate the efficiency of protective measures taken. Research objects are the production and injection wells of PJSC Tatneft in terms of its Field Offices: Aznakayevskneft – AzN, Almetyevskneft – AN, Bavlyneft – BN, Jalilneft – JN, Elkhovneft – EN, Leninogorskneft – LN, Nurlatneft – NN, Prikamneft – PN, and Yamashneft – YaN. We have considered the wells with and without cathodic protection, broken down by their ages: 0-5; 6-10; 11-15. 16-20; 21-25; 26-30; and 31+ years.

The cathodic protection efficiency criterion is reducing the number of oil-well casing failures (Fig. 1.21). Measured data is approximated with relevant curves indicating the initial data validity factors of the trend model selected.

Analyzing the dependencies obtained, we can conclude that cathodic protection affects strongly the injection wells that have been operated for less than 25 years. Apparently, a lower protective effect on injection wells aged over 25 years is related to the effects provided by internal corrosion that is not affected by cathodic protection. In case of production wells, the critical age in terms of failures is that of 26-30 years, which is most probably related to the ageing of cement. Understandably, the youngest wells aged under 5 years the least corrodible. The equivalent number of failures within this age group of wells with and without cathodic protection is related to pulling the cement sheath up to the well head and to using the advanced cement slurries.

Characteristic that is inverse to failures can be evaluated using the efficiency of cathodic protection, i. e., the protection level characterizing decrease in the casing corrosion velocity due to cathodic protection. Mathematically, it can be found as the difference between the specific frequency of oil-well casing failures with, $n_3(t)$, and without, $n(t)$, cathodic protection, divided by the specific frequency of failures without cathodic protection:

$$Z = \frac{n(t) - n_3(t)}{n(t)}.$$

Efficiency values for individual Field Offices reach 1. while the average value of efficiency lies within the range of 0.5-0.6 (Fig. 1.22). For injection wells, this value is 0.4-0.5 in average.

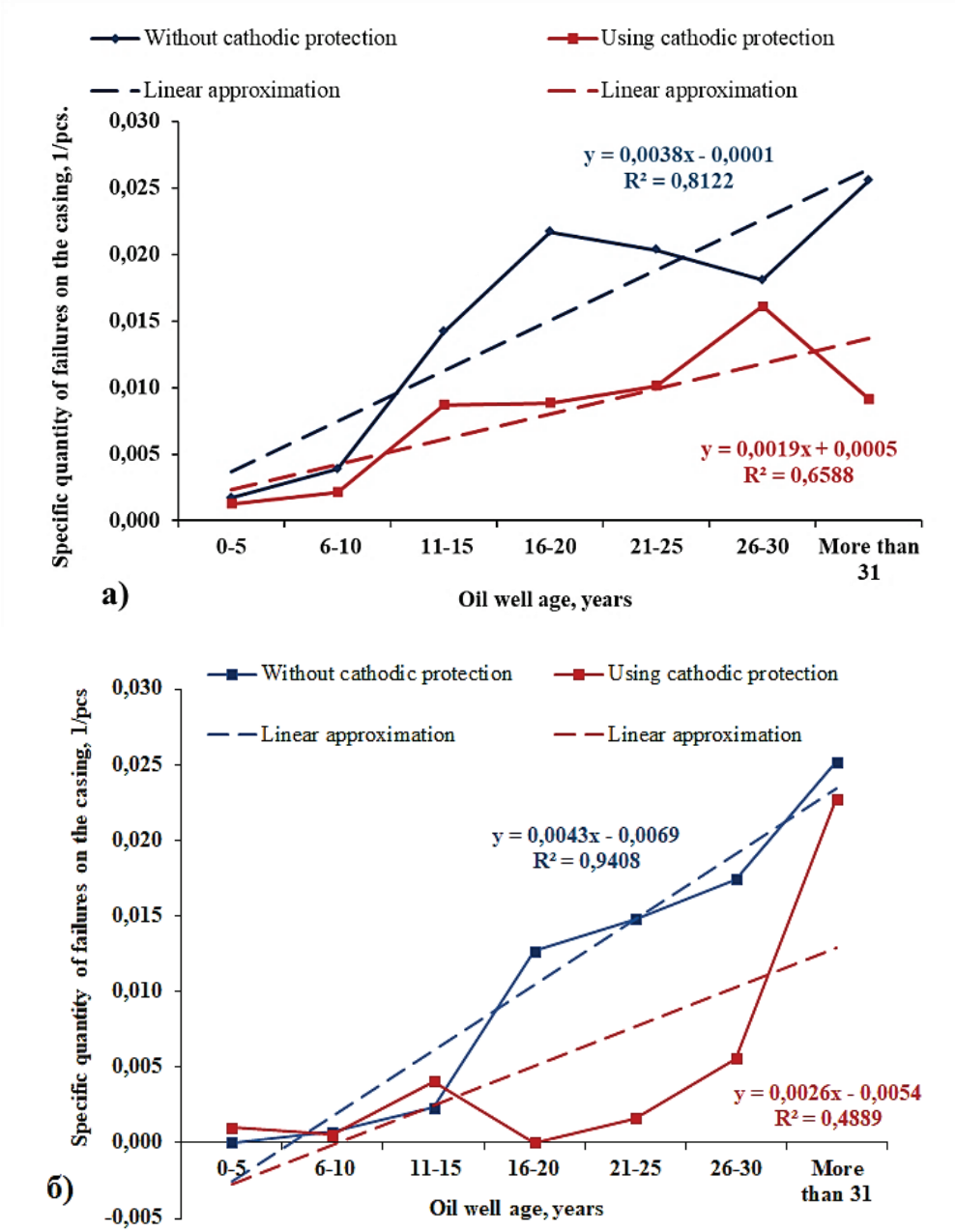

Fig. 1.21. Comparative changes in the specific frequency of failures in production (a) and injection (b) wells, depending on the availability of cathodic protection, over the years 2003-2015

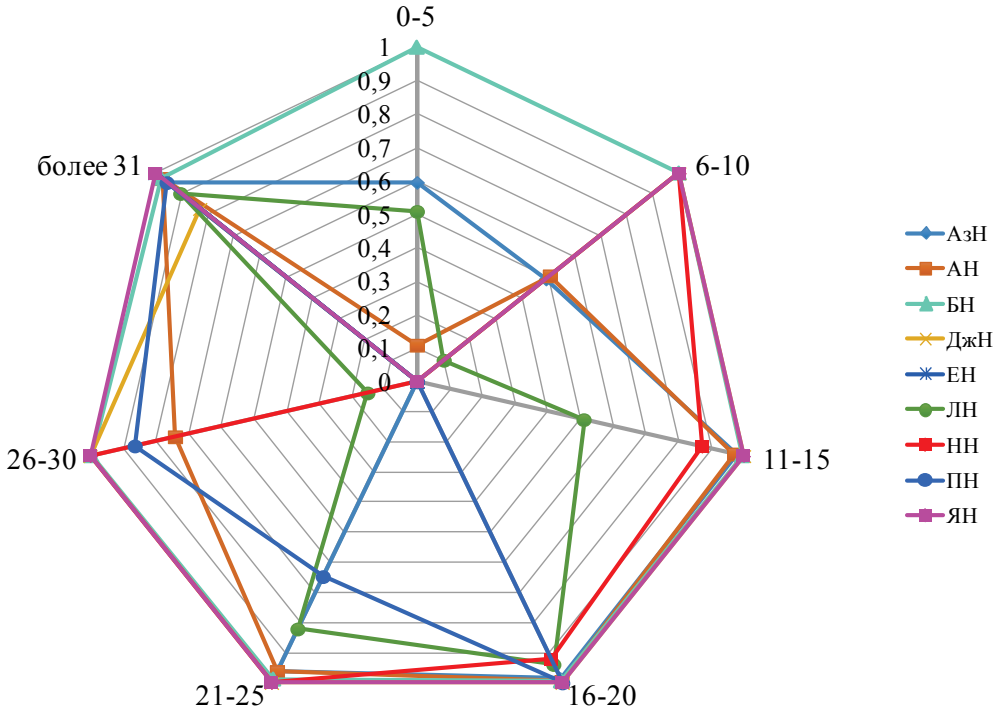

Fig. 1.22. Efficiency of cathodic protection technology for production wells of different age groups by Field Offices over the years 2003-2015

The highest efficiency of cathodic protection is observed in wells having been operated for 11-25 years in individual Field Offices, which is proven by the values of failure reduction factor defined as the ratio of the specific number of failures without cathodic protection to that with cathodic protection (Fig. 1.23). For injection wells, the value of 4-8 is observed at AN, BN, and AzN.

The equipment reliability can be characterized to the fullest extent by the probability of survival, i. e., the probability of no failure within the given operation time, i. e., within the predefined time interval relevant to the well age, which is defined mathematically as a ratio of the difference between the total number of *N*-aged wells and the number of failures *n(t)* in wells aged *t* to the total number of wells:

$$P(t)=\frac{N-n(t)}{N}.$$

Linear dependencies obtained by mean values without considering extreme points show that the no-failure probability decreases down to 0.9 for the old stock of both types of wells without cathodic protection (Fig. 1.24). When forecasting this indicator for unprotected wells aged about 40 years, this value decreases by 0.1 and makes about 0.8. At the same time, the protected wells retain this probability up to 0.98 within the entire service life.

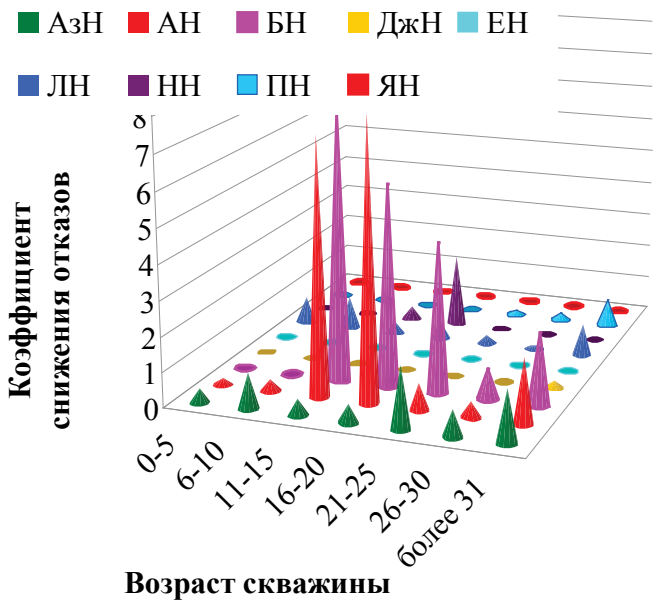

Fig. 1.23. Failure reduction factor for production wells depending on their ages over the years 2003-2015

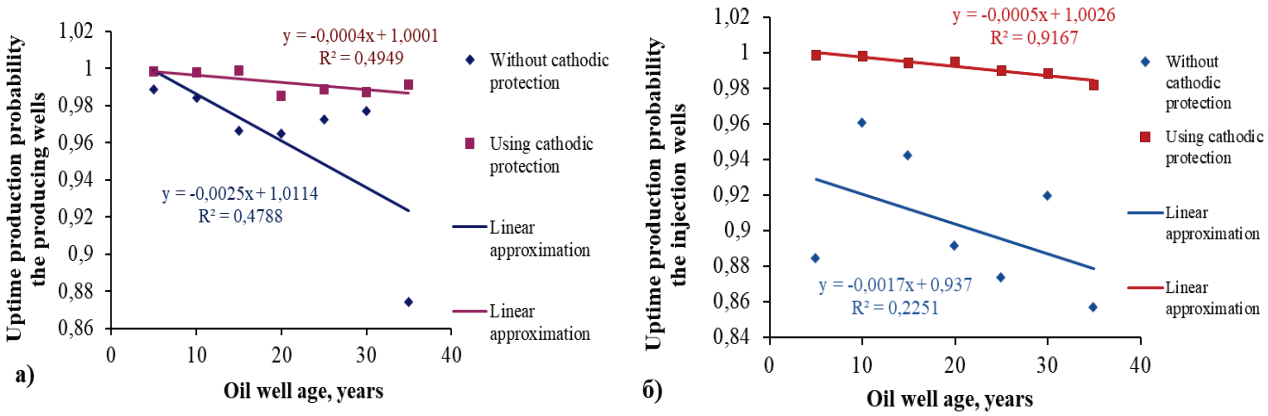

Fig. 1.24. Probability of the non-failure operation of production and injection wells, depending on their ages and on the availability of cathodic protection

At the same time, the average failure probability, i. e., the probability of at least one failure occurring within a given operation time (within the predefined time interval relevant to the well age):

$$Q(t) = 1 - P(t) = \frac{n(t)}{N}$$

makes 0.15 for unprotected wells.

1.6. Forecasting the Corrosion-Caused Failures of Casings [10]

When counting the number of corrosion-caused casing failures within the total number of failures caused by loss of tightness, we exclude those

caused by permeability of threaded joints of casings. Other failure causes are uncommon.

To identify more precisely the causes of existing or future failures, the following procedures, either alone or in combination:

– Measuring the mean pipe wall thickness using geophysical thickness gages (Fig. 1.25);

– Casing logging with geophysical defect detectors, such as MI-5X introscope (Fig. 1.26); and

– Removing and visually inspecting the casings (Fig. 1.27).

Fig. 1.25. Geophysical thickness gage

Fig. 1.26. Magnetic introscope MI-5X

Economic efficiency of oil-well casing CP is measured using the accumulated number of failures as per a well, counted considering the forecasted growth over the CP service life, as well as service lives with and without protection.

Corrosion failure without protection are forecasted for a group of wells of the same category and design.

Fig. 1.27. Visual inspection of casings

If the basic number of the wells in the selected group were drilled within a short time interval (at most 10 years), then for all wells one dynamic series

is made for the corrosion-caused failures accumulated over t years of operation, the t time reference being taken from the weighted mean drilling year of the wells in group T_{mn}.

As a predictable property, we take the ratio of the number of annual failures over t years of operation to the well stock of the group, i. e., the number of failures accumulated over t years in average per well:

$$\bar{F}(t) = \sum_{i=t_0}^{t} n(i)/N_f, \tag{1.1}$$

where t_0 means the mean operation period of the wells in group, counted from year T_{mn} up to the year of the first corrosion-caused failures appearing; $n(i)$ means the number of corrosion-caused failures in the wells in group in the i^{th} year of operation; and N_f means the number of wells in the group.

For further calculation, the dynamic series $\bar{F}(t)$ obtained is approximated by an as simple analytic function as possible, such as exponential or power function. If the wells of the selected group were drilled within a longer period (over 10 years), then for the purpose of forecasting $\bar{F}(t)$, a subgroup of the oldest wells from this group is chosen, which contains as many oldest wells drilled within a short time interval of at most 10 years as possible. Function $\bar{F}(t)$ defined for this subgroup will be statistically true for all the wells in the group.

The accumulated number of failures with cathodic protection ensuring the P corrosion protection degree, is calculated by formula:

$$\overline{F}_{gr}(t) = \overline{F}\left[(1-P)\,t + Pt_{gr}\right], \tag{1.2}$$

where t_{gr} means the time of operating the wells before introducing the protection, year.

The value of the casing protection degree is taken as $P = 0.7 \div 0.8$. Decrease in the number of failures accumulated due to CP over any reference period of CP action, t', is calculated by formula

$$\Delta\overline{F}(t') = \overline{F}(t_{gr} + t') - \overline{F_{gr}}(t_{gr} + t'). \tag{1.3}$$

Annualized decrease in failures due to CP over period t' is found from formula

$$\Delta\overline{f}(t') = \Delta\overline{F}(t')/t'. \tag{1.4}$$

No-CP casing service life, T, is found considering the accumulated failures from expression

$$\overline{F}(T) = N_c, \tag{1.5}$$

where N_c is the critical number of failures calculated as per 1 well over time T, is defined based on technical and economic calculations by comparing the costs related to handling failures and the sequences thereof, and the costs of drilling a new well or running a new production string [10].

CP-equipped production casing service life, T_{gr}, is calculated by formula

$$T_{gr} = \left(T - Pt_{gr}\right)/(1 - P). \quad (1.6)$$

Chapter Review

1. Oil production process exemplified by PJSC Tatneft.
2. Typical oil well designs and factors defining the choice of the design.
3. Types of oil-field casing corrosion by the nature of corrosive destruction.
4. Cathodic protection system operation practices and impacts on the statistics of production casing failures.

Chapter 2. CATHODIC PROTECTION SYSTEMS FOR OIL WELLS

Cathodic protection that has been used since 1913 is the only way of actively protecting casings against ground corrosion. Developing a time-continuous ECP capable of efficiently protect a casing is still an urgent task of scientific research [14].

Cathodic polarization of the structure leads to increasing the content of electrons in the lattice, i. e., to increasing electron density, which manifests in shifting the potential into the cathodic region. Increasing the electronic density of metal prevents from transforming its atoms into positively charged ions that pass into solution, or corrosion products remaining on the surface, i. e., the anodic reaction of metal ionization is incumbered. As a result, cathodic processes run on the surface of metal, while anodic processes causing corrosion pass to auxiliary electrodes (anodic earthing). Electrochemical protection of underground pipelines must be time-continuous and ensure the cathodic polarization of underground structures over the entire surface.

Cathodic protection unit consists of a DC source, anodic earthing, and connection cables (Fig. 2.1-2.3). The structure to be protected is connected to the negative contact of the current source, while its positive contact is connected to the second electrode, i.e., anode bed. Anode beds are made of low-alloyed steel or cast iron, including using a coke filling, iron-silicon alloy, and graphite materials or graphite-reinforced plastics (Fig. 2.2). Anode beds can be shallow (anode is installed below freezing depth), pile-supported (they are used in swamp areas), and deep well anodes.

To prevent casing corrosion, they use a cathodic protection system with series-connected anodes (bracelet anodes), louvered anodes consisting of multiple separate plates that work on the principle of a louvre, and cable anodes.

A shot hole is drilled for the anode bed. Electrodes are run into the shot hole. A test station is installed on the anode bed.

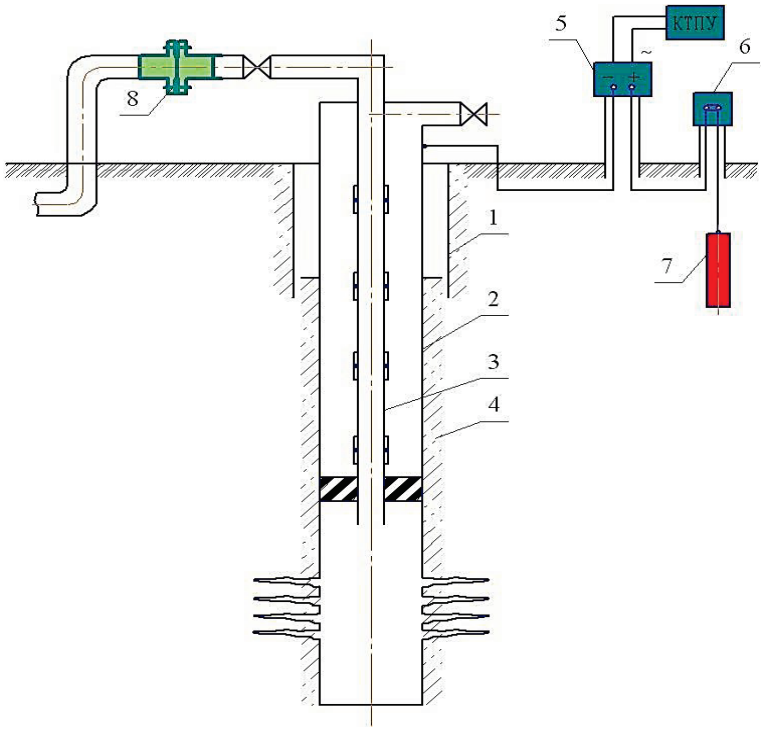

Fig. 2.1. Oil-well casing cathodic protection system: 1 – conductor; 2 – production casing; 3 – OWT; 4 – cement ring; 5 – cathodic protection station; 6 – test post; 7 – anode bed; 8 – nonconductive joint

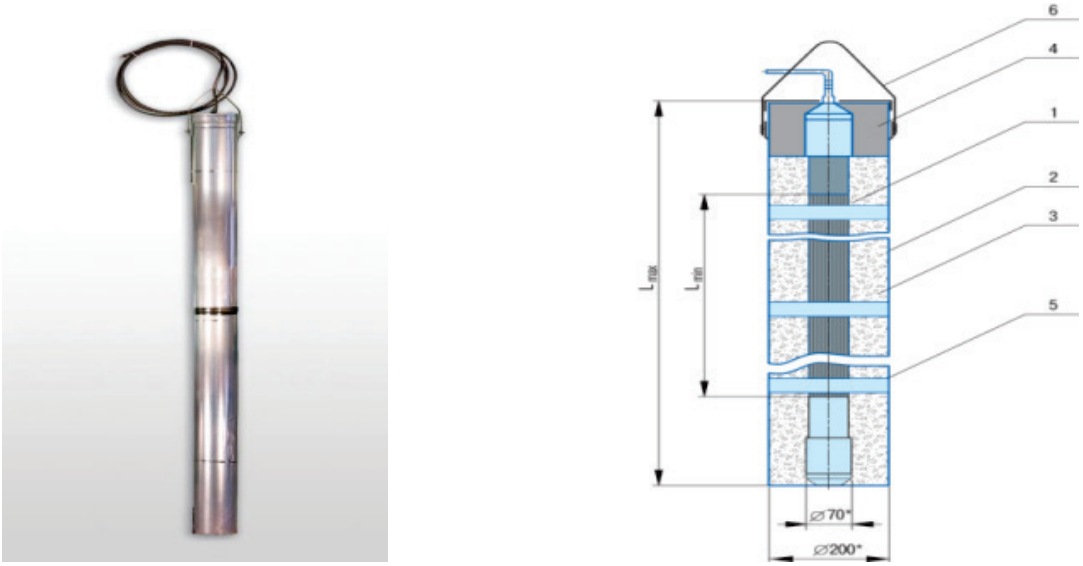

Fig. 2.2. Anode bed ELER 5K (for the wells of at least 324 mm in diameter; it has been manufactured since 2008): 1 – electrode; 2 – container made of galvanized steel sheets; 3 – coke fines; 4 – plastic filling; 5 – centering ring; 6 – weight handling device

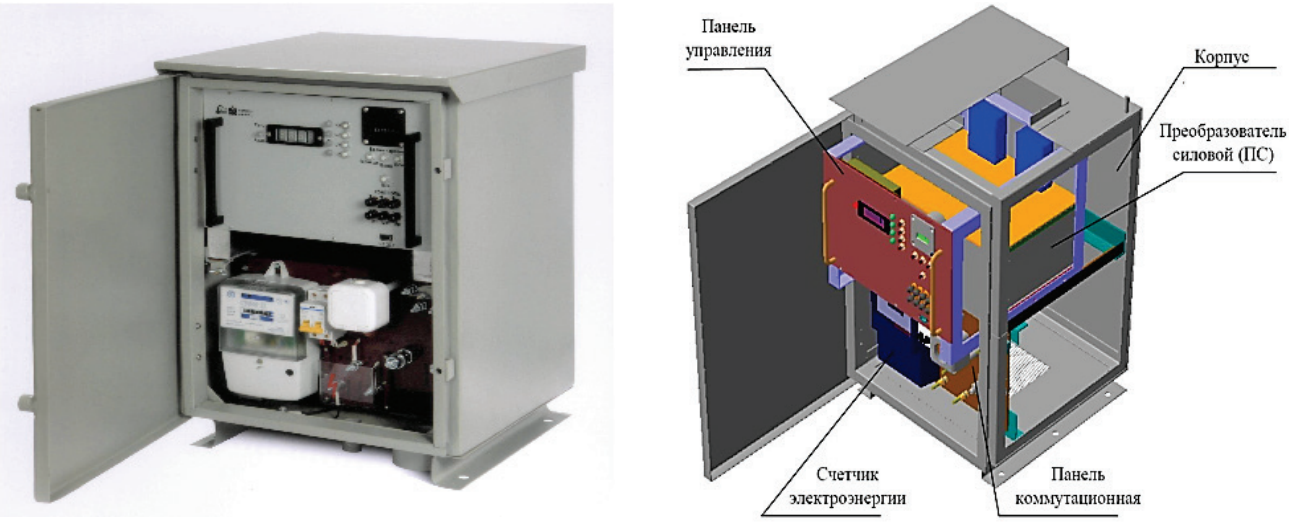

Fig. 2.3. Cathodic protection station

2.1. Cathodic Protection Schemes [10]

Oil-well casing cathodic protection is performed by cluster well scheme and individual well scheme (Fig. 2.4-2.7).

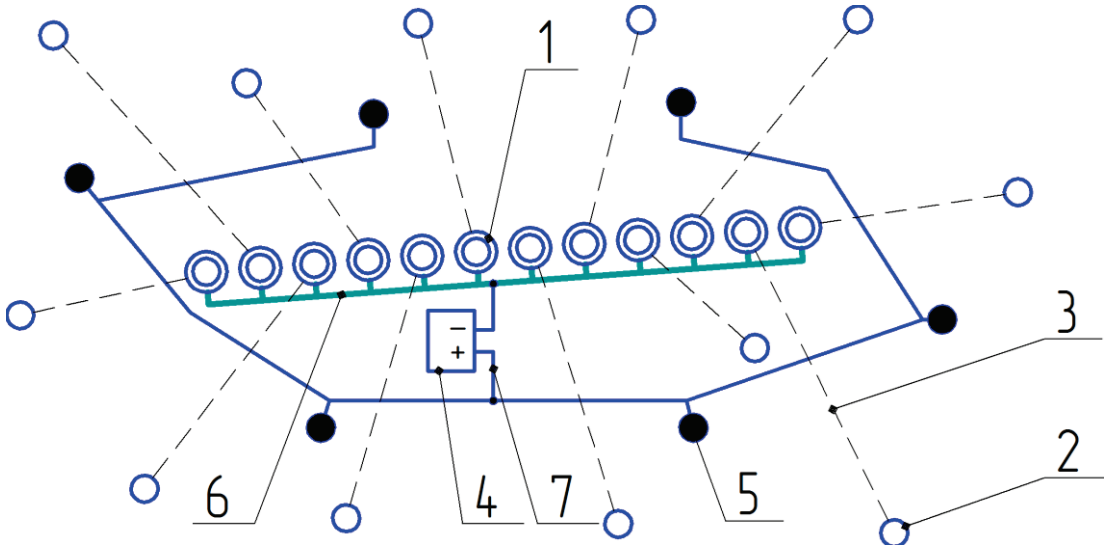

Fig. 2.4. Cluster well cathodic protection scheme: 1 – well heads; 2 – bottom holes; 3 – casings; 4 – cathodic protection station; 5 – anode beds; 6 – steel rails; 7 – drainage cable

Applying a cluster scheme of cathodic protection using well flow lines or distribution water lines as current ducts to casings is related to high currents (proportionally to the number of wells in the group) running off a limited area where anode beds are located. This creates a risk of the adverse

effect provided by stray currents upon other pipelines running at the distance of 1-2 km. Therefore, this protection scheme is not recommended for mass adoption at oil fields having dense underground piping.

In case of individual scheme, one or several adjacent wells separated by at most 200 m from each other are protected by a single C(S)PU. An individual separated casing CP scheme (Fig. 2.5) is implemented by electrically disconnecting a flow line or a distribution water line from the string to be protected, using an electrically insulating gasket installed at the well head. This scheme is used, if FL/DWL has already been protected electrochemically, i. e., has a cathodic or sacrificial protection.

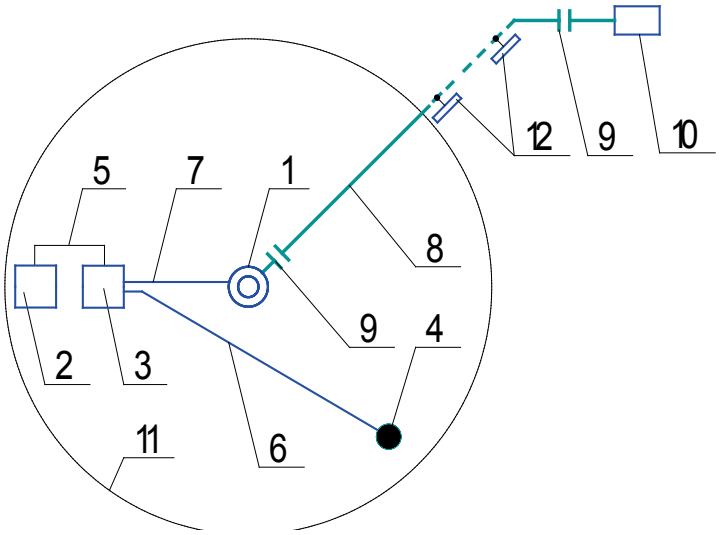

Fig. 2.5. Individual well casing cathodic protection scheme:
1 – well; 2 – package transformer substation; 3 – CPS; 4 – AB;
5 – power line 220 V; 6 – anodic drainage cable; 7 – cathodic drainage cable;
8 – flow line (distribution water line); 9 – EIG;10 – GMS (CPS);
11 – well boundary; 12 – sacrificial protection unit FL (DWL)

An individual shared CP scheme of a casing and FL (DWL) is implemented (Fig. 2.6) without installing an EIG at well heads. In this scheme, the EIG is installed at the other end of the FL (DWL). The shared cathodic protection of a casing is used where FL (DWL) does not have its own ECP.

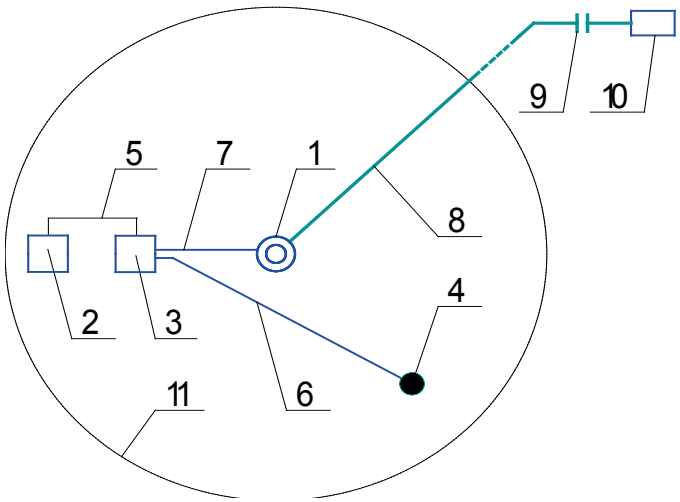

Fig. 2.6. Shared cathodic protection scheme of a casing and FL (DWL): 1 – well; 2 – package transformer substation; 3 – CPS; 4 – AB; 5 – power line 220 V; 6 – anodic drainage cable; 7 – cathodic drainage cable; 8 – flow line / distribution water line; 9 – EIG; 10 – GMS (CPS); 11 – well boundary

An individual CP scheme can be implemented using a cathodic protection assembly (CPA) embedded in the deep well pumping unit control panel of each well (Fig. 2.7). In this case, the CP system is simplified essentially, and the length of cable drainage lines is reduced.

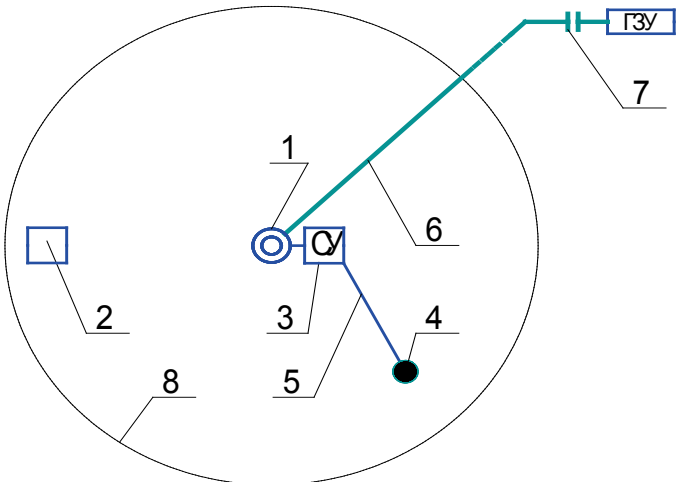

Fig. 2.7. Shared cathodic protection scheme of a production-well casing and FL, using a CPA: 1 – well; 2 – PTS; 3 – DWPU control panel with a CPA; 4 – AB; 5 – anodic drainage cable; 6 – flow line; 7 – EIG; 8 – well boundary

A cluster cathodic protection scheme is used where production wellheads are arranged in clusters. For this scheme, if all the wells in a cluster are similar in design, the casings are interconnected via a steel bus welded on them and having the section of at least 300 $mm^{2.}$ to be protected as a single object. To evenly distribute the protective current among the

strings, it is recommended to use several ABs distributed along the cluster perimeter so that its casings do not screen each other.

If there are different-type wells within a cluster, then they are divided into groups by their designs, and then each group is protected as a single object. The groups should be protected by separate C(S)PUs. In case of the cluster protection scheme, FLs are not disconnected electrically from the casings to be protected, i. e., they are involved into the shared protection. EIGs are installed on the collection header. Casings within a cluster can also be protected according to the individual shared scheme, using CPAs embedded in the deep-well pumping unit control panel of the wells. Decision between the cluster and the individual CP schemes of the cluster wells is made based on a feasibility study.

Independent on the scheme chosen, the CP system must ensure supplying the precomputed protective current to each casing and exclude harmful effects provided by stray currents upon the neighboring underground structures.

If there is at least one well subject to or having CP in the cluster, then all the wells in the cluster must be protected, whether they need it or not. Cathodic protection is also obligatory for any well with the expected service life of at least 10 years, located within the radius of at most 100 m from a cathode-protected well or cluster, whether it needs CP or not.

2.2. Determination of Necessity and Priority for the Cathodic Protection of Oil-Well Casings

The necessity to provide the cathodic protection of new wells is determined considering the identified need for and efficiency of the cathodic protection of the existing wells of a similar design, operating in similar hydrogeologic conditions [10].

2.3. Methods of Choosing Wells for Cathodic Protection

Wells for introducing cathodic protection or for repair-and-renewal operations are selected, based on comparing some parameters characterizing their development status, service life, and general status [10].

For each parameters, there should be found the value of function μ_i (membership function) that ranges from 0.1 through 0.9 and, in each case,

has a form determined by the physical significance of the parameter and by the action type (cathodic protection or repair-and-renewal operations). From the values of μ_i for the methods being compared by the maximum value of the minimums ($max\mu_{min}$), cathodic protection or repair-and-renewal operations are selected for a given well. For example, if the values of μ_{min} for CP and WO are 0.25 and 0.15. respectively, then CP is chosen for this well, since the minimum value of μ_i for cathodic protection is higher than for WO. If the minimum values of μ_i, obtained for both methods are equal to 0.1 or less, then both methods are considered inefficient for a given well. Then other, more thoroughgoing actions must be planned, such as drilling a new well, replacing the string followed by completely cementing it, running a smaller-diameter string followed by completely cementing the ring space around it, etc. In case of obtaining comparable (differing by at most 25 %) data on the minimums of individual functions, the products of all μ_i are found for CP and for WO. The highest value of the products, $max\,\Pi\,\mu_i$, indicates the action type preferable for a given well. For example, if the values of $\boldsymbol{\Pi\mu_i}$ for CP and WO are 0.35 and 0.6. respectively, then WO shall be chosen for this well.

When selecting wells for an action, the inputs are studied comprehensively, such as deposit development status, well design, statuses and numbers of repairs performed, service life for continued operation, and changes in the operation conditions.

We have defined seven parameters for production wells and eight parameters for injection wells, based on which the wells can be selected objectively to achieve the best effect:

1) Parameter X_1 – well category: production and injection (for production well, $X_1 = 1$; for injection well, $X_1 = 2$).

2) Parameter X_2 – well age since completing the drilling (in years).

3) Parameter X_3 – well service life for continued operation, counted starting from the year of introducing the protection (in years).

4) Parameter X_4 – status of the casing-string annuluses (presence of cement). $X_4 = 1$ – for the wells with the cement sheath level above the surface pipe / preceding casing shoe, $X_4 = 2$ – for the wells with the cement sheath level below the surface pipe shoe, and $X_4 = 3$ – for the wells with the cement level above the surface pipe shoe, but having some intervals of poor quality cementing.

5) Parameter X_5 – number of repairs aimed at re-sealing the production casing in the well by the time of implementing protective actions.

6) Parameter X_6 – diameter (in mm) of the production casing. This parameter is considered, because the diameter tolerance available allows prolonging the service life of wells by running smaller-diameter casings.

7) Parameter X_7 – wall capacity. For production wells, the current capacity value is defined for pipeline oil (without water – t/day). For an injection well, this parameter is equal to the current value of injectability – m^3/day.

8) Parameter X_8 – the ETL length to the nearest voltage source, the construction of which is necessary to power the CPS. Parameter X_8 (for injection wells only) is defined by the ETL kilometers (km). If the power supply is available on the well site, then we take $X_8 = 0$.

Selecting membership function μ_i. Formulas and parameters of functions μ_i are defined for each parameter X_i for all actions to be compared. When determining functions μ_I, the following reasons are considered:

a) With increasing parameter X_i favorable to a given action, function μ_I increases (within the range of 0.1-0.9);

b) With increasing X_i that is an adverse factor for a given action, μ_i decreases;

c) If using the method is technically or economically inefficient at certain parameters X_i, then μ_i takes the minimum value, i.e., $\mu_i = 0.1$;

d) If parameter X_i changing within a certain range provides an immaterial or unidentified effect, then μ_i = const within such range;

e) If the applicability or efficiency of the method leaps or changes abruptly at changing parameter X_i, then function μ_i is selected to be power or exponential; while, if these changes are gradual, the straight-line function is selected.

Membership function μ_i for CP and WO of production and injection wells, found for the environment of PJSC Tatneft, are presented in Appendix 2.

Priorities of connecting the selected wells to CP are determined by making a list ranking by the values of μ_{min}, in which the wells are arranged in the descending order of this value. If the values of μ_{min} for several wells turn out to be equal or close to each other (i.e., the difference does not exceed 10%), then the wells within that group shall be ranked by the value of $\boldsymbol{\Pi\mu_i}$: The larger this product is, the closer to the top of the list is the well [10].

Let us consider an example of selecting a well for cathodic protection. A production well is operated, and its age is 10 years. The planned service life for continued operation of the well is 20 years. Cement sheath level is

above the service pipe shoe. Over the operation time, two workovers of the well have been performed. Casing diameter is 146 mm. Oil production for pipeline oil is 5 t/day. The task is to decide whether using cathodic protection, in this case, will be reasonable or the workover of the well should be performed.

We register the well inputs through parameters X_i and for each parameter, using Appendix 2. and then select the relevant value of membership function μ_i for cathodic protection and for workover (Table 2.1).

Table 2.1

Values of Parameters X_i and Membership Functions μ_i

X_1	X_2	X_3	X_4	X_5	X_6	X_7
1	10 years	20 years	1	2	146 mm	5 t/day
μ_1	μ_2	μ_3	μ_4	μ_5	μ_6	μ_7
Values of μ_i for cathodic protection						
0.9	0.9	0.9	0.75	0.368	0.9	0.9
Values of μ_i for workover						
0.9	0.9	0.9	0.9	0.5	0.9	0.1

The highest values of the minimums for the two actions being compared were 0.368 (CP) and 0.1 (WO). In this case, cathodic protection is chosen for the well.

2.4. Constructing the Cathodic Protection System

CPS is mounted on a base made of pipes or welded structures near the package transformer substation (PTS) in accordance with a standard design solution or an individual design.

The recommended CPS mounting height is 1.4-1.7 m above the ground level. The station must be installed to a true vertical (allowable variation of at most 2°). Wire/cable holes in the CPS casing must be fitted with insulating bushes. Cable ends to be introduced into the CPS shall be protected against mechanical damages with pipes or ducts, the bottom part of which is deepened into the ground to 0.3-0.4 m. Where the CPS is mounted on a special base/foundation, then its casing shall be earthed in the common ground grid in accordance with the requirements of the Electrical Installation Regulations.

CPS is connected to the AC network using an individual automatic switch via cable AVRB 2×4 mm^2 or a similar one.

Cables are connected to the oil-well casing, anode bed, and cathodic protection station. A cathodic drainage cable from the CPS to the well casing is connected using a contact plate welded to the casing. The contact plate represents an L-shaped strip 25 mm wide and 4 mm thick, with cadmium coating and flanges 50 and 30 mm long. The plate is welded to the casing with its longer flange, while in the shorter flange a hole is drilled with the diameter of 10.5 mm for the M10 fixing bolt. It is allowed to connect the cathodic drainage cable to the pumping unit frame or to the chain transmission of the deep-well pumping unit, using the contact plate welded to it.

When using as a protective current source the cathodic protection unit built in the control station of the deep-well pumping unit, the cathode lead from the cathodic protection block shall be connected to the control station casing (Fig. 2.8 and 2.9) [10].

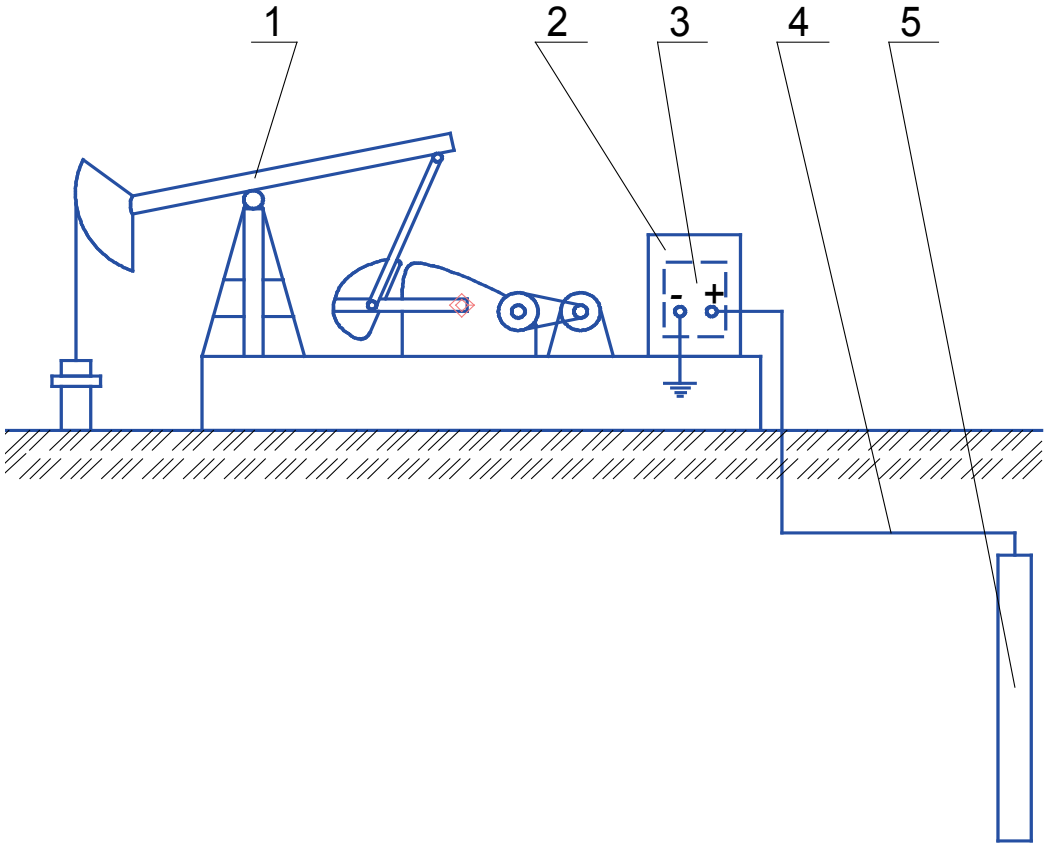

Fig. 2.8. Cathodic protection scheme for a production well casing using the cathodic protection block of the control station of a sucker-rod pumping unit: 1 – beam unit; 2 – control station; 3 – cathodic protection station; 4 – anode drainage cable; 5 – anode bed

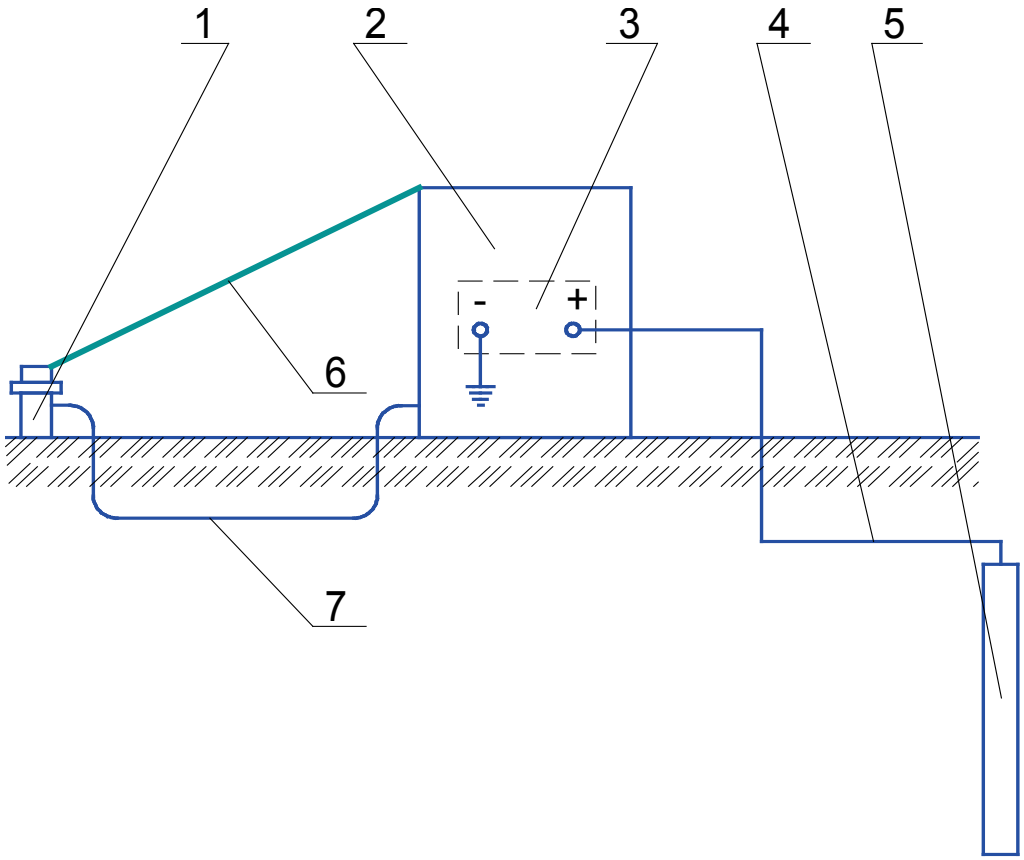

Fig. 2.9. CP scheme of a production well casing, using the cathodic protection block of the control station of a submersible centrifugal pump system: 1 – well; 2 – control station; 3 – cathodic protection block; 4 – anode drainage cable; 5 – anode bed; 6 – electrical motor power cable; 7 – electrical connection between the control station casing and the well casing

Chapter Review

1. Cathodic protection principle and components.
2. Oil-well casing cathodic protection schemes.
3. Algorithm of selecting the wells for using cathodic protection.

Chapter 3. CATHODIC PROTECTION ENGINEERING

3.1. Methods of Cathodic Protection Engineering [10]

Parameters of the cathodic protection of well casings depend on well designs. Therefore, all the deposit wells intended for cathodic protection are grouped by this parameter. The mean characteristics of the wells in a group are used in engineering the cathodic protection for each group.

The inputs for cathodic protection engineering are:

a) Ion and gas compositions and the pH values of produced water;

b) Distribution of the specific electric resistance of rocks along the well depths;

c) Distribution of thicknesses, H_i, and specific electric resistances, ρ_i, surface soils (down to the depth of 50 m);

d) Mean values of the diameters, wall thicknesses, and lengths of well casings;

e) Top of the cement in the borehole annulus of the wells;

f) Length, diameter, wall thickness, burial depth, and outer insulating coating resistance of the flowline or a distribution water duct of the wells; and

g) Topographical survey of above- and underground structures located within a radius of at least 200 m from the well or the cluster of wells to be protected.

Cathodic protection engineering follows some experimental works, as a result of which the following primary materials are obtained for each group of wells:

a) Stationary cathodic polarization curves “current density – cathodic polarization value” of pipe steel for the most aggressive stratal water of the well logs; and

b) Curves of distributing the voltage drops on a production string along the well depth, taken with a two-contact probe for the most typically designed wells in each group during the test cathodic protection at three values of protective current: 5. 10. and 20 A.

The main parameters of cathodic protection are defined as follows:

1. Stationary cathodic polarization curves $\boldsymbol{\Delta\phi = \Delta\phi(j)}$ are taken.

Polarization curves of the pipe steel in stratal water are taken in a water-proof cell using Luggin-Haber capillary and an auxiliary anodic electrode made of carbon steel. Before starting the polarization, a working

(cathode-polarized) pipe-steel electrode is held in the stratal water under research within 10 days in order to obtain sulfides on it and to establish a stationary potential. Electrochemical cell for taking the curves, having the volume of at least 2 l, is filled completely (without the gas cap) with natural or artificial stratal water under research. When using artificial stratal water model, before introducing any aggressive gases, it is carefully de-aerated by bubbling a pure inert gas, such as helium, argon, hydrogen, or nitrogen. If the temperature of the stratum within the interval under research differs from room temperature by over 10°, then the tests are made by dipping the electrochemical cell in a constant-temperature bath.

Stationary cathodic polarization curves are taken with registering the stationary values of the electrode potential at different values of the polarizing current density. The stationary value of potential is found by measuring the potential every polarization hour on the first day, and then the measurements are performed less frequently, such as two times a day. Polarization duration at each current density value must be at least two days. The recommended values of the current densities to be defined at the hydrogen-sulfide corrosion: 5. 20. 50. and 100 mA/m^2. Only one value of current density is imposed on one working electrode.

The polarization curve obtained is approximated by a possibly simpler analytical dependence:

$$\Delta\phi = \Delta\phi\ (j), \tag{3.1}$$

where $\Delta\varphi = \varphi - \varphi_c$, V; φ is electrode potential at cathodic polarization, V; and ϕ_c is the stationary potential before imposing the current, V.

2. Found is the dependence of the current density in the controlled string interval on the polarizing current: $\boldsymbol{j = j(\bar{I}_o)}$.

This dependence is found experimentally by taking the curves of voltage drop on the well casing by a two-contact probe, at least at three values of protective current $\bar{I}_o$: 5. 10. and 20 A and with the exposure time at each current value of at least 24 h (in Fig. 3.1. this is exemplified by showing the curves of voltage drops at the currents of 10 and 20 A, obtained in Jalilneft).

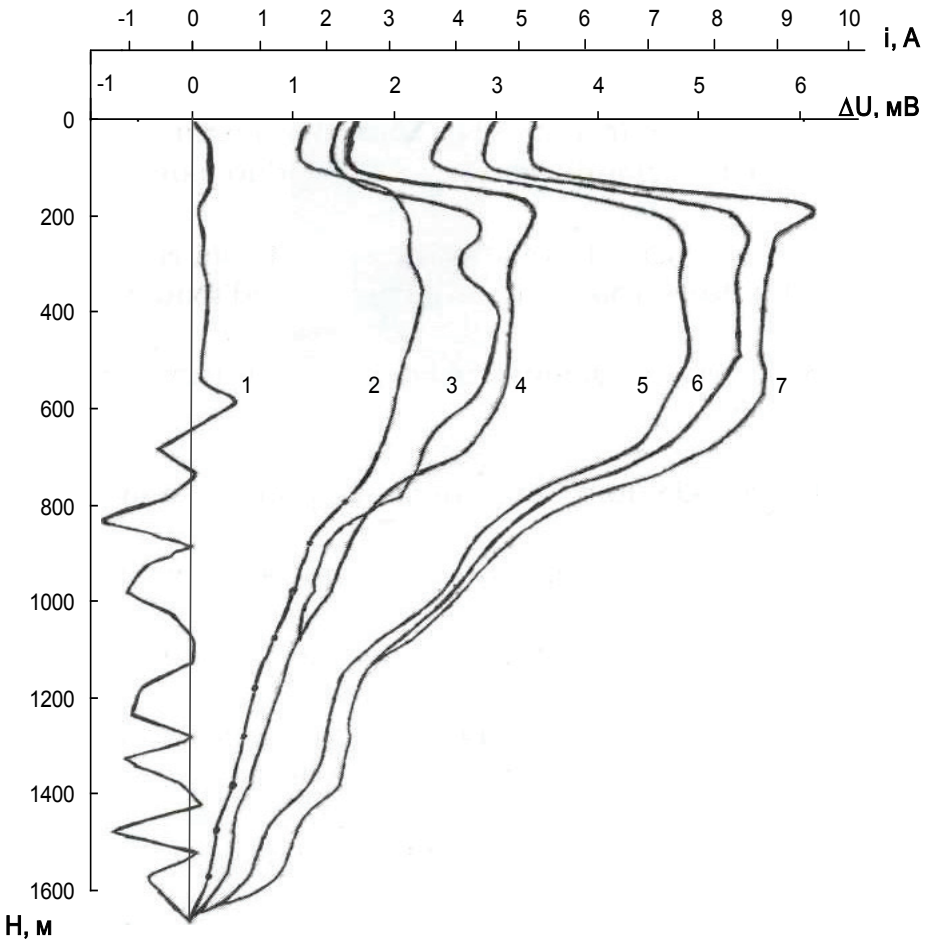

Fig. 3.1. Curves of distributing the voltage drops on a well casing (ΔU) and the current in it (i) along the well depth: Voltage drop and current: 1 – in a natural condition; 2-4 – at the polarization time of 0. 6. and 24 h respectively, with the current of 10 A; 5-7 – at the polarization time of 0. 6. and 24 h, respectively, with the current of 20 A

Voltage drops at the casing is measured with a two-contact probe in every 50 m within the interval under research in 30 s upon stopping the probe. To measure voltage drops, measuring tools are used, such as milli- and microvoltmeters, the input resistance of which must be at least 1 MOhm. Current density on the surface of the well casing, according to the data obtained by measuring the voltage with a two-contact probe, is calculated by the following formula:

$$j = \frac{\Delta U_1 - \Delta U_2}{\pi r_k D_k l_p \Delta L}, \text{ A/m}^2. \quad (3.2)$$

where ΔU_1 and ΔU_2 are well-casing voltage drops measured at two points, between which the leakage current density is found, V; r_k – input resistance of the well casing, Ohm/m; D_k – outer diameter of the well casing, m; l_p – distance between the probe contacts (normally, l_p = 7.5 m), m; and ΔL – distance between measuring points ΔU_1 and ΔU_2 , m.

Using the current density values corresponding with different values of polarizing current, the dependence of $j = j(\bar{I}_o)$ is found, approximating it by a possibly simple analytical formula (this dependence can be approximately taken as linearly proportional).

In grounds that are layer-by-layer inhomogeneous by their specific electrical resistance, the current density can be found in any interval of the production casing, using the approximated analytical formula:

$$j_i = \frac{\bar{I}_o c\square[\alpha_k(L_k - \bar{Z}_i)]}{\pi D_k \rho_i \sum_{i=1}^{n} H_i c\square[\alpha_k(L_k - \bar{Z}_i)]/\rho_i}, \text{ A/m}^2. \quad (3.3)$$

where α_k is leakage coefficient, m^{-1}; L_K is the production casing length, m; $\bar{I}_o$ is the polarizing current, A; $\bar{Z}_i$ is the coordinate of the midpoint of the i^{th} layer, m; ρ_i is the specific resistance, Ohm·m; H_i is the thickness of the i^{th} layer, m; and n is the number of layers along the well casing, within which ρ is roughly constant.

To calculate by this formula, the curve is used that shows distributing the rock specific electrical resistance along the well depth. The total well profile by the value of this parameter is divided into intervals (layers), the thickness of the layer under research being not to exceed 100 m.

The most aggressive (in terms of the contents of aggressive components in stratal water or the confinement of failures) interval is chosen as the controlled interval of the production casing. Then we find the dependence of the casing cathodic polarization in the controlled interval of the casing on the polarizing current intensity, $\bar{I}_o$, by substituting the value of the current density, $j = j(\bar{I}_o)$, for the interval under research into function $\Delta\phi = \Delta\phi(j)$ obtained in the stratal water of the same interval, i.e.:

$$\Delta\phi = \Delta\phi(j) = \Delta\phi[j(\bar{I}_o)] = \Delta\phi_1(\bar{I}_o), \text{ V}. \quad (3.4)$$

The value of cathodic polarization is calculated depending on the predefined degree of well casings protection in the controlled interval of string $P = 0.7 \div 0.8$ by formula:

$$\Delta\phi_k = 0.08\, lg(1 - P), \text{ V}. \quad (3.5)$$

The casing protection current intensity, $\bar{I}_o$, is found that ensures the predefined protection degree in the controlled interval by substituting the values of $\Delta\varphi_k$ in function $\Delta\phi = \Delta\phi_1(\bar{I}_o)$, i.e., $\bar{I}_o = \bar{I}_o\ (\Delta\phi_k)$.

In experimentally finding the dependence of $j = j(\bar{I}_o)$, the anode bed is placed at a certain test distance from the wellhead, ℓ_a^e, selected within 50-100 m, while the actual distances of ABs from wellhead ℓ_a, produced by the CP project on the wells, usually differ from ℓ_a^e. To eliminate the dependence of the found protective current value on ℓ_a^e, a correction factor is introduced:

$$I_o = \bar{I}_o / K_a(\ell_a^e), \quad (3.6)$$

where $K_a(\ell_a^e)$ is a factor considering the influence of the AB distance upon the protective current value; I_0 is the protective current corresponding with l_a=∞. Factor considering the influence of the AB-well distance on the protective current value is calculated for a vertical AB by empirical formula

$$K_a = 0.23 L_1^{0.31} \ell_a^{-0.1}, \quad (3.7)$$

where L_1 is the well depth, m, at which the casing protection degree is controlled.

The optimal distance between AB and the wellhead is selected within the following ranges for individual and cluster schemes:

$$l_a = 30 \div 50 \text{ m at } L_1 = 600 \div 1.200 \text{ m} \quad (3.8)$$
$$l_a = 50 \div 80 \text{ m at } L_1 = 1.200 \text{ m}.$$

Computations that are ultimately aimed at finding the production string protection current value, $I_{0.}$ were performed by TatNIPIneft for the standard conditions of Romashkino Oil Deposit. The following protective current values were obtained from the above computations:

– For the wells with the cement tops below the surface pipe shoe, I_0 = 8 A; and

– For the wells with the cement tops above the surface pipe shoe, I_0 = 6 A.

These protective currents are true for all the wells of the above deposits with the depths of 1.600÷1.900 m. For the wells of another depth L, the protective current value, $I_{0.}$ is recommended to be adjusted by formula

$$I_0(L) = \boldsymbol{I_o L / 1,750}. \quad (3.9)$$

The CPS current intensity I for protecting one well, considering the design value of l_a and spending a part of current on protecting an FL or a DWL (in case of combined protection), shall be found by formula:

$$I = K_m K_a I_o, \text{ A}, \quad (3.10)$$

where K_m is the factor considering the FL/DWL CPS current consumption.

$$K_m = \frac{r_k \alpha_m ct\square(\alpha_k L_k)}{r_m \alpha_k ct\square(\alpha_m L_m)} + 1. \quad (3.11)$$

where L_k is the length of the well casing, m; r_m is the longitudinal resistance of the flow line, Ohm/m; α_T is the flow line leakage factor, m^{-1}; L_m is flow line length, m; $cth(\alpha L)$ is the hyperbolic cotangent of argument αL.

At the separate CP scheme, as well as in case of external polymer insulation of FL (DWL) at the combined protection of $K_m = 1$.

The leakage factors of the casing and of the flow line are found by formula

$$\alpha = \sqrt{r/R},\ \text{m}^{-1}. \quad (3.12)$$

where r and R are the longitudinal and transitional resistances of an extended underground structure, Ohm/m.

The longitudinal resistance of an extended structure can be found by formula

$$r = 0.32\frac{\rho_{st}}{\delta(D-\delta)},\ \text{Ohm/m}, \quad (3.13)$$

where ρ_{st} is the specific resistance of pipe steel, ρ_{st} = 0.24 Ohm·mm^2/m; δ is the pipe wall thickness, m; and D is the outer diameter of pipes, m.

Transitional resistance of an FL (DWL) is found by solving the transcendent equation

$$R_m = \frac{R_u}{\pi D_m} + \frac{\rho_g}{2\pi} ln \frac{R_m}{D_m \square_m r_m},\ \text{Ohm·m}, \quad (3.14)$$

where R_u is the resistance of external insulation, Ohm·m^2; D_m is diameter, m; h_m is the occurrence depth, m; ρ_g– is the mean specific ground resistance in the area of an FL (DWL), Ohm·m.

Transitional resistance of a well casing for the standard conditions of Romashkino Oil Deposit is taken as R_k = 150 Ohm·m. In other cases, the transitional resistance of a casing is found by solving transcendental equation:

$$R_k = \frac{\rho_n}{2\pi} ln \frac{2}{D_k\sqrt{r_k/R_k}},\ \text{Ohm·m}, \quad (3.15)$$

where ρ_n is the average specific resistance of strata in the well profile, Ohm·m.

$$\rho_n = \frac{L_k}{\sum_{i=1}^{n} H_i/\rho_i},\ \text{Ohm·m}, \quad (3.16)$$

where ρ_i is the specific electrical resistance, Ohm·m; H_i is the thickness of the i^{th} stratum, m; and n is the number of strata along the well casing length, within which ρ is approximately constant.

Let us consider an example of finding the protective current of a well casing

1. Inputs.

1.1. Borehole logs are of the same type for all the production wells of the deposit. We group the wells by their production string annular cement levels: Group 1 – wells where cement has not reached the preceding

string (in our case, conductor) shoe; Group 2 – wells where cement is above the conductor shoe. This group also includes the wells having the low-quality cementing sections longer than 5 m within the range of aggressive water-bearing strata. We perform computations for Group 1.

Intensive inter-stratal water flows were not detected in the borehole annuli, i.e., well casing corrosion takes place in static conditions.

1.2. Distribution of apparent strata resistivity in a generalized well log is shown in Table 3.1.

Table 3.1

Distribution of Apparent Strata Resistivity in a Generalized Well Log

Depth ranges, m	0 – 200	200 – 270	270 – 670	670 – 710	710 – 800	800 – 1.020	1.020 – 1.220	1.220– 1.320	1.320 – 1.580	1.580 – 1.700
Range #	1	2	3	4	5	6	7	8	9	10
$\rho_i, Ohm \cdot m$	30	470	324	130	45	202	90	330	141	60
Layer thickness H_i, m	200	70	400	40	90	220	200	100	260	120

1.3. Average specific resistivity of the upper ground layers at a deposit (down to 10 m), ρ_i = 40 Ohm□m.

1.4. Casings in the group have the following average characteristics: Length L_k = 1.700 m; diameter D_K = 0.146 m; and wall thickness δ_k = 8 mm.

1.5. Flow lines have the following average characteristics: Length L_m = 800 m; diameter D_m = 0.1 m, wall thickness δ_m = 5 mm, external insulation resistance R_u = 20 Ohm·m; and depth of laying h_m = 1 m.

1.6. In the generalized hydrogeologic section of the wells, two aggressive water-bearing horizons are notable: One horizon with the stratum water hydrogen sulfide concentration of 100 mg/l within the range of 600-700 m; the other one – with the H_2S concentration of 300 mg/l within the range of 700-820 m.

1.7. The stationary polarization cathodic curves obtained for stratum water of the two aggressive horizons are shown in Fig. 3.2. Without such curves, in case of hydrogen sulfide corrosion, the curves shown in Fig. 3.3 can be used as a first approximation.

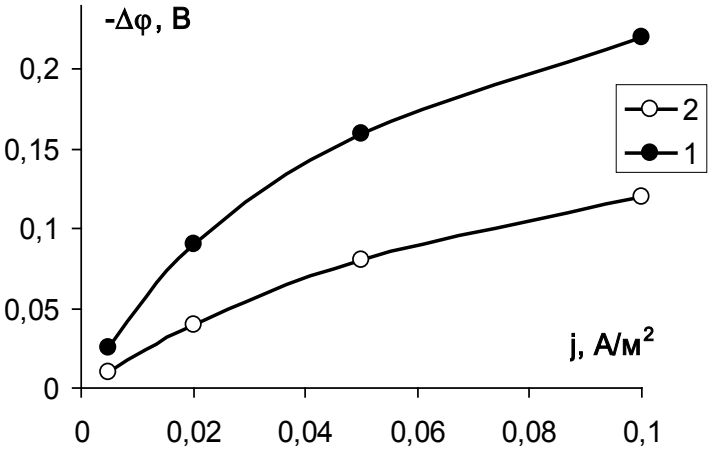

Fig. 3.2. Stationary polarization cathodic curves for pipeline steel in the stratum water of the first (curve 1) and the second (curve 2) aggressive water-bearing horizons

1.8. We obtained the curves of distributing the voltage drops at the production string, taken using a two-contact probe at the protection currents of 10 and 20 A (distance between the well head and the anode bed l_a^e= 100 m; the value of the voltage drop at any string point is approximately proportional to the polarizing current intensity; therefore, we did not take the curve at the current of 5 A). The curves are shown in Fig. 3.1.

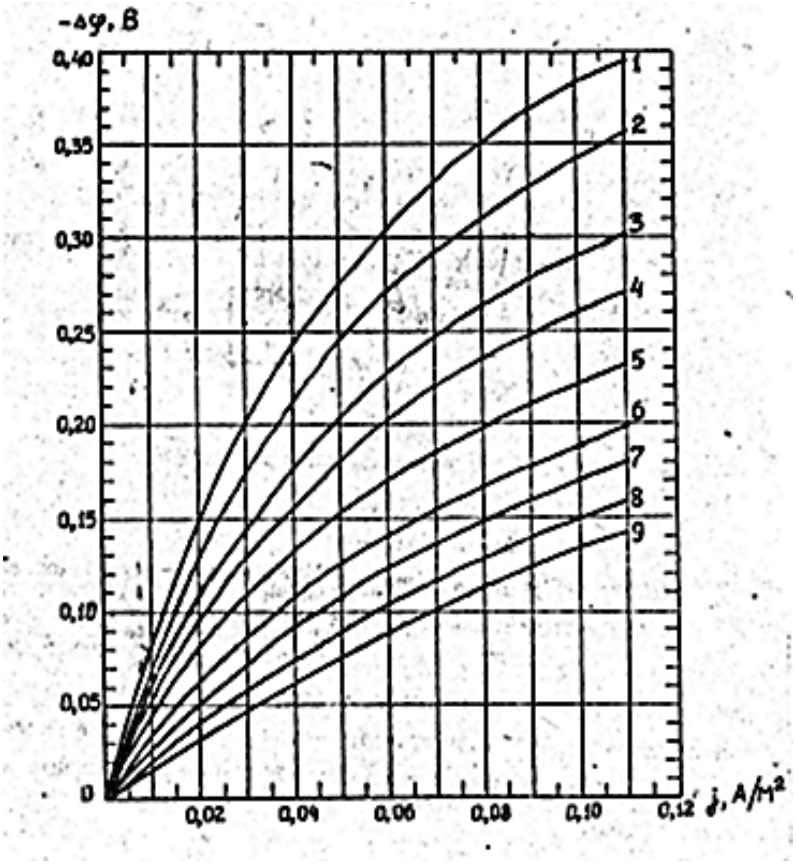

Fig. 3.3. Stationary polarization cathodic curves of pipeline steel in hydrogen sulfide-containing stratum water (t = 15-35° C). The curves correspond with the H_2S concentration in mg/l: 1 – 0÷5; 2 – 5÷30; 3 – 30÷60; 4 – 60÷80; 5 – 80÷120; 6 – 120÷170; 7 – 170÷250; 8 – 250÷350; 9 – 350÷450

2. Finding the functional dependencies among the cathodic protection parameters.

2.1. We compute the average longitudinal resistances of casings and flow lines by formula (3.13):

$$r_k = 0.32\frac{0.24}{8(146-8)} = 69.6 \cdot 10^{-6} O\square m/m\,;$$
$$r_m = 0.32\frac{0.24}{5(100-5)} = 162 \cdot 10^{-6} O\square m/m\,.$$

2.2. Then we calculate the current densities within the range of the first aggressive horizon (600-700 m) by formula (3.2) on the values of voltage drops from curves 4 and 7 (Fig. 3.1):

– At the current of 10 A

$$j(10) = \frac{0.00305 - 0.00267}{3.14 \cdot 69.6 \cdot 10^{-6} \cdot 0.146 \cdot 7.5 \cdot 100} = 0.016\frac{A}{m^2}\,;$$

– At the current of 20 A

$$j(20) = \frac{0.0056 - 0.00508}{3.14 \cdot 69.6 \cdot 10^{-6} \cdot 0.146 \cdot 7.5 \cdot 100} = 0.022\frac{A}{m^2}\,.$$

2.3. We calculate the current densities within the range of the second aggressive horizon (700-820 m):

$$\bar{j}(10) = \frac{0.00267 - 0.00180}{3.14 \cdot 69.6 \cdot 10^{-6} \cdot 0.146 \cdot 7.5 \cdot 120} = 0.030\frac{A}{m^2}\,;$$

$$\bar{j}(20) = \frac{0.00508 - 0.0036}{3.14 \cdot 69.6 \cdot 10^{-6} \cdot 0.146 \cdot 7.5 \cdot 120} = 0.052\frac{A}{m^2}.$$

2.4. Since for the current equaling to 0 the current densities are 0 within all the ranges, we can draw straight lines by three points to find the dependence of the current density on the polarizing current intensity for both ranges:

– For the first range: $\bar{j}(I_0) = 0.00125 \cdot \bar{I_0}$;

– For the second range: $\bar{j}(I_0) = 0.00243 \cdot \bar{I_0}$.

2.5. Then we use formula (3.12) to find the leakage coefficients of casings and flow lines:

$$\alpha_k = \sqrt{69.6 \cdot 10^{-6}/151} = 0.68 \cdot 10^{-3}, m^{-1}\,;$$
$$\alpha_m = \sqrt{162 \cdot 10^{-6}/167} = 0.97 \cdot 10^{-3}, m^{-1}.$$

2.6. We compute the sum in formula (3.3), using the data from Table 3.1:

$$\sum_{i=1}^{10} H_i c\square\left[0.68\cdot 10^{-3}(1.700-\overline{Z_i})\right]/\rho_i$$

$$=\frac{200c\square[0.68\cdot 10^{-3}(1.700-100)]}{30}+$$

$$+\frac{70c\square[0.68\cdot 10^{-3}(1.700-235)]}{470}+\frac{400c\square[0.68\cdot 10^{-3}(1.700-470)]}{324}$$

$$+$$

$$+\frac{40c\square[0.68\cdot 10^{-3}(1.700-690)]}{130}+\frac{90c\square[0.68\cdot 10^{-3}(1.700-755)]}{45}$$

$$+$$

$$+\frac{220c\square[0.68\cdot 10^{-3}(1.700-910)]}{202}$$

$$+\frac{200c\square[0.68\cdot 10^{-3}(1.700-1.120)]}{90}+$$

$$+\frac{100c\square[0.68\cdot 10^{-3}(1.700-1.270)]}{330}$$

$$+\frac{260c\square[0.68\cdot 10^{-3}(1.700-1.450)]}{141}+$$

$$+\frac{120c\square[0.68\cdot 10^{-3}(1.700-1.640)]}{60}=23.6.$$

2.7. We calculate the current densities by formula (3.3) within ranges No. 4. 5. and 6. within which the aggressive horizons are located (at $I_0 = 8$ A):

$$j_4 = I_0\frac{c\square[0.68\cdot 10^{-3}(1.700-690)]}{3.14\cdot 0.146\cdot 130\cdot 23.6}=0.009\cdot I_0=0.009\cdot 8$$
$$=0.072\ \text{A/m}^2;$$

$$j_5 = I_0\frac{c\square[0.68\cdot 10^{-3}(1.700-755)]}{3.14\cdot 0.146\cdot 45\cdot 23.6}=0.0025\cdot I_0=0.0025\cdot 8$$
$$=0.02\ \text{A/m}^2;$$

$$j_6 = I_0\frac{c\square[0.68\cdot 10^{-3}(1.700-910)]}{3.14\cdot 0.146\cdot 202\cdot 23.6}=0.00053\cdot I_0=0.00053\cdot 8$$
$$=0.004\ A/m^2.$$

2.8. Since the first aggressive horizon (600-700 m) is completely located within the fourth range, the for it

$$j(I_0)=0.072A/m^2.$$

2.9. The second aggressive horizon (700-820 m) is located within the fifth and sixth ranges; therefore, we find the mean-weight value of the current density for it:

$$j(I_0) = \frac{0.0025 \cdot 100 + 0.00053 \cdot 20}{120} \cdot I_0 = 0.0022 \cdot I_0 = 0.0022 \cdot 8 = 0.0176 \text{ A/m}^2.$$

2.10. In the cathodic protection practice, the casing protection current does not usually go beyond the limit of $I_0 = 0 \div 30$ A, the relevant currents of which in the first and the second horizons are 0-0.04 and 0-0.07 A/m^2. Within this range, the polarization curves shown in Fig. 3.2 can be approximated with the following functions:

– For the first curve, $\Delta\varphi = -1.3 \cdot j^{0.7}$; and

– For the second curve, $\Delta\varphi = -1.8 \cdot j$.

2.11. We find the dependencies of polarization in the horizons under research on the polarization current intensity, substituting the values of current densities from 2.4 into the expressions in 2.10:

– For the first horizon, $\Delta\varphi = -1.3 \cdot (0.00125 \cdot \bar{I}_0)^{0.7} = -0.012 \cdot \bar{I}_0^{0.7}$; and

– For the second horizon, $\Delta\varphi = -1.8 \cdot (0.00245 \cdot \bar{I}_0)^{0.7} = -0.0044 \cdot \bar{I}_0$.

2.12. At the casing protection rate of 0.8 within the string range under control, the value of cathodic polarization [formula (3.5)] is

$$\Delta\varphi_c = 0.08 \cdot \lg(1-P) = -0.056 \text{ V}.$$

2.13. We find the coefficient considering the influence of the AB distance from the well upon the protective current value at $L_1 = 760$ m (coordinate of the middle of the most aggressive horizon (700+820) / 2 = 760 m) and $l_a = 35$ m (for a vertical AB, expression 3.7 is true)

$$K_a = 0.23 \cdot 760^{0.31} \cdot \ell_a^{-0.1} = 1.8 \cdot 35^{-0.1} = 1.26.$$

2.14. We calculate the mean specific resistivity of the well log formation by formula (3.16)

$$\rho_n = \frac{1.700}{\sum_1^{10} H_\iota/\rho_\iota} = \frac{1.700}{200/30 + 70/470 + 400/324 + 40/130 + 90/45 + 220/202 + 200/90 + } =$$

$$= \frac{}{+100/330 + 260/141 + 120/60} = 95 \text{ Ohm} \cdot \text{m}.$$

2.15. We compute the mean transitional resistivity of well casings by formula (3.15) using the method of sequential approximations (on the first approximation, we take $R_c = \rho_n = 95$ Ohm·m):

$$R_c = \frac{95}{2 \cdot 3.14} ln \frac{2}{0.146\sqrt{69.6 \cdot 10^{-6}/95}} = 150 \ \ \text{Ohm} \cdot \text{m} \ .$$

On the second approximation, we substitute the value obtained:

$$R_c = \frac{95}{2 \cdot 3.14} ln \frac{2}{0.146\sqrt{69.6 \cdot 10^{-6}/150}} = 151 \ \ \text{Ohm} \cdot \text{m} \ .$$

Since the latter value does not considerably differ from the former one, the computations can be finished.

2.16. Similarly, we compute the mean transitional resistivity of flow lines by formula (3.14), taking on the first approximation $R_m = R_u + \rho_g = 20 + 40 = 60$ Ohm·m;

$$R_m = \frac{20}{3.14 \cdot 0.1} + \frac{40}{2 \cdot 3.14} \cdot ln \frac{60 \cdot 10^6}{0.1 \cdot 1 \cdot 162} = 161 \ O\square m \cdot m \, ;$$

$$R_m = \frac{20}{3.14 \cdot 0.1} + \frac{40}{2 \cdot 3.14} ln \frac{161 \cdot 10^6}{0.1 \cdot 1 \cdot 162} = 166 \ O\square m \cdot m \, ;$$

$$R_m = \frac{20}{3.14 \cdot 0.1} + \frac{40}{2 \cdot 3.14} ln \frac{166 \cdot 10^6}{0.1 \cdot 1 \cdot 162} = 167 \ O\square m \cdot m.$$

2.17. Then we compute the coefficient that considers the current consumed by CPS FLs or DWLs by formula (3.11):

$$K_m = \frac{69.6 \cdot 10^{-6} \cdot 0.97 \cdot 10^{-3} ct\square (0.68 \cdot 10^{-3} \cdot 1.700)}{162 \cdot 10^{-6} \cdot 0.68 \cdot 10^{-3} ct\square (0.97 \cdot 10^{-3} \cdot 800)} + 1 = 1.486 \ .$$

3. Finding the optimal value of protective current. We find the CPS current intensity for protecting one well, Ic, considering the design value of l_a and the consumption of a part of current for protecting the FL or DWL (in case of joint protection) by formula (3.10):

$$I = 1.486 \cdot 1.26 \cdot 8 = 14.98 \ A \approx 15 \ A \, .$$

3.2. Anode Bed Engineering [10]

Anode bed type, i.e., vertical, horizontal, deep, or buried, is selected based on ground conditions, such as ground water level or the at-depth distribution of the ground resistivity, the availability of free sites within the area of the wells to be protected, and the proximity of the neighboring

underground structures that may be adversely affected by stray currents created by the AB.

For a dense underground pipework networks in the well area, it is recommended to use vertical ABs 20-50 m long, fitted with low-soluble (carbon and graphite or ferrosilite) electrodes. In case of protecting several wells using a single cathodic protection unit and where there is a high specific resistivity of surface ground and a low resistivity of deeper layers, it is reasonable to erect deep or buried ABs up to 100 m long. In a deep AB, the total computed length of electrodes is shorter than that of the wellbore by the ground freezing depth, i.e., by 2-3 m. In a buried AB, the wellbore depth is only determined by ground conditions or by the requirements regarding the elimination of harmful effects provided by stray currents, while the total length of electrodes is computed.

If there are no independent structures (FL/DWL of the well to be protected is not an independent structure) in the area of wells with a radius of less than 70 m and at a low ground water level (below 20-30 m), it is economically feasible to erect subsurface ABs (vertical, down to 10 m deep, horizontal, mixed).

The required total resistivity of the anode bed or of a circuit of anode beds is computed by formula

$$R_s^{tot} = \frac{U_m}{I_{tot} C_s} - R_{pr}, \text{ Ohm}, \quad (3.17)$$

where U_m means the maximum nominal voltage at the CPS outlet, V (specified in the CPS data sheet and chosen within the range of 24-48 V); C_s means the voltage storage coefficient, C_s is taken as 2; and I_{tot} means the total CPS current, A

$$I_{tot} = C_{in} \sum_{i=1}^{n} I_i, \quad (3.18)$$

where n means the number of wells protected by one C(S)PU; I_i is the C(S)PU current used to protect one well and computed by formula (3.10); R_{pr} means the resistivity of drainage cables, Ohm; and C_{in} means interference coefficient (for individual scheme, C_{in} = 1. while for clustering scheme, C_{in} = 1.2).

When erecting several ABs connected into one circuit, the required resistivity of one grounding protection is found from the following formula:

$$R'_{gr} = N_{gr} K_s R_{gr}^{tot}, \text{ Ohm}, \quad (3.19)$$

where N_{gr} means the number of grounding protections within the circuit; and K_{sh} means the shielding coefficient to be defined from Appendix 3.

Distance b between single grounding protections within circuit is selected by a design engineer, the minimal value of b having to be at least a half of the length of a single grounding protection within the circuit, i.e., $b \geq \ell/2$.

The resistivity of a single grounding protection installed vertically in the ground is computed by the following formula:

$$R_{gr} = \frac{\bar{\rho}_g}{2\pi\ell_e}\left(ln\frac{2\ell_e}{d} + 0.5\,ln\frac{4t_e+3\ell_e}{4t_e+\ell_e}\right), Ohm, \quad (3.20)$$

$$\ell_e = \ell - \ell_n; \quad (3.21)$$

$$t_e = t + \ell_n, \quad (3.22)$$

where $\bar{\rho}_g$ means the average specific ground resistivity around the anode bed, Ohm·m; l_e means the efficient (operating) length of the anode bed, m; l means the total length of the anode bed electrodes, m; d means the external diameter of the anode bed electrodes, m; t_e means the efficient burial of the anode bed, m; t means the designed burial of the anode bed (the distance from the ground surface to the upper end of the anode bed), m; to be taken as at least as deep as the soil frost depth, i.e., 1.8-2.0 m; and l_n means the length of the non-operating part of the anode bed, determined by lowering the level of the substance filling the bore pit in the process of operation. For vertical anode beds 20-40 m deep and at the ground water level of h_{gw} = 5÷15 m, the following values of l_n can be taken approximately:

l_n = 0 m – when using a solid free-flowing conductive filling (coke breeze) to fill the borehole;

l_n = 2 m – when using as a filler a centrally prepared mud solution thickened with gel powder;

l_n = 4 m – when using a gel-powder-thickened mud solution prepared while drilling the borehole; and

l_n = 6 m – when filling the borehole with a mud solution (without adding any gel powder).

For all filler types, $l_n \leq h_{gw}$ (for example, in case of filling the borehole with a mud solution at h_{gw} = 5 m, we take l_n = 5 m, while at h_{gw} = 10 m we take l_n = 6 m).

Resistivity of a single horizontal grounding protection is found by the following formula:

$$R_{gr} = \frac{\bar{\rho}_g}{2\pi\ell}\left(ln\frac{2\ell}{d} + ln\frac{\ell+\sqrt{\ell^2+16\square_e^2}}{4\square_e}\right), \text{Ohm}, \quad (3.23)$$

where h_e is the burial depth of the anode bed electrodes (distance from the ground surface to the electrode midpoint), m, to be taken as at least the ground frost depth.

In case of designing the anode bed electrodes in carbon (coke) filling, d is substituted with the filling diameter (the resistivity of the carbon filling itself can be neglected).

Formulas (3.19) – (3.23) are used to solve the inverse problem: By the required total resistivity R_{gr}^{tot}, the anode bed parameters are calculated, i.e., l and t, as well as their number, N_{gr}. In designing ABs, the following computing algorithm is recommended:

1) We primarily define N_{gr} =1. then K_e = 1 and $R_{gr}^{'} = R_{gr}^{tot}$.

2) Then we define l = 20 m and compute R_{gr} using formula (3.20) or (3.23).

3) If $R_{gr} < 1.2R_{gr}^{'}$ (*), then the defined values of N_{gr} and l are accepted.

4) If $R_{gr} > 1.2R_{gr}^{'}$, then we gradually increase l (at 20% intervals) to continue computing R_{gr}, until the condition is met (*).

5) If the condition (*) is not met at increasing l up to 50 m, then we take N_{gr} = 2.

6) Define the largest possible distance between two anode beds, b, considering the site plan within the radius of 30-50 m around the well.

7) Define l = 30 m, compute b / l, and define K_e from the table (if b / l is non-integral, then K_e shall be found by interpolating the values of K_e for the nearest two integers of b / l).

8) Compute $R_{gr}^{'}$ by formula 3.19.

9) Compute R_{gr} by formula (3.20) or (3.23); of the condition (*) is met, then the values of N_{gr} and l are accepted.

10) If the condition (*) is not met, then increase l up to 50 m and iterate computing $R_{gr}^{\prime}$ and R_{gr}, until the condition (*) is met.

Where such approximations lead to obtaining the values of N_{gr} and l, which are not acceptable for the local conditions, then select a higher voltage at the CPS output (U_m = 48-96 V) and repeat the computations.

Along with computing the anode bed by flowing resistance, the total mass of electrodes M (with the service life at least as long as that of the entire system) is computed by formula:

$$M = m_o \ell N_{gr}, \text{ kg}, \qquad (3.24)$$

where

$$m_o = \frac{I_{tot} T_{gr} q K_i}{\ell_e N_{gr} K_u}, \text{ kg}, \quad (3.25)$$

where m_0 means the required mass of 1 m of the running length of an electrode, kg/m; q means the anodic dissolution rate of the material of electrodes, kg/A·year (Appendix 4); T_{gr} means the design life of the anode be, years; K_u means the coefficient of using the mass of electrodes, to be taken as 0.75; K_i means the coefficient of the irregularity of current flowing along the anode bed length, to be taken as 1.5.

Should m_0 exceeds the actual mass of 1 m of the running length pf the electrodes used (for ferrosilide electrodes ZZhK-1500. GAZ-M, and graphitized electrodes EGT, it is 19.5. 22.9. and 7 kg/m, respectively), then we increase l (which leads to increasing l_e) and/or N_{gr}, until the necessary results are obtained (i.e., m_0 becomes less than or equal to the actual mass of 1 m of the running length of the electrodes used).

The required power at the CPS output is found by formula

$$N = I_{tot} U_m K_{pr}, \text{ W}, \quad (3.26)$$

where K_{pr} means the power reserve coefficient, to be taken as K_{pr}=1.5÷2.

The type of CPS is chosen by power and by its maximum rated output voltage.

To prevent the harmful effects provided by the cathodic protection currents on non-involved structures, it is reasonable to take technological measures, such as selecting the type and design of AB and keeping a safe distance between an AB and a non-involved structure. Safe distance between an AB and a non-involved structure, depending on the parameters of the cathodic protection system and on the type and dimensions of the AB at ρ_g ~ 20 Ohm·m, is selected by the curves shown in Figs. 3.4 and 3.5.

At the insulation resistivity R_u= 0 Ohm·m and the current of 10 A, safe distances are taken from the relevant curve for the current of 20 A. Linear resistance of the pipeline insulation (Ohm·m) is found by dividing the surface resistance (Ohm·m^2) by πD_m.

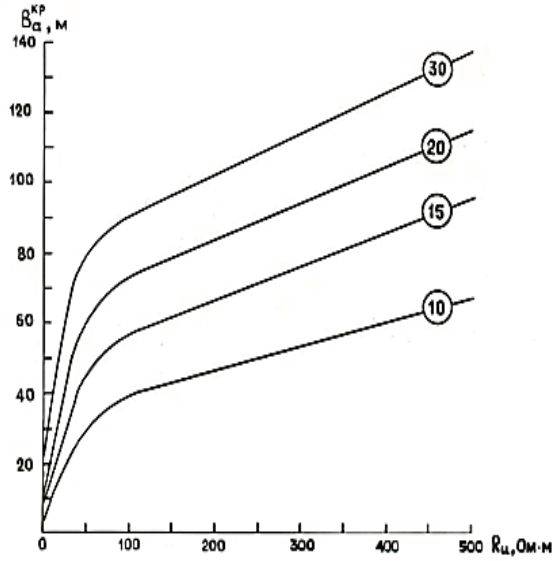

Fig. 3.4. Safe distances for vertical ABs , depending on the AB length, l, current (shown in circles) and the linear resistance of the pipeline insulation R_u: 1 – R_u=0; 2 – R_u=50 Ohm□m; 3 – R_u= 500 Ohm□m

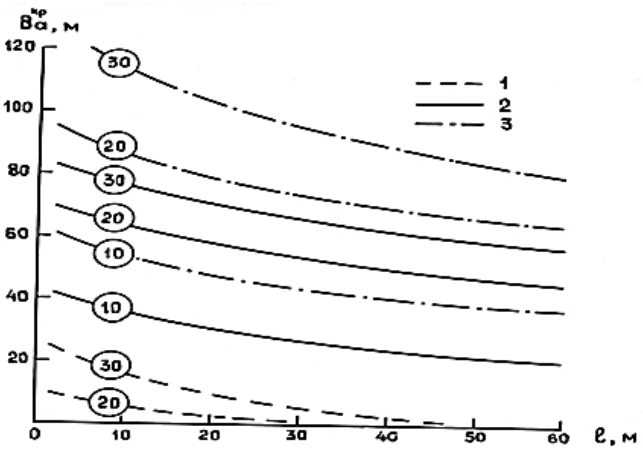

Fig. 3.5. Safe distances for horizontal ABs, depending on current (shown in circles) and the linear resistance of the pipeline insulation, R_u

The safe distance is counted from the midpoint of the horizontal anode bed to the nearest point of the pipeline and does not practically depend on the anode bed length or its attitude relative to the pipeline.

Let us consider exemplary computations of the parameters of a cluster cathodic unit

1. Inputs.

1.1. Number of wells in the cluster, K = 10.

1.2. Average characteristics of the casings of all the wells in the cluster are similar and coincide with the example used in the computations above.

1.3. All wells in the cluster work for a single common flow line – a collector having the following characteristics: L_m = 10.000 m, D_m = 0.3 m, δ_m = 7 mm, R_u = 500 Ohm□m, and h_m = 1.2 m.

1.4. Average specific resistivity of the ground along the flow line, ρ_g = 60 Ohm□m, and the average resistivity of strata in the well log, ρ_n = *95* Ohm□m. Specific ground resistivity distributions at the depth of down to 50 m within the cluster area are shown in Table 3.2.

Table 3.2

Specific ground resistivity distribution

Ranges, m	0-10	10-25	25-40	40-50
Stratum #	1	2	3	4
Stratum thickness, □$_i$, m	10	15	15	10
$\rho_{gi}, O□m \cdot m$	40	30	20	85

1.5. Casing protection current value is I_0 = 8 A.

2. Computing the CU parameters.

2.1. Compute the electrical parameters of the cluster casings (see Section 3.1 and subclauses 2.1. 2.5. and 2.15):

$$r_c = 69.6 \cdot 10^{-6} Ohm/m;\ \alpha_к = 0{,}68 \cdot 10^{-3}\ м^{-1};\ R_c = 151\ O□m \cdot m.$$

2.2. Compute the equivalent electric parameters of the cluster casings:

$$r_c^e = \frac{r_k}{K} = \frac{69.6 \cdot 10^{-6}}{10} = 7 \cdot 10^{-6} O□m/m\ ;$$

$$\alpha_c^e = \alpha_c = 0.68 \cdot 10^{-3} m^{-1}\ .$$

2.3. Compute the electric parameters of the flow line by formulas (3.12) – (3.14):

$$r_m = \frac{0.32 \cdot 0.24}{7(300-7)} = 37.4 \cdot 10^{-6}\ \ \frac{O□m}{m};$$

$$R_m = \frac{500}{3.14 \cdot 0.3} + \frac{60}{2 \cdot 3.14} ln \frac{500+60}{0.3 \cdot 1.2 \cdot 37.4 \cdot 10^{-6}} = 698\ \ \text{Ohm} \cdot \text{m},$$

$$R_m = \frac{500}{3.14 \cdot 0.3} + \frac{60}{2 \cdot 3.14} ln \frac{698}{0.3 \cdot 1.2 \cdot 37.4 \cdot 10^{-6}} = 700\ \ \text{Ohm} \cdot \text{m},$$

$$\alpha_m = \sqrt{37.4 \cdot 10^{-6}/700} = 0.23 \cdot 10^{-3} m^{-1}.$$

2.4. Compute the coefficient considering the CPS current consumption by formula (3.11):

$$K_m = \frac{7 \cdot 10^{-6} \cdot 0.23 \cdot 10^{-3} ct\square(1.700 \cdot 0.68 \cdot 10^{-3})}{37.4 \cdot 10^{-6} \cdot 0.68 \cdot 10^{-3} ct\square(10.000 \cdot 0.23 \cdot 10^{-3})} + 1 = 1.08.$$

2.5. Select the distance of anode beds from the nearest well heads: l_a = 30 m (L_l = 760 m), the coefficient being, according to (3.7):

$$K_a = 0.23 \cdot 760^{0.31} \cdot 30^{-0.1} = 1.28.$$

2.6. Find the total CU current by formula (3.18):

$$I_{tot} = \text{K} \cdot K_{\text{in}} \cdot K_m \cdot K_a \cdot I_0 = 10 \cdot 1.2 \cdot 1.28 \cdot 1.08 \cdot 8 = 133 \text{ A}.$$

2.7. Using formula (3.17), compute the total AB resistivity ($U_M = 48\ B, R_{pr} = 0.05\ O\square m$) :

$$R_{gr}^{tot} = \frac{48}{133 \cdot 2} - 0.05 = 0.13 \text{ Ohm}.$$

2.8. Compute the average specific resistivity of the upper ground layers within the anode bed area by the data of Table 3.2:

$$\rho_{gr} = \frac{\sum_1^n \square_i}{\sum_1^n \square_i/\rho_{gri}} = \frac{10 + 15 + 15 + 10}{\frac{10}{40} + \frac{15}{30} + \frac{15}{20} + \frac{10}{85}} = 31 \text{ Ohm} \cdot \text{m}.$$

2.9. We select vertical ABs with the electrode lengths of l = 40 m and diameter of d_e = 0.114 m (electrodes EGT-2500. material used for electrodes is graphite-reinforced plastic, mass of 1 running m, $m^f{}_0 = 7\ kg/m$). At the same time, in our case, l_n = 2 m, t = 2 m. Accordingly, the effective length and the burial of the anode bed, according to (3.21) and (3.22) will be:

$$l_e = 40 - 2 = 38\ m, \qquad t_e = 2 + 2 = 4\ m.$$

Compute the resistivity of a single AB by formula 3.20.

$$R_{gr} = \frac{31}{2 \cdot 3.14 \cdot 38} \cdot \left(ln\frac{2 \cdot 38}{0.114} + 0.5 \cdot ln\frac{4 \cdot 4 + 3 \cdot 38}{4 \cdot 4 + 38} \right) = 0.902 \text{ Ohm}.$$

2.10. Define approximately the number of ABs without considering the shielding coefficient:

$$N'_{gr} = R_{gr}/R_{gr}^{tot} = 0.902/0.13 = 6.94 \approx 7\ .$$

2.11. Locate the ABs uniformly along the cluster perimeter. Average distance between the suggested AB location points is taken as $b = 70\ m$. The b:l ratio is:

$$b/\ell = 70/40 = 1.75.$$

From Appendix 3. find the shielding coefficient for $b/\ell = 2$.

$N_з = 10; K_e = 0.75$.

2.12. Re-specify the number of ABs by formula (3.19):

$$N_{gr} = 0.902/0.75 \cdot 0.13 \approx 9\,.$$

2.13. Considering the number of ABs obtained, re-specify their locations.

2.14. By formula (3.25), compute the required mass of 1 running m of electrodes without using any filling (T_{gr} = 10 years, the minimum-resistance ground stratum is composed of loam, therefore, according to Appendix 4. q = 1.1 kg/A·year for graphite-reinforced plastics):

$$m_0 = \frac{133 \cdot 10 \cdot 1.1 \cdot 1.5}{38 \cdot 9 \cdot 0.75} = 8.6 \text{ kg/m}.$$

The value obtained is higher than the actual mass (7 kg/m) of the electrodes selected. This means that the computed service life of ABs will not be reached. Therefore, we use the coke filling of electrodes by filling the AB wells upon running the electrodes, with coke breeze. Then q = 0.3 kg/A□year. In this case,

$$m_0 = \frac{133 \cdot 10 \cdot 0.3 \cdot 1.5}{38 \cdot 9 \cdot 0.75} = 2.3 \text{ kg/m},$$

which is below the actual mass of 1 running meter of electrodes.

2.15. Using formula (3.21), compute the total mass of electrodes by their service life that must be longer than or equal to that of the system:

$$M = 2.3 \cdot 40 \cdot 9 = 828 \text{ kg}.$$

2.16. Using formula (3.26), find the CPS output power at the cathodic unit of the cluster:

$$N = 133 \cdot 48 \cdot 1.7 = 10.852.8 \text{ W} = 10.8 \text{ kW}\,.$$

Chapter Review

1. Necessary source data for engineering and designing the cathodic protection of casings.
2. Methods of recording cathodic polarization curves.
3. Methods of recording stress drop profiles along the casing depth.
4. Anode bed calculation algorithm.

Chapter 4. STANDARD DESIGN SOLUTIONS [16]

Currently, according to PJSC Tatneft's Regulations, cathodic protection must be ensured for any well, the expected service life of which is at least 10 years, and which is located within the radius of at least 100 m from the cathodic-protected wells. As well, if there is at least one well in a cluster, which is subject to cathodic protection, then all the other wells in that cluster must be protected, whether they need such protection or not.

The following inputs are required to implement the cathodic protection project:

– Design assignment;

– Topographical survey of elevated and underground structures within the radius of 200 m from the well or cluster to be protected, scaled 1:500; and

– Results of measuring the specific electric resistivity of ground at the entire depth at the location where an anode bed would be erected.

4.1. General Provisions

CPSs are selected by reference power, considering the voltage reserves in accordance with the current Regulations. Cathodic protection stations are installed strictly vertically (deviation may not exceed 2.0 %) on a substructure near the power supply source (transformer substation) with the installation height of 0.8-1.2 m from the ground surface (Fig. 4.1). Cathodic protection station must have a protective grounding used to prevent electrical shocks, in case of insulation damages, and can be connected into the common ground grid in the transformer substation with a band of 5x30 mm or have its dedicated ground grid (Fig. 4.2). At the same time, the dissipation resistance of the ground greed may not exceed 4 Ohm.

CPS power supply should be from the alternating current mains via an individual automatic switch of the low voltage board of the transformer substation. In case of no transformer substation 6/0.4 kV wells to be protected on the site, powering the CPS is provided for:

a) If the well to be protected is remote up to 200 m from the transformer substation, from the low voltage board of that transformer substation;

b) By a to-be-designed FL 6(10) kV 1.000 m long with installing a to-be-designed transformer substation 6(10)/0.4 kV; and

c) By a to-be-designed double-wire FL 0.22 kV 500 m long, from the existing transformer substation 6 (10)/0.4 kV.

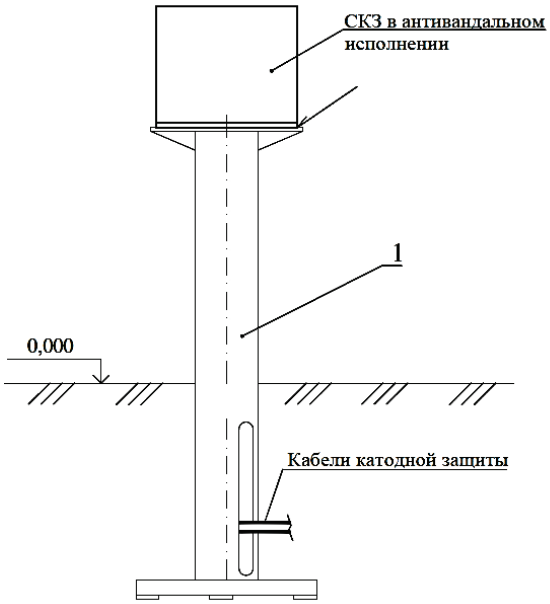

Fig. 4.1. Installing a vandal-proof CPS: 1 – CPS substructure

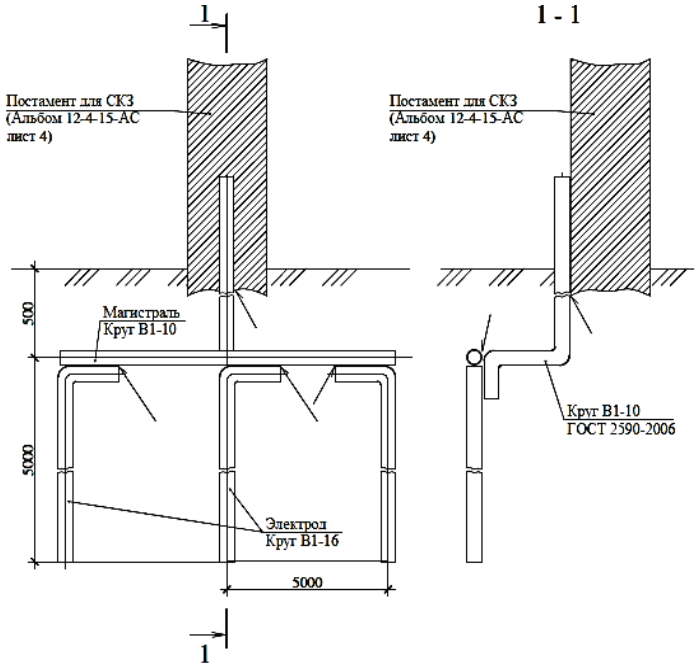

Fig. 4.2. Protective grounding

To avoid cable damages, lead-in of power cables into the transformer substation and lead-in of both power and electrochemical protection cables into the CPS substructure must be performed under mechanical protection. As electrochemical protection anodic and cathodic cables, we use a copper-conductor cable with a cross-section of 16 mm^2 and a double polyethylene or polypropylene insulation. Power cable and electrochemical protection cables should be laid in an open trench at a depth of at least 1 m and with the extensive length sufficient to compensate possible seismic motions or temperature transformations of the cables themselves. To prevent mechanical damages, cables should be additionally protected with a signal tape that is laid in the trench under the cables at the distance of 250 mm from their external surfaces.

Should the to-be-designed cable cross any other cables, both must be separated by a ground layer at least 0.5 m thick. In case of cables crossing any motor roads, they must be laid via pipes BNT 100-2950 at a depth of at least 1 m from the roadbed.

In Fig. 4.3. options are shown of how to connect a cathodic drainage cable to be laid from the cathodic protection station to the casing drainage point (direction).

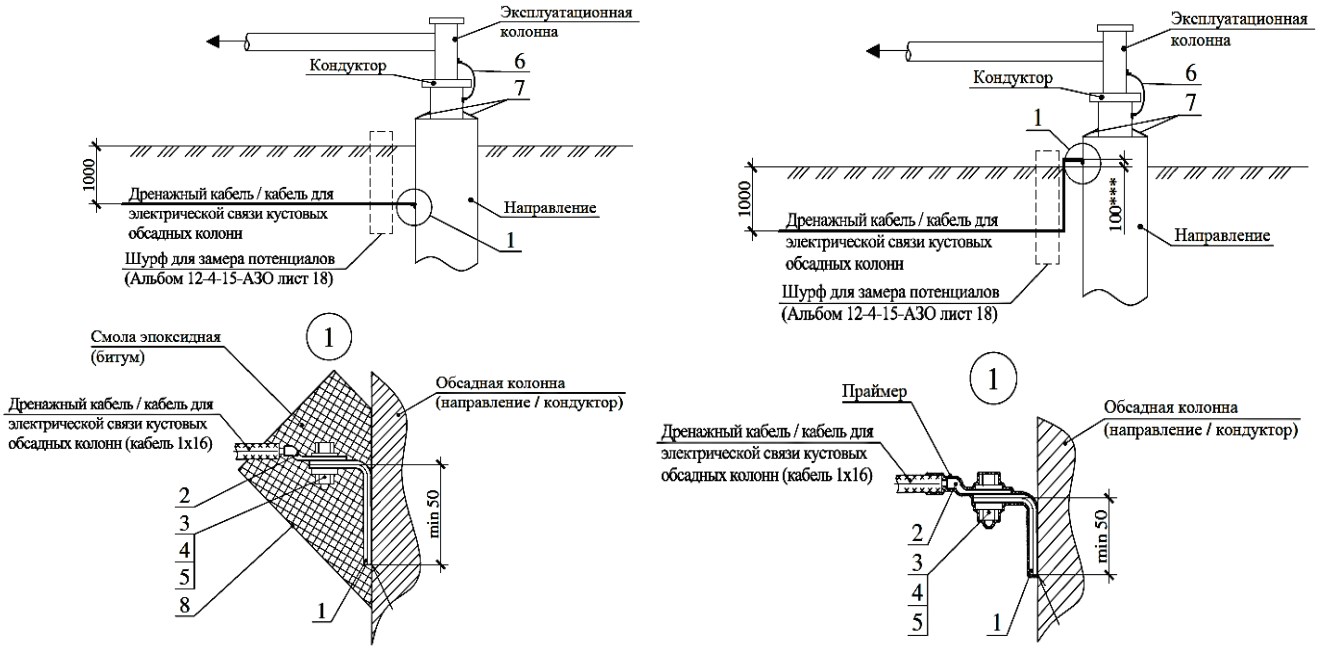

Fig. 4.3. Cable-to-casing connection unit in the ground (left) and above the ground (right): 1 – Band V-4x30; 2 – Cable thimble; 3 – Bolt; 4 – Nut; 5 – Washer; 6 – String-conductor girt; 7 – Band ON-4x40; 8 – Pipe PE80; 8 – Leak-tight metal sleeve in a PVC jacket

Drainage cable is connected to the production string guide at the depth of 1 m (Fig. 4.3. on the left). At the connection point, a mold is installed to be filled with plasticized bituminous mastic. The guide is connected to the conductor with two sections of a band sized 4x40. The conductor is joint to the production string with a steel cable jumper. The band and the steel cable are connected using electric arc welding. If the production string guide is deeper than 1 m from the ground surface, drainage cable shall be connected to the conductor. In the second option (Fig. 4.3. on the right) the cable is connected to the production string guide at the height of 0.1 m from the grade elevation opposite the coupling location. The junction point is coated with a primer (bitumen-gasoline solution at the ratio 1:3).

For clustered wells, the cathodic drainage cable to be laid from the CPS to the drainage point is connected to one of the wells within the cluster. Electric linking all the wells within the cluster is performed with a cable identic with the drainage one. Anodic drainage cable is connected to the anode bed output in clamps at the test point.

Anode bed type (deep, subsurface vertical, or horizontal) and length (depth) are selected based on ground conditions, such as groundwater level, distribution of the ground specific electrical resistivity along the depth, and presence of high-permeability intake formations; availability of free sites

within the area of wells to be protected, and the proximity of neighboring underground structures that may be adversely affected by stray currents generated by anodic protection, namely:

a) In grounds where ground water level does not exceed 20 m and in the absence of high-permeability intake formations down to the depth of 20-50 m, deep fluid-filled ABs are chiefly used;

b) In grounds where ground water level does not exceed 5 m (river flood plains) and in the absence of intake formation down to the depth of 50 m, deep ABs are chiefly used without any special filler (clay mud is used as a filler in the well);

c) In grounds where ground water level does not exceed 5 m (river flood plains) and in the presence of intake formations at the depth of lower than 10 m, subsurface vertical ABs are chiefly used with a filler of thickened clay mud or without any special filler (at the ground water level lower than 2 m);

d) In grounds where ground water level is above 20 m and in the presence of high-permeability intake formations down to the depth of 50 m, deep or subsurface vertical ABs are chiefly used with dry fillers;

e) If the suggested AB erecting location provides no site free of underground communications or no sufficient dimensions considerably exceeding the design length of the AB, only deep AB is selected; and

f) If the specific electric resistivity (SER) of the upper ground layers (down to 5 m) is considerably, at least two times, lower than the average SER of the lower layers (5-50 m), then horizontal ABs are chiefly used (the mean values of the SERs of upper and lower ground layers are found by measuring the SER with a four-electrode probe at the distances of 2 and 20 m between electrodes).

If there is no special data, the ground water level is evaluated qualitatively by the ground shape: If the topography is flat within at least 1 km around the AB erection site, the ground water level is usually above 20 m; in uplands with cliffs starting at the distance of less than 1 km from the AB, it is below 20 m; and it is above 5 m on flood plains or in waterlogged lands.

AB parameters should be computed considering the geometric parameters and the materials of the electrodes selected. Optimal distances between the AB and the head of well to be protected shall be chosen within 30-80 m, depending on the depth of this well. If there are several ABs on the well site, the distance between them shall be taken according to the calculations made in compliance with the current Regulations.

Individual joint cathodic protection of a casing and a FL/DWL is performed without installing an EIG at the well head. EIG is installed at the other end of the FL/DWL. Joint cathodic protection of a casing and a FL/DWL is used, if the pipeline is not protected electrochemically.

Elimination of anode zones on a pipeline is achieved by changing the cathodic protection station current intensity. At the same time, the current tapped to the well casing should not reduce by more than 20 %, as compared to the design value. If no complete protection of a pipeline is ensured along its entire length in the joint cathodic protection of a casing and the pipeline connected to it (for the wellhead pipeline potential that does not exceed the standard protective potential value), then the pipeline is additionally equipped with cathodic or sacrifice protection.

You are allowed not to install an EIG at the pipeline end located on the GMS (CPS) site, provided that all the three conditions below are met:

- The pipeline is not insulated externally or is insulated with bitumen (external insulation resistivity is below 200 Ohm·m^2);
- The pipeline length exceeds 1.000 m; and
- No need for the pipeline ECP against external corrosion is proven.

In the standard solutions below, we consider the cathodic corrosion protection for:

a) Casing of a single well;
b) Casing of a cluster of two wells;
c) Casing of a cluster of three wells;
d) Casing of a cluster of four wells; and
e) Casing of a cluster of five wells.

Legend keys used in the diagrams below are given in Table 4.1.

Table 4.1

Legend keys for standard design solutions

Обозначение	Ниаменование
	Станция катодной защиты (СКЗ)
	Анодный заземлитель (АЗ)
—W—	Кабель электрохимзащиты
—$W_ш$—	Шина для создания электрической связи скважин
—N—	Кабель электропитания
	Контрольно-измерительная колонка (КИК)
ЭИС	Электроизолирующее соединение

For cathodic protection of a cluster of six or more wells, the combinations of the options above should be used.

Protection current of a well/cluster is taken in accordance with the computations described in Chapter 5 below. Cathodic protection efficiency is controlled at the wellhead using a portable copper-sulfate electrode (Fig. 4.4). Potential measuring unit skid shall be located at the opposite side of the clutch location (near the location of the cathodic cable drainage point). At wells where wellhead access platforms are concreted, the hole is located externally of the concreted site, close to curb. Internal space of the pipe is filled with sand to enable measuring the polarization potentials using a portable copper-sulfate electrode.

Fig. 4.4. Potential measuring pit:
1 – PE80 pipe; 2 – Copper-sulfate electrode; 3 – Cap

4.2. Process Diagrams of Cathodic Protection Units

In Fig. 4.5. the layouts are shown for locating cathodic protection tools on a single well. Where possible, ABs are placed on the well site opposite the flow line, considering the location plan.

In case of dehumidification of filling and of the ground around AB due to electroosmosis, the AB operability can be completely restored by injecting water or thickened mud fluid via the cover from the pit. Mud, clay, mud-clay mixture, or coke fines (coke breeze) can be used as an electroconductive filling for ABs.

In Figs. 4.6-4.9. various layouts are shown for the cathodic protection tools, depending on the number of wells in the cluster and on the number of anode beds. As an example, one of diagrams of connecting the cathodic protection station to five casings is shown in Fig. 4.9.

Vertical and horizontal versions of anode beds used in the electrochemical protection of oil well casings are shown in Figs. 4.11 and 4.12. Draining out gases generated in the operation of an AB, a perforated polyethylene tube is fastened along its entire length, the upper end of which is drained out into the cover.

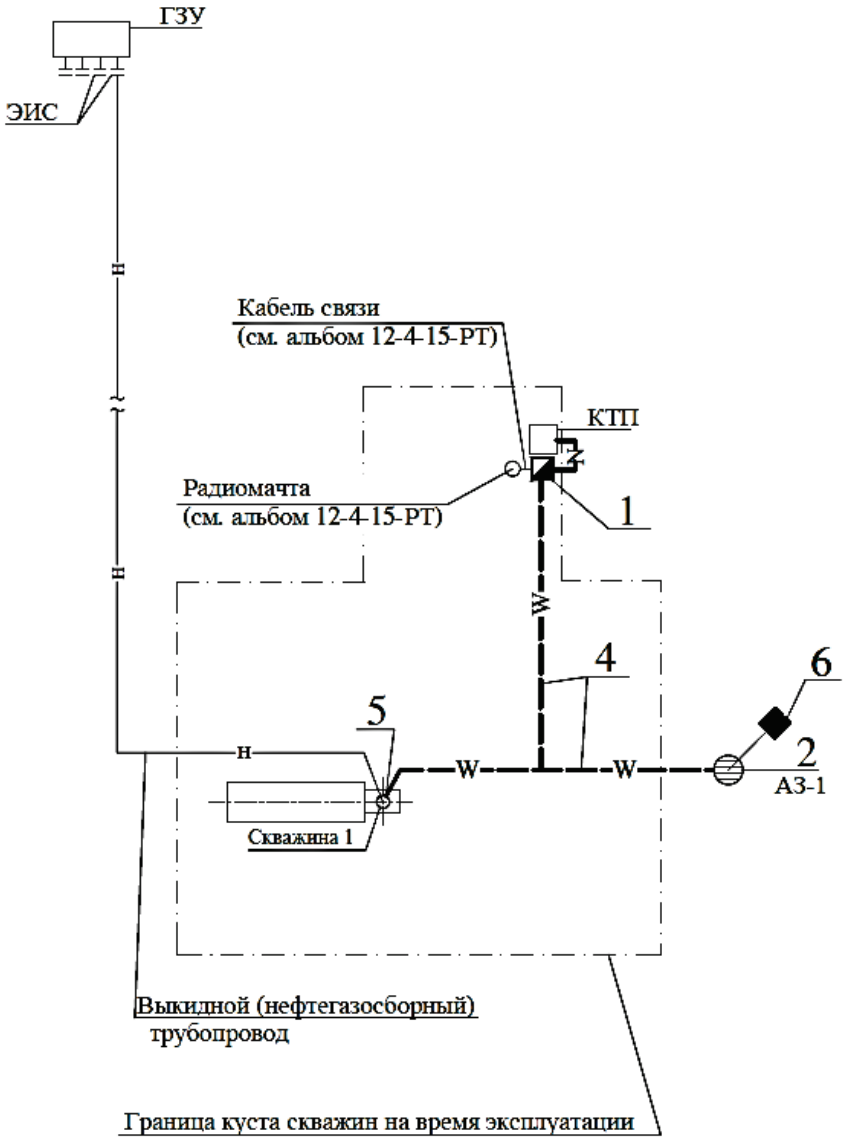

Fig. 4.5. Layout of cathodic protection tools on a single well:
1 – Cathodic protection station; 2 – Anode bed; 3 – Electroconductive filling for AB;
4 – Cable 1x16; 5 – Assembly of connecting the cable to casing string;
6 – Metering Operation Center (MOC); and 7 – MOC guard

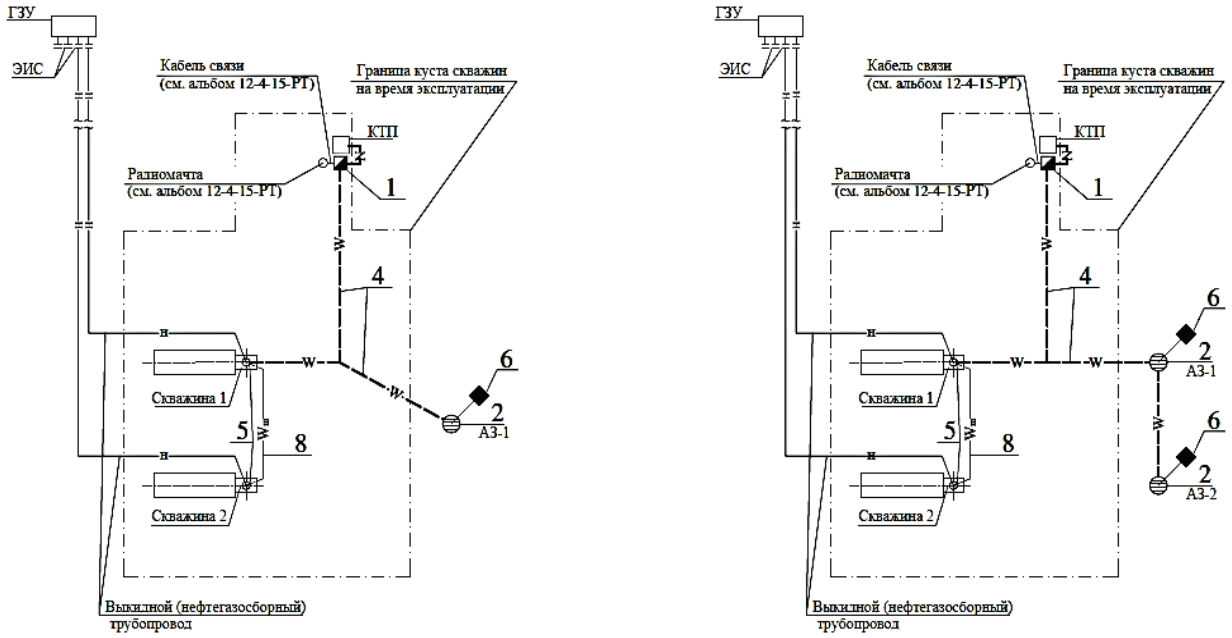

Fig. 4.6. Layout of cathodic protection tools on a cluster of two wells with one (left) and two (right) ABs: 1 – Cathodic protection station; 2 – Anode bed; 3 – Electroconductive filling; 4 – Cable 1x16; 5 – Assembly of connecting the cable to the casing string; 6 – MOC; 7 – MOC guard; and 8 – Cable 1x16

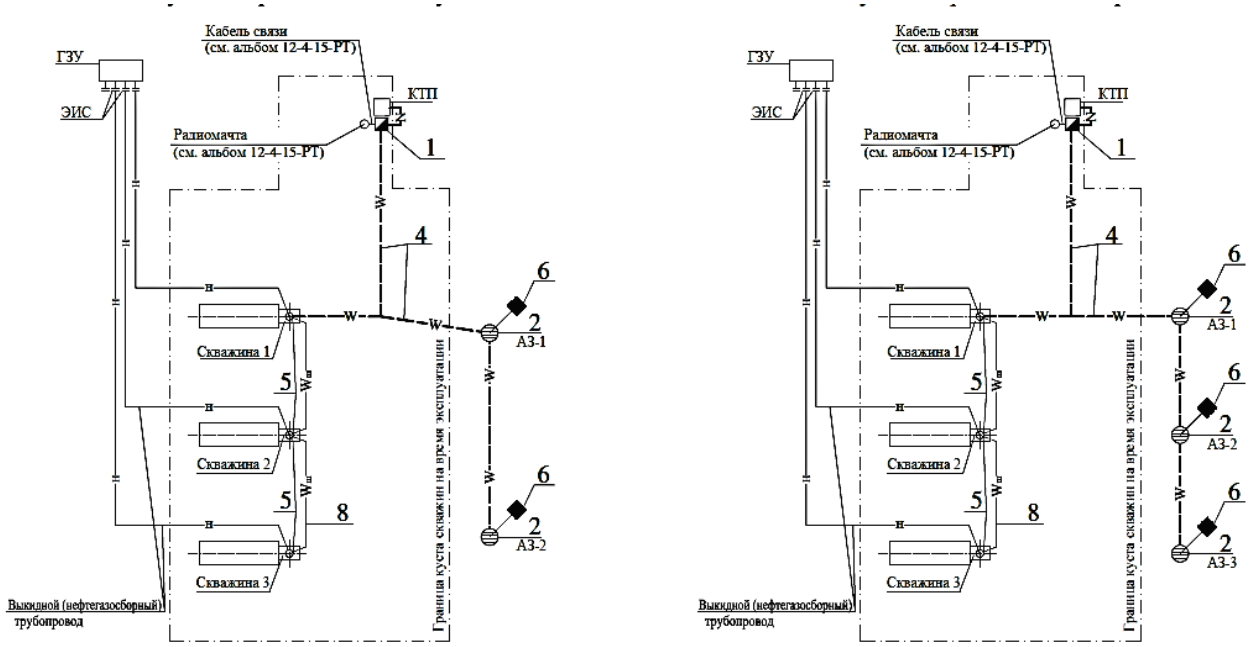

Fig. 4.7. Layout of cathodic protection tools on a cluster of three wells with two (left) and three (right) ABs: 1 – Cathodic protection station; 2 – Anode bed; 3 – Electroconductive filling; 4 – Cable 1x16; 5 – Assembly of connecting the cable to casing string; 6 – MOC; 7 – MOC guard; and 8 – Cable 1x16

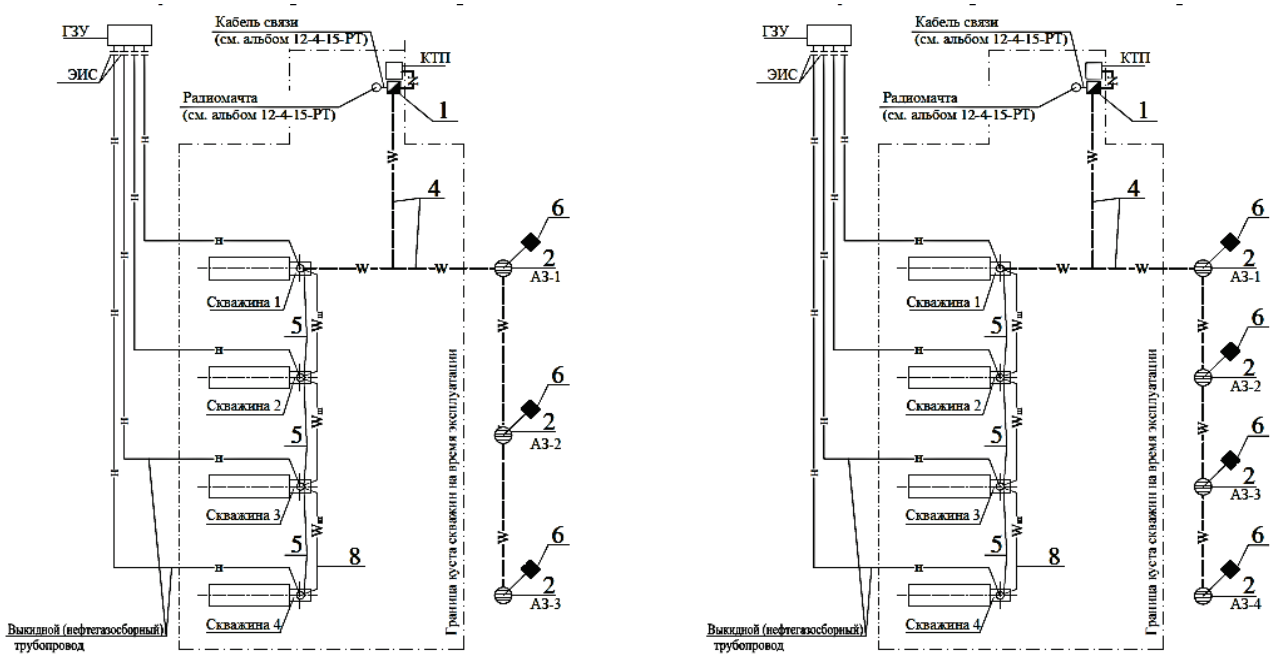

Fig. 4.8. Layout of cathodic protection tools on a cluster of four wells with three (left) and four (right) ABs: 1 – Cathodic protection station; 2 – Anode bed; 3 – Electroconductive filling; 4 – Cable 1x16; 5 – Assembly for connecting the cable to casing string; 6 – MOC; 7 – MOC guard; and 8 – Cable 1x16

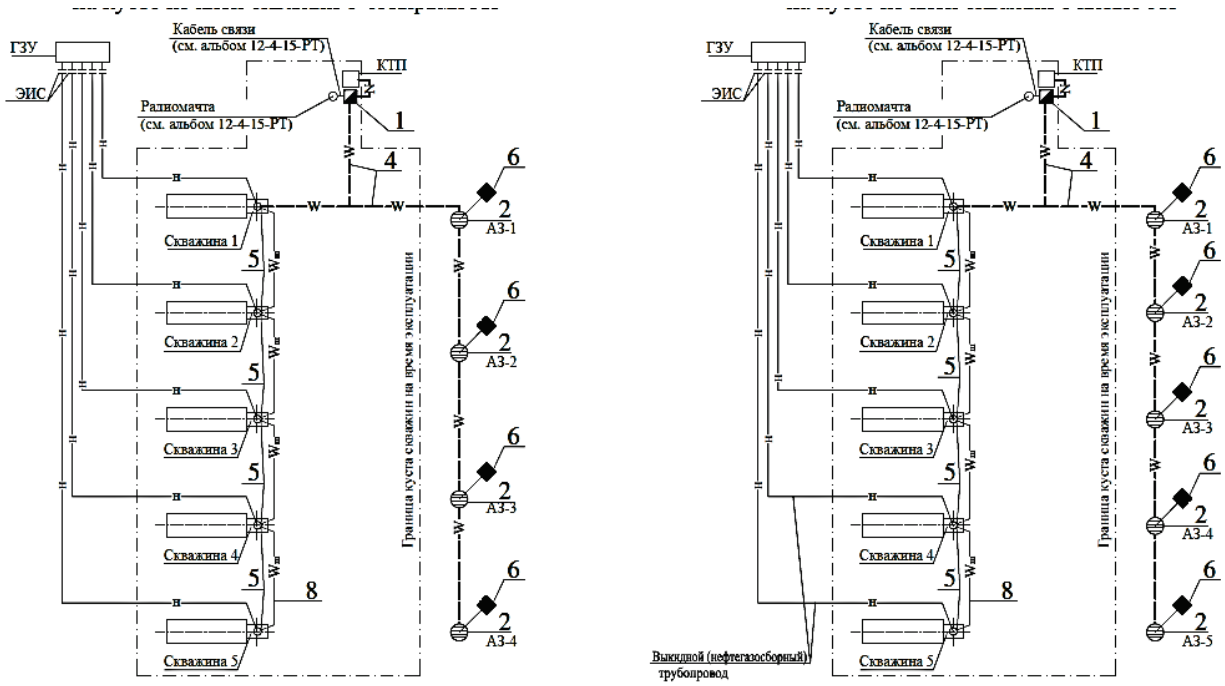

Fig. 4.9. Layout of cathodic protection tools on a cluster of five wells with four (left) and five (right) ABs: 1 – Cathodic protection station; 2 – Anode bed; 3 – Electroconductive filling; 4 – Cable 1x16; 5 – Assembly for connecting the cable to casing string; 6 – MOC; 7 – MOC guard; and 8 – Cable 1x16

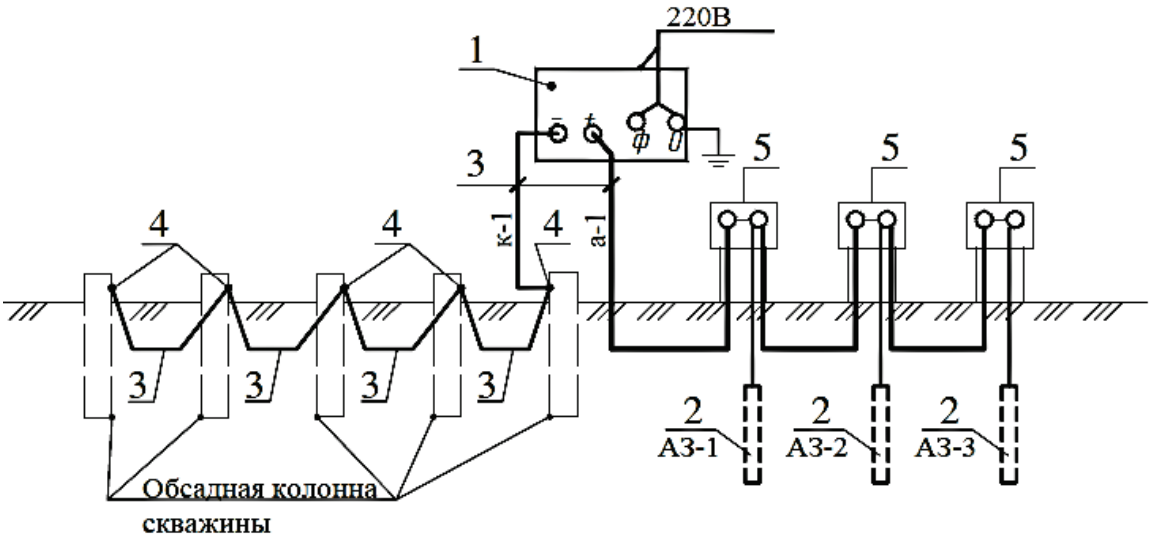

Fig. 4.10. Layout of cathodic protection tools on five well casings: 1 – Cathodic protection station; 2 – Anode bed; 3 – Cable 1x16; 4 – Assembly for connecting the cable to casing string; 5 – MOC; and 6 – MOC guard

To reduce the dissipation resistance and enhance seasonal stability, as well as to reduce the rate of anodic dissolution of electrodes, dry and liquid (in initial condition) active and inactive fillers surrounding the electrodes can be used. If the design provides for using a dry filler (coke breeze), the well is filled with a dry composition down to the lower end of the casing polyethylene tube of the cover. Coke breeze is poured via a keyseat into the AB pit cover in batches, 100-150 kg each. Each batch of coke breeze is poured with 40-50 l of sweet water, it being necessary to prevent blockages. Considering the consolidation/shrinkage of the filling, the pit is filled up to the level of installing the cover.

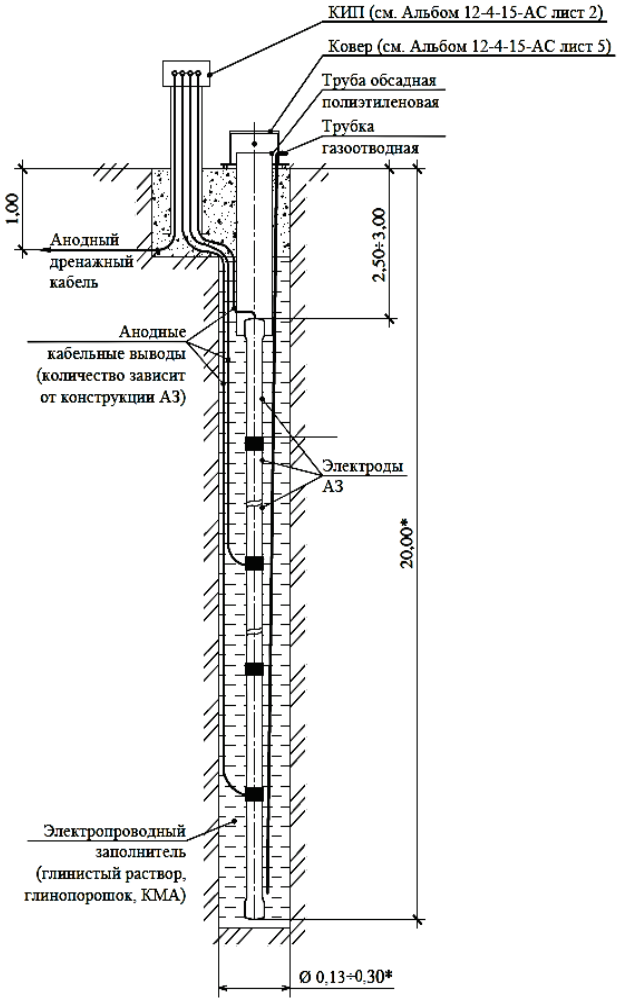

Fig. 4.11. Vertical anode bed

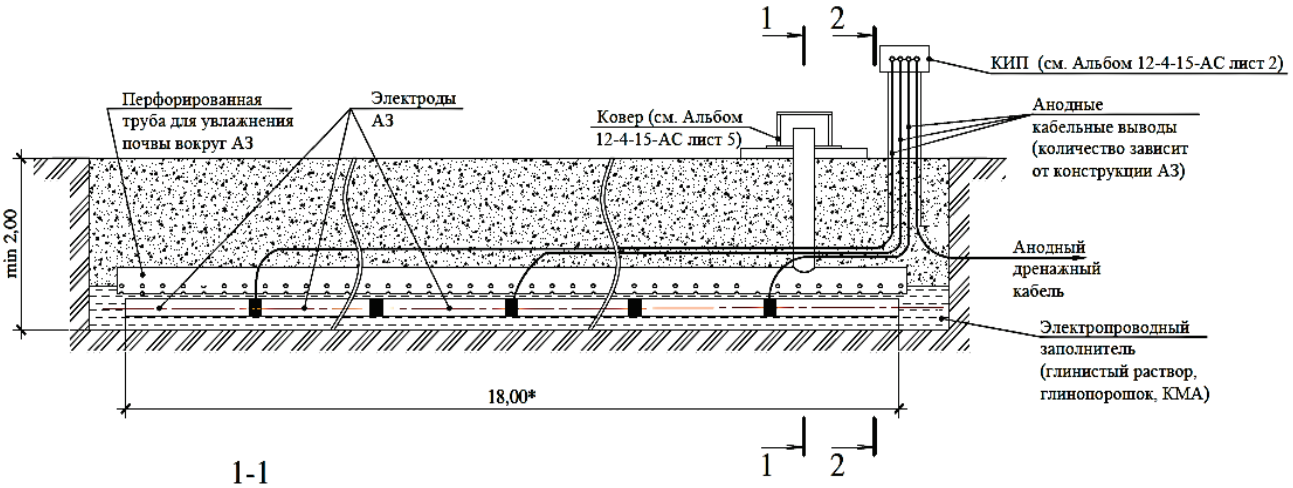

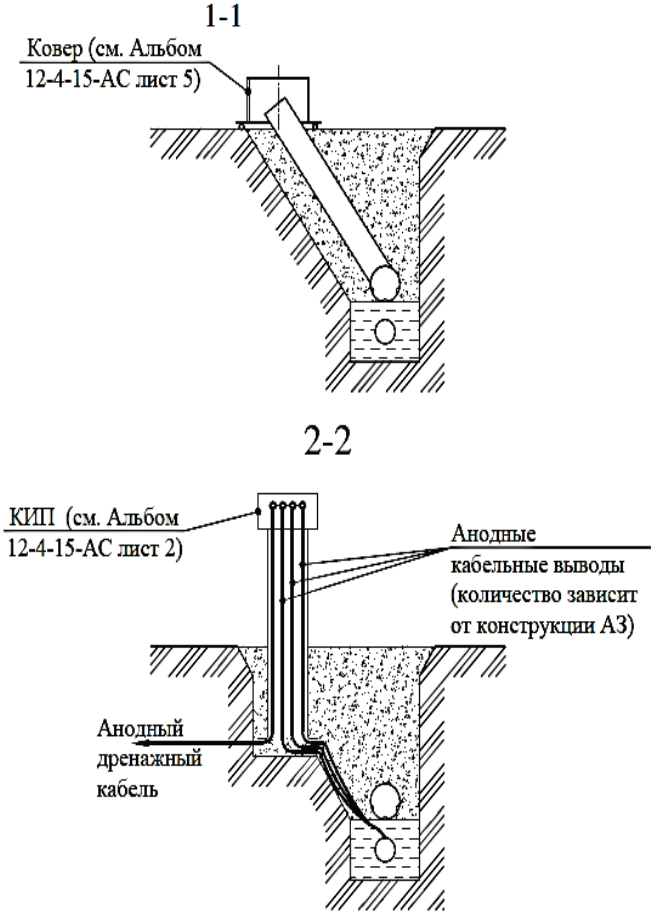

Fig. 4.12. Horizontal anode bed

Total amount of coke breeze and water depends on electrode brands and pit depth and is re-specified when associating with a specific facility. Mean coke breeze consumption is 40-50 kg per an electrode (1.5 m long).

Over the AB, near the cover, an MOC is installed (strictly vertically), in which anode outputs are connected to the drainage cable from the CPS. On the MOC head, a red plate is placed, in which the following is given in white: AB number, CPS number, well number, and contact phone number (Fig. 4.13).

MOC and cover are installed within a common protective guard. The guard flag is colored in red, and the flag direction corresponds with the anodic drainage cable direction. MOC, cover, and their guard are colored in yellow.

Well depth for installing a deep AB is 2.5-3 m (AB burial) longer than the design one. The well within the AB burial range is drilled out with the diameter of 295 mm to install a cover with a casing PE tube.

AB pit corresponds with the diameter within the ranges of:

– 130-190 mm when filling the pit with clay mud; and

– 190-300 mm when filling the pit with dry fillers.

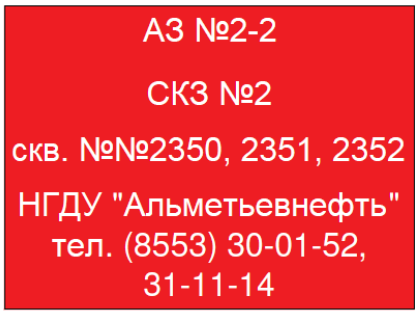

Fig. 4.13. A sample plate containing the AB MOC data

Upon drilling completion, immediately before running the electrodes, the well is filled with normal clay mud or special mud powder PBMV thickened to creamy consistency. Into the well opening (burial), under the AB, a cover is installed, fastened with a polyethylene pipe with a diameter of 250 mm, which cases the well wall within the burial range. When mounting the AB, electrodes are run using a well drill or special tools tested and accepted for pulling and running operations.

Before starting the mounting, the AB elements undergo receiving inspection for their compliance with the requirements of design and regulatory documents. At inspection, the following is checked:

– Actual amounts and brands of electrodes and other anode bed elements, their integrity, and compliance with design documents;

– Brands, sections, and lengths of anode terminal cables and their compliance with design documents (cable terminals must have a length reserve of 2-3 m); and

– Availability of auxiliary materials and tools.

Chapter Review

1. Using standard design solutions, describe cathodic protections for a single-well casing and for the casing of a cluster of two or more wells.
2. Give the type codes of standard design solutions.
3. What conditions should be considered when selecting a type of anodic earthing?

Chapter 5. EXAMPLES OF ESTIMATING THE PROTECTION CURRENT USING DIFFERENT METHODS [17. 18]

The key parameter of cathodic protection is the value of protective current. For casing structures, protective current is considered to be sufficient, if the measurement results show that electric current directed to the well casing has eliminated all the anodic areas [6]. There are some methods that allow finding the value of the required cathodic protection current [6. 7]:

– Method of polarization curves (electric logging);

– Method for identifying the voltage drop profile in a production casing;

– Method of calculating the potential shift in the wellbore and the resistance in the well-ground system; and

– Method of modeling the cathodic protection for a well.

5.1. Method of Polarization Curves

Method of polarization curves is easy to perform, while its validity is proven by laboratory tests. It is based on the fact that the difference of potentials between the casing structure and the reference electrode changes where the current is delivered through ground to the well casing. For this current intensity, the shift of potential depends on the polarization duration and current density. With increasing the current intensity, the casing surface polarization strengthens. Minimum required value of protective current is found using dependence $E - \log I$.

Electric logging method is implemented as follows. Equipment required for performing a study is laid out in accordance with Fig. 5.1. Upon preparing the required equipment, the potential of "natural state" is measured and registered. Then, through the anode bed, the casing is being fed with current (usually 0.1 A) within a certain time interval (2-3 min.), upon elapse of which the current is cut and potential is measured. Within a fraction of a second, potential drops rapidly, and then it decreases gradually. Of interest is the value that is reached after the rapid drop (before the gradual decrease starts). This value is named a potential at the instantaneous current cutout. Current cutout lasts for at most 2 s. Then the casing is fed with the current of a higher value (increments are 0.1-0.2 A).

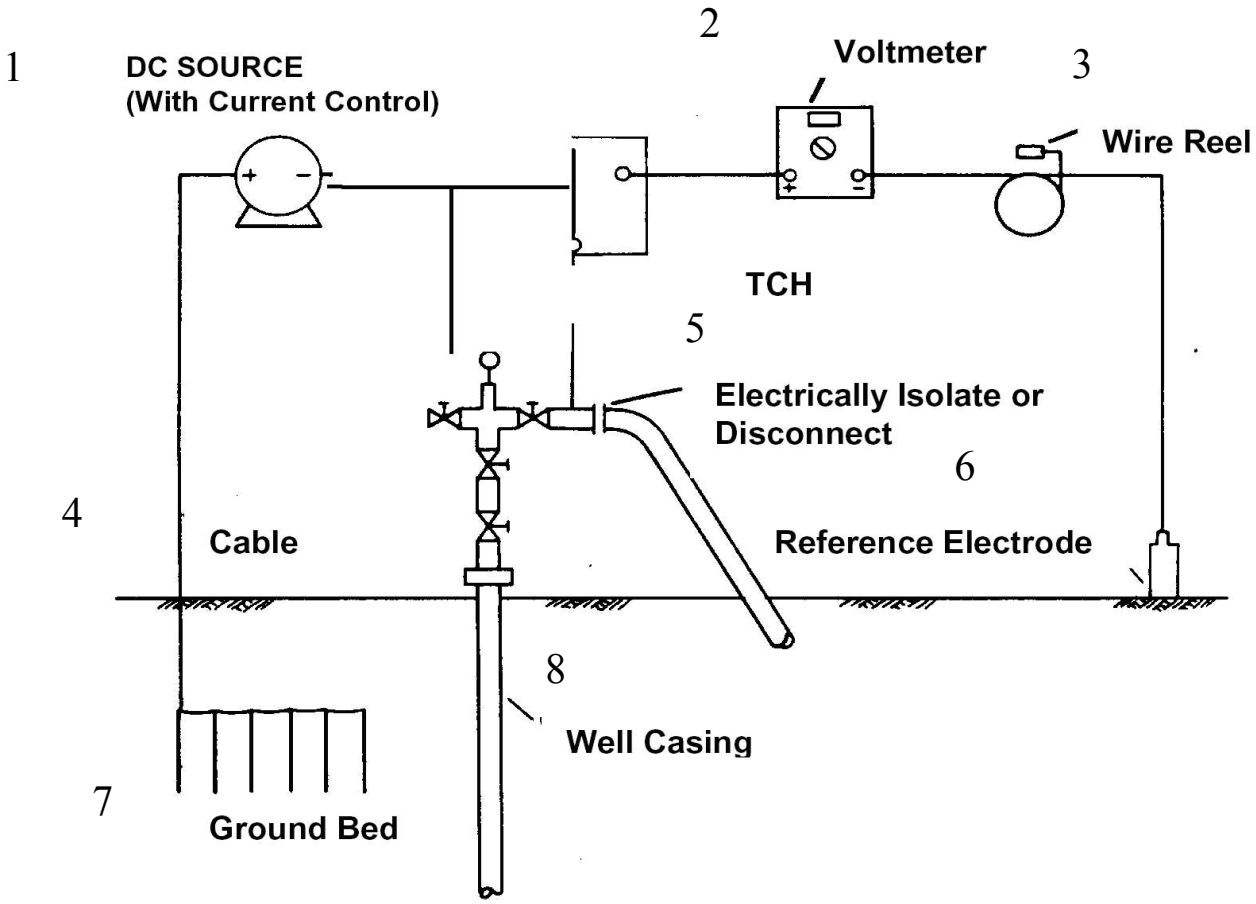

Fig. 5.1. Scheme of testing by the electric logging method: 1 – DC source; 2 – Voltmeter; 3 – Wire drum; 4 – Cable; 5 – Electrically insulating gasket; 6 – Reference electrode; 7 – Anode bed; and 8 – Well casing

Fig. 5.2 shows the results of identifying the cathodic protection current (for one of the casings of PJSC Tatneft) by the electric logging method. The curve has two clearly linear sections, 1 and 2. extrapolating which to the crossing point allows finding the minimum protection current value that ensures the satisfactory cathodic protection against corrosion. In this case, this value is 4.8 A.

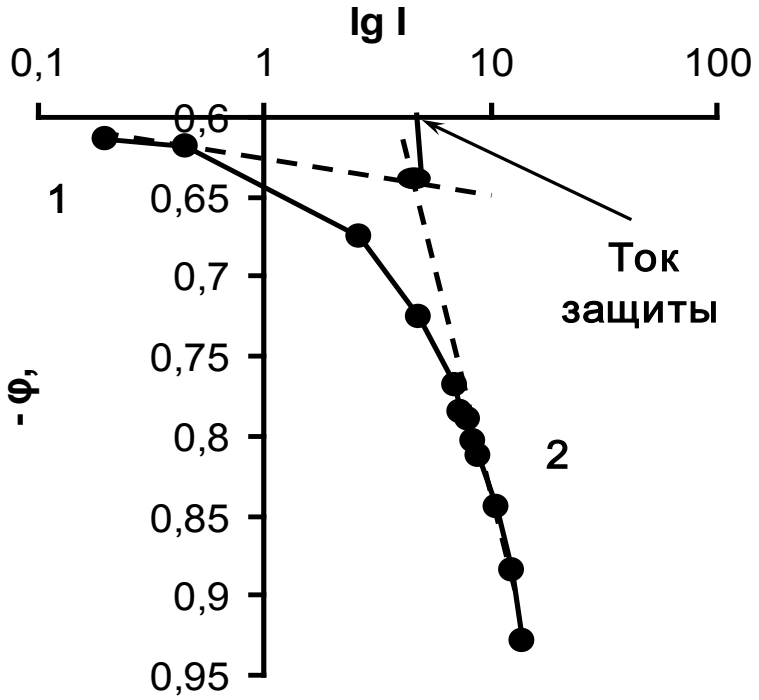

Fig. 5.2. Polarization curve of the casing of well No. 22505 of OGPD Bavlyneft

5.2. Calculating the Potential Shift in the Wellbore and the Resistance in the Well-Ground System

Knowing the value of protection current and the potential shift at wellhead and using the method of calculating the potential shift in the wellbore and the resistance within the well-ground system, we can compute the potential shift at the bottom hole [7]. Below is an example of computing for the casing of well No. 22505 of OGPD Bavlyneft, consisting of three sections, i.e., guide, conductor, and production string (Fig. 5.3). Computations are performed for each section of the casing, from bottom hole through the wellhead.

First stage of computations includes determining the geometric and electrical parameters of the structure in accordance with the well type and characteristics. Ad hoc, the cross section of a metal structure is found according to diagram [7] shown in Fig. 5.4.

Formula of finding the total cross-section area of the sections is represented as follows:

$$S_k = \sum \pi \cdot d \cdot e\,,\ \text{m}^2 \qquad (5.1)$$

where *d* means the external diameter of the pipe; and *e* means the pipe wall thickness.

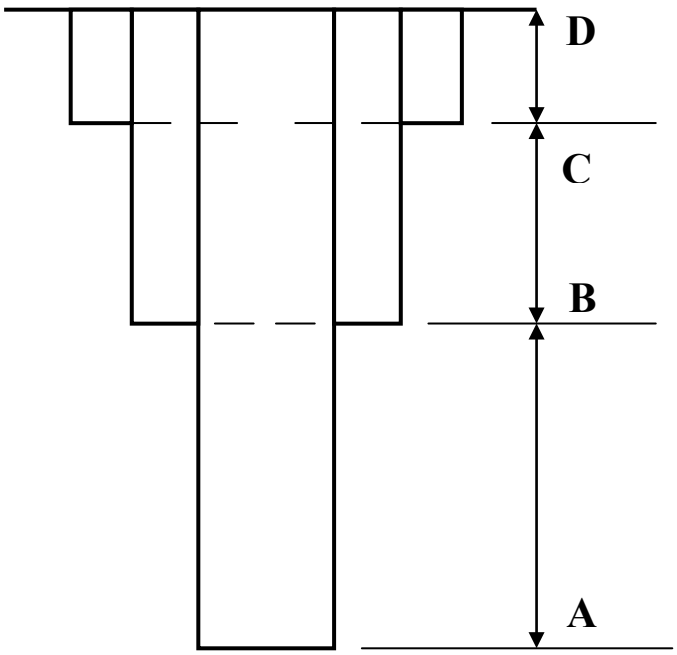

Fig. 5.3. Three-step casing: AB – production string; BC – conductor; CD – guide

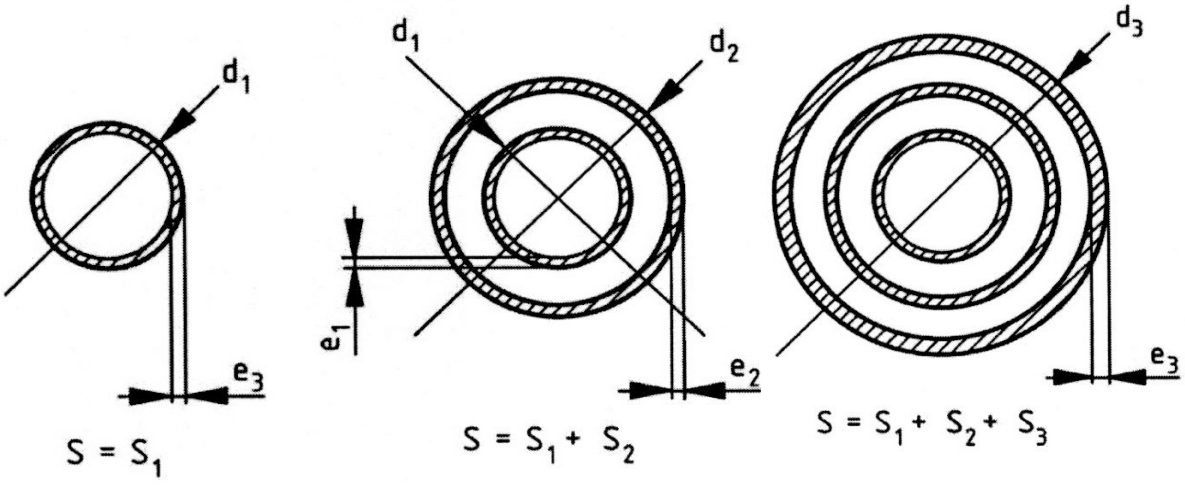

Fig. 5.4. Diagram of computing the cross section of a casing consisting of three sections (from left to right): Production string; production string + conductor; production string + conductor + guide

Cross-section areas of the sections of the casing under research, considering their changes in height, were:

– Section 1 (production string): AB = 1.757 m; d_1 = 146 mm; e_1 = 7.7 mm; $S_1 = \pi \cdot d_1 \cdot e_1 = 35.3 \cdot 10^{-4}$ m^2;

– Section 2 (conductor): BC = 274 m; d_2 = 245 mm and d_1 = 146 mm; e_2 = 8.9 mm and e_1 =7.7 mm; $S_2 = \pi \cdot (d_1 \cdot e_1 + d_2 \cdot e_2) = 103.7 \cdot 10^{-4}$ m^2;

– Section 3 (guide): CD = 32 m; d_3 = 324 mm, d_2 = 245 mm and d_1 = 146 mm; e_3 = 9.5 mm, e_2 = 8.9 mm and e_1 = 7.7 mm; $S_3 = \pi \cdot (d_1 \cdot e_1 + d_2 \cdot e_2 + d_3 \cdot e_3) = 200.4 \cdot 10^{-4}$ m^2.

Longitudinal ohmic resistance is found by formula:

$$r_k = \frac{\rho \cdot 1}{s_k}, O\Omega m \cdot m^{-1} \ , \tag{5.2}$$

where ρ = 18·10^{-8} Ohm□m means steel resistance; *1 (one)* means the length of a section. For the three sections under consideration, they were: r_1 = 51·10^{-6} Ohm□m^{-1}; r_2 = 7.3·10^{-6} Ohm□m^{-1}; and r_3 = 9·10^{-6} Ohm□m$^{-1.}$ respectively.

In computing, the system of electric parameters includes coefficient of attenuation, α_k, and characteristic impedance, γ_k, both determined by the relevant formulas:

$$\alpha_k = \sqrt{\frac{\frac{r_k}{r_{co}}}{\pi \cdot d_k}} = \sqrt{r_k \cdot \frac{\pi \cdot d_k}{r_{co}}}, [m^{-1}] \ , \tag{5.3}$$

$$\gamma_k = \sqrt{\frac{r_{co}}{\pi \cdot d_k} \cdot r_k}, O\Omega m, \tag{5.4}$$

where r_k means longitudinal ohmic resistance; r_{co} means specific coating resistance; d_k means the external diameter of the casing section.

At the first computation stage, parameters α_k and γ_k are unknown, since they depend on the value of r_{co}. At the second stage, testing is performed with current feed, at which the current intensity, I_n, and potential shift at the wellhead, U_n, are measured, and the U_n/I_n. ratio is computed.

In our case, potential at the wellhead before current feed was –0.650 V (CSE), while upon current disconnection it is (3 A) – (-0.760) V (CSE), which is relevant to the potential shift of 0.110 V. The ratio computed was:

$$\frac{U_n}{I_n} = \frac{0.110}{3} = 0.037\ V/A. \tag{5.5}$$

At the third stage, the value of r_{co} is found using the successive-approximation method. Computations are performed, starting from the lower section, taking the spontaneous potential shift as $U_{0.}$ such as U_0 = 1.

For the casing under consideration, consisting of three sections, three systems of equations are used. For the first section (bottom hole):

$$\text{A} \begin{cases} U_1 = U_0 \cdot cosh\ (b_1) \\ I_1 = \frac{U_0}{\gamma_1} \cdot sin\Omega(b_1) \end{cases} \tag{5.6}$$

For the second section:

$$\text{B} \begin{cases} U_2 = U_1 \cdot cosh\ (b_2) + \gamma_2 \cdot I_1 \cdot sinh\ (b_2) \\ I_2 = \frac{U_1}{\gamma_2} \cdot sin\Omega(b_2) + I_1 \cdot cos\Omega(b_2) \end{cases} \tag{5.7}$$

For the third section:

$$C \begin{cases} U_3 = U_2 \cdot \cosh(b_3) + \gamma_3 \cdot I_2 \cdot \sinh(b_3) \\ I_3 = \frac{U_2}{\gamma_3} \cdot \sin(b_3) + I_2 \cdot \cos(b_3) \end{cases} \quad (5.8)$$

In the equations above:

$$b_k = \alpha_k \cdot L_k, \quad (5.9)$$

where α_k means the coefficient of attenuation; L_k means the section length.

These techniques suggest that the r_{co} value representing the specific coating resistance remains unchanged over the entire surface of the well for all sections.

To solve the system of equation, the expressions for U_1 and I_1 of system A are substituted in system B, and, respectively, expressions U_2 and I_2 obtained in system B are substituted in system C. Resulting from such substitutions, we obtained system C$^{/}$:

$$U_3 = U_0 \cdot \begin{bmatrix} \cos(b_1) \cdot \cos(b_2) \cdot \cos(b_3) + \frac{\gamma_2}{\gamma_1} \cdot \sin(b_1) \cdot \sin(b_2) \times \\ \times \cos(b_3) + \frac{\gamma_3}{\gamma_2} \cdot \cos(b_1) \cdot \sin(b_2) \cdot \sin(b_3) + \\ + \frac{\gamma_3}{\gamma_1} \cdot \sin(b_1) \cdot \cos(b_2) \cdot \sin(b_3) \end{bmatrix} \quad (5.10)$$

$$I_3 = U_0 \cdot \begin{bmatrix} \frac{1}{\gamma_3} \cos(b_1) \cdot \cos(b_2) \cdot \sin(b_3) + \frac{\gamma_2}{\gamma_1 \cdot \gamma_3} \cdot \sin(b_1) \cdot \sin(b_2) \times \\ \times \sin(b_3) + \frac{1}{\gamma_2} \cdot \cos(b_1) \cdot \sin(b_2) \cdot \cos(b_3) + \frac{1}{\gamma_1} \cdot \sin(b_1) \times \\ \times \cos(b_2) \cdot \cos(b_3) \end{bmatrix} \quad (5.11)$$

Value of the U_3/I_3 ratio does not depend on the value of U_0; it only depends on the values of parameters b_1. b_2. b_3. γ_1. γ_2. and γ_3 that are functions of r_{co}. Substituting parameter r_{co} in the expression for U_3 and I_3 and setting the U_3/I_3 ratio to the experimentally obtained value of this ratio, equaling to 0.037 V/A, we compute the value of r_{co} by the method of successive approximations.

In our case, computations were performed at the following values of r_{co} (Ohm·m^2): 100. 50. 25. and 20. The value of r_{co}, in our case, fell within the range of 25-20 and was taken as 23 Ohm·m^2.

At the last stage, we substitute the value of r_{co} in all expressions for b_1. b_2. b_3. γ_1. γ_2. and γ_3. As a result, we represent system C$^{/}$ as:

$$C^{/} \begin{cases} U_3 = U_0 \cdot 3.26 \\ I_3 = U_0 \cdot 79.78 \end{cases} \quad (5.12)$$

The equations obtained link the values of the wellhead potential shift, U_3. to the bottom hole potential shift (U_0), and the value of the bottom hole potential shift, U_0. to the value of the protective current, I_3.

Using equation system $C^{/}$, we can compute the potential shifts at the wellhead and at the bottom hole for any predefined current intensity. Particularly, substituting the results of computing the protective current intensity by the electric logging method (4.8 A) in equation system $C^{/}$, we will find that the value of the bottom hole is:

$$I_3 = U_0 \cdot 79.78\ (A) \rightarrow U_0 = 0.060\ V.$$

At the same time, the computed value of the wellhead potential shift will be:

$$U_3 = U_0 \cdot 3.26\ (V) \rightarrow U_3 = 0.196\ V.$$

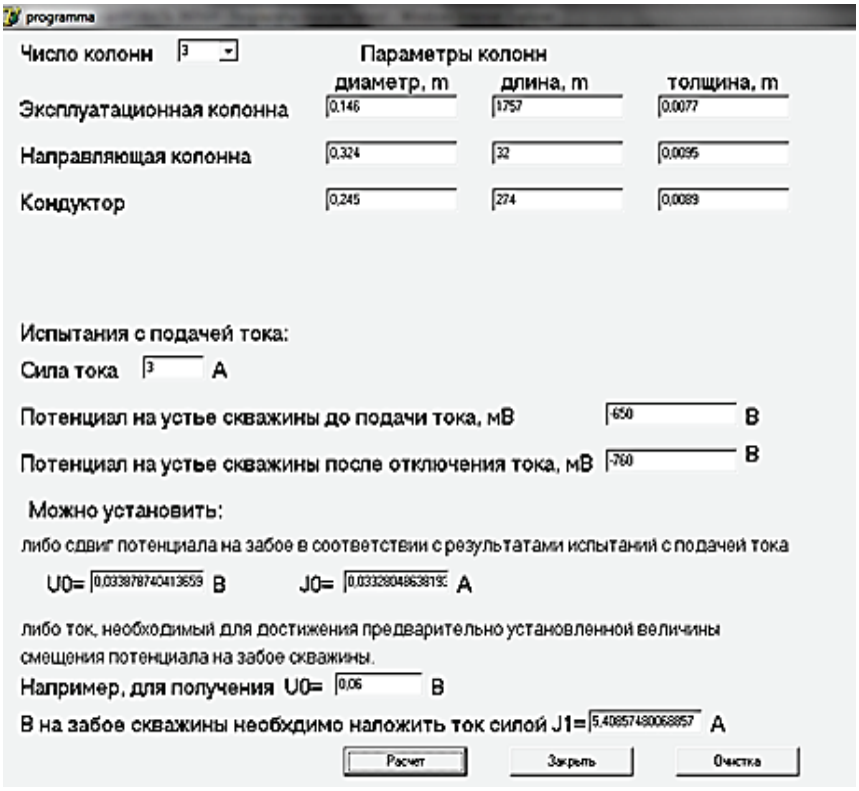

Fig. 5.5. Development environment Delphi 7 and software

To compute the potential shift in the well bore and the resistivity in the well-ground system, a software program for Windows was developed – imperative, structured, and object-oriented programming language, Delphi 7 (Fig. 5.5).

5.3. Method for Identifying the Voltage Drop Profile in a Production Casing

The method of measuring potential profiles has been known for relatively long time; it was first published in 1948. The techniques proposed for computing the current density distribution along the depth of a casing are based on the materials stated in Regulations 153-39.0-531-07. *Guidelines for the Cathodic Protection of Well Casings and Flow Lines (Distribution Water Lines) against External Corrosion*. These techniques additionally consider changes in the metal cross-section area and changes in the area of the external surface of the sections of a casing along its height. Computing the cathodic protection current density along the casing depth is based on the voltage drop measurement results obtained using a two-contact probe (Fig. 5.6).

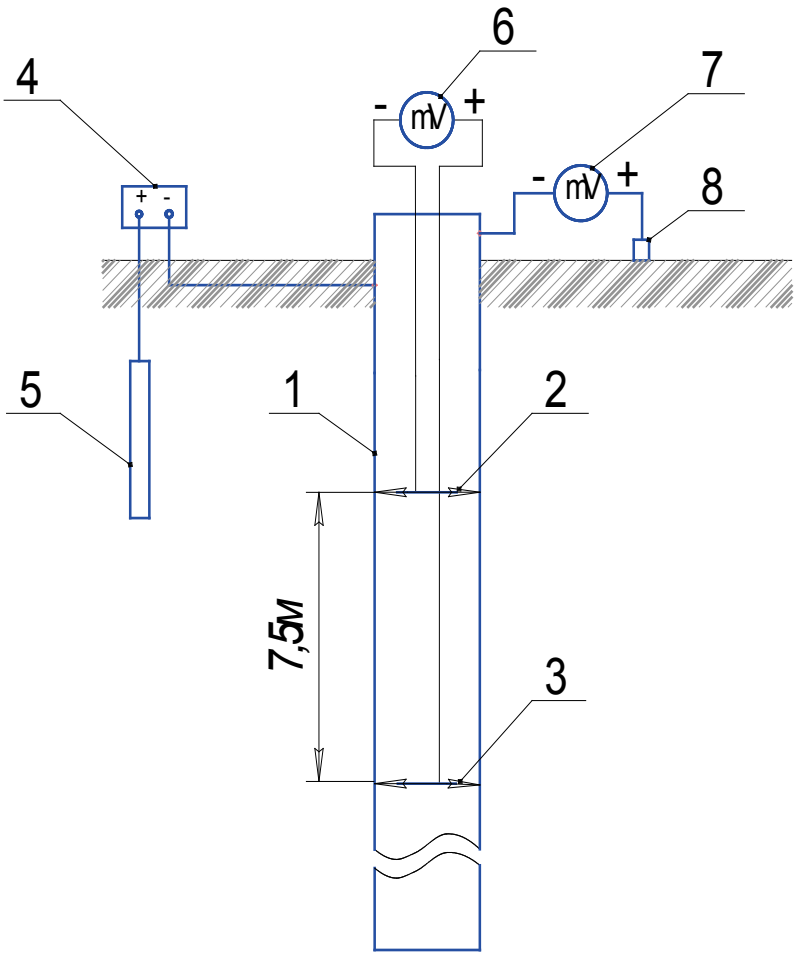

Fig. 5.6. Diagram of measuring the voltage drop on a well casing:
1 – Well casing; 2 – Upper contact unit of the probe; 3 – Lower contact unit of the probe; 4 – Adjustable DC source; 5 – Anode bed;
6 – Milli(micro)voltmeter; 7 – Millivoltmeter; and 8 – CSRE

Voltage drops on the casing are measured using a two-contact probe every 50 m within the studied interval in 30 s after the probe has been stopped. To measure voltage drops, measurement tools, such as millivoltmeters or microvoltmeters, are used, the input resistance of which must be at least 1 MOhm.

As an example, we have shown in Fig. 5.7 the voltage drop distribution among the probe contacts along the depth of the casing of well No. 22505 at OGPD Bavlyneft at the disabled cathodic protection (natural condition of the well casing) and at the protection current intensity of 6 and 12 A.

Analysis of experimental findings regarding the voltage drop along the casing depth has shown that discontinuous changes are observed at the depths of 50. 100. 150. 250. 300. 350. and 850 m. The changes observed can be related either to changing the casing metal resistance within the section under research or to the specifics of current running in the casing.

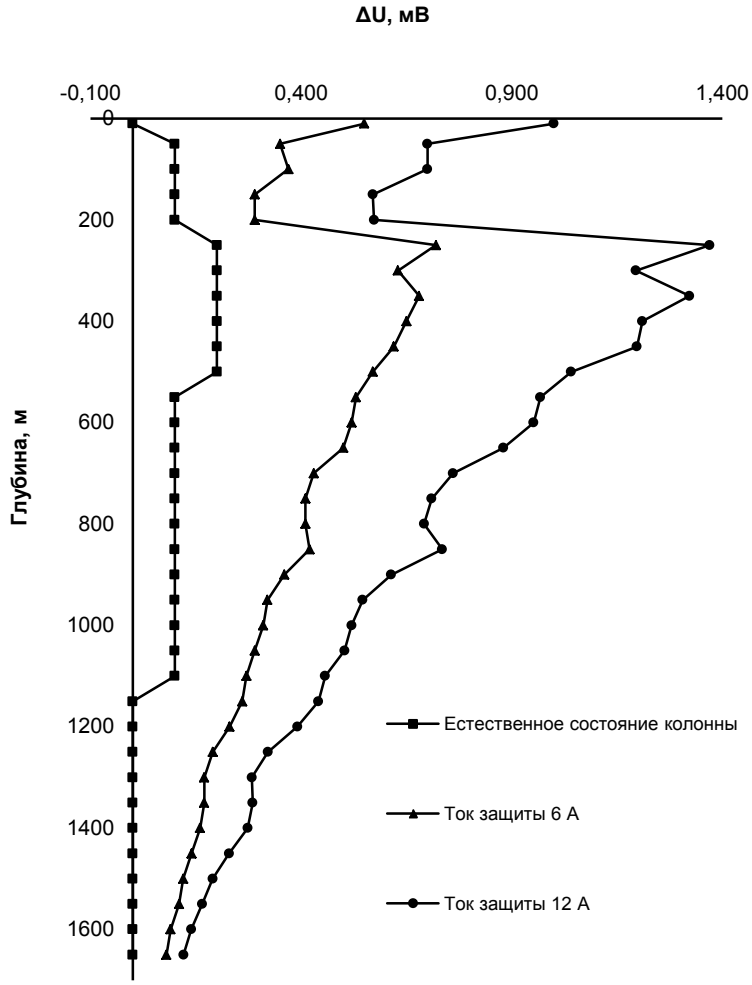

Fig. 5.7. Voltage drop distribution among the probe contacts along the depth of the casing of well No. 22505 at OGPD Bavlyneft

When computing the values of the intensity of current running through the relevant sections of the casing, based on data shown in Fig. 5.6. it was considered that the casing consists of three sections (Fig. 5.3) differing in their cross-section areas.

Cross-section areas of a casing at its different sections were computed by the known formulas:

– Production string $S_1 = \pi \cdot d_1 \cdot e_1$.

– Conductor $S_2 = \pi \cdot (d_1 \cdot e_1 + d_2 \cdot e_2)$, and

– Guide $S_3 = \pi \cdot (d_1 \cdot e_1 + d_2 \cdot e_2 + d_3 \cdot e_3)$,

where $d_{1–3}$ means the diameters of external pipe surfaces; $e_{1–3}$ means pipe thickness.

Cross-section areas of the sections of the casing under research, considering their changes in height, were:

– Section 1 (production string): AB = 1.757 m; d_1 = 146 mm; e_1 = 7.7 mm; $S_1 = \pi \cdot d_1 \cdot e_1 = 35.3 \cdot 10^{-4}$ m^2;

– Section 2 (conductor): BC = 274 m; d_2 = 245 mm; d_1 = 146 mm; e_2 = 8.9 mm; e_1 = 7.7 mm; $S_2 = \pi \cdot (d_1 \cdot e_1 + d_2 \cdot e_2) = 103.7 \cdot 10^{-4}$ m^2; and

– Section 3 (guide): CD = 32 m; d_3 = 324 mm; d_2 = 245 mm and d_1 = 146 mm; e_3 = 9.5 mm; e_2 = 8.9 mm and e_1 = 7.7 mm; $S_3 = \pi \cdot (d_1 \cdot e_1 + d_2 \cdot e_2 + d_3 \cdot e_3) = 200.4 \cdot 10^{-4}$ m^2 .

Resistivity of the casing sections between the probe contacts was found by formula:

$$R = \frac{\rho \cdot l}{S} \ (Ohm),$$

where ρ means the specific resistance of steel, equal to $18 \cdot 10^{-8}$ Ohm·m; l means the section length equaling to 7.5 m; S means the area of the transversal section, m^2.

For the casing under consideration, the resistances of the sections between the probe contacts are:

$$R_1 = \frac{\rho \cdot l}{S} = \frac{18 \cdot 10^{-8} \cdot 7.5}{35.3 \cdot 10^{-4}} = 3.8 \cdot 10^{-4} \ Ohm; \ R_2 = \frac{\rho \cdot l}{S} = \frac{18 \cdot 10^{-8} \cdot 7.5}{103.3 \cdot 10^{-4}} = 1.3 \cdot 10^{-4} \ Ohm; \ R_3 = \frac{\rho \cdot l}{S} = \frac{18 \cdot 10^{-8} \cdot 7.5}{200.4 \cdot 10^{-4}} = 6.7 \cdot 10^{-5} \ Ohm.$$

Current running through the controlled sections of the casing is computed by formula:

$$I = \frac{\Delta U}{R}, A,$$

where ΔU means the voltage drop between the probe contacts and R means the resistance of the casing section between the probe contacts.

Currents distribution along the casing length for the example under consideration is shown in Fig. 5.8.

Results of computing the distribution of currents along the casing depth, using its geometric characteristics (Fig. 5.7. curves 1 and 1*), have shown that, at the depth of 250 m, a rapid current intensity growth (5.53 A and 10.54 A for protection currents 6 and 12 A, respectively) is observed, followed by a similarly rapid drop. A probable reason for this current growth is the non-coincidence of the beginning of another section (conductor) with the position of the metal contact point between the production string and the conductor (aligner position). Due to that, the production casing resistivity was used in the computations of current intensity relevant to the depth of 250 m. Curves 2 and 2* represent the adjusted dependences reflecting the changes in the current intensity along the casing depth.

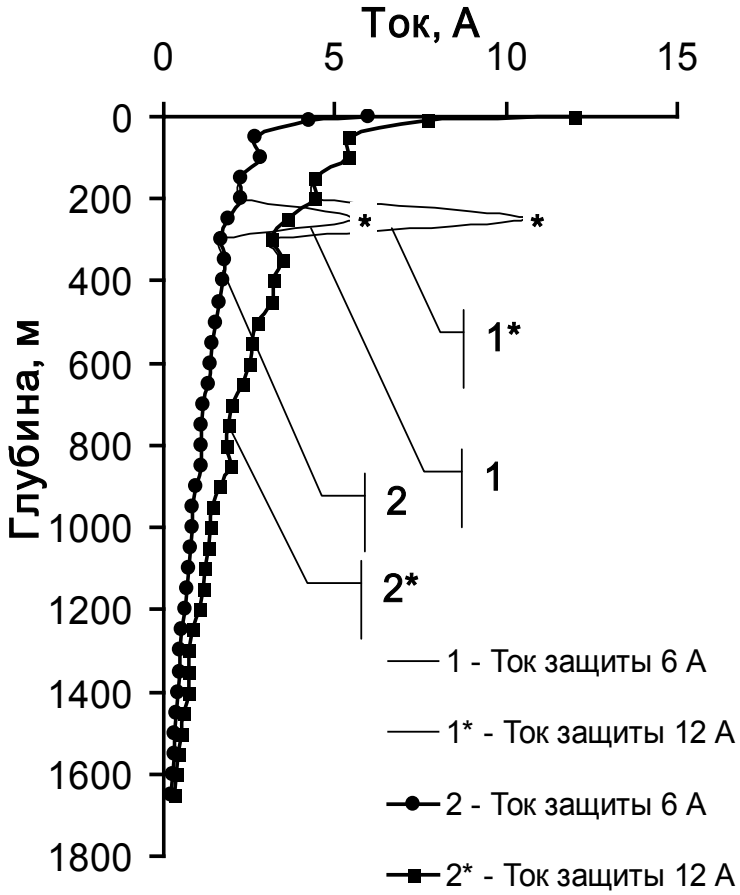

Fig. 5.8. Distribution of currents along the casing depth of well No. 22505 of OGPD Bavlyneft, at protection current 6 and 12 A: 1 – Computing by the geometric characteristics of the casing; 2 – Computing considering the position of a metal contact between sections

Observable decrease in the intensity of current flowing through the production casing, at the depth of 350-300 m, can be explained, in our

opinion, by the occurrence of stray current flowing from the production casing onto the conductor. At the depth of 100-50 m, a similar decrease in the current intensity is observed, explainable by the current flowing down from the conductor onto the guide.

Current flowing onto the production casing within each range (50 m), was computed by formula:

$$I = I_1 - I_2.$$

where I_1 means the current value at the initial point of the range (located above), A; I_2 means the current value at the end point of the range.

Some results of computing the intensity of current running onto the production casing between sections (including the one where the current flows from the casing) are given in Table 5.1.

Table 5.1

Results of computing the intensity (A) of current running onto the production casing

Range M		…	200 – 250	250 – 300	300 – 350	350 – 400	…
Protection current	6		0.34	0.24	–0.13	0.08	
	12		0.8	0.46	–0.33	0.29	

External surface area relevant to different well casing depth intervals was computed by formula:

$$S = \pi \cdot D_i \cdot l,$$

where D_i means the diameter of the i^{th} section of the casing, m; l means the distance of 50 m, at which the measurements are done.

Considering the diameters of the guide, conductor, and production string (D_1 = 146 mm; D_2 = 245 mm; and D_3 = 324 mm), the surface area of the i^{th} section was:

$$S_1 = 3.14 \cdot 0.146 \cdot 50 = 22.92 \text{ m}^2;$$
$$S_2 = 3.14 \cdot 0.245 \cdot 50 = 38.47 \text{ m}^2; \text{ and}$$
$$S_3 = 3.14 \cdot 0.324 \cdot 50 = 50.87 \text{ m}^2.$$

Cathodic protection current density distribution along the depth of a casing was computed by formula:

$$i = \frac{I_1 - I_2}{\pi \cdot D_i \cdot l}, \text{A/m}^2,$$

where I_1 means the current value at the initial point of the range, A; I_2 means the current value at the end point of the range, A; D_i means the diameter of the i^{th} section of the casing, m; and l means the distance interval, at which measurements are done.

Analysis of computation results (Fig. 5.9) has proven that the production string at its entire length is located under the cathodic protection, except for anode areas within the depth ranges of 300-350 and 800-850 m. Anode current density is 0.0057 and 0.014 A/m^2 for the first range and 0.0011 and 0.0049 A/m^2 for protection currents 6 and 12 A, respectively.

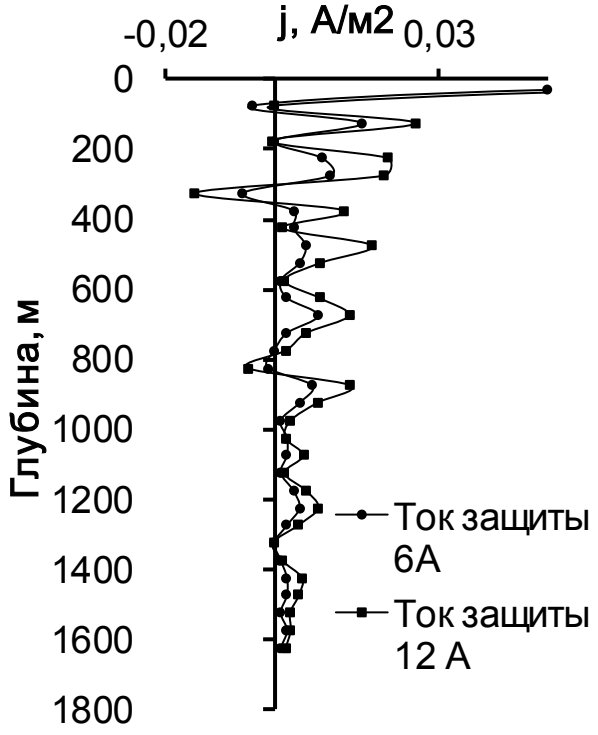

Fig. 5.9. Distribution of current densities along the casing length of well No. 22505 of OGPD Bavlyneft, at the protection current intensity of 6 and 12 A

Chapter Review

1. Finding protective current, using the method of polarization curves (electrical logging).
2. Finding protective current, using the method of identifying the voltage drop profile on the production casing.
3. Finding protective current using the method of calculating the potential shift in the wellbore and the value of resistance in the well-ground system.

Chapter 6. CONTROLLING THE CATHODIC PROTECTION SYSTEM PARAMETERS

6.1. Telemetric Control System Features

To enhance the operation reliability of an ECP system, it is necessary to ensure a high-level control over its electrochemical parameters.

Since 2010. telemechanization of cathodic protection rectifiers have been used on the premises of PJSC Tatneft to control and quickly and efficiently manage the ECP tools from central control rooms, which protection is realized by installing telemetry elements into cathodic protection stations [19-21]. The system can be installed directly in the rectifier-equipped cabinet or in a separate by-standing cabinet (Fig. 6.1).

Fig. 6.1. Cathodic protection stations of OGPD Leninogorskneft with the telemechanization system located inside CPS (left) and in a single cabinet (right)

Telemechanization devices for CPSs are currently widely used to control the ECP efficiency of oil pipelines at PJSC Transneft and gas pipelines at PJSC Gazprom. Information on equipping the CPS with the telemechanization system for different OGPDs of PJSC Tatneft as of November 21. 2017 are given in Table 6.1.

Table 6.1

Changes in introducing the telemechanization system
at PJSC Tatneft as of November 21. 2017

OGPD	CPSs, pcs.	Telemetry-equipped CPSs, pcs.	% of coverage
BN	526	526	100
AN	959	959	100
PrN	283	283	100
AzN	938	78	8.3
EN	601	218	36
LN	953	345	36.2
NN	719	0	0
NN (SVN)	222	0	0
YaN	334	127	38.0
YaN (SVN)	59	0	0
JN	1.212	279	23
Total for PJSC Tatneft	**6.806**	**2.815**	**41.4**

The main functions of a telemechanic cabinet are to collect analog and discrete signals and transfer data to the upper level. System telemetry performed: CPS output current, CPS output voltage, pipeline potential, and voltage regulation (setup).

Monitoring system ensures performing the following key tasks:

– Prompt and continuous control of main, such as potential, voltage, and current, and additional, such as operation mode, security alarm, etc., analog and discrete parameters of a CPS (Fig. 6.2);

– Remote control of the cathodic protection system; and

– Equipment diagnostics of CPS and TM (telemechanic) system.

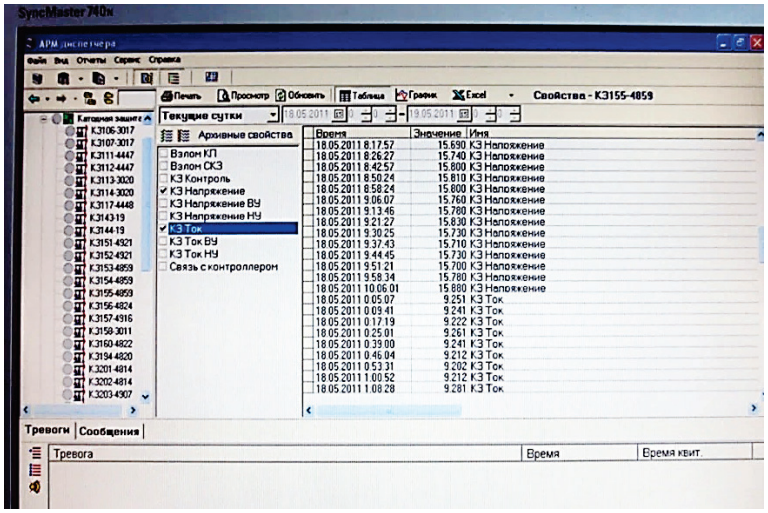

Fig. 6.2. Visualizing the cathodic protection station parameters in the personal computer monitor

Information is transferred to an upper level by the lower level initiative, i.e., in case of changing discrete signals or exceeding the analog value of the predefined sensitivity threshold, or by the top-down approach, i.e., when a command to update database is received from the upper level. This approach allows efficiently using low-bit rate links (radio channels) in data transfer.

All data is transferred from the lower level to the upper-level controller to the ECP service operator. Through the upper-level controller, the lower level is uploaded, diagnosed, and dECPgged remotely. The telemechanization system data types are telesignalization, telemeasurements, and telecontrol (Fig. 6.3).

Cathodic protection station information is necessary for the ECP services located at the distance of several hundreds of kilometers from each other.

Requirements to be met by a telemetric control system (TCS) include [21]:

– TCS consists of a telemetric cathodic protection efficiency control module (hereinafter, the “module”), the data from which are transferred via the well controller to the upper level, i.e., to the operator’s AWS of the Oil&Gas Production Workshop and to corrosion engineer’s workstation;

– TCS must ensure transferring the indications, such as current intensity, voltage, and unauthorized access, from the CPS via the module and the existing controller located on the well, considering various communications channels, to the operator’s AWS of the Oil&Gas Production Workshop and to corrosion engineer’s workstation, as well as

signaling the unauthorized access, archiving the indications, and viewing the data over the reporting period; and

– Informing with an emergency alarm on an outward/inward current intensity deviation by more than 20 % from the value set at commissioning, to the operator's AWS and corrosion engineer's workstation;

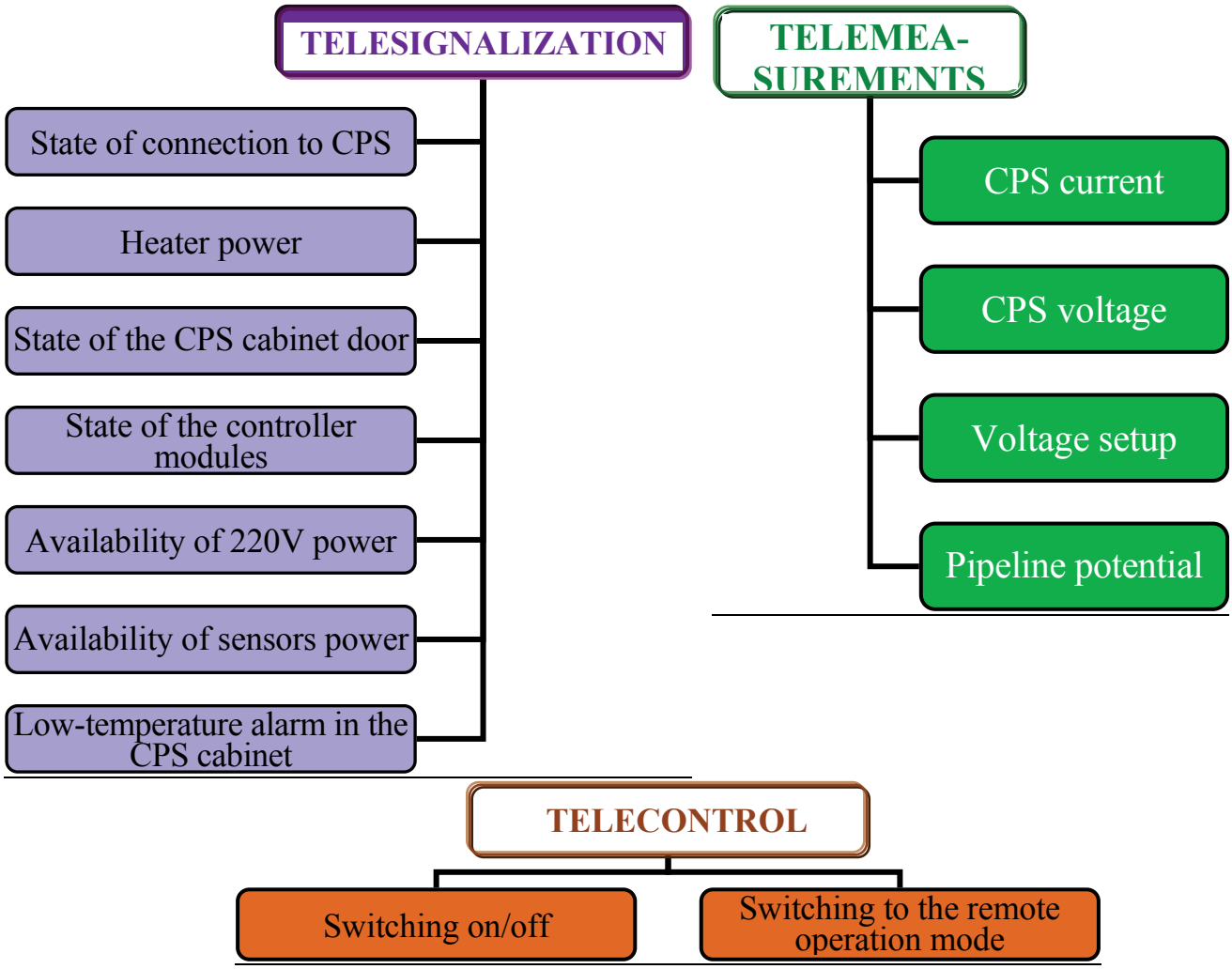

Fig. 6.3. Information transferred by the telemechanization system

– Archiving the values of the CPS current intensity and voltage at least once a week in the normal operation mode, and immediately archiving if the current intensity set at commissioning deviates from that value (in such a case, archiving must further take place at least once a day). Archive data must be stored with the corrosion engineer within the CPS service life and with the control center of the Oil&Gas Production Workshop within 6 months; and

– Viewing the values of the CPS current intensity and voltage over any time period in tabular and graphical forms. In Fig. 6.4. as an example, the changes in the current intensity and voltage values are shown graphically

that have been registered within 3 months using TCS. Graphics obtained in such a manner allow tracking parameters changing with the time and observing visible fluctuations (deviations) from the preset values, which can occur due to some reasons, such as seasons, cathodic protection station operation specifics, power outages, etc.

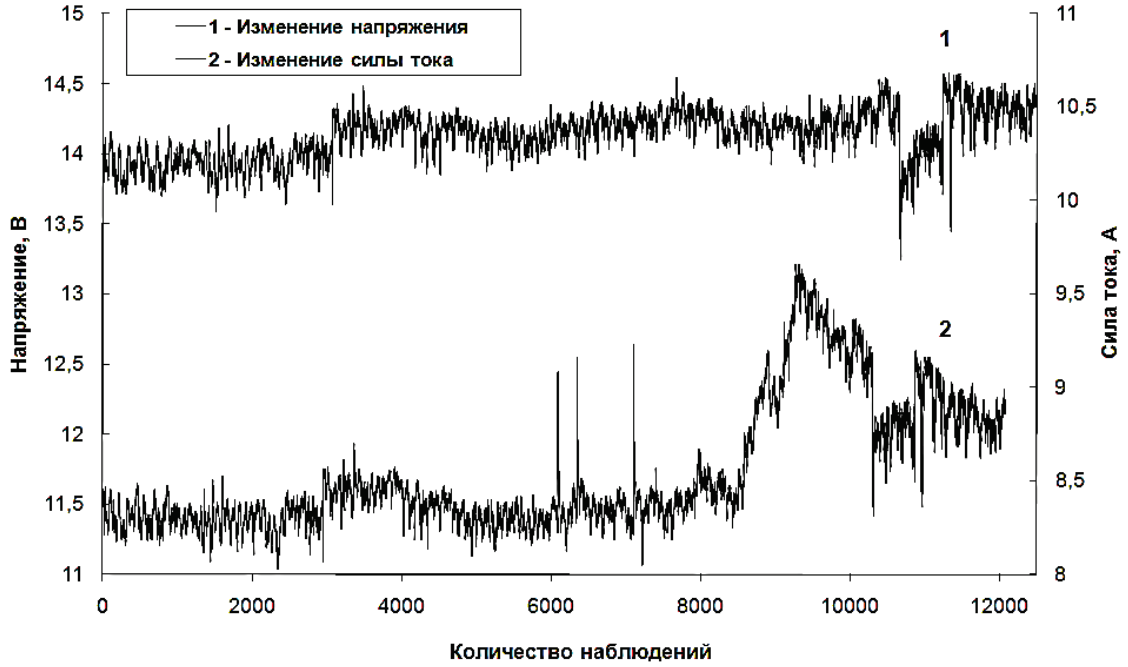

Fig. 6.4. Values of current intensity and voltage obtained using TCFs for well No. 172 at OGPD Bavlyneft

6.2. Modules of Controlling the Cathodic Protection Station Parameters

Any cathodic-protected well can be connected to the CPS parameters control system. A module is used to measure the CPS parameters, transform analog signals to digital signals, if necessary, and transmit signals.

According to technical specifications, 6 module options can be used at PJSC Tatneft, depending on the presence of a well telemechanization controller near the CPS and the distance between the CPS and such controller, as well as on the existing communications channel to transfer information via a modem [20]:

– Option 1 – Measuring the parameters and wire transfer of analog signals 4-20 mA to the analog inputs of the well controller;

– Option 2 – Analog sampling and wire transfer of a discrete signal to the RS 485 input of the well controller;

– Option 3 – Analog sampling and transferring the signal via a modem by radio channel FM 433;

– Option 4 – Analog sampling and transferring the signal via a modem by radio channel FM 160;

– Option 5 – Analog sampling and transferring the signal via a modem by cellular channel GSM; and

– Option 6 – Analog sampling and transferring the signal via a modem by a broadband wireless access channel.

Module option shall be selected in accordance with the conditions given in Table 6.2.

Table 6.2

Functional limits in selecting module options

Module options	Module application limits
Option 1	1. Presence of a well telemechanization controller near the CPS, with the required number of analog inputs 2. Distance from the CPS (module) to the telemechanization controller does not exceed 10 m
Option 2	1. Presence of a well telemechanization controller near the CPS, with free entrance RS 485 and Modbus protocol 2. Distance from the CPS (module) to the telemechanization controller does not exceed 1.000 m 3. Possibility to lay a twisted-pair wire from the module to the controller
Option 3	1. No well telemechanization controller near the CPS 2. Data can be transferred via a radio modem within the band of 433 MHz 3. Maximum communications distance is 400 m within the line of sight up to the signal receiver
Option 4	1. No telemechanization controller near the CPS 2. Data can be transferred via a radio modem within the band of 160 MHz 3. Maximum communications distance is 20 km
Option 5	1. No well telemechanization controller near the CPS 2. Data can be transferred via a GSM/GPRS modem
Option 6	1. No telemechanization controller near the CPS 2. Data can be transferred via the broadband wireless access channel 3. There must be a line of sight up to the signal receiver

If it is possible to transfer data via several channels, the lower-cost module option should be preferred. Upon selecting an option, the module is connected to the CPS and to the well telemechanization controller, if necessary, in accordance with the user manual of the specific module.

Upon mounting, the module operability is verified, and measurement channels are calibrated as follows:

– Testing the CPS current value for its compliance with the design value; if necessary, the current value must be adjusted;

– Opening the CPS cabinet door and registering the emergency door opening signal at the operator's AWS;

– Measuring current and voltage (and potential, if there is a potential measuring channel) at the CPS output with a control devices marked as calibrated, and registering the values of the same parameters at the operator's AWS. Measurements are performed for three current intensity values: The one relevant to the design/working value, the one 20 % higher, and the one 20 % lower than the working value. Current intensity must be measured by CPS conducting bridge voltage drop (the module must be connected to the same bridge);

– Should the control device indications differ from those at the operator's AWS by more than 10 %, then adjustment factors must be entered in APCS so that the APM indications correspond with those of the control device;

– The values of the upper and lower current intensity limiting values shall be set at the operator's APM, at which values the alarm must actuate. The lower limit must be 20 % lower than and the upper limit must be 20 % higher than the working value of current. The limits must be set with an accuracy of up to 0.1 A; and

– Testing alarm actuation, in case of the current intensity deviating from the working value; for this purpose, the current intensity of the facility shall be increased/decreased by more than 20 %.

Within the entire CPU operation period, parameters must be registered in the APCS and in the Pipework System Operation Accounting & Analysis program. In APCS, the parameters must be archived in the operation mode (if the current value changes by at most 20 % of the design value) at least once every two hours, while in emergency mode (if the current intensity deviates by more than 20 % from the design value) they must be archived immediately upon reaching the limit value, and then at least once an hour; in the Pipework System Operation Accounting & Analysis program, the

values measured in the operation mode must be archived at least once a week.

Should the CPS operation parameters deviate from working values, ECP service professionals should be sent to the well to identify the causes of such deviation. If possible, the deviation cause is eliminated on site or CPS/C(S)PU repair request is submitted.

Chapter Review

1. Telemetry system and its purpose.
2. Selecting a telemetry system module.

Chapter 7. METHODS OF MONITORING THE TECHNICAL AND CORROSION CONDITION OF AN OIL-WELL CASING

7.1. Essential Elements of Monitoring

Integrity and environmental safety of a well as a complex engineering structure are largely determined by the technical and corrosion condition of its casings that are its key support elements. Technical condition shall mean the cluster of the object properties that may change while being operated and that are characterized at a certain moment by the features defined in the object technical specifications or to be defined at certain time intervals [22].

Key tasks of monitoring are:

– Obtaining background curves characterizing the initial technical condition of casings and of the cement sheath in order to generate a "data sheet" of the technical conditions of the well supports;

– Identifying the wearing zones of well casings, the residual pipe thicknesses, and their residual strengths;

– Detecting leaks and cracks along the bodies of casing pipes, as well as identifying their nature, i.e., whether they are longitudinal, transversal, or directed at an angle to the casing axis;

– Identifying the intervals of intense corrosion and through-corroded areas of well casings;

– Detecting leaking socking joints or other leakages in well casings; and

– Identifying the condition of the cement sheath and detecting the intervals of behind-casing fluid movements.

Technical condition of wells is studied using geophysical methods at all stages of the well life, i.e., construction, operation, workover, and abandonment. Completeness and integrity of data obtained are determined by well design (presence of oil-well tubing or underground equipment, multistring structures, etc.), well conditions, monitoring techniques, the GIS complex used and the technical capabilities of geophysical well appliances, and the system-based approach to measurements.

7.2. Geophysical Research Methods

Currently, a variety of geophysical research methods exists and is successfully used to study the technical condition of well casings (Fig. 7.1), and activities continue aimed at improving them [23].

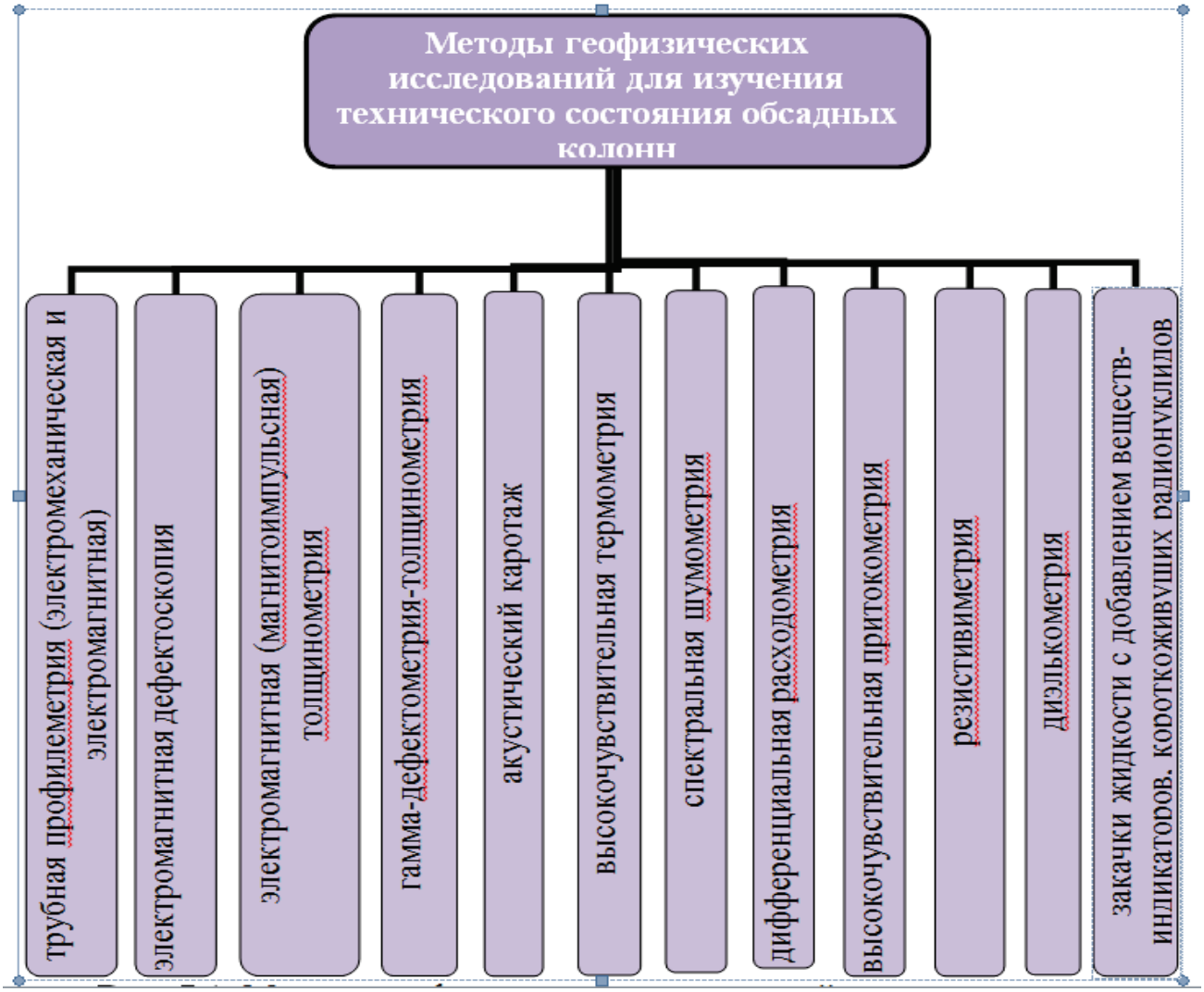

Fig. 7.1. Geophysical research methods used to study the technical condition of well casings

Geophysical research in wells are conducted using special installations that include surface and downhole equipment interconnected via a communication channel, i.e., a logging cable, as well as a pulling-and-running mechanism ensuring the movements of downhole devices along the well cellar.

Below are some methods directly applicable to evaluating the corrosion condition of well casings.

7.3. Electromagnetic Inspection

7.3.1. Electromagnetic Detectors of the EMDS-TM and EMD-S Series [24]

Hardware and software of an electromagnetic inspection and gaging complex (EMWD–TM), based on analyzing the electromagnetic field in the non-stationary mode allows solving the problems of qualitative and quantitative in-process inspections of well casings (for example, measuring the well thickness with an accuracy of up to 0.5 mm) through the oil-well tubing of production and injection wells. Hardware tools differ in the numbers and dimensions of probes, in signal registration time intervals, and, accordingly, in their release capabilities.

In Fig. 7.2. the block diagram is shown for the design of well apparatus EMWD–TM–42. One of the advantages of such a complex of probes is the presence of the smaller, *C*, and the larger, *A*, axial probes, which allows quite uniquely associating the defects detected with the first (internal) or second (external) string.

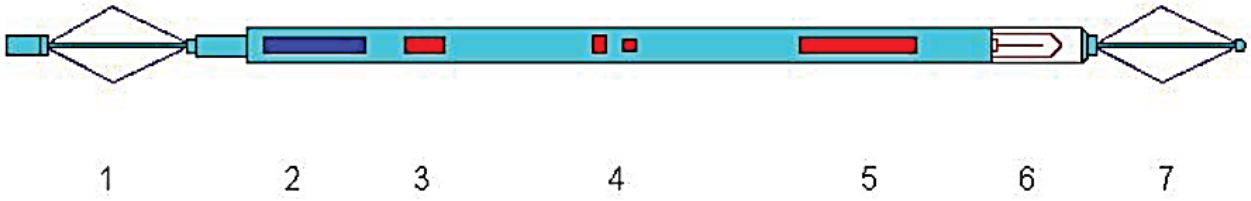

Fig. 7.2. Layout of the probes of the EMWD-TM-42 series small electromagnetic detector: 1 – Upper centering aligner; 2 – Block-gamma; 3 – Short axial probe C; 4 – Transversal probes B and BB; 5 – Long axial probe A; 6 – Thermometer; 7 – Lower centering aligner

Steel string defects, such as longitudinal or near-longitudinal ones, are registered relatively easily by the intensive anomalies of the axial probe that is primarily used in gaging. To enhance the vertical characteristic of the probe (reducing the dependence on the non-uniformity of the electromagnetic parameters of a string), it is reasonable to shorten it to the length of approximately 5 cm. With increasing the crack length, the anomaly amplitude increases; the crack width is not significant for the crack interrupts eddy currents along the pipe circle. Using the non-stationary measurement mode allowed combining the exciter coil and the pickup coil and creating a small transversal probe measuring the radial component of electromagnetic field.

Basic technical specifications of electromagnetic inspection machinery EMWD-TM-42:

– Maximum diameter of the external pipe – 426 mm;

– Minimum internal diameter of the internal pipe – 60 mm;

– Maximum wall thickness of one pipe – 12 mm;

– Minimal wall thickness of one pipe – 3 mm;

– Maximum wall thickness of two pipes – 25 mm;

– Acceptable value limits of relative measurement error: Relative change in the wall thickness in a single pipe – at most 5 %; and that of the thickness of the relative change in the external pipe wall in two-string structures – at most 15 %;

– Minimum length of the crack-type defect along the pipe axis, available to detection, must be, in mm: When inspecting a single pipe with the 500-mm diameter – 50-225 mm; when inspecting the internal pipe of two- and three-string structures, 75 mm; when inspecting the external pipe of two coaxial pipes, in mm: 100 for the diameter of 146 mm, 150 for the diameter of 168 mm, 175 for the diameter of 245 mm, and 200 for the diameter of 324 mm; and

– Maximum allowed rate of running the downhole device along the well to achieve better granularity (at least one measurement per each 5 cm): 0.166 m/s (400 m/h) in basic observations and 0.055 m/s (200 m/h) in detailed observations.

Based on theoretic and model studies, the main constructs of probe systems were created to solve the problems of measuring the string wall thickness and to solve the problems of searching for minor local defects (series EMWD–C, Fig. 7.3).

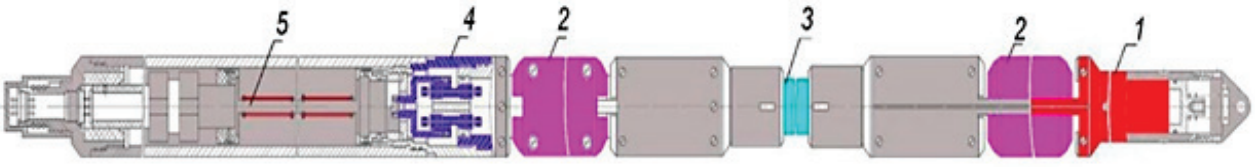

Fig. 7.3. Block diagram of an electromagnetic detector with scanning elements, EMWD-C: 1 – Protector module; 2 – Sensors module; 3 – Generator module; 4 – Switch module; and 5 – Electronics module

EMWD–C is designed for solving the following problems:

– Closely investigating a string by several elements, detecting defects, and identifying their forms and sizes;

– Identifying the string wall thickness by several elements and averaging it along the circle; and

– Detecting and locating drilling and cumulative perforation holes.

The main feature of these devices is placing probes intended for registering minor defects into special hold-down containers sliding over the well wall. This design allows essentially enhancing the ratio between the defect signal and the background fluctuations determined by the inhomogeneity of the electromagnetic properties of a casing. Anomaly from a minor hole-type defect decreases rapidly with moving away from the wall (quicker than $1/R^2$), while anomalies from electromagnetic inhomogeneities reduce remarkable slower with the distance increasing.

Probe part of the devices is limited with four contact probes, each of which explores a casing sector of 90 degrees, slightly overlapping. Granularity is quite sufficient for separating by components the components of perforation holes created by perforator PK-105 punching in four directions.

Four probes for differential wall thickness measurements in individual sectors were placed in the same hold-down containers as the probes for minor defects. Along with contact probes, the detector contains four integral probes – two axial and two transversal ones, both located on the device axis. Integral probes allows distinguishing and confidently recognizing the types of defects, such as longitudinal and transversal cracks or corrosion areas, as well as identifying the wall thickness averaged along the circle.

When logging, the detector represents a rigid assembly. When being transported, the electronics module can be detached from other modules. Casing device contains a theoretically reasonable group of electromagnetic probes, differently sized, oriented, and configured. Alternating electromagnetic field generated by exciter coils launches eddy currents in the casing, while measuring coils, i.e., sensors, register the secondary magnetic field of eddy currents. Time-series field amplitude depends on the casing wall thicknesses and on the presence of string defects.

For all four differential sensors, one exciter coil is used, located in the generator module, while other exciter coils are placed in combination with relevant measuring coils. Signals from sensors modules are transmitted to the electronics module through a sealed connector in the switch module. Here, signals from all sensors are amplified, pre-processed, digitized, and transmitted to the surface via a telemetric communication line. The module operates in two mutually exclusive modes: “Thickness” and “Defects.”

Basic technical specifications of the EMWD–C electromagnetic detectors:

– Casing wall thickness measurement range – 3-12 mm;

– Basic relative error of measuring the casing wall thickness averaged along the circle – 10 %;

– Basic relative error of measuring the casing wall thickness for each sector – 20 %;

– Minimum length of crack- and pit-type defects – 75 x 0.5 mm;

– Minimal dimensions of local hole-type defects available to detection – 12 mm;

– External diameter of the casing under study – 146-168 mm;

– Maximum temperature in the well – 120° C;

– Maximum hydrostatic pressure – 80 MPa;

– Power consumption – 15 W; and

– Dimensions of the casing device: Diameter 112 mm; length 3.100 mm; detector weight 110 kg; ground-based control console weight 6 kg.

In Figs. 7.4-7.7. flaw patterns are shown that have been obtained from the electromagnetic inspections of well casings.

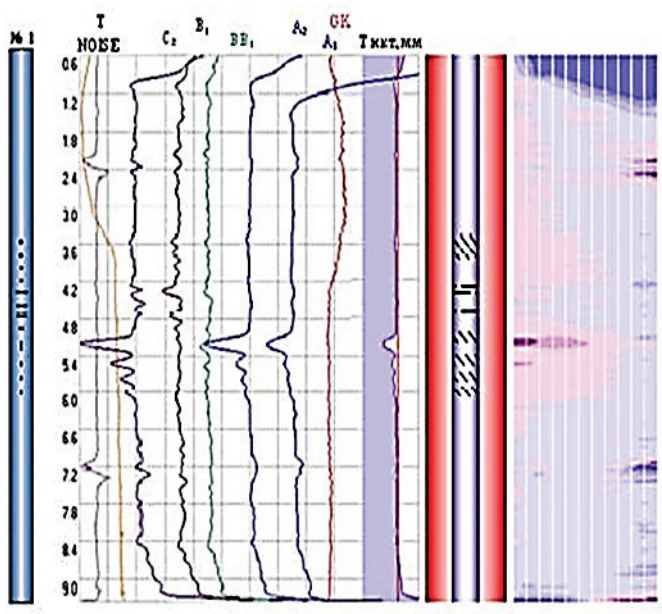

Fig. 7.4. Crevice-type string damages detected in single- and multistring structures

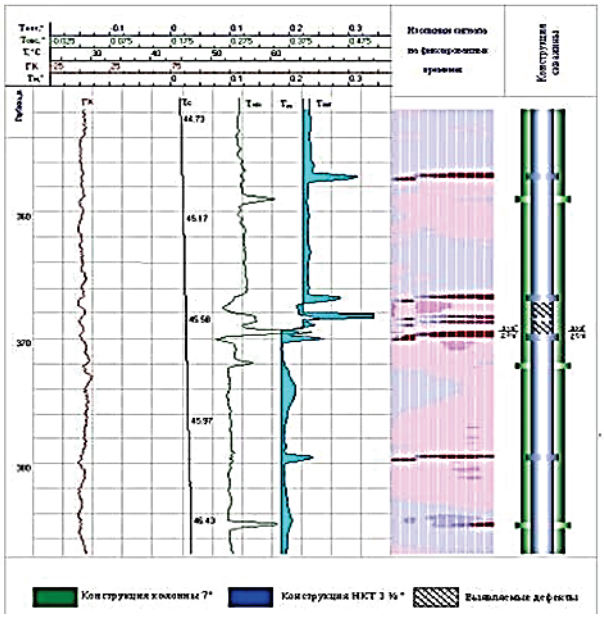

Fig. 7.5. Effects of EMWD–TM–42. Fahud-97 Deposit, Oman

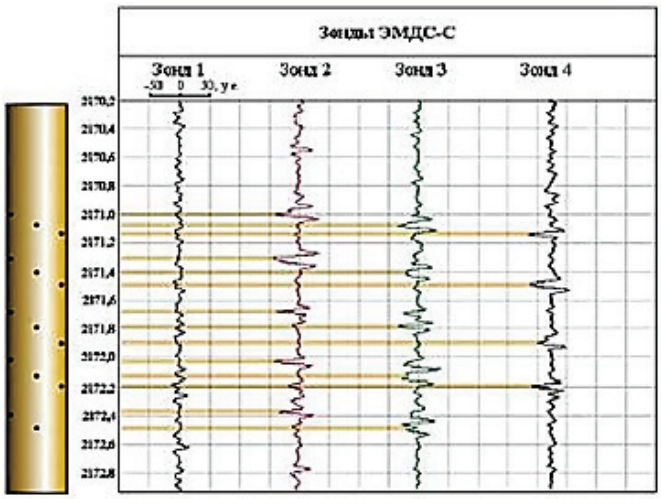

Fig. 7.6. Effects of using EMWD-C in detecting perforation holes PK-105C. 10 holes/m, string 168 mm. Well 2. Nizhnevartovsk, Russia

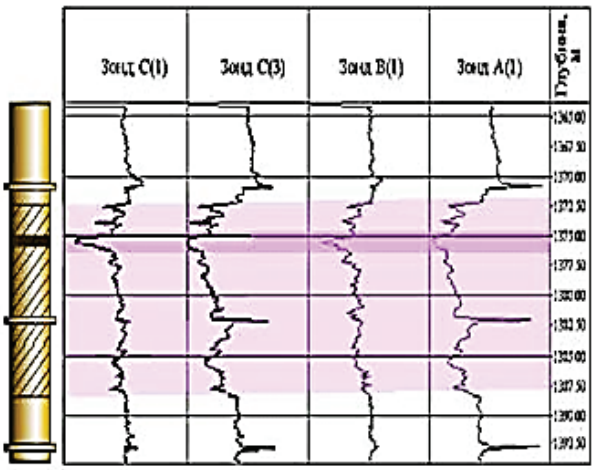

Fig. 7.7. Effects of using EMWD-C in detecting corrosion development intervals. Well. 704. Tuymazy Oil Field, Russia

7.3.2. Magnetic-Pulse Testing-Based Technology [25]

Currently, it is a relevant task to develop a technique aimed at solving the problems of defect detection in non-killed wells without pulling the OWT in the conditions of multistring structures. MID-K, the equipment designed for performing magnetic-pulse testing and gaging, can be successfully used to control the technical conditions of well casings directly in oil and gas wells being operated, while information obtained in such testing and gaging would be important for making further decisions regarding the operation modes of such wells (Fig. 7.8).

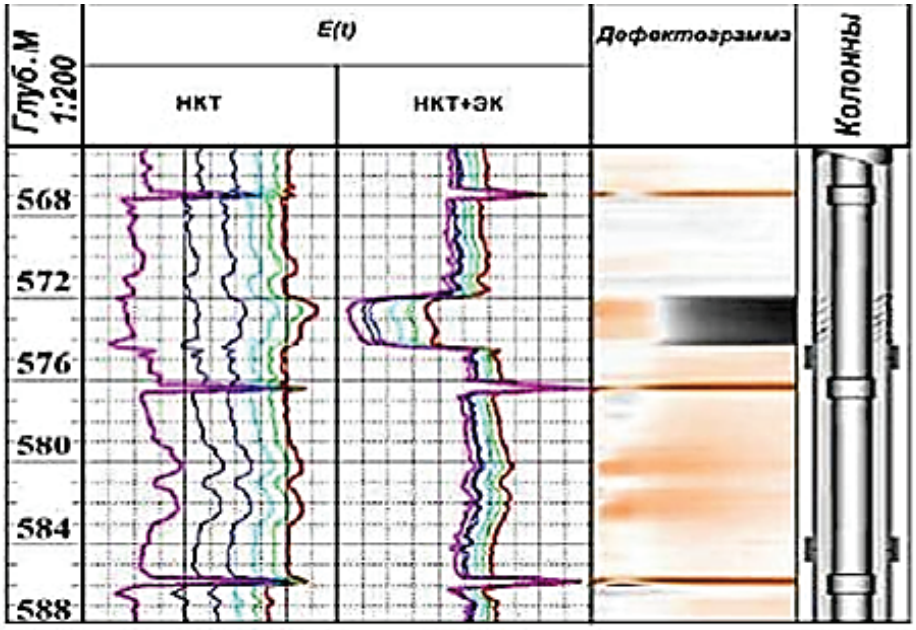

Fig. 7.8. Exemplary testing in a production string via TBG

7.3.3. Electromagnetic Detectors of the Pipe Analysis Logs Series [26]

Well casing quality evaluation with electromagnetic detectors of pipe analysis logs includes separating of internal and external defects of a well casing. This method is primarily used to detect small holes or defects. High-frequency eddy current identifies the defects on the internal wall of a string, while MFL reflects the thickness of the entire casing. Using such measurements, minor defects and corrosion areas are distinguished that can be identified on the internal or external side of a casing. The device registers signals from 24 sensors (12 magnetic flux sensors and 12 high-frequency eddy flux sensors) to ensure the complete coverage of the casing surface. Combining this device with other tools, such as geometry tool and sonic imager, it is possible to detect and identify defects on internal and external strings in two-string structures.

In Fig. 7.9. PAL registration is shown, aimed at evaluating the casing corrosion. Perforated within the intervals of 1.145-1.160 feet.

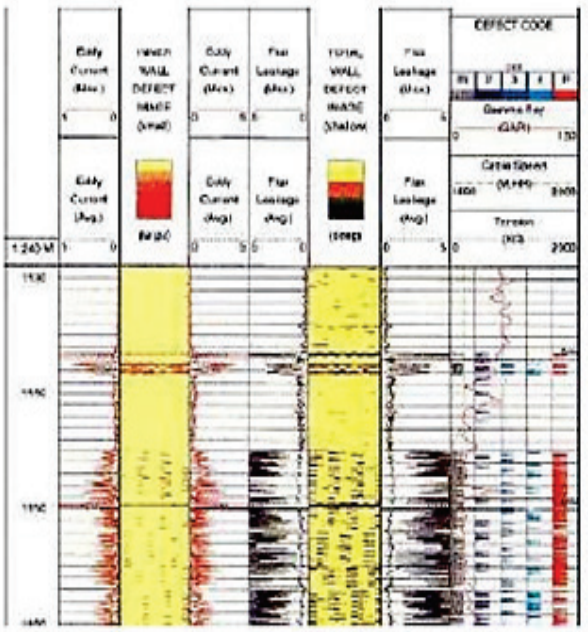

Fig. 7.9. PAL recording to evaluate the string corrosion. Perforated within the intervals of 1.145-1.160 feet

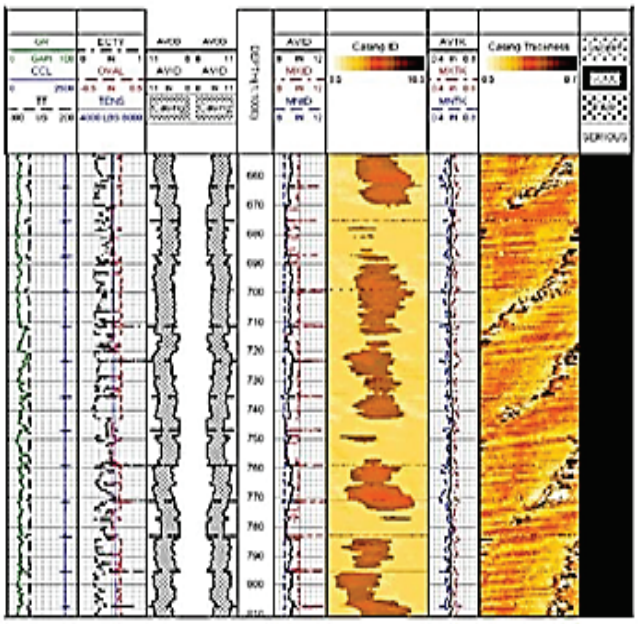

Fig. 7.10. Diagram with corrosion areas outside and inside the string

Corrosion areas inside and outside the string are shown in Fig. 7.10. Development of the casing ID) shows the ovality of the string: Dark red is the larger diameter, pale is the smaller diameter. Development of the casing thickness shows possible cracks in the string (Fig. 7.10).

7.3.4. Multifrequency Electromagnetic Thickness Tool METT Schlumberger [27]

Multifrequency electromagnetic thickness measurer METT (Fig. 7.11) uses non-destructive and non-contact induction methods to detect metal losses and changes in the casing form, independently of what fluid type was used to fill the casing. METT is usually applied to detecting large-scale corrosion damages and can also be used to detect metal losses on the external casings of multi-casing wells.

Fig. 7.11. Multifrequency electromagnetic thickness measurer METT

Applications:

– Locating corrosion damages in arrangement with one or more casings;

– Evaluating the residual resource of a casing; and
– Evaluating the corrosion protection system efficiency.

7.3.5. Metal Thickness Tools Sondex [28]

Corrosion damage degree can be evaluated by combining metal gaging and external visualization with internal radial measurements. Sondex offers two additional tools ensuring, along with multifinger imaging tool, the visualization of the entire pipe, as well as extremely accurate data on metal thickness.

Ultrasound gaging tool with a diameter of 21/8 inches is equipped with six transceivers installed on shoes that move on the internal surface of the pipe under research. The output signal of the device is determined by the run period of ultrasound pulses running through the resting metal and echoing from the opposite side.

Magnetic Thickness Tool (MTT) distinguishes through small dimensions (its diameter is 111/16 inches), due to which it rungs through the production OWT to study the main casing (Fig. 7.12). The tool generates an alternating magnetic field that extends over the external metal surface. The tool is rigged with 12 sensors located along the circle inside the casing or OWT under research. Each sensor registers local deviations determined by the deviation thickness in an alternating magnetic field when it returns to the casing. Twelve output signals ensure the sufficient amount of data for a three-dimensional visualization of the thickness under research.

Combining the three control techniques above ensures obtaining the best possible information on the well condition, which helps plan well workovers more accurately.

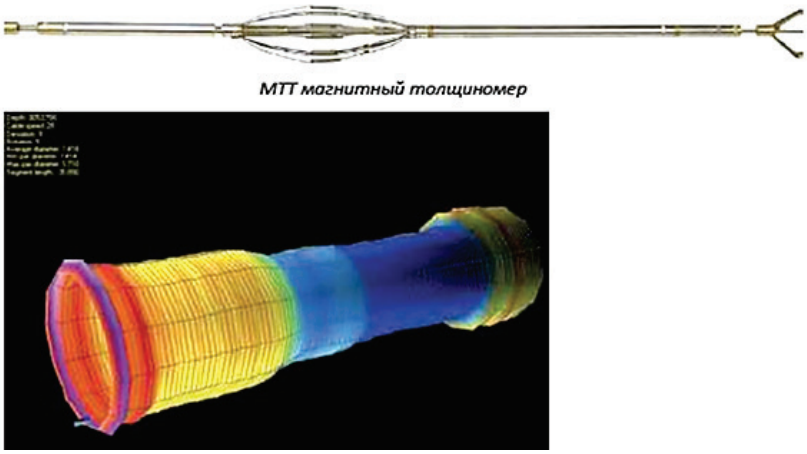

Fig. 7.12. A three-dimensional image demonstrating the decrease in thickness of a single well-casing section

7.4. Diagnosis Technology Using Scanning Magnetic Introscopes [29]

Using their experiences in diagnosing and monitoring the states of pipelines, Tatar Oil Research and Design Institute (TatNIPIneft) and Technical Diagnosing Center Introsco have developed a FS diagnosis technology using scanning magnetic introscopes (SMIs) [30]. SMI operation [31. 32] is based on magnetic flux leakage (MFL) registration method. SMI contains (Fig. 7.13) a magnetizer and a multielement system of MFL sensors.

Magnetizer creates a magnetic flux in the FS walls. When it passes through the area of an FS wall having defects or other specificities, a magnetic pattern is formed at the internal surface of the FS wall, represented as the superposition of the magnetizing field and stray magnetic field from the FS defects and specificities. As the SMI moves within the FS, the magnetic pattern is read, the sizes and nature of which can infer the parameters and defects of the FS wall.

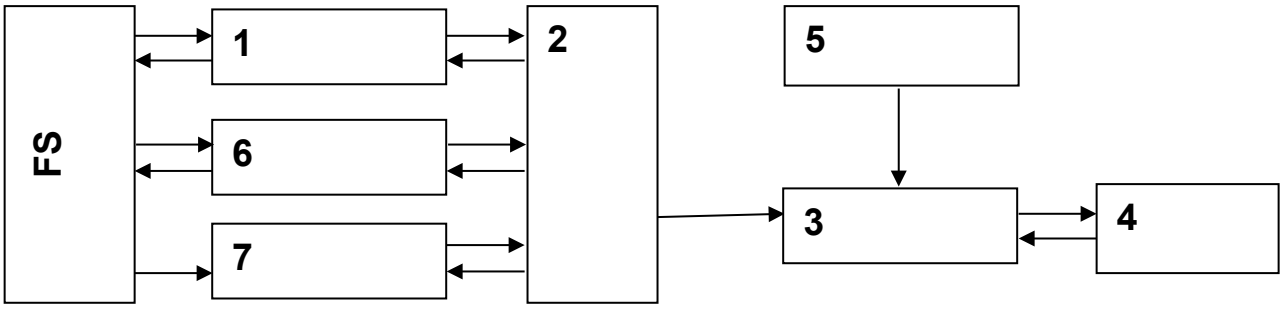

Fig. 7.13. Block diagram of the scanning magnetic introscopy system:
1 – Main magnetometering system; 2 – Onboard controller;
3 – Ground controller; 4 – Personal computer; 5 – Selsyn;
6 – Additional module; 7 – Complexation sensors

Advantages of SMI in solving the key tasks of well inspection, using the MI-5X series introscopes, are linked in Table 7.1.

In design terms, the well module of scanning Introscope MI-50 consists of three units (Fig. 7.14) located in a single casing: Magnetic introscopy unit (Introscope scanner), magnetic-pulse thickness gaging unit (thickness gage), and gamma ray (GR) logging unit. The GR unit serves for "anchoring" the entire obtained information to the geological profile, as well as for detecting radio-geochemical anomalies that may be an indirect sign of the fluid leaking beyond the string within the range of its defects,

while the thickness gaging unit is intended for identifying the FS wall thickness averaged by circle.

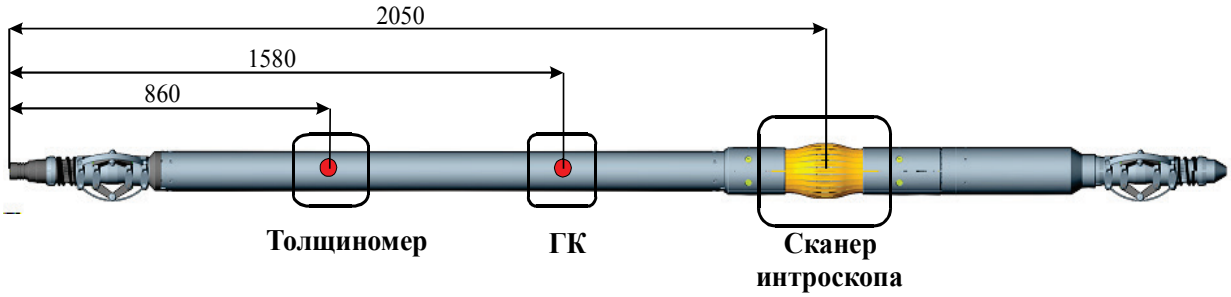

Fig. 7.14. Design of the magnetic well Introscope MI-50

Table 7.1

Advantages of using SMI in diagnosing the corrosion state of a well casing

Sl. No.	Main tasks of well inspection	Features of magnetic Introscope MI-5X
1	Detecting the poor tightness of strings	Detecting through-holes of D > 4 mm and cracks > 30 mm long
2	Detecting the locations of intervals and the perforation quality	Measuring the coordinates of and counting perforation holes, the positions and lengths of perforation intervals along the string depth with a measurement accuracy of ± 1 cm
3	Evaluating the quality of socket joints and of the FS design elements geometry	Identifying and measuring the dimensions and positions of sockets (with identifying the annuli), aligners, cement shoe, and other ferromagnetic design elements
4	Calculating the pipe wall thicknesses	Detecting the integral thickness of pipe walls with an absolute accuracy of 0.4 mm
5	Evaluating the defectiveness of pipes	Measuring the coordinates of defects along the string depth, measurement accuracy being ± 1 cm. The unit registers the coordinates, types, forms, geometry, and orthographic sizes of defects, such as “metal loss” or “crack” exceeding in depth 0.2 of the string wall thickness

Indications of all SMI units are set to correspond with the FS depth, using an odometric unit (selsyn) to be installed at the well head. Information on the defects detected is registered with a stationary or portable computer of the logging station. Defects are detected, recognized,

and evaluated by analyzing the magnetograms obtained while logging. Software supplied as part of the Introscope allows decoding magnetograms and interpreting the inspection data, as well as preparing reports and archiving the control results (Fig. 7.15).

The software (SW) allows processing the data obtained from all the SMI functional units: Magnetic introscopy, thickness gaging, and gamm-logging. The SMI depth counting system is calibrated in laboratory conditions, using special standard length samples. The necessity of it is determined by using for determining a depth the standard odometric equipment of geophysical crew, the accuracy of which cannot be pre-evaluated in manufacturing the SMI. To gage the SMI indications, an FS sample is used, which has standard defects. While gaging, the indications from standard defects are registered. Going forward, they are used in interpreting diagnostic data to evaluate the parameters and specificities of FS. In geophysical activities aimed at inspecting a FS, recording the diagnostic data into computer memory is accompanied with a simultaneous display on its monitor the current diagnostic information that allows rotating the image, eliminating clutter, selecting the correspondence of color and indications, etc.

Interpretation is the most important stage of processing diagnostic information. Currently, interpretation can be performed manually or semi-automatically.

Main characteristics of magnetic Introscope MI-50:

– Maximum wall thickness of the well casing to be inspected – 11 mm;

– Maximum diagnostics rate – 0.2 km/h;

– Minimum diameter nominal of the through-hole-type defect to be detected – 4 mm;

– Minimum size of the corrosion-cavern-type defect to be detected (length/width) – 10/10 mm;

– Minimum size of the transverse-crack-type defect to be detected (length/opening) – 30/10 mm;

– Depth as percentage of the wall thickness – 40 %; and

– String thickness gaging error – 0.4 mm.

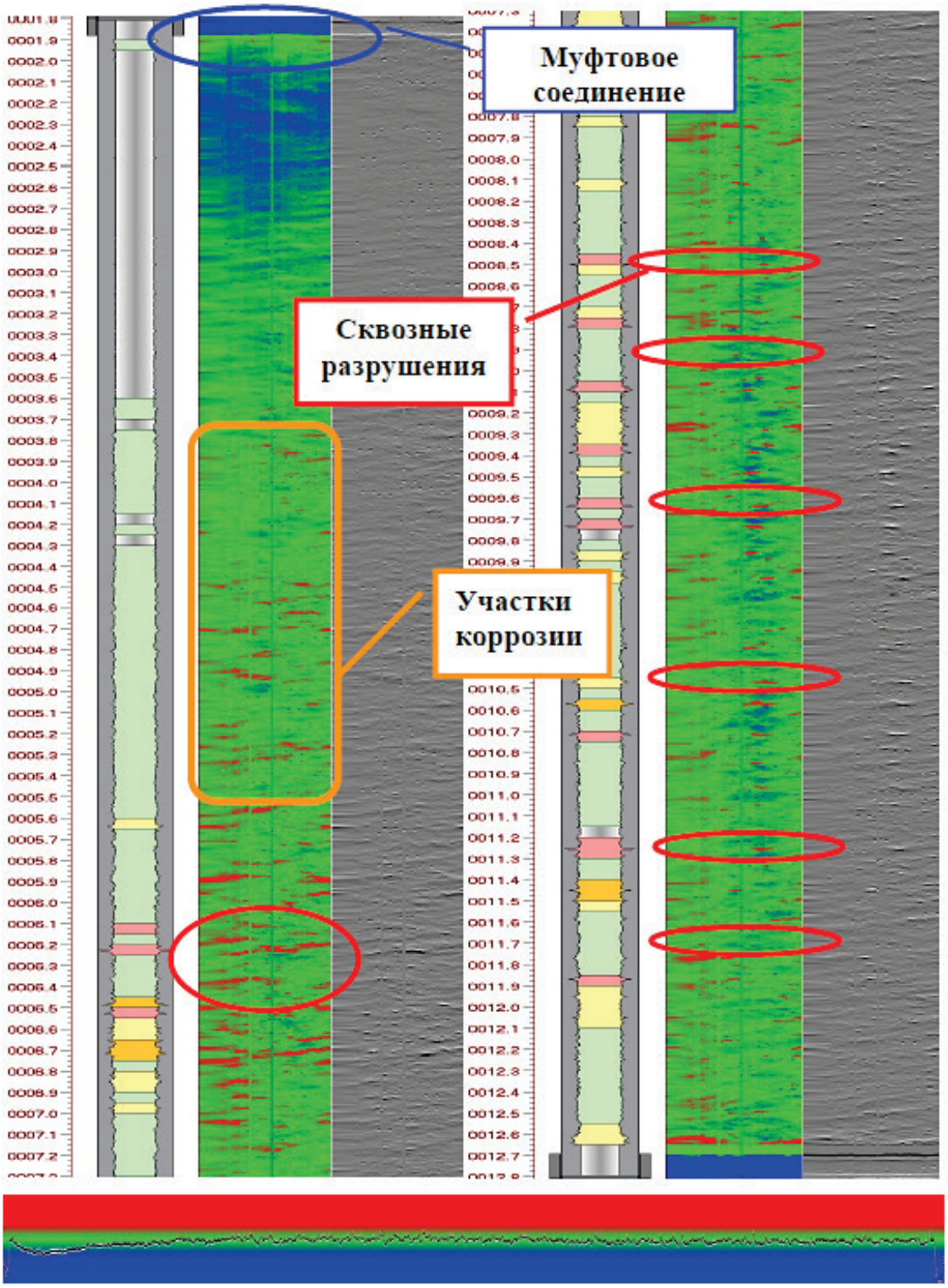

a

Fig. 7.15. Magnetogram of the sections of FS No. 2691 at OGPD Aznakaevskneft within the intervals: a – 1.8-12.8 m; b – 149.9-157.5 m

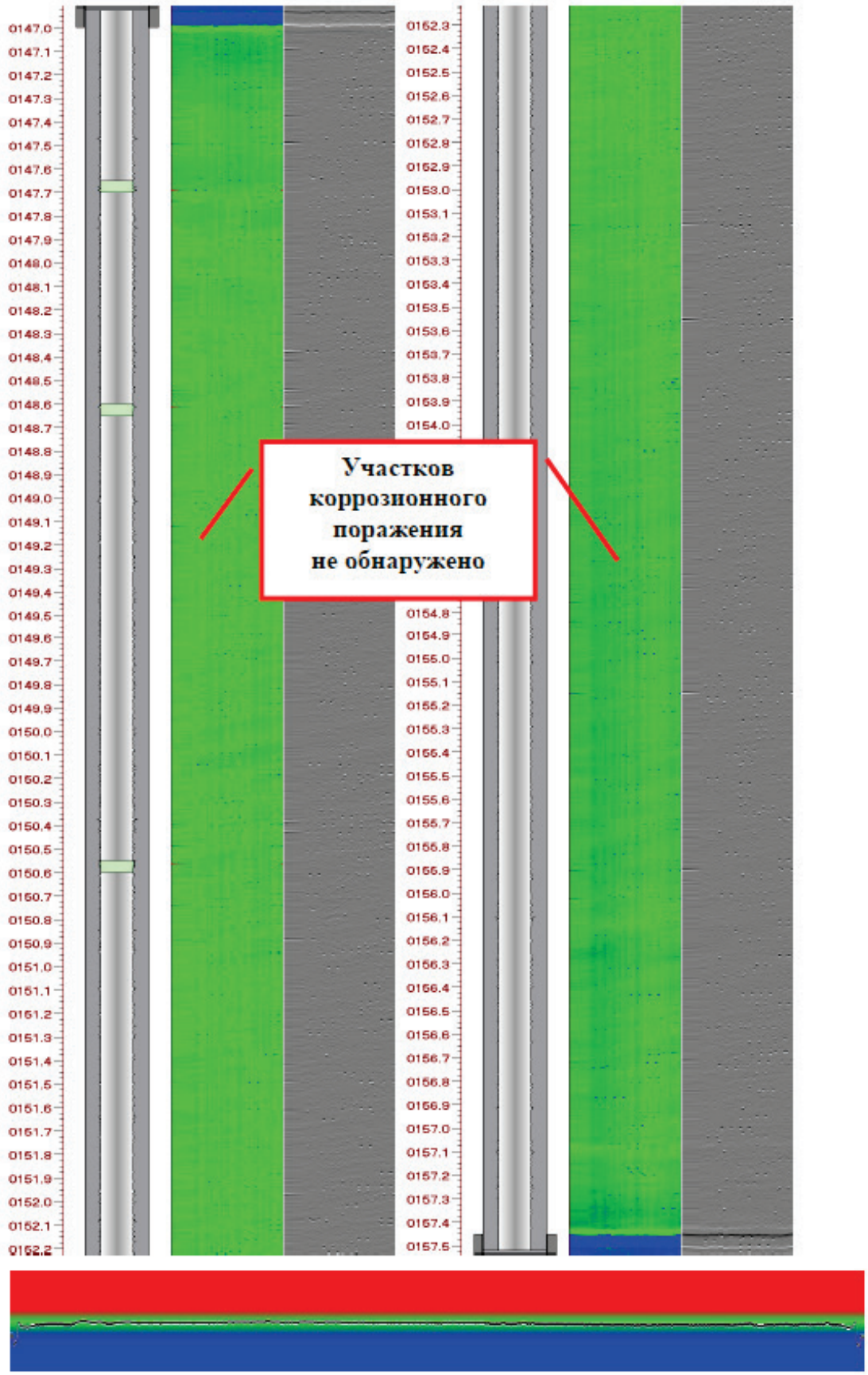

b

Fig. 7.15. (End). Magnetogram of the sections of FS No. 2691 at OGPD Aznakaevskneft within the intervals: a – 1.8-12.8 m; b – 149.9-157.5 m

Technical and operational parameters of magnetic Introscope MI-50 allow us per a round trip: To register the FS defects and specificities; detect corrosion and fatigue cracks, caverns, pits, metal losses, and the FS design features, such as packer blocks, clutches, aligners, perforations, etc.; and evaluate the results of exposing the FS wall to repair, production, and drilling machinery.

To perform diagnostics using a SMI, there is no need for cleaning the FS walls to metal or for ensuring the high dispersion ability of the well fluid. A criterion of the FS suitability for performing the survey is the drift passage.

The most typical defects identified by the FS magnetic introscopy are shown in Fig. 7.16 below.

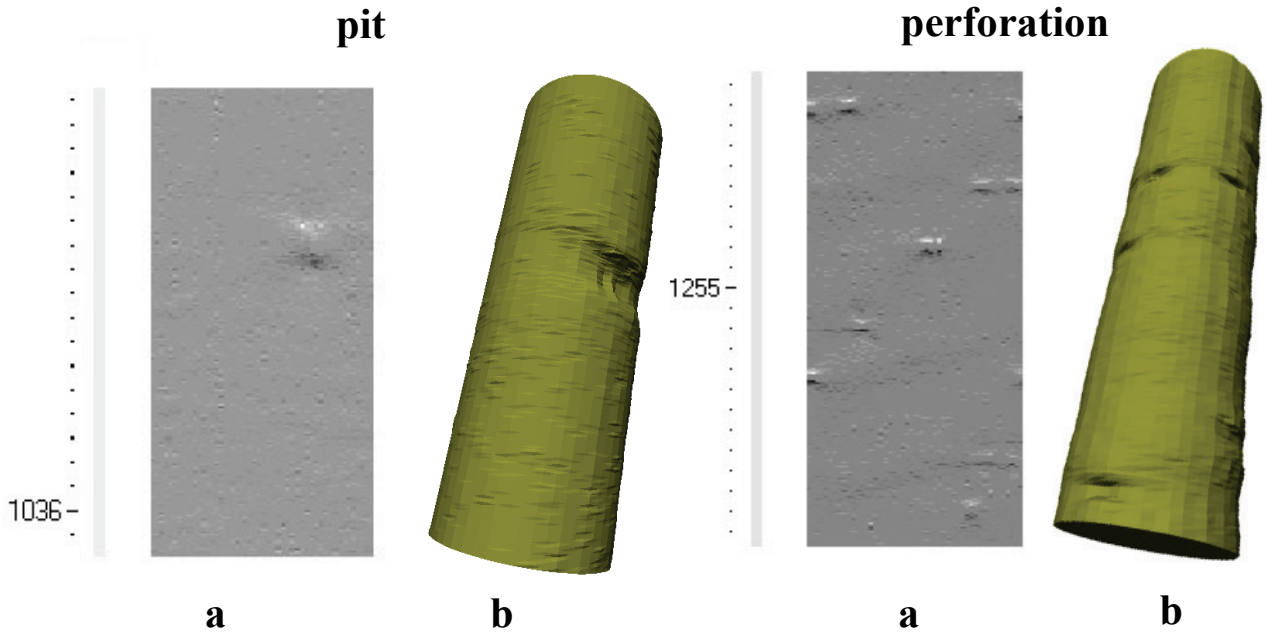

Fig. 7.16. Two-dimensional (a) and three-dimensional (b) images obtained using introscope MI-50 (well 766 at OGPD Bavlyneft)

Over the year 2007-2010. 146 wells have been studied at PJSC Tatneft. According to diagnostic findings, over thousand FS defects have been detected and localized. Table 7.2 presents the form of collecting data based on diagnosing with magnetic Introscope MI-50.

As of now, there have been developed and put into effect reference documents regulating the use of the magnetic introscopy technology [31].

Table 7.2

Information on the findings obtained with magnetic introscope MI-50 for the wells of PJSC Tatneft

№ п/п	Скважина, площадь	Дата строительства	Дата исследования	Тип скважины	Заказчик, НГДУ	Интервал исследования, м	Характер выявленных нарушений
1	2	3	4	5	6	7	8
1	1307 Акташская	12.1972	28.12.05	нагн	НГДУ «Заинскнефть», Альметьевское УПНП и КРС	0-830	Многочисленные интервалы коррозионного поражения обсадной колонны; 5 возможно сквозных нарушений.
2	2629 Акташская	01.1964	29.12.05	нагн	НГДУ «Азнакаевскнефть», ЦППД	0-1658	Незначительная коррозия по колонне; 2 сквозных нарушения.
3	4401 Азнакаевская	10.1958	25.01.06	доб	НГДУ "Азнакаевскнефть", ЦДНГ-5	0-600	Незначительная коррозия по колонне; 3 возможно сквозных нарушения.
4	8465 Зеленогорская	01.1969	26.01.06	доб	НГДУ "Азнакаевскнефть" ЦКРС-4	0-600	Незначительная коррозия по колонне; 4 возможно сквозных нарушения.
5	2045 Павловская	07.1956	30.01.06	доб	НГДУ "Азнакаевскнефть" ЦДНГ-5	0-600	Незначительная коррозия по колонне; имеются многочисленные нарушения, возможно сквозные
6	8169 Березовская	05.1974	03.04.06	нагн	Альметьевский ЦППД	0-409	Коррозия не выявлена; имеется 1 недоворот в муфтовом соединении.
7	10032 Сев.-Альметьевская		05.04.06	нагн	Альметьевский ЦППД	0-319	Незначительная коррозия по колонне; 2 возможно сквозных нарушения.
8	2078 Ново-Елховская	10.1976	13.04.06	доб	НГДУ "Елховнефть" Миннибаевский ЦКРС	0-402	Коррозия не выявлена; 1 недоворот в муфтовом соединении.
9	295д Бавлинская	05.1989	15.04.06	доб	Лениногорское УПНП и КРС, ЦКРС-1	1287.5 -1378	В интервале исследования колонна сильно корродированна; 2 возможно сквозных нарушения; 2 недоворота в муфтовом соединении.

7.5. Acoustic Logging

One of efficient methods to control the internal surfaces of well casings is the acoustic reflection method [33]. Small-diameter televiewer AVK-42M allows obtaining a video image of the internal surface of the well wall in two parameters: Amplitude and time (Fig. 7.17). It uses the principle of registering the changes in internal surface reflectance when scanning the string with ultrasound pulses, the changes in the reflected echo pulse arrival time being registered, too. These principles underly the USI hardware manufactured by Schlumberger, indigenous Russian televiewers, such as ARKTs-T-1. SAT–4 by Geofizika, AVK-42 by PAO NPP VNIIGIS, AKTs SV by NPP Geometr, and Schlumberger scanners: CET-CE/G/J, CET-V V/N/F, Computalog-PET, and Baker Atlas-CBT.

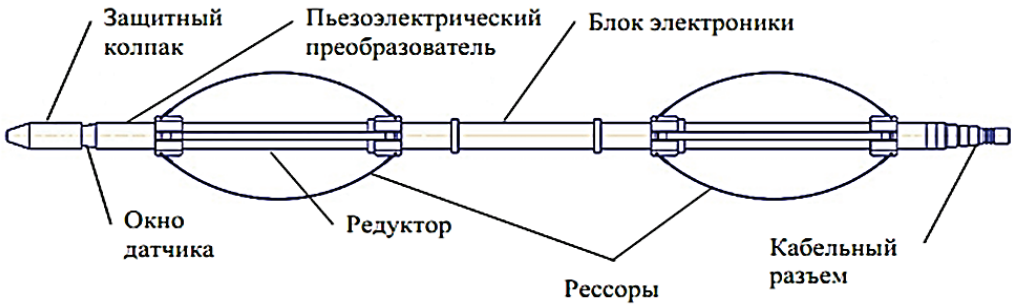

Fig. 7.17. Diagram of borehole televiewer AVK-42M

Small diameter of the AVK-42M hardware allows surveying wells 75-250 mm in diameter, while its low weight and rigid centralizers ensure a good centering adjustment and passing through angled holes, including horizontal wells.

When surveying old well stock, a complex of two scanning methods has proven to be good, i.e., acoustic and electromagnetic techniques, which complex allows well distinguishing intervals containing the internal and external corrosion areas in the well casing. In Fig. 7.18. an example is shown of distinguishing the internal and external area corrosion of the well casing, based on electromagnetic inspection findings obtained using devices EMWD-C and AVK-42M. At the depth of 1.832 m and below, multiple pits occur in the string, the largest ones being noted within the interval of 1.836-1.839 m with EMWD–C, while AVK-42M registers intense internal area corrosion. Thickness probes of EMWD-C register here a significant decrease in the well wall thickness, while the visible record of AVK-42M shows paint coating darkening related to the reduction of echo intensity. Starting from the depth of 1.838 m and below, no defects are observed on the internal surface, according to the AVK-42M visual record, while the

EMWD-C data show defects down to the depth of 1.839 m, which says for the presence of defects on the external side of the string.

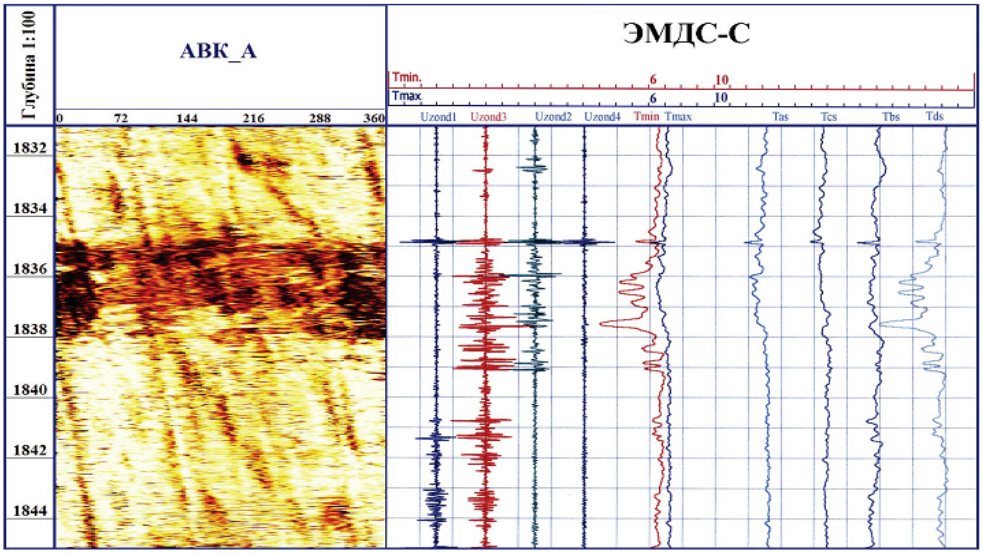

Fig. 7.18. Example of distinguishing the interval of the internal and external area corrosions of the well casing

The visual record shown in Fig. 7.19 demonstrates the signs of a corrosion pit at the depth of 1.184.8 m, which is confirmed by the three-extremum anomaly in curves U2 and U4 of electromagnetic inspection with EMWD-C; on the right, there are the cement-bond acoustic logging findings obtained with ZAS-TSh-36. which show the bad quality of cementing within the range of 1.184-1.187 m.

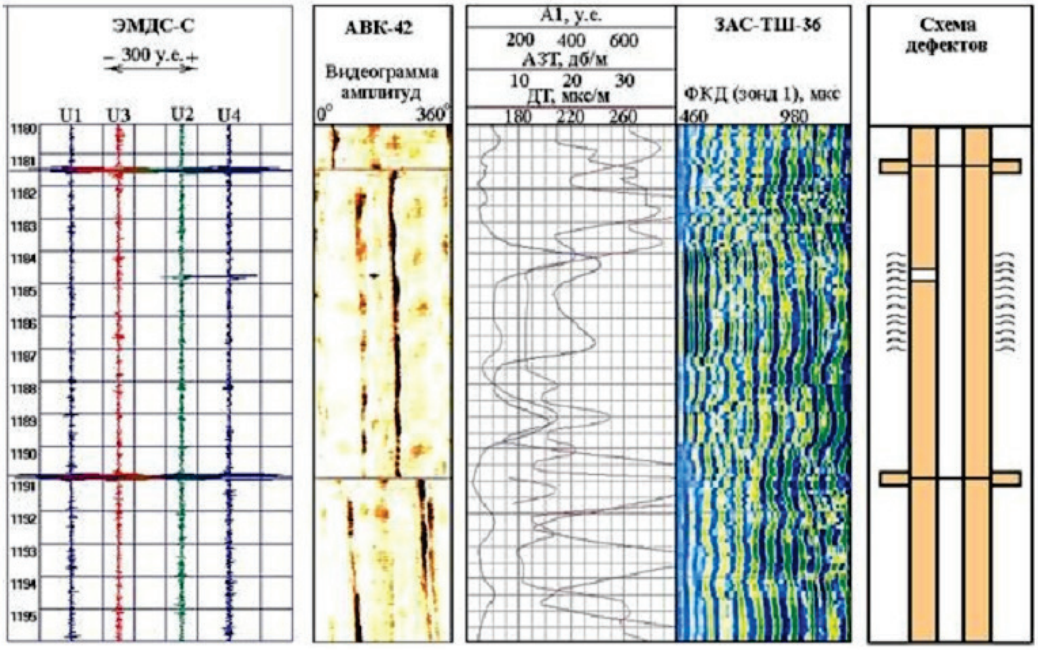

Fig. 7.19. Example of selecting a separate corrosion spot and a breakdown of cement column

7.6. Gamma-Gamma Thickness Gaging

Gamma-gamma thickness gaging is a radioactive method to register the intensity of scattered gamma-radiation using a probe containing the source of medium-energy γ-radiation and a detector of scattered gamma-radiation. The probe length is selected as about 9-12 cm to eliminate the influence upon the results of measuring the annulus medium density and ensure the maximum sensitivity of the method towards changing the casing wall thickness.

The method is used to find the perimeter-average thickness of the casing, the locations of clutches, casing centralizers, packers, and other elements of the well structure and to evaluate the degree of mechanical and corrosive wear of pipes. The device is centered in the well.

To quantitatively interpret the findings, calibration functions are used that relate the probe counting rate (pulses/min) to the steel casing thickness. In interpreting, corrections are made for the natural gamma-radiation background, as well as for the effects provided by the density of the wellbore and annulus filler. A set of pipes having different diameters and wall thicknesses is used as a gaging tool [34].

Chapter Review

1. Main goals of monitoring the technical and corrosion statuses of casings.
2. Survey methods used in monitoring the corrosion statuses of casings.
3. Magnetic introscopy technology in diagnosing the statuses of oil-well production casings.

Chapter 8. PERFORMANCE AND ECONOMIC EFFICIENCY OF USING CATHODIC PROTECTION FOR CASINGS AND FLOWLINES [35–41]

Currently, cathodic protection is covering over 11.000 well casings and over 11.000 km of the production and distribution water flow lines of injection wells at PJSC Tatneft [36–39]. For a feasibility study of using cathodic protection, we have analyzed the frequency of corrosion-caused well casing failures at production and injection wells under 30 years, relevant to the design working life of a cathodic protection unit, exemplified by the comparative evaluation of the operation of wells at Jalilneft OGPD without cathodic protection that have been operated since 1985 and equipped with electrochemical protection since 2003 – the time of actively introducing cathodic protection.

At the initial stage, we gathered summary data on the amount of well casing failures (in pcs.) falling within the sequence number of the year of well operation (1-30). Failures in the first operation year were classified as construction defects and were considered irrelevant.

To find the specific well failure rates at the production and injection wells, falling within various well service lives, the concept of specific well failure rate was introduced, defined as the quotient of the number of well failures happened in the N^{th} operation year by the total well stock, for which there are operation statistics in the N^{th} year. As is seen from Fig. 8.1. SWFR is ranged within 0-0.0272 and 0.007-0.093 (failures happened every year) for production and injection wells, respectively.

Best practices in operating production wells that have been equipped with cathodic protection since they were commissioned show that no actual corrosion-caused well failures have been registered over 14 years (years 2003-2016 were the period of obligatorily equipping all the newly commissioned wells with cathodic protection), so the SWFR is taken as zero for subsequent calculations.

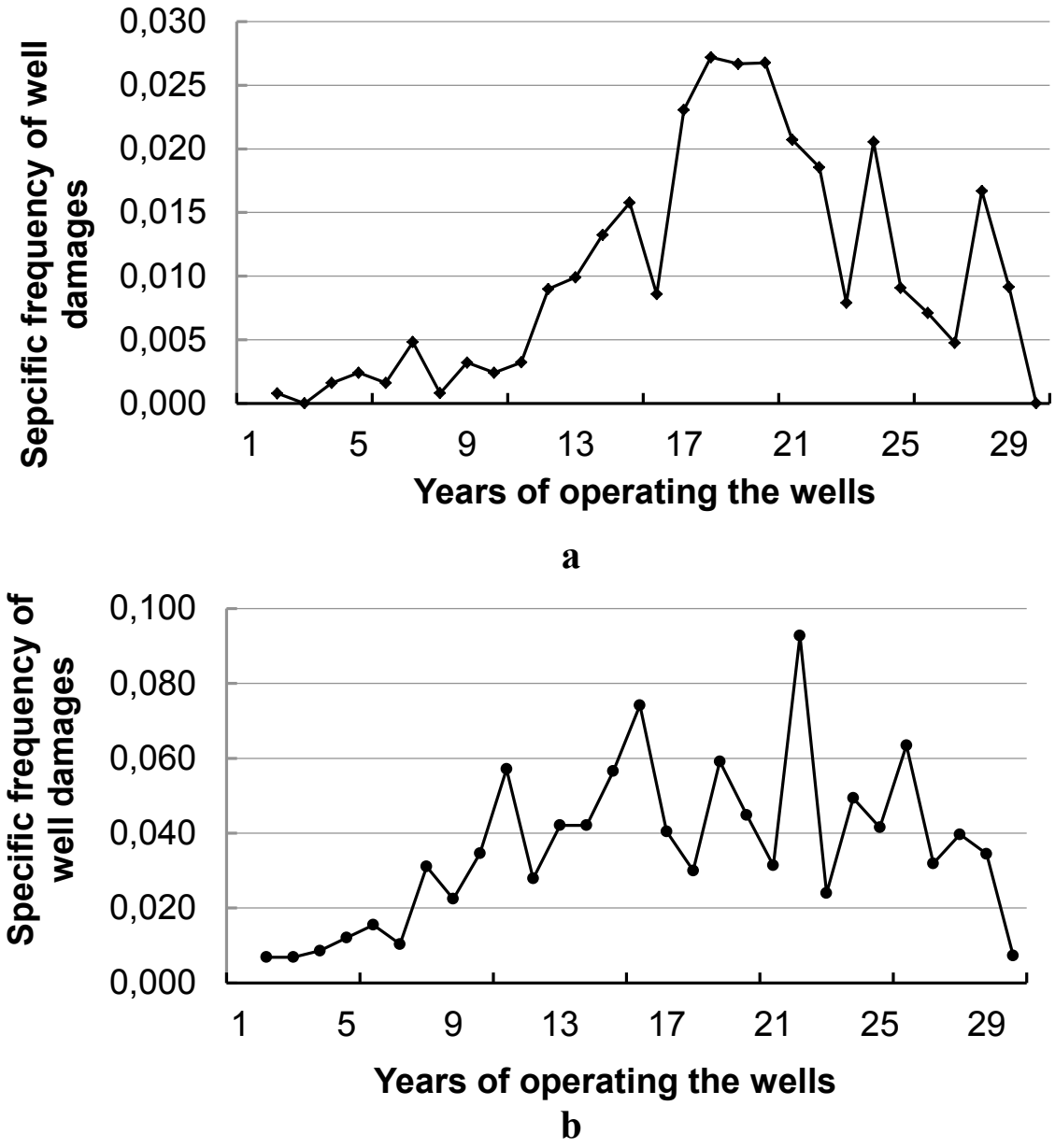

Fig. 8.1. Changes in the specific well failure rates of production (b) and injection (b) wells without cathodic protection

Over the period under research, corrosion-caused failures were registered at injection wells with cathodic protection in the 5^{th}, 8^{th}, and 10^{th} operation year (Fig. 8.2), which had been caused by corrosion processes localized on the internal surface of the casing. Currently, the solution of this problem is the use (pumping) of anti-corrosion liquid and installation of packers inside the casing to reduce pressure on the casing.

To be able to forecast the values of SWFR for developing the methods of evaluating the efficiency of cathodic protection, we propose to use its mean value for the OGPD over the period under research.

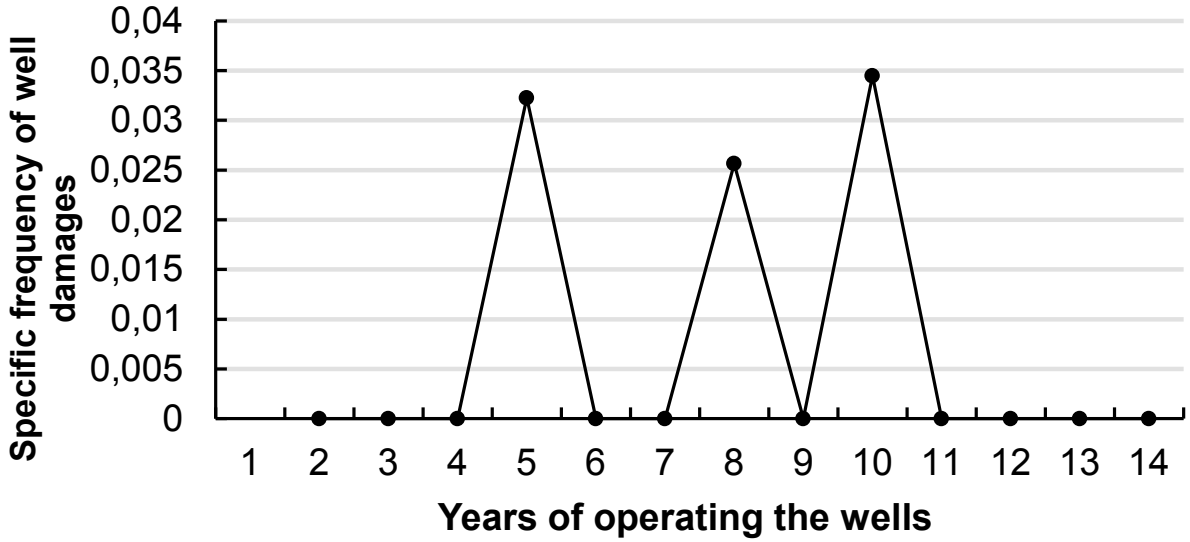

Fig. 8.2. Changes in the specific well failure rates at injection wells with cathodic protection

Decreasing SWFR observed in using the active protection method allows reducing the duration of the well downtime while waiting for and during workover, which results in ensuring the full compliance with productivity standards.

At the next stage of studies, a correlation-regression analysis (Fig. 8.3) was performed to ensure a deeper insight into the possible dependence of the well downtime in WWO, registered prior to the occurrence of problems related to a production string failure on the well capacity. For the wells with a capacity of 8-11 t/day, the WWO time made 30-35 days, while for 1-2 t/day it was 80-110 days, i.e., high-performance wells are repaired quicker, while decisions on performing WO at lower-capacity wells are postponed. The nature of a trend line constructed (Fig. 8.3) provides evidence of the negative correlation between the parameters under consideration, i.e., there is an inverse relationship between the well capacity and the WWO.

Determination index $R^{2.}$ or the approximation reliability degree, of the regression equation obtained as a power function (Fig. 8.3) shows that, in most cases (62 %), changes in WWO depend on those in the well capacity, while their lesser part falls within some other factors that have not been considered in this model. To evaluate the model quality and the statistical reliability of the regression equation obtained, Fischer test, F_R, is used, the actual value of which was 20.94. Tabular value, F_k, is found using Fischer-distribution tables. At the significance point of a=0.05 (a probability of discarding a correct hypothesis, provided that it is true) and the degrees of freedom k_1=2–1 and k_2=15–2. tabular value F_k=4.67. Therefore, $F_R > F_k$, and

the regression equation is considered statistically reliable. Evaluating the correlation index (R=0.785) by Chaddock scale provides evidence of a highly strong correlation between the variables under consideration.

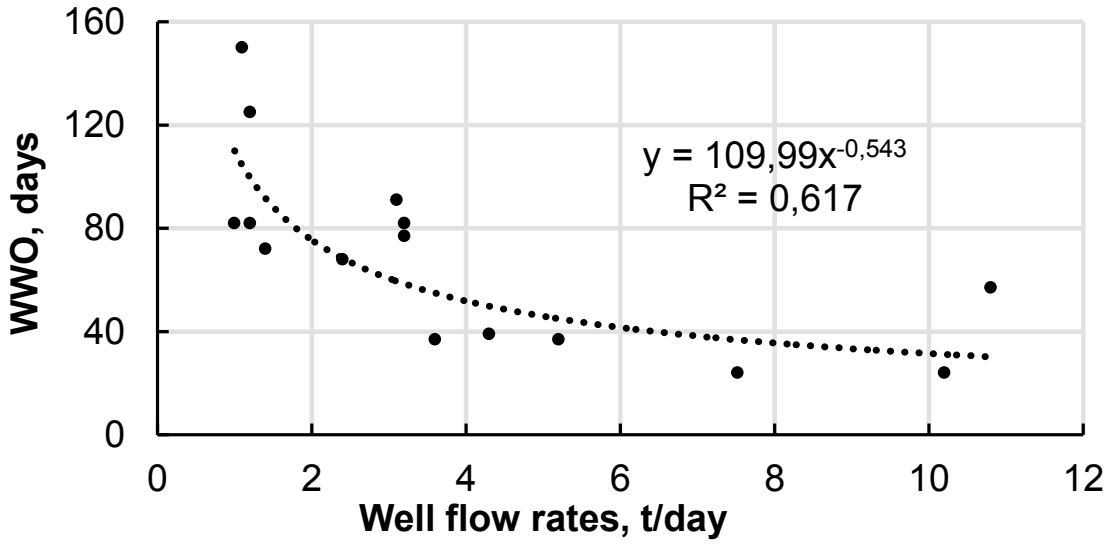

Fig. 8.3. Dependence of the production wells WWO duration on their capacities

For the injection wells for the group of reacting production wells with the capacities of 1-5 t/day, the WWO duration is 75-85 days, with 7-10 t/day it is 60-65 days, and with over 15 t/days, it is 45-50 days, i.e., inverse correlation is also observed among the parameters under consideration (Fig. 8.4).

However, unlike the above dependence, for production wells the approximation reliability degree of the exponential function equation obtained is less than 25 % (Fig. 8.4), and its correlation index is less than 50 %, which provides evidence of a weaker (according to Chaddock scale) correlation between the variables under consideration. For the model constructed, the actual value of F_R was 4.23. tabular value F_k=4.67. Therefore, $F_R<F_k$, and the mathematical model synthesized in such conditions is of no practical importance. In other words, in the conditions of the OGPD considered, no functional dependence was found between an injection well in the WWO and the oil capacity for a group of reacting wells. In this case, it is recommended to use the mean value of the injection well WWO in the computations for any capacity values in a group of reacting wells.

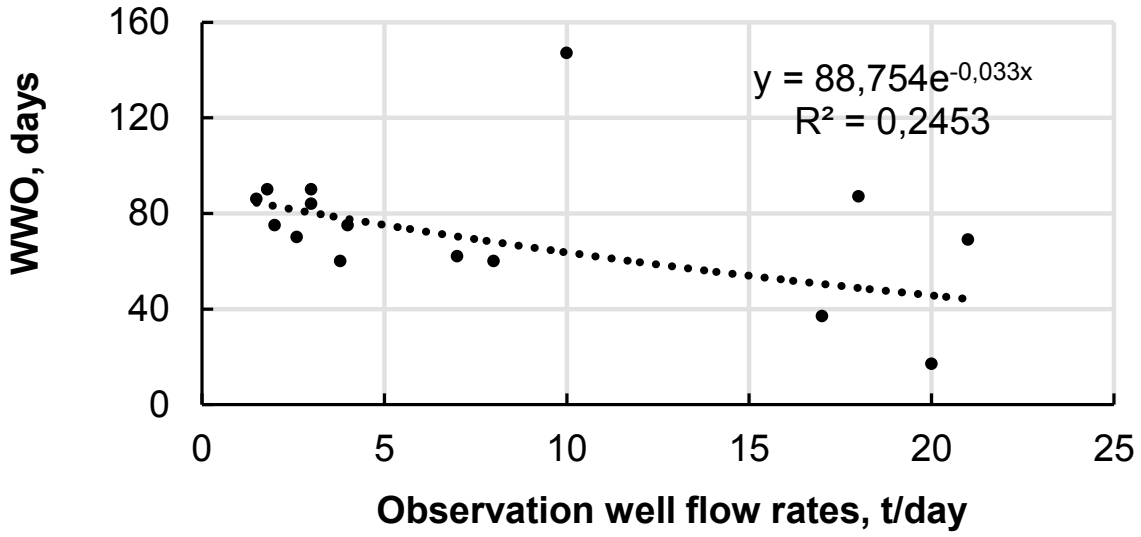

Fig. 8.4. Dependence of the injection well WWO duration on their capacities for a group of reacting wells

Starting from 2015 (RD 153–39.0–935–15), along with production and injection wells, flow lines and water distribution lines have become a single asset under cathodic protection on the premises of PJSC Tatneft, for which previously sacrifice anodes were provided as their protection technology. The reason for changing the protection means was the disadvantages of that technology, such as the limited electrochemical capacity of the anodes and the need for replacing them every 5 years. The benefit from using the combined cathodic protection of well casings and flow lines or distribution water lines is the manageability of cathodic protection technology, i.e., a cathodic protection station can be used to obtain practically any value of the current intensity necessary for protecting the well casing and the pipeline. At the same time, the anode bed is replaced just once every 15 years.

Then, based on the actual statistics on the number of workovers for the OGPD Jalilneft's wells placed in operation in 1985-2016 and according to the regulation documents of PJSC Tatneft, the methods are proposed for computing the economic efficiency of the cathodic protection of well casings, which may be a feasibility study for using such cathodic protection.

The performance indicators of wells without the CP of their casings and with the sacrifice protection of their pipelines are taken as the comparison base. In our case, the SWFRs of wells with CP are compared to those of wells without CP for the wells placed in operation at OGPD Jalilneft over the years 1985-2016.

Economic effect of using the cathodic protection of well casings and pipelines is computed in accordance with RD 153–39.0–620–09 – Regulations on Identifying the Economic Efficiency of Implementing Intellectual Property Assets by the formula:

$$E_T = R_T - C_T,$$

where R_T is the cost estimate of the results of performing the activities; and C_T is the estimate of the costs of the activities performed.

Cost estimates of the results obtained from performing the activities are formed through:

– Saving the operational costs of WO;

– Increasing the earnings of oil sales, since the underperformance of oil production is reduced due to reducing the well downtime duration waiting for WO; and

– Excluding the expenditures on the sacrificial protection of well flow lines / water distribution ducts.

Saving the operational WO costs in the N^{th} year of operating the well is found by multiplying the average WO cost by changing the SWFR in the N^{th} year of operating the well. In defining the WO cost, we selected the workover presupposing the installation of an additional string, as known more reliable as compared to the production string damage elimination technique, such as grouting. Installing an additional string is a relatively expensive workover; however, considering waiving to re-grout, in case of an unsuccessful primary grouting, this technique finally turns out to be less cost-consuming than cementing. Changing the SWFR represents the difference between the new and the basic SWFR options.

Increasing the earnings of oil sales in the N^{th} year of operating the well represents the product of the mean-weight oil sale price (exclusive of VAT, export duties, and selling expenses) and the specific reduction of underperformances in oil production in the N^{th} year of operating the well. The specific reduction of underperformances in oil production in the N^{th} year of operating the well is computed by multiplying the daily production rate in the N^{th} year of operating the well by the specific reduction of WWO- and WO-caused well downtime in the N^{th} year of operating the well.

Changes in the daily production by the years of well operation are found as follows: The average initial oil production rate is used in the first year; in the subsequent years, the oil production decline factor is applied to the production year of the preceding year, which factor is determined by PJSC Tatneft's Process Department for Developing Oil Deposits and

Geologic Formations for each OGPD. Specific reduction of WWO- and WO-caused well downtime in the N^{th} year of well operation is computed by multiplying the well downtime duration due to one well damage in the N^{th} year of well operation by changing the SWFR in the N^{th} year of well operation.

In turn, the well downtime duration caused by one well damage in the N^{th} year of well operation is composed of the WWO duration in the N^{th} year of well operation and the average WO duration for liquidating the well casing damage. To find the WWO duration, it is necessary to perform the correlation-regression analysis of statistics for an OGPD. Based on the analysis results, a mathematical model must be obtained and estimated, which describes the functional dependence of the WWO duration and production rate. Then the following is used in finding the WWO duration in the N^{th} year of well operation:

a) The WWO value computed by the regression equation, where the regression equation obtained from the analysis is estimated as statistically valid, shows a high correlation between the parameters under consideration, while the trendline built provides the evidence of a negative correlation between the WWO duration and the well production rate that had been registered before the issues occurred, related to the production string damage; and

b) The average WWO duration typical of a given OGPD, in the opposite case.

Costs of the sacrificial protection of the well flow lines / water distribution ducts are composed of the investment costs related to implementing the sacrificial protection plant of the well pipeline, the specific current expenditures on maintaining the GPU, and the subsequent operational costs of the SP workover consisting in periodically replacing the worn-out components of the SP. SP includes a protective group, a guarded test post, and 2 electrically insulating gaskets at the ends of each pipeline to be protected. As a manner of experience, protectors are replaced every 5 years, test posts every 10 years, and EIG and guard every 15 years.

Estimation of costs related to performing an activity is composed of the specific, i.e., related to one well, one-time costs of implementing a cathodic protection unit and of the subsequent CP workover consisting in replacing the worn-out components of the CP, the specific current costs of electrical energy and of the C(S)PU maintenance, as well as the increase in the variable costs of oil production, MET, and income tax. CP includes a

cathodic protection station, anode beds, guarded test posts, and 1 EIG at the end of each pipeline to be protected.

Specific per-well costs are computed by dividing the costs per one C(S)PU by the number of wells protected by this unit. Increasing variable costs of oil production in the N^{th} year of well operation is computed by multiplying the statutory ratio of the variable costs of producing 1 t of oil, which ratio is annually communicated to the OGPD by the Economic Department of PJSC Tatneft, by the specific reduction of oil underperformance in the N^{th} year of well operation. Increase in MET in the N^{th} year of well operation is computed by multiplying the MET rate calculated considering tax exemptions granted for oil production a given subsoil area, by the specific reduction of oil underperformances in the N^{th} year of well operation.

The methods developed do not consider any potential accompanying effects of implementing CP, such as increase of service life and environmental benefits.

Preliminary data analysis of OGPD Jalilneft has shown the following:

– Registered are the isolated cases of liquidating the injection and production wells in the 12^{th} and 14^{th} years of operation, caused by the production string corrosion, which allows us to state the insignificance of the effect of increasing the well service life in the OGPD; and

– Environmental effects cannot be evaluated due to the complexity of their actual estimation.

For OGPD Jalilneft considered herein, as of April 2017 and provided that one C(S)PU is implemented for two new wells, the net present value over the accounting period was RUB 144.4 thousand per production well and RUB 825.2 thousand per injection well. Investments in CP for a production well pay back within 14.2 years, while the payback period for an injection well is 9.2 years. Yield index of discounted expenditures is 1.9 unit fractions for a production well and 3.5 unit fractions for an injection well.

In efficiency calculations, it is recommended to use statistics and inputs not so much for the OGPD in general as for individual sites/deposits having identical development conditions, which would allow identify the efficient areas of using cathodic protection at an OGPD. If some indicators for the wells in 2003-2016 are unavailable or insufficient (in case of no wells without cathodic protection or of their number being insufficient to perform analyses), it is necessary to use sample wells implemented before

2003. as it was shown in the techniques developed. Should the continued operation of a well be less than 30 years, considering shifting the well from production to injection according to the decision of the head of the oil and gas development service of an OGPD, then this period of time is taken as a reference period [35].

Chapter Review

1. Methods of analyzing the cost-benefit ratio of joint cathodic protection.
2. Effects provided by the major workover waiting time of production and injection wells on reliability, depending on their production rates.
3. Return on investments in cathodic protection of a production well and an injection well.

Chapter 9. CALCULATORY TASKS

9.1. Selecting Wells to Connect Cathodic Protection

A commercial injection well is being operated, aged X_2 years. The scheduled time of further operation for this well is X_3 years. Cementing quality is X_4. Over the operation period, X_5 well workovers have been performed. Casing diameter is X_6. The oil production well for pure oil is X_7. Find out whether it would be reasonable to use cathodic protection in this example or it is necessary to perform the workover of the well. Initial data for analysis is given in Table 9.1.

Table 9.1

Values of Parameters X_i

Version #	X_1	X_2, years	X_3, years	X_4	X_5	X_6, mm	X_7, t/day (X_1=1) m^3/day (X_1=2)	X_8, Km
1	**2**	**3**	**4**	**5**	**6**	**7**	**8**	**9**
1	1	15	15	1	2	146	5	–
2	1	20	15	1	3	146	5	–
3	1	25	5	2	2	168	4	–
4	1	10	25	1	1	178	6	–
5	1	5	30	1	0	140	5	–
6	1	30	10	2	3	168	6	–
7	1	35	10	1	1	140	6	–
8	1	20	20	3	2	178	2	–
9	1	25	10	3	3	194	3	–
10	1	40	10	3	4	146	4	–
11	2	15	15	1	2	146	45	0
12	2	20	15	1	3	146	100	0.04
13	2	25	5	2	2	168	200	0.03
14	2	10	25	1	1	178	200	1
15	2	5	30	1	0	140	150	0.02
16	2	30	10	2	3	168	70	0
17	2	35	10	1	1	140	200	0
18	2	20	20	3	2	178	160	0
19	2	25	10	3	3	194	40	0
20	2	40	10	3	4	146	100	0

9.2. Evaluating the Casing Pipe Protection Current

Calculate the oil-well casing pipe protection current. Mean characteristics of the casing pipes in all wells are roughly the same and coincide with the example described in Section 3.1.1 (L_c = 1000 m). Distribution of the apparent noninvaded formation resistivities in the geological column of wells is given in Table 9.2. In the geological column of wells, there are two aggressive water-bearing horizons: The first one with the hydrogen sulfide concentration in the stratum water being 100 mg/l within the range of 600-700 m; the second horizon with the H_2S concentration of 300 mg/l within 700-820 m. Stationary cathodic polarization curves for stratum water in two aggressive horizons are shown in Fig. 3.2. Production casing voltage decrease distribution curves taken with a double-contact probe at the protection currents of 6. 7. and 12 A are shown in Fig. 9.1.

Table 9.2

Distribution of the Apparent Noninvaded Formation Resistivities in the Geological Column of Wells

1	Depth ranges, m	0 – 280.4	280.4–289.4	289.4–295.6	295.6–305.6	305.6–307.7	307.7–310.4	310.4–313	313–317.5	317.5–328.4
2	Range #	1	2	3	4	5	6	7	8	9
3	ρ_i, Ohm·m	89.7	31.9	30.6	78.6	65.9	52.8	64.5	48.07	83.2
4	Thickness of layer H_i, m	280.4	9	6.2	10	2.1	2.7	2.6	4.5	10.9

Table 9.2 (continued)

1	328.4–331.4	331.4–337.5	337.5–339.6	339.6–341.1	341.1–345.1	345.1–347.1	347.1–349.7	349.7–353.6	353.6–362.1	362.1–364	364–366.5	366.5–369.7	369.7–374.1	374.1–375.8
2	10	11	12	13	14	15	16	17	18	19	20	21	22	23
3	19.0	83.0	53.3	9.9	82.0	19.6	41.2	23.8	59.8	18.0	32.1	6.2	30	51.4
4	3	6.1	2.1	1.5	4	2	2.6	3.9	8.5	1.9	2.5	3.2	4.4	1.7

Table 9.2 (continued)

1	375.8–378.2	378.2-390.5	390.5–395.8	395.8–397.4	397.4–400.8	400.8–408.9	408.9–412	412–417.7	417.7–422.6	422.6–424.5	424.5–426.8	426.8–429.6	429.6–432.1	432.1–462.2
2	24	25	26	27	28	29	30	31	32	33	34	35	36	37
3	98.9	45.5	18.2	32.8	73.1	81.0	31.2	73.0	96.2	78.5	113.	74.8	113.1	79.6
4	2.4	12.3	5.3	1.6	3.4	8.1	3.1	5.7	4.9	1.9	2.3	2.8	2.5	30.1

Table 9.2 (continued)

1	462.2–466.8	466.8–470.2	470.2–474.1	474.1–488	488–494.3	494.3–499.6	499.6–509.9	509.9–518.3	518.3–521.2	521.2–527.4	527.4–529.2	529.2–538.5	538.5–542.3	542.3–554.9
2	38	39	40	41	42	43	44	45	46	47	48	49	50	51
3	56.1	38.4	61.4	45.8	27.9	52.1	98.6	72.3	39.6	49.4	77.4	46.2	53.3	72.1
4	4.6	3.4	3.9	13.9	6.3	5.3	10.3	8.4	2.9	6.2	1.8	9.3	3.8	12.6

Table 9.2 (continued)

1	554.9–556.8	556.8–560.7	560.7–567.9	567.9–569.1	569.1–573.1	573.1–575.3	575.3–577.3	577.3–583.3	583.3–591.6	591.6–596	596–620.2	620.2–623.6	623.6–630.6	630.6–634.4
2	52	53	54	55	56	57	58	59	60	61	62	63	64	65
3	78.0	49.1	70.1	48.3	99.2	54.0	73.8	42.1	56.4	81.7	55.9	89.2	53.0	80.1
4	1.9	3.9	7.2	1.2	4	4.2	2	6	8.3	4.4	24.2	3.4	7	3.8

Table 9.2 (continued)

1	634.4–641.5	641.5–651.2	651.2–653.3	653.3–655.7	655.7–663.8	663.8–666.8	666.8–677.1	677.1–678.5	678.5–684.6	684.6–689.6	689.6–691.9	691.9-693.7	693.7-697.8	697.8-699.2
2	66	67	68	69	70	71	72	73	74	75	76	77	78	79
3	48.9	76.7	45.2	82.0	47.4	80.3	79.2	45.0	72.0	43.7	64.3	43.3	101.4	46.2
4	7.1	9.7	2.1	2.4	8.1	3	10.3	1.4	6.1	5	2.3	1.8	4.1	1.4

Table 9.2 (continued)

1	699.2–718.9	718.9–720.3	720.3–723.3	723.3–727.9	727.9–738.9	738.9–742.9	742.9–771.1	771.1–777.2	777.2–781	781–784.5	784.5–790	790–802.8	802.8–808.4	808.4–814.1
2	80	81	82	83	84	85	86	87	88	89	90	91	92	93
3	51.1	35.6	58.3	108	66.3	107	58.6	86.3	50.1	72.5	51.2	89.7	52.5	37.7
4	19.7	1.4	3	4.6	11	4	28.2	6.1	3.8	3.5	5.5	12.8	5.6	5.7

Table 9.2 (continued)

1	814.1–816.2	816.2–823.2	823.2–828.4	828.4–834.2	834.2–852.7	852.7–855.1	855.1–861.4	861.4–887.8	887.8–891.9	891.9–900	900–911.3	911.3–915.9	915.9–926	926–952.2
2	94	95	96	97	98	99	100	101	102	103	104	105	106	107
3	50.7	82.8	36.6	27.0	98.7	53.1	98.9	75.5	16.9	41.7	57.9	91.8	73.7	97.3
4	2.1	7	5.2	5.8	18.5	2.4	6.3	26.4	4.1	8.1	11.3	4.6	10.1	26.2

End of Table 9.2

1	952.2–956.5	956.5–962.2	962.2–970.5	970.5–981.5	981.5–989.4	989.4–995.7	995.7–1000.4
2	108	109	110	111	112	113	114
3	81.8	27.2	100.4	85.0	79.5	80.8	97.2
4	4.3	5.7	8.3	11	7.9	6.3	4.7

Average resistivity in the upper ground layers on the oilfield (to the depth of 10 m) ρ_i = 50 Ohm·m.

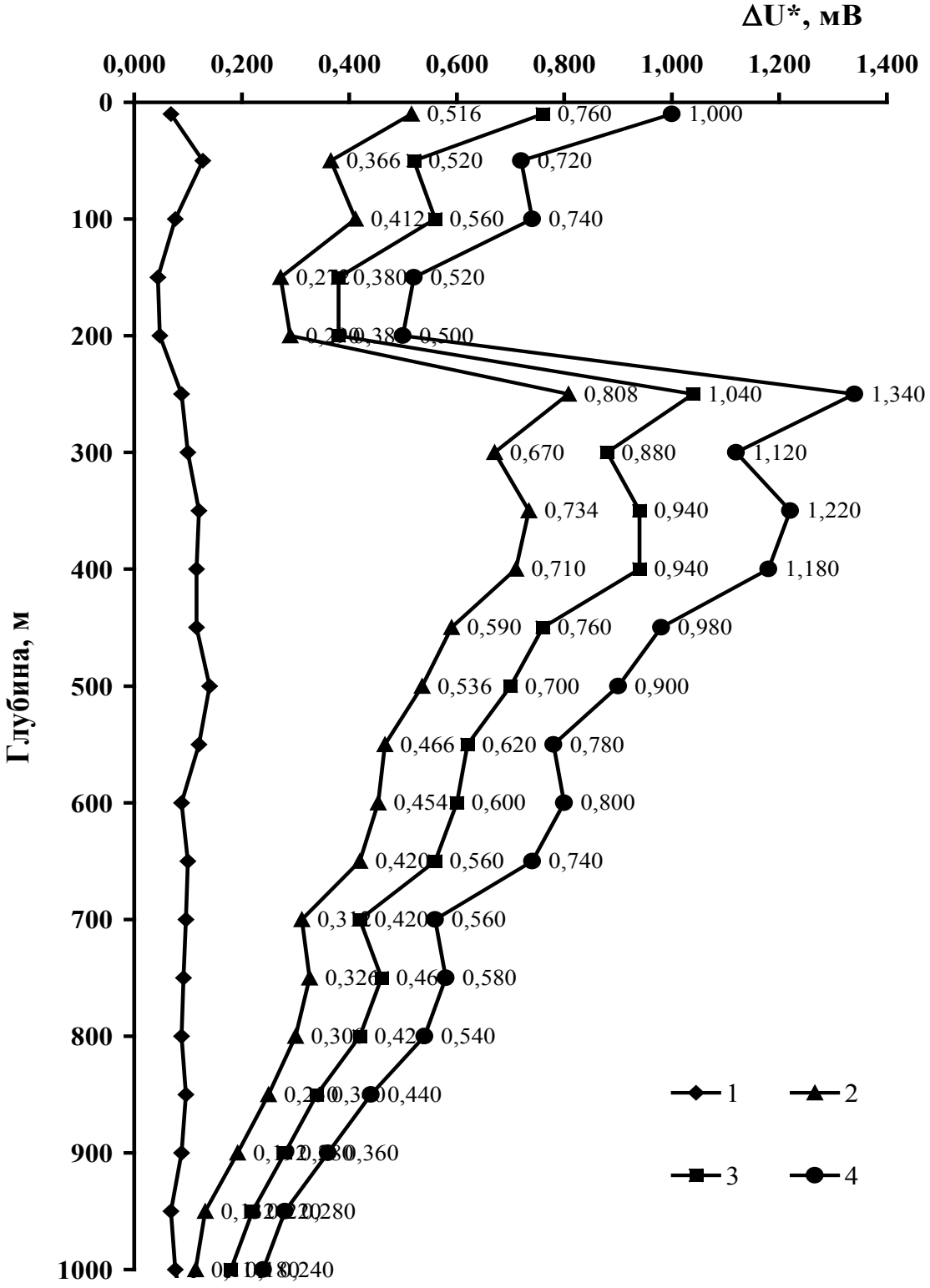

Fig. 9.1. Casing pipe voltage decrease distribution curves, ΔU, at the well depth: 1 – in natural condition; 2 – protection current 6 A; 3 – protection current 9 A; 4 – protection current 12 A

*** Experimental data regarding the voltage decrease were obtained using a 500-time amplifier.*

9.3. Analyzing the Protection Current, Using the Method of Calculating the Potential Shift in the Well Shaft and the Resistance Value within the Well/Ground System

Analyze the necessary protection current to reach the potential of 0.1 V at the oil-well casing bottom (see Fig. 5.2). Geometric characteristics of casing pipes are given in Table 9.3. In testing with supplying the current of 3 A, the potential shift was 0.1 V.

Table 9.3

Geometric Characteristics of Casing Pipes

Version	Outside diameter of casings, mm			Pipe wall thickness, mm			Sector length, m		
	Direction	Conductor casing	Production casing	Direction	Conductor casing	Production casing	Direction	Conductor casing	Production casing
1	193.7	168.3	114.3	9	8	7	20	200	1.700
2	193.7	168.3	127.0	9	8	7	20	200	1.700
3	219.1	193.7	139.7	10	9	8	25	220	1.750
4	273.1	244.5	168.3	10	9	8	25	230	1.800
5	273.1	244.5	177.8	11	10	9	30	240	2.000
6	298.5	273.1	193.7	11	10	9	30	250	2.000
7	323.9	298.5	219.1	12	10	9	30	255	2.100
8	193.7	177.8	127.0	10	9	8	30	260	2.200
9	244.5	219.1	139.7	11	10	9	30	270	2.300
10	273.1	244.5	168.3	12	10	9	30	270	2.400

9.4. Analyzing the Current Density Distribution at the Casing Pipe Depth, Using the Method of Identifying the Voltage Decrease Profile

Analyze the current density distribution at the oil-field casing pipe depth (see Fig. 5.2), based on the results of measuring the voltage decrease with a double-contact probe (Table 9.4). Geometric means of the casing sectors of all wells are roughly the same and coincide with the example described in Section 5.3.

Table 9.4

Results of Measuring the Voltage Decrease at the Casing Pipe Depth with a Double-Contact Probe

Version	1	2	3	4	5	6
Protection current, A	3	6	9	12	6	6
Depth, m	ΔU*, mV					
10	0.304	0.516	0.760	1.000	0.055	0.315
50	0.206	0.366	0.520	0.720	0.038	0.050
100	0.242	0.412	0.560	0.740	0.045	0.038
150	0.194	0.272	0.380	0.520	0.046	0.037
200	0.200	0.290	0.380	0.500	0.124	0.040
250	0.548	0.808	1.040	1.340	0.046	0.043
300	0.458	0.670	0.880	1.120	0.045	0.039
350	0.500	0.734	0.940	1.220	0.027	0.038
400	0.486	0.710	0.940	1.180	0.072	0.039
450	0.394	0.590	0.760	0.980	0.020	0.029
500	0.350	0.536	0.700	0.900	0.014	0.030
550	0.312	0.466	0.620	0.780	0.036	0.025
600	0.316	0.454	0.600	0.800	0.030	0.022
650	0.284	0.420	0.560	0.740	0.030	0.021
700	0.228	0.312	0.420	0.560	0.048	0.019
750	0.234	0.326	0.460	0.580	0.039	0.026
800	0.210	0.300	0.420	0.540	0.018	0.031
850	0.164	0.250	0.340	0.440	0.033	0.027
900	0.134	0.192	0.280	0.360	0.056	0.027
950	0.104	0.132	0.220	0.280	0.054	0.028
1000	0.092	0.114	0.180	0.240	0.015	0.029
1050	0.060	0.086	0.140	0.200	0.052	0.028
1100	0.048	0.076	0.120	0.160	0.029	0.027
1150	0.030	0.032	0.060	0.100	0.023	0.023
1200	0.026	0.020	0.040	0.060	0.024	0.021
1250	0.006	0.010	0.000	–0.020	0.022	0.012

* Experimental data regarding the voltage decrease were obtained using a 500-time amplifier.

APPENDICES

Appendix 1 [Reference Data]

Table P1.1

Dimensions of Oil Case Pipes Having Standard Thread Lengths

Nominal diameter, mm	Pipe dimensions, mm			Inches
	Outside diameter	Wall thickness	Inside diameter	
1	2	3	4	5
114	114.3	6	102.3	4 ½
		7	100.3	
		8	98.3	
127	127.0	6	115	5
		7	113	
		8	111	
		9	109	
140	139.7	6	127.7	5 ½
		7	125.7	
		8	123.7	
		9	121.7	
		10	119.7	
		11	117.7	
146	146	6.5	133	5 ¾
		7	132	
		8	130	
		9	128	
		10	126	
		11	124	
168	168.3	6	155.3	6 ¾
		7	154.3	
		8	152.3	
		9	150.3	
		10	148.3	
		11	146.3	
		12	144.33	
178	177.8	7	163.8	7
		8	161.8	
		9	159.8	
		10	157.8	
		11	155.8	
		12	153.8	

Table P1.1 (continued)

1	2	3	4	5
194	193.7	7	179.7	6 ¾
		8	177.7	
		9	175.7	
		10	173.7	
		12	169.7	
219	219.1	7	205.1	8 ¾
		8	203.1	
		9	201.1	
		10	199.1	
		12	195.1	
245	245.0	8	228.5	9 ¾
		9	226.5	
		10	224.5	
		12	220.5	
273	273.1	8	257.1	10 ¾
		9	255.1	
		10	253.1	
		12	249.1	
299	298.5	8	282.5	11 ¾
		9	280.5	
		10	278.5	
		11	276.5	
		12	274.5	
324	323.9	9	305.9	12 ¾
		10	303.9	
		11	301.9	
		12	299.9	
340	339.7	9	321.7	13 ¾
		10	319.7	
		11	317.7	
		12	315.7	
		9	333	
351	351	10	331	
		11	329	
		12	327	
		9	359	
377	377	10	357	
		11	355	
		12	353	
		9	388.4	

Table P1.1 (end)

1	2	3	4	5
407	406.4	10	386.4	
		11	384.4	
		12	382.4	
		10	406	
426	426	11	404	16 ¾
		12	402	
		11	486	
508	508			

Appendix 2

Table P2.1

Pertain Functions of μ_i for Development Wells

Parameter X_i	Cathodic protection		Capitalized workover	
	Value X_i	Value μ_i	Value X_i	Value μ_i
1	2	3	4	5
Well category X_1	$X_1 = 1$	$\mu_1 = 0.9$	$X_1 = 1$	$\mu_1 = 0.9$
Well age X_2	$X_2 \le 30$ $30 < X_2 < 46$ $X_2 \ge 46$	$\mu_2 = 0.9$ $\mu_2 = 2.4 - 0.05X_2$ $\mu_2 = 0.1$	$X_2 \le 30$ $X_2 > 30$	$\mu_2 = 0.9$ $\mu_2 = 1.7 - 0.0267X_2$
Duration of continued operation X_3	$X_3 \le 10$ $10 < X_3 < 20$ $X_3 \ge 20$	$\mu_3 = 0.1$ $\mu_3 = 0.08X_3 - 0.7$ $\mu_3 = 0.9$	$X_3 > 0$	$\mu_3 = 0.9$
Cementing quality (sufficiency) X_4	$X_4 = 1$ $X_4 = 2$ $X_4 = 3$	$\mu_4 = 0.75$ $\mu_4 = 0.9$ $\mu_4 = 0.7$	$X_4 = 1$ $X_4 = 2$ $X_4 = 3$	$\mu_4 = 0.9$ $\mu_4 = 0.9$ $\mu_4 = 0.9$
Number of workovers X_5	$X_5 < 3$ $X_5 \ge 3$	$\mu_5 = 0.9 - 0.266X_5$ $\mu_5 = 0.1$	$X_5 < 4$ $X_5 \ge 4$	$\mu_5 = 0.9 - 0.2X_5$ $\mu_5 = 0.1$
Diameter of production casing X_6	$X_6 > 0$	$\mu_6 = 0.9$	$X_6 \ge 146$ $X_6 < 146$	$\mu_6 = 0.9$ $\mu_6 = 0.4$
Oil yield X_7	$X_7 \le 0.5$ $0.5 < X_7 < 5$ $X_7 \ge 5$	$\mu_7 = 0.1$ $\mu_7 = 0.011 + 0.178X_7$ $\mu_7 = 0.9$	$X_7 \le 2$ $2 < X_7 < 5$ $X_7 \ge 5$	$\mu_7 = 0.9$ $\mu_7 = 1.434 - 0.267X_7$ $\mu_7 = 0.1$

Table P2.2

Pertain Functions of μ_i for Injection Wells

Parameter X_i	Cathodic protection		Capitalized workover	
	Value X_i	Value μ_i	Value X_i	Value μ_i
1	2	3	4	5
Well category X_1	$X_1 = 2$	$\mu_1 = 0.85$	$X_1 = 2$	$\mu_1 = 0.9$
Well age X_2	$X_2 \le 30$ $30 < X_2 < 46$ $X_2 \ge 46$	$\mu_2 = 0.9$ $\mu_2 = 2.4 - 0.05X_2$ $\mu_2 = 0.1$	$X_2 \le 30$ $X_2 > 30$	$\mu_2 = 0.9$ $\mu_2 = 1.7 - 0.0267X_2$
Duration of continued operation X_3	$X_3 \le 10$ $10 < X_3 < 20$ $X_3 \ge 20$	$\mu_3 = 0.1$ $\mu_3 = 0.08X_3 - 0.7$ $\mu_3 = 0.9$	$X_3 > 0$	$\mu_3 = 0.9$
Cementing quality (sufficiency) X_4	$X_4 = 1$ $X_4 = 2$ $X_4 = 3$	$\mu_4 = 0.75$ $\mu_4 = 0.9$ $\mu_4 = 0.7$	$X_4 = 1$ $X_4 = 2$ $X_4 = 3$	$\mu_4 = 0.9$ $\mu_4 = 0.9$ $\mu_4 = 0.9$
Number of workovers X_5	$X_5 < 3$ $X_5 \ge 3$	$\mu_5 = 0.9 - 0.266X_5$ $\mu_5 = 0.1$	$X_5 < 4$ $X_5 \ge 4$	$\mu_5 = 0.9 - 0.2X_5$ $\mu_5 = 0.1$
Diameter of production casing X_6	$X_6 > 0$	$\mu_6 = 0.9$	$X_6 \ge 146$ $X_6 < 146$	$\mu_6 = 0.9$ $\mu_6 = 0.4$
Injectability X_7	$X_7 \le 50$ $50 < X_7 < 200$ $X_7 \ge 200$	$\mu_7 = 0.1$ $\mu_7 = -0.165 + 0.053X_7$ $\mu_7 = 0.9$	$X_7 \le 50$ $50 < X_7 < 200$ $X_7 \ge 200$	$\mu_7 = 0.9$ $\mu_7 = 1.165 - 0.0053X_7$ $\mu_7 = 0.1$
Length of power transmission lines X_8	$X_8 \le 0.05$ $0.05 < X_8 < 2$ $X_8 \ge 2$	$\mu_8 = 0.9$ $\mu_8 = 1 / (0.883 + 4.558\ X_8)$ $\mu_8 = 0.1$	$X_8 \ge 0$	$\mu_8 = 0.9$

Appendix 3

Screening Factors for Anode Bed

Ratio of the distance between ground devices to the length of one ground device, b / l	Number of ground devices within the grounding circuit, N_{gr}	Screening factor of ground devices, K_{gr}
For vertical ground devices		
1	2	0.84 – 0.87
2	2	0.90 – 0.92
3	2	0.93 – 0.95
1	3	0.76 – 0.80
2	3	0.85 – 0.88
3	3	0.90 – 0.92
1	5	0.67 – 0.72
2	5	0.79 – 0.83
3	5	0.85 – 0.88
1	10	0.56 – 0.62
2	10	0.72 – 0.77
3	10	0.79 – 0.83
For horizontal ground devices		
1	2	0.85 – 0.87
2	2	0.92 – 0.94
3	2	0.95 – 0.97
1	3	0.79 – 0.81
2	3	0.89 – 0.91
3	3	0.93 – 0.94
1	5	0.72 – 0.74
2	5	0.84 – 0.86
3	5	0.88 – 0.90

Appendix 4

Anodic Dissolution Rates of Electrode Materials, kg/A·year

Electrode Material	Medium or Filling				
	Clay	Loam	Sand	Small-sized coke	
				in slightly wet grounds	in very wet grounds
Steel	10	10	10	2–4	4–7
Cast iron	5–7	5–7	5–7	1–3	3–5
Ferrosilite	0.25–0.35	0.25–0.35	0.25–0.35	0.1–0.2	0.2–0.3
Graphite and graphite fiber composite	1.3–1.4	1.1–1.2	0.9–1.0	0.20–0.25	0.25–0.30

Appendix 5

CONTINUOUS AND FORMATIVE ASSESSMENT TEST TASKS [40]

Questions below are intended for students' individual work and for testing their knowledge of protecting metals against corrosion. Along with quizzes, this section contains reference materials that briefly sum up the basic contents of the corrosion protection questions under consideration, which will both allow them to independently assess their knowledge when preparing for tests and/or examinations and enables correcting such knowledge.

General Characterization of Corrosive Processes

1. Which of the statements below defines the term of corrosion?
   a) Failure of metals and alloys due to mechanical damages.
   b) Spontaneous failure of metals and alloys due to environment.
   c) Failure of metals in acid solutions.
   d) Failure of metals in alkalis.
   e) Failure of metals in sea water.

The word 'corrosion' derives from the Latin word 'corrodere' meaning "to gnaw to pieces." Metal corrosion means the spontaneous failure of metals and alloys due to their interaction with the environment.

2. What types of processes are corrosive processes?
   a) Heterogeneous processes. b) Homogeneous processes.

Corrosive process runs at the metal-environment phase boundary, i. e., it is a heterogeneous process.

3. Which of the statements below defines a corrosive process running by a chemical mechanism?
   a) Corrosion, in which oxidation-reduction processes run within one action.
   b) Corrosion, in which oxidation-reduction processes do not run within one action.
   c) Corrosion of metals in gaseous medium.

d) Corrosion of metals in non-electrolytes.
e) Corrosion of metals in atmospheric conditions.

By the process mechanism, a distinction is made between the chemical and electrochemical corrosion of metals. Chemical corrosion is a process of the metal interaction with a corrosive medium, in which metal oxidation and the reduction of the oxidative component of the medium run simultaneously within one action. The interaction products are not divided spatially.

4. Which of the statements below defines a corrosive process running by an electrochemical mechanism?

a) Corrosion, in which the oxidation and reduction processes run within one action.
b) Corrosion, in which the ionization of metal atoms and the reduction of the oxidative component of the corrosive medium do not run within one action and their velocities depend on the electrode potential.
c) Corrosion of metals when exposed to electrical current.
d) Corrosion of metals in alkalis.
e) Corrosion of metals in acids.

Electrochemical corrosion is a process of the metal interaction with a corrosive medium (electrolyte solution), in which the ionization of metal atoms and the reduction of the oxidative component of the corrosive medium do not run within one action and their velocities depend on the electrode potential.

Electrochemical corrosion processes run according to the electrochemical kinetics rules, where the total interaction reaction may be divided into two, considerably independent, electrode processes: Anodic process, i. e., metal passing into solution as ions and keeping the equivalent amount of electrons in the metal, and cathodic process, i. e., assimilating by oxidizers the excessive electrons occurring in the metal.

5. What definitions of corrosive process classify corrosion by the type of corrosive medium?

a) Atmospheric
b) Contact
c) Gaseous
d) In-ground
e) Fluid
f) Microbiological

By the type of corrosion medium, a distinction is made between the following corrosions: Gaseous, atmospheric, in-ground, microbiological, and fluid.

Gaseous corrosion is the corrosion of metals in a gaseous medium, which runs by a chemical mechanism.

Atmospheric corrosion is the corrosion of metals in the atmosphere of air or any wet gas, which is observed under visible condensation mist layers on the metal surface (humid atmospheric corrosion) or under the finest invisible adsorption mist layers (wet atmospheric corrosion).

Underground (soil, in-ground) corrosion is a corrosion caused by the effects provided on the metal by soil or ground that represents, in terms of corrosion, a specific electrolyte.

Microbiological corrosion is a corrosion running as influenced by the activity of microorganisms.

Fluid corrosion is the corrosion of metals in fluid media. A distinction is made among the salt, alkalic, seawater, and freshwater corrosions of metals.

By the conditions of fluid medium influencing on the metal, this type of corrosion is also divided into the following types: Full-immersion corrosion, partial-immersion corrosion, and intermittent-immersion corrosion.

6. What features are used in classifying corrosion by the types of additional effects?

a) Contact corrosion
b) Radiation corrosion
c) Corrosion cavitation
d) External-current corrosion
e) Corrosion under mechanical attack

By the types of additional effects, there can be the following: Contact corrosion, radiation corrosion, external-current corrosion, corrosion on stress, corrosion cavitation, and fretting corrosion.

Contact corrosion means corrosive processes in a system consisting of several metals located within one electrically conducting corrosive medium and being electrically interconnected.

Radiation corrosion means corrosive processes in the conditions of radioactive irradiation.

External-current corrosion means corrosive processes in the conditions of electrical current flowing through the metal surface.

Corrosion under mechanical attack. The most characteristic types of such destruction are:

a) Corrosion cracking occurring where the metal is simultaneously attacked by an aggressive medium and mechanical stresses. Cracks are typically formed in this process.

b) Corrosion fatigue caused by a corrosive medium and reversed or fluctuating mechanical stresses. This type of destruction is also characterized by forming inter- and transcrystallite cracks.

c) Corrosion cavitation is usually the consequence of an energetic mechanical effect provided by a corrosive medium upon the metal surface. Such corrosive-mechanical effects may lead to the quite strong local destructions of metal structures, such as for marine propeller screws.

d) Corrosive erosion caused by the mechanical abrasive effects provided by another solid body in the presence of a corrosive medium or by the direct abrasive effects provided by the corrosive medium itself.

e) Fretting corrosion caused by vibrations and a corrosive medium simultaneously.

7. What definitions classify corrosion by the nature of changes in the metal surface?

a) Fretting corrosion
b) Local corrosion
c) Total surface corrosion
d) Corrosion cavitation

By the nature of changes in the metal/alloy surface, a distinction is made among several types of corrosive destructions.

Corrosion is called total surface corrosion, if it covers the entire surface of the metal. Total surface corrosion can be uniform and nonuniform. In case of selective corrosion, one structural constituent or one alloy component is destructed.

Local corrosion covers some individual sectors of the metal surface. Local corrosion can appear as spots, pits, or points, penetrating deeply into metal. Subsurface corrosion begins on the surface, but then it spreads in the depth of the metal.

Intercrystallite corrosion is characterized by the metal destruction at the grain boundaries (Fig. 1).

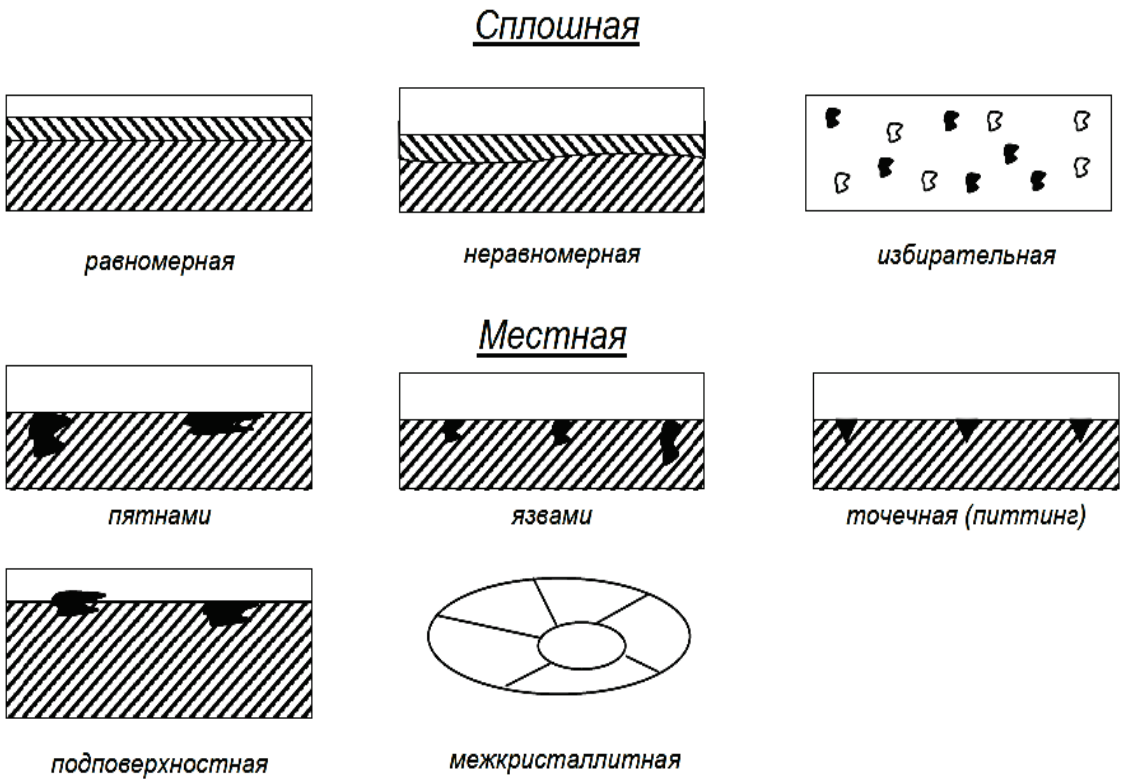

Fig. P 5.1. Types of Corrosion Failures.

8. What parameters are used to compute the time allowed for operating the structures designed, t_{all}?

a) Highest permissible corrosion velocity.

b) Highest corrosion velocity.

c) Corrosion depth.

d) Technical (or maximum permissible) corrosion depth.

Corrosion depth (h) is a normal coordinate of a certain corrosion front point reckoned from the initial surface of metal.

Technical (or maximum permissible) corrosion depth (h_t) is the inmost corrosion depth allowed in the conditions of a given technical task.

Corrosion velocity (v) is the rate of the imaginary continuous movement, at which the observed corrosion front point would have moved into the metal to a depth equaling to the one actually observed, over the observation time.

Technical, or highest permissible, corrosion velocity (v_t) is the highest corrosion rate allowed for a given structure.

Highest corrosion velocity (v_{max}) is the highest corrosion rate expected.

Corrosion wear (C) is the mass of metal passed into a compound on a unit of the surface of its contact to the corrosive medium per time unit.

In case of uniform corrosion, the above variables of h, v, and C are interrelated. Therefore, having measured one of them, you can find the values of the two other variables.

Knowing the above values, you can find the estimated permissible operation time of the structures designed:

$$t_{all} = \frac{h_t}{V_{max}}.$$

9. Corrosion velocity (mm/year) found based on metallographic studies characterizes:

a) Mean metal corrosion velocity over testing time.
b) True metal corrosion velocity at the completion of testing.
c) Highest metal corrosion velocity over testing time.
d) Lowest metal corrosion velocity over testing time.

Metal corrosion velocity found based on metallographic studies is the mean velocity over testing time. True metal corrosion velocity at a given time can be found by graphical differentiation (by the slope of the tangent to the corrosion-time curve).

10. If a metal has the uniform corrosion velocity of 0.0005 mm/year, then, according to the 10-to-1 metal corrosion-resistance scale, it is

a) Highly resistant
b) Non-resistant
c) Sensitive
d) Totally resistant

To qualitatively and quantitatively evaluate metal corrosion resistance and choose protection means in specific conditions, there are several corrosion-resistance scales. Most common is the 10-to-1 metal corrosion-resistance scale (Table P 5.1). To roughly estimate the corrosion resistance of metals, you should be guided by resistance groups, while score should be used for precise evaluation.

Table P 5.1

10-to-1 Metal Corrosion-Resistance Scale

Resistance Group	*Metal Corrosion Velocity, mm/year*	*Score*
Totally resistant	*Below 0.001*	*1*
Highly resistant	*Above 0.001 up to 0.005*	*2*
	Above 0.005 up to 0.01	*3*
Resistant	*Above 0.01 up to 0.05*	*4*
	Above 0.05 up to 0.1	*5*
Low-resistant	*Above 0.1 up to 0.5*	*6*
	Above 0.5 up to 1.0	*7*
Sensitive	*Above 1.0 up to 1.5*	*8*
	Above 5.0 up to 10.0	*9*
Non-resistant	*Above 10.0*	*10*

11. If a metal has the uniform corrosion velocity of 0.05 mm/year, then it is

a) Highly resistant
b) Low-resistant
c) Resistant
d) Sensitive

See the answer to Question 10.

12. If a metal has the uniform corrosion velocity of 0.5 mm/year, then it is

a) Resistant
b) Low-resistant
c) Sensitive
d) Non-resistant

See the answer to Question 10.

Metal Corrosion in Electrolyte Solutions

13. Choose the conditions, in which the electrochemical corrosion of metals runs.

a) Freshwater or seawater
b) Atmospheric conditions
c) Soil
d) Dry gas
e) Wet gas

Most metal structures get destructed in electrolyte solutions. These are the destruction of metal products in freshwater or seawater, in atmosphere, and in soil; destruction of machines and devices in chemical industry; losing metals when descaling them in pickling solutions; etc.

14. Thermodynamics provides information

a) On the possibility/impossibility of spontaneous corrosion process.

b) On corrosion process velocity.

c) On both above.

Thermodynamics provides comprehensive information on the possibility/impossibility of spontaneous corrosion process in the conditions considered. The process will run spontaneously ($\Delta G < 0$), if the difference of the balanced potentials of the anodic metal oxidation reaction (Ea) and the cathodic oxidizer reduction reaction (Ec) is a negative value in the given conditions. However, thermodynamics does not answer the following question: What will be the velocity of a thermodynamically possible corrosion process?

15. In how many groups are all metals divided by their thermodynamic stability depending on the value of the standard electrode potential?

a) 4; b) 5; c) 6; d) 7; e) 8.

By their thermodynamic stability, all metals are divided into five groups, depending on the value of the standard electrode potential. The groups are separated from each other by the balanced potentials of possible cathodic reactions. In this case, these are the balanced potentials of the hydrogen electrode and oxygen electrode in neutral and acidic media (Table P 5.2).

Table P 5.2

Potentials of the Hydrogen Electrode and Oxygen Electrode in Neutral and Acidic Media

E_{N^+/H_2}		E_{OH^-/O_2}	
Medium			
Neutral	*Acidic*	*Neutral*	*Acidic*
–0.415	*0.000*	*0.815*	*1.23*

Group 1:

Metals of increased thermodynamic instability, such as Na, Mg, Be, Al, Zn, etc. Their standard potentials are more negative than the balanced potential of the hydrogen electrode in neutral media (–0.415 V). Therefore, they corrode even in neutral aqueous media that do not contain oxygen.

Group 2:

Thermodynamically instable metals, such as Cd, Mn, Ni, Sn, Pb, etc. Their standard potentials range within the values of the balanced potentials of hydrogen electrode in neutral (–0.415 V) and acidic (0.000 V) media. In the absence of oxygen, they are stable in neutral media and corrode in acidic media.

Group 3:

Metals of intermediate thermodynamic stability, such as Bi, Re, Cu, Rh, Ag, etc. Their standard potentials range within the values of the balanced potentials of hydrogen electrode in acidic media (0.000 V) and of oxygen electrode in neutral media (0.815 V). They are stable in acidic media in the absence of oxygen and corrode in neutral media in its presence.

Group 4:

High stability metals, such as Ir and Pt. Their standard potentials range within the values of the balanced potentials of oxygen electrode in neutral media (0.815 V) and acidic media (1.23 V). They are stable in neutral media in presence of oxygen, but they corrode in acidic media in its presence.

Group 5:

Full stability metals, such as Au. Their standard potentials are more positive than the balanced potential of oxygen electrode in acidic media (1.23 V). They are stable in neutral and acidic media and in presence of oxygen.

16. Which metals belong to the group of increased thermodynamic instability?

a) Cd, Mn, Ni, Sn, Pb
b) Na, Mg, Be, Al, Zn
c) Bi, Re, Cu, Rh, Ag
d) Ir, Pt
e) Au

See the answer to Question 15.

17. Which metals are thermodynamically instable?

a) Cd, Mn, Ni, Sn, Pb
b) Na, Mg, Be, Al, Zn
c) Bi, Re, Cu, Rh, Ag
d) Ir, Pt
e) Au

See the answer to Question 15.

18. Pourbix diagrams allow finding

a) Boundaries of the thermodynamic possibility of corrosion process.

b) Thermodynamically possible cathodic process.

c) Corrosion process velocity

d) Expected corrosion products.

Pourbaix diagrams, i. e., diagrams showing the condition of the metal-water system, can be used to set the boundaries of the thermodynamic possibility of electrochemical corrosion of metals, the thermodynamically possible cathodic process, and the expected corrosion products.

19. What basic stages does corrosion process consist of?

a) Transferring the reacting substances to the phase boundary

b) Heterogeneous reaction

c) Removing the reaction products

d) All the above

Normally, corrosion process consists of at least three basic stages: 1) Transferring the reacting substances to the phase boundary, i. e., to the reaction area; 2) heterogeneous reaction itself; and 3) Removing the reaction products from the reaction area. Each of these basic stages can, in turn, consist of elementary stages that run successively.

20. What is the range of the roughness coefficient representing the true-to-visible metal surface ratio?

a) 1-1.5; b) 2-4; c) 4-6.

The ratio between the true surface and the geometric surface is characterized by the roughness coefficient: $V_r=S_{true}/S$, the values of which usually range within 2-4.

21. Which of the equations below describes an individual anodic reaction:

$Me \rightarrow Me^{z+} + ze$?

a) $\vec{i} = k_1 \exp[+\frac{a(E_P+\Delta E)zF}{RT}]$;

b) $\overleftarrow{i} = k_2 c^1 \exp[-\frac{\beta(E_P+\Delta E)zF}{RT}]$.

The equation of the individual polarization curves of anodic and cathodic reactions running on the surface of metal immersed in the solution of its salt, in case of the inhibited stage of the charge transfer process, is represented as:

For anodic reaction $Me \rightarrow Me^{z+} + ze$*:*

$$\vec{\imath} = k_1 \exp[+\frac{a(E_P + \Delta E)zF}{RT}]$$

For cathodic reaction $Me^{z+} + ze \rightarrow Me$*:*

$$\overleftarrow{\imath} = k_2 c^1 \exp[-\frac{\beta(E_P + \Delta E)zF}{RT}].$$

22. Is this statement correct? Changing the value of balanced potential gives rise to concentration polarization, i. e., potential difference determined by the difference of balanced potentials.

a) Yes, it is correct. b) No, it is not correct.

Slowness of the diffusion stage of electrochemical process leads to the difference in the concentrations of reaction participants in the solution volume and on the metal surface, which, in turn, changes the balanced reaction potential computed by Nernst equation. Changes in the value of balanced potential gives rise of concentration polarization, i. e., potential difference determined by the difference of balanced potentials, the value of which can be represented by the following equation:

$$\Delta Econc = E_p - E_{p0} = 2.3(\frac{RT}{zF}) \times \lg(\frac{c}{c_0}),$$

where E_p *is the balanced potential relevant to the concentration of ions at the metal surface;* E_{p0} *is the balanced reaction potential relevant to the concentration of ions in the solution; c is the concentration of diffusing substance near the corroding metal; and* c_0 *is the same in the solution volume.*

23. In what sequence, in a general case, does the metal surface condition change when the potential shifts from the balanced value to positive area?

a) Passivity disturbance, transition range, passive state, and active dissolution.

b) Active state, transition range, and passive state.

c) Active state, transition range, passive state, and passivity disturbance.
d) Passive state, transition range, active state, and passivity disturbance.
e) Transition range, passivity disturbance, active dissolution, and passive state.

Dependence of the anodic dissolution rate on potential for most metals has a typical form (Fig. P 5.2). In this dependence, some areas are identified, which are relevant to different states of the metal surface. There active state, transition range, passive state, and the passivity disturbance area.

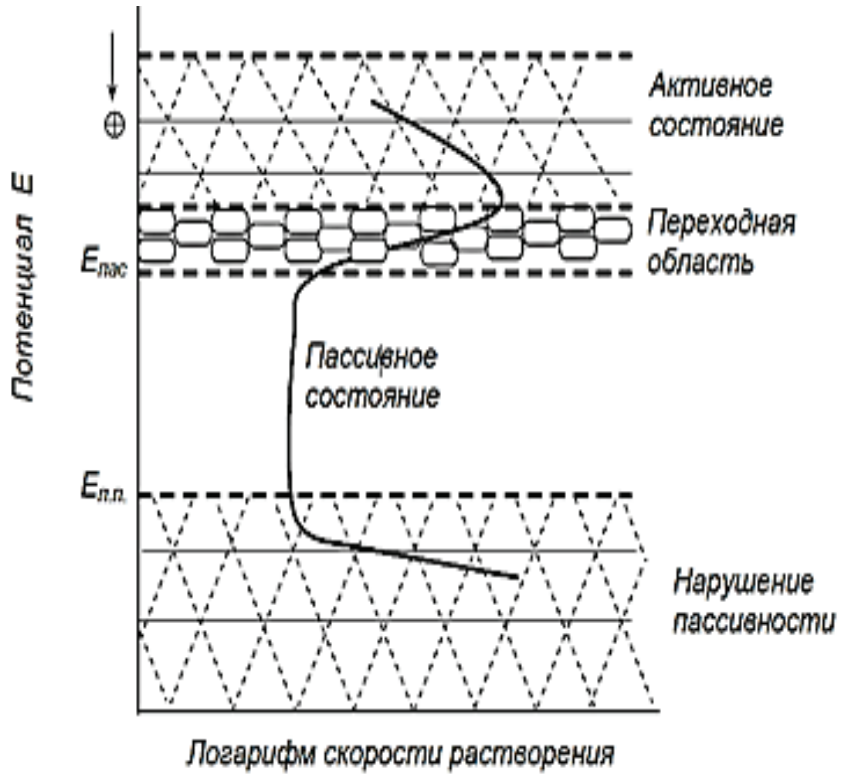

Fig. P 5.2. Dependence of the Metal Dissolution Rate on Potential

24. When a metal enters the passive state at anodic dissolution, the following is observed:
a) Shift-down of the anodic dissolution rate of metals in the potentiodynamic polarization conditions;
b) Significant shift of the potential to the positive side in galvanodynamic conditions.

Beginning of the passive state of metals is characterized by the following phenomena:

a) Shift-down of the anodic dissolution rate of metal in the poentiodynamic polarization conditions;

b) Significant shift of the metal potential to the positive side in the galvanodynamic polarization conditions.

25. Passivators that bring a metal into passive state are:

a) Oxidizers, such as $NaNO_3$. HNO_3. K_2CrO_4. $NaNO_2$. and Na_2WO_4;

b) Ions, such as Cl^-, Br^-, and J^-;

c) Reducing agents, such as Na_2SO_3 and $Na_2S_2O_3$.

Passive state of metals is caused by oxidizers or anodic polarization. Substances or processes that cause the passive state of metals in certain conditions, are called passivating factors or passivators.

Passivators are: 1) Oxidizers, such as HNO_3. $NaNO_3$. $NaNO_2$. Na_2WO_4. and K_2CrO_4; 2) anodic polarization from an external supply source of direct current or where the metal works as anode with another metal working as a cathode.

Substances or processes that disturb the passive state of metals or hindering the passivity, are called activators. Activators are:

1) Reducing agents, such as hydrogen, $Na_2 SO_3$. $Na_2 S_2O_3$. etc.;

2) Cathodic polarization;

3) Some ions, such as H^+, haloid ions, such as Cl^-, Br^-, and I^-; SO_4^{2-}, etc.;

4) Increasing temperature; and

5) Mechanical damage of the passive surface of the metal.

26. Activators that bring the metal from passive state into active state are:

a) Reducing agents, such as hydrogen, $Na_2 SO_3$. $Na_2 S_2O_3$. etc.;

b) Cathodic polarization;

c) Some ions, such as H^+, haloid ions, such as Cl^-, Br^-, and I^-; SO_4^{2-}, etc.;

d) Increasing temperature;

e) Mechanical damage of the passive surface of the metal.

See the answer to Question 25.

27. What is the steady-state (corrosive) potential of metal?

a) Unbalanced electrode potential;

b) Balanced electrode potential;

c) The value of unbalanced electrode potential, relevant to the balance of the sums of the rates of anodic and cathodic processes.

Potentials of metals, in which exchange processes involve both their own ions and other ions and molecules, are called unbalanced electrode potentials.

The value of an unbalanced electrode potential, relevant to the balance of sums of rates of anodic and cathodic processes, is called the steady-state potential. A special case of a steady-state potential is the potential of corrosion (corrosion potential).

28. Which of the statements below regarding Evans Diagram is true?
    a) A diagram, in which the value of potential is plotted on the abscissa, while the current values are plotted on the ordinate;
    b) A diagram, in which the negative values of potential are plotted up on the ordinate, while the values of anodic and cathodic currents are plotted on the abscissa;
    c) A diagram, in which the positive values of potential are plotted up on the ordinate, while the values of anodic and cathodic currents are plotted on the abscissa.

Corrosion systems are usually analyzed using Evans Diagrams, in which the kinetics of anodic and cathodic reactions is reflected graphically. In these diagrams, the negative values of potential are plotted up on the ordinate, while the absolute values of anodic and cathodic currents are plotted on the abscissa.

29. What types of corrosion monitoring do you know?
    a) Anodic; b) Cathodic; c) Mixed; d) Ohmic.

Corrosion runs under anodic inhibition, if the displacement of corrosion potential from the balanced potential of anodic reaction considerable exceeds its displacement from the balanced potential of cathodic reaction. Corrosion runs under cathodic monitoring, if the displacement of corrosion potential of the balanced potential of cathodic reaction considerably exceeds its displacement from the balanced potential of anodic reaction. If the displacements of corrosion potential from the balanced potentials of anodic and cathodic reactions are comparable, then mixed monitoring takes place. If the resistance of the corrosive medium is high, then the process runs under ohmic monitoring.

30. Which of the statements below are true for corrosion processes in neutral media?

a) Corrosion velocity depends on the nature of the electrolyte.
b) Corrosion velocity does not depend on the concentration of dissolved salts.
c) Corrosion velocity grows with mixing.
d) Corrosion velocity does not depend on mixing.

Characteristics of the oxygen ionization cathodic reaction affect markedly the metal corrosion velocity. Due to the insignificant solubility of oxygen in aqueous media, the inhibited stage is usually the transfer of oxygen to the metal surface within the diffusion layer. In this case, the highest oxygen ionization reaction rate in natural convection conditions is relevant to the diffusion current limit. Oxygen solubility depends on the electrolyte nature and decreases with increasing the concentration of salts dissolved. Moreover, the concentration of dissolved oxygen decreases with increasing the solution temperature and reducing the oxygen partial pressure in gas phase. Low solubility of oxygen in aqueous solutions determines the low values of the diffusion current limit in the natural convection conditions. One of the factors changing the efficient thickness of the diffusion layer is the solution mixing. Electrolyte velocity provides a major influence upon metal corrosion in neutral media, which runs with oxygen depolarization.

31. What are the causes of electrochemical heterogeneity of the metal-electrolyte interface?

a) Inhomogeneity of metal phase
b) Inhomogeneity of liquid phase
c) Inhomogeneity of physical conditions
d) Inhomogeneity of metal surface
e) Inhomogeneity of the internal stresses in metal
f) Submicroscopic (atomic) inhomogeneity of metal surface
g) Inhomogeneity of protective films on the metal surface

Surface of a corroding metal usually represents a complex galvanic cell, i.e., a galvanic cell that consists of several electrodes that differ from each other. Causes of electrochemical heterogeneity, i.e., inhomogeneity, of the metal-electrolyte interface in the electrochemical corrosion of metals are given in Table 3 below.

32. Metal phase inhomogeneity that leads to the electrochemical heterogeneity of the metal-electrolyte interface is caused by

a) Macro- and microinclusions
b) In homogeneity of the alloy
c) Presence of grain boundaries in crystals
d) Emergence of dislocations on the metal surface

See the answer to Question 31.

Table P 5.3.

Causes of the electrochemical heterogeneity of the metal-electrolyte interface

General Cause of Heterogeneity	Specific Cause of Heterogeneity	Polarity of Sectors
1	2	3
Inhomogeneity of metal phase	Macro- and microinclusions	Inclusions with a more positive potential – cathodes
	Inhomogeneity of the alloy	Sectors enriched with a component having a more positive potential – cathodes
Inhomogeneity of metal surface	Grain boundaries in crystals	Boundaries may be both cathodes and anodes
	Emergence of dislocations on the metal surface	Emergence region is an anode
	Anisotropy of metal crystal	Various edges of monocrystals may be both anodes and cathodes
Submicroscopic (atomic) inhomogeneity of the metal surface	Presence of dissimilar atoms in a solid solution	Atoms or atom clusters with a more negative potentials

End of Table P 5.3

1	2	3
Inhomogeneity of protective films on the metal surface	Macro- and micropores in the oxide film	Metal in pores is an anode
	Inhomogeneous distribution of corrosion after-product on the metal surface	Sections under the corrosion products are usually anodes
Inhomogeneity of internal stresses in metal	Inhomogeneous deformation	The deformed section is an anode
	Inhomogeneity of external stresses	Stressed sectors are anodes
Inhomogeneity of liquid phase	Difference in the concentration of the own ions of the metal in the electrolyte	Sections contacting the more dissolved solution are anodes
	Difference in the concentration of neutral salts	Sectors contacting more concentrated solutions of salts with an active anion are anodes, while those with the solutions of passivating salts are cathodes
	Difference in pH	Sections, in which pH is lower, are anodes
	Difference in the concentration of oxygen or another oxidizer	Sections, in which the oxidizer concentration is higher, are cathodes
	Difference in temperature	Heated sections are anodes
Inhomogeneity of physical conditions	Inhomogeneous distribution of radiant energy	Intensively irradiated sections are anodes
	Inhomogeneous electric field	Sections, in which positive charges are included in electrolyte, are anodes

33. In a corrosive system, the inclusions in metal phase, having a more positive electrode potential, are:

a) Anodes; b) Cathodes; c) Can be both anodes and cathodes.

See the answer to Question 31.

34. In a corrosive system, the metal sections under the corrosion products are usually:

a) Anodes; b) Cathodes; c) Can be both anodes and cathodes.

See the answer to Question 31.

35. With increasing the temperature, the corrosion velocity usually:

a) Increases; b) Decreases.

With increasing the temperature, the corrosion velocity usually increases. This is caused by the following basic factors:

a) Increasing rate of the diffusion of oxidizer to the metal surface and of the corrosion products from the surface;

b) Reducing over-stresses and increasing the rate of electrochemical reactions;

c) Increasing the rate of intermediate reactions;

d) Growth of the solubility of corrosion products.

The increased temperature may also decrease the corrosion velocity. For instance, if a metal corrodes in neutral media, where oxidizer is oxygen, since its solubility in water decreases with increasing temperature.

36. With increasing pressure, the corrosion velocity usually:

a) Increases; b) Decreases.

With increasing pressure, the corrosion velocity usually increases, since the solubility of oxygen increases and mechanical stresses in metal grow.

37. Alternating current flowing through the metal surface:

a) Increases the corrosion velocity;

b) Decreases the corrosion velocity.

External anodic current accelerates corrosion, while the cathodic one inhibits it. Polarizing with the external alternating current strengthens corrosion. This happens, because the rate of anodic process (metal ionization) increases during anodic half-period, while no metal ions discharge during cathodic period.

38. Presence of aerobic or anaerobic bacteria in the corrosive medium:
a) Increases corrosion velocity; b) Decreases corrosion velocity.

Aerobic bacteria promoting corrosion can be sulfur-oxidizing and iron-precipitating. The former ones can oxidize sulfur to sulfuric acid, the local concentration of which may reach 10 %.

Iron-precipitating bacteria adsorb iron in an ionic state and excrete it as insoluble compounds. Non-equilibrium retention of those compounds at different sections of the metal surface results in the values of their potentials becoming inequal. Electrochemical heterogeneity occurring on the surface enhances corrosion.

Anaerobic bacteria are basically sulfate-reducing. They reduce the sulfate ions into sulfide ions that accelerate corrosion remarkably.

Metal Corrosion in Natural and Industrial Conditions

39. What types of metal corrosion are observed in natural media?
a) Corrosion by gases
b) Soil corrosion
c) Seawater corrosion
d) Atmospheric corrosion

Most metal structures are operated in natural conditions. A considerable number of steel structures are operated in atmospheric conditions. Main and upstream pipelines, water ducts, and well casings at oil and gas oilfields operate below the ground. Metal structures of ports, mooring berths, and vessels contact seawater permanently and are exposed to seawater corrosion. All types of corrosive processes in natural conditions run by the electrochemical mechanism.

40. Provided that there is a mist adsorption layer on the metal surface, the rate of atmospheric corrosion is controlled by:
a) Anodic process; b) Cathodic process.

Provided that there is a shallow-thickness mist adsorption layer on the metal surface, oxygen penetrates through it unhinderedly, and cathodic process is unhampered. Anodic process is complicated by the fact that corrosion products shield the metal surface.

41. Which of the product design features below promote atmospheric corrosion?
a) Polished surface of the product
b) Crevices or gaps in the structure parts

c) Pores in the protective coating or oxide layer
d) Leaks in threaded and screwed joints
e) Rough surface of the product

Narrow crevices and gaps, in which capillary condensation and moisture stagnation, promote atmospheric corrosion and can lead to forming corrosion pits. Atmospheric corrosion can also be intensified due to pores in the protective coating or oxide layer, as well as to leaks in threaded and screwed joints.

42. Which of the statements below regarding soil corrosion processes are true?

a) Velocity depends on the soil humidity
b) Velocity depends on the pH of the environment
c) Velocity depends on the air permeability of soil
d) Steady corrosion rate
e) Velocity depends on the mineralogical content and grading of soil

With increase in the soil humidity, its corrosive activity grows until it reaches a certain critical level. Further increase in the humidity decreases such activity. This is related to lower oxygen access.

In most soils, their pH=6.0-7.5. There are also alkali loams and saline lands that have pH=7.5-9.5 and acidic humus and marshy soils having pH=3.0-6.0. both are highly aggressive. Mineralogic content and grading of grounds influences their ohmic resistance.

Air permeability of soils is of great importance. Inhibiting oxygen access decreases the corrosion velocity. In most soils, corrosive processes run under cathodic inhibition due to the hampered oxygen transport. In loose, well aerated soils, anodic inhibition is observed.

In case of corrosion couples occurring, in which anodic and cathodic sections are considerably distant from each other, then the process is characterized by ohmic inhibition.

Along with steady-rate corrosion, underground metal structures are exposed to pitting corrosion that most frequently occurs on the bottom parts of pipelines.

43. Under which control does the soil corrosion process run most frequently?

a) Anodic control;
b) cathodic control;
c) ohmic control;
d) anode-cathode control.

See the answer to Question 42.

44. How do stray currents affect the corrosion of underground utility systems and structures?

a) They inhibit corrosion velocity
b) They stop corrosion
c) They do not affect corrosion velocity
d) They accelerate corrosive processes
e) Alternating current inhibits corrosion

Stray currents cause serious the corrosive damages of underground utility systems or structures and occur due to the earth leakage of the direct current drawn by overhead and underground rail transport, such as tube railroad, tram, or electrified railways, and by electrical welding machines. Areas where stray currents enter from the earth into a metal structure become cathodes, while those where the current leaks into the earth are anodes. Intensity of corrosive damages directly depends on the values of stray currents and follows the Faraday's law. Alternating stray current is also dangerous, but it destructs metals at a rate that is many times lower than that of direct current.

45. Which of the statements below regarding local corrosion are true?

a) Destruction of comparatively small sectors
b) Difficulties in detecting
c) High rate of corrosion front-line advance
d) Probabilistic nature

A distinctive feature of local corrosion processes is that they damage small sections on the surfaces of metal structures made of metals, the dissolving rate of which considerably exceeds that of the main part of the surface. Most local corrosion processes are probabilistic. The increased danger of local corrosion processes is related to the fact that, due to small dimensions of the surface areas damaged by them and due to high metal dissolving rates in them, the existence of a corrosion area is often detected just at the time of failure.

46. Which of the statements below regarding pitting corrosion are true?
a) Pitting corrosion of metals in aqueous media is stimulated by the ions of Cl^-, Br^-, and J^-
b) By their action efficiencies, activating anions are ranked as $Br^- > Cl^- > J^-$
c) OH^-, NO_3^-, SO_4^{2-}, and ClO_4^- can be passivators for the metal
d) Water can be passivator for the metal
e) Pits are formed on the surfaces of metals that are in a passive state

Pitting corrosion of metals in aqueous media is stimulated by the ions of Cl^-, Br^-, and J^-. By the relative efficiency of their action, the activating anions are arranged as Cl^-, Br^-, and J^-. Metal passivators can be various anions usually containing oxygen, such as OH^-, NO_3^-, SO_4^{2-}, and ClO_4^-*), but water is the most universal passivator.*

47. Which of the statements below regarding pitch corrosion are true?
a) Pitch corrosion is typical of metals in active state
b) Pitch corrosion is typical of metals in passive state
c) Sulfide non-metal inclusions enhance the metal resistance against pitch corrosion
d) Tendency to pitch corrosion increases when forming a network of finely dispersed perlite precipitate
e) Manganous sulfide inclusions in carbon steels increase the tendency to pitch corrosion

Pitch corrosion usually runs on the surfaces of metals that dissolve in active state. Carbon and low-alloy steels used in aqueous chloride-containing media tend to pitch corrosion. Resistance of carbon and low-alloy steels against pitch corrosion largely depends on their structural and structural-phase components. Abrupt decrease in the resistance of steels against pitch corrosion happens in separating sulfide non-metal inclusions in their structures. Manganous sulfide inclusions are dangerous for carbon steels. For steels having a ferrite-perlite structure, tendency to pitch corrosion increases when forming a continuous network of fine-dispersed perlite precipitate.

48. Which of the statements below regarding the crevice corrosion processes are true?

a) Crevices, gaps, or pockets in the structure result in crevice corrosion
b) Processing defects, such as micro-cracks or micro-crevices, on the metal result in crevice corrosion
c) Only metals capable of passivation can be attacked by crevice corrosion
d) Tendency to crevice corrosion decreases with increasing the doping level of steel
e) Intensification of crevice corrosion is promoted by changes in the properties of the solution in crevices or gaps

Crevice corrosion occurs where the structure has narrow crevices, gaps, or pockets, or if the metal has processing defects, such as micro-crevices or micro-cracks. Intensification of crevice corrosion is promoted by changes in the properties of the solution in crevices or gaps – it acidifies with the time and becomes more concentrated with aggressive anions. Tendency to crevice corrosion decreases with increasing the doping level of steels.

49. Which of the statements below regarding the contact corrosion are true?

a) Contact corrosion develops in the solutions of electrolytes at the contact of steady-potential metals
b) Anode of a corrosion couple will be the metal having a more negative potential
c) Cathode of a corrosion couple will be metal having a more negative potential
d) Dangerous is the combination of the small surface of cathode and the large surface of anode in the corrosion couple

Two metals contacting each other and having different electrode potentials form in the electrolyte a galvanic element, the activity of which affects the corrosion velocity of each of those metals: Corrosion of a more electronegative metal usually strengthens, in most cases, while the corrosion of a more electropositive metal weakens or sometimes stops completely.

Contact corrosion may be observed in a structure made of the same metal, if there is a difference in the electrochemical potentials of its different parts. For example, in welded structures, the welded seam

potential may differ from the base metal potential. Contact corrosion is the more dangerous, the higher is the ratio of the cathode surface are to the anode surface area.

50. What types of corrosive and mechanical damages do you know?
a) Fretting corrosion b) Corrosion fatigue
c) Corrosion cracking d) Corrosion cavitation

The following types of mechanical-stress-induced corrosive damages to metal are known:

– Corrosion cracking is metal destruction due to the occurrence and development of crevices at the simultaneous effects provided by tensile stresses and corrosive medium;

– Corrosion fatigue is metal destruction induced by the periodic dynamic load at stresses that are considerably lower than the strength limit;

– Corrosion cavitation is metal destruction determined by both corrosive and impact effects of a corrosive medium;

– Fretting corrosion is corrosion induced by both vibration and a corrosive medium; and

– Corrosion erosion usually means metal surface destruction caused by the mechanical abrasive effects provided by another solid object and simultaneously by a corrosive medium or by the direct abrasive effect provided by the corrosive medium itself.

51. Which of the statements below regarding corrosion erosion are true?
a) It is the metal surface destruction caused by mechanical abrasive effects and by the action of a corrosive medium
b) Additional abrasive effects reduce the corrosion velocity
c) Additional abrasive effects increase the corrosion velocity

Term "corrosion erosion" usually means the metal surface destruction caused by the mechanical abrasive effects provided by another solid object at the simultaneous action of a corrosion medium, or by the direct abrasive action of the corrosion medium itself. If oxide coatings or adsorption films are skimmed mechanically and permanently, the corrosion velocity can increase by several orders.

52. Under cavitation attack, metal corrosion:
a) Accelerates; b) Decelerates; c) Remains unchanged.

Under cavitation attack, metal corrosion accelerates and leads to forming deep local caverns.

Cavitation is the process of forming and collapsing small bubbles in the unsteady flow of liquid that flows around a solid body. The bubbles disappear accompanied by a pressure surge leading to the destruction of both protective coatings and the structure of the metal itself. At the same time, the corrosion velocity may increase up to 75 mm per year. Bubbles are formed in the low-pressure regions and collapse in the high-pressure regions.

53. Fire resistance means

a) Ability of the metal to resist the corrosive effects provided by gases at high temperatures
b) Ability of the metal to retain rather high mechanical properties at high temperatures

Fire resistance characterizes the ability of a metal to resist the corrosive effects provided by gases at high temperature. Fire resistance means the ability of a metal to retain at high temperatures its high mechanical properties, such as long-term strength and creep-resistance.

54. How does introducing chrome, aluminum, and silicon into the composition of steel affect its oxidation rate?

a) It does not practically affect it
b) It inhibits it strongly
c) It stops corrosion completely
d) It accelerates it strongly

Protective properties of surface films depend on the nature and composition of the alloy. Chrome, aluminum, and silicon strongly inhibit iron oxidation due to forming strong protective oxide coatings. These elements are widely used to alloy steels to enhance their fire resistance.

Chrome introduced into steel in the amount of up to 30 % increases its fire resistance considerably.

Aluminum is introduced into steel in the amount of up to 10 %, which increases its fire resistance even more. A similar property is typical of silicon introduced into steel in the amount of up to 5 %. Sulfur, phosphor, nickel, and manganese that are present in an alloy do not practically affect the high-temperature oxidation of iron.

Vanadium, wolfram, and molybdenum accelerate steel oxidation strongly at high temperature. This is determined by the fugitiveness and high fusibility of the oxides formed by those elements.

55. How do sulfur, phosphor, nickel, and manganese affect the steel oxidation rate when introduced into the steel?

a) It stops corrosion completely
b) It inhibits it strongly
c) It does not practically affect it
d) It accelerates it strongly

See the answer to Question 54.

56. How do vanadium, wolfram, and molybdenum affect the steel oxidation rate when introduced into the steel?

a) It accelerates it strongly
b) It inhibits it strongly
c) It stops it completely
d) It does not practically affect it

See the answer to Question 54.

57. At high temperatures, increasing the carbon contents in steel leads to:

a) Increasing the oxidation rate;
b) Decreasing the oxidation rate;
c) No influence upon the oxidation rate.

At high temperatures (800° C or higher), with increasing the carbon contents in steel, its oxidation rate decreases due to the more intensive formation of carbon oxide, which leads to inhibiting the iron oxidation process, as well as resulting from decreasing the solubility and diffusion rate of iron in scale saturated with carbon oxide and strengthening the formation of gas bubbles in the scale.

58. How do mercaptans, hydrogen sulfide, and elemental sulfur affect the corrosive activity of oil?

a) They increase it; b) They reduce it; c) They do not affect it.

High corrosive activity is imparted to oil by sulfur compounds dissolved in it, such as mercaptans (thio-alcohols R – S – H) that destruct Co, Ni, Pb, Cu, and Ag, forming the relevant mercaptides, such as $[(CH_3S)_2$ *Pb,* $(CH_3S)_2$ *Cu, etc.; hydrogen sulfide that affects Fe, Pb, Cu, and Ag forming sulfides, such as FeS, PbS, etc.; and elemental sulfur that is corrosively active towards copper and silver and also forms sulfides.*

Corrosion Resistance of High-Priority Metals and Alloys

59. Which of the statements below regarding the iron corrosion products are true?

a) Insoluble iron corrosion products are rust;
b) Rust has weak adhesion to metal surfaces;
c) Rust coats metal with a loose layer;
d) Rust protects iron well against further corrosion;
e) Rust composition is expressed by the general formula:
$nFe(OH)_2 \times mFe(OH)_3 \times qH_2O$, where n, m, and q are integers.

In the most media, except for the solutions of mineral acids, insoluble iron corrosion products (rust) are formed. Rust is formed in a solution in proximity of the corroding surface. Rust coats metal with a loose layer. Its adhesion to the metal surface is weak; therefore, it does not protect iron well against corrosion. Rust composition can alternate, and it is expressed with the following general formula:
$nFe(OH)_2 \times mFe(OH)_3 \times qH_2O$, where n, m, and q are integers.

60. The boundary concentration of carbon between steels and cast irons is, in %:

a) 2.03; b) 1.83; c) 2.08; d) 2.53; e) 3.02.

$Fe\text{-}Fe_3C$ systems are divided into steels and cast irons, depending on their carbon contents. Steels are alloys, in which carbon content does not exceed 2.03 %.

61. Which of the statements below regarding steel classification are true?

a) Ferrite steels – steel structure contains no more than 0.1 % of C
b) Ferrite steels – steel structure contains more than -.1 % of C
c) Ferrite-austenite steels – steel structure contains 0.1-0.51 % of C
d) Austenite steels – steel structure contains 0.51-2.03 % of C

Steel structure is determined by carbon contents. Steels containing less than 0.1 % of C have a purely ferrite structure. Steels containing 0.1-0.51 % of carbon have a ferrite-austenite structure. Alloys containing 0.51-2.03 % of C have a purely austenite structure.

62. Which of the statements below regarding the corrosion properties of iron in organic media are true?

a) Carbon steels are highly corrodible in organic acids;
b) Steel corrosion velocity in organic acids decreases in presence of oxygen;
c) With rising temperature, the steel corrosion velocity in organic acids increases;
d) Carbon steels are resistant in alcohols and benzene;
e) Carbon steels are resistant in organic solvents.

In organic acids, carbon steels are highly corrodible, and this corrosion increases in presence of oxygen and with rising temperature. Iron-carbon steels are corrosion-resistant in alcohols, benzene, and organic solvents.

63. Which of the alloying elements below increase the corrosion resistance of steels in the solutions of electrolytes?

a) Chrome
b) Nickel and copper
c) Molybdenum and wolfram
d) Titanium and niobium
e) Nitrogen

Introducing nickel into steel facilitates passivation and increases the stability of passive state, including in media inducing the development of local corrosion processes, such as pitting or crevice corrosion.

To increase the corrosion resistance even more, molybdenum is introduced into the content of chrome-nickel stainless steels, which enhances the ability of steels to passivate in non-oxidizing media, narrowing the active dissolution region, and promotes the essential reduction of their tendency to pitting and crevice corrosion.

Wolfram, like molybdenum, enhances the corrosion resistance of steels; however, its actions is not so efficient.

Carbon is a necessary alloying element in martensitic steels, such as 30X13. 40X13. 95X18. etc., where it ensures high strength characteristics. Nitrogen is a strong austenite-promoting element. It is very useful in austenitic and austeno-ferritic steels. Nitrogen strengthens a solid solution stronger than carbon, increases resistance against pitting corrosion, and inhibits separating carbide and intermetallic phases.

When introduced into steels, copper enhances their resistance in mineral acids.

Titanium and niobium form carbides, TiC and NbC, and, doing so, eliminate carbon from the solid solution. When introduced into steel, they enhance the resistance of steels against local corrosions.

64. Choose the correct combinations of element names and symbols.
a) X – Cr; b) H – Ni; c) M – Mo; d) Г – Mn; e) Ю – W.

The following Russian letters are assigned to each of alloying elements: Х – Cr; Н – Ni; М – Mo; Г – Mn; Ю – Al; Ф – W; С – Si; М – Ti; Д – Cu; Б – Nb; А – N.

65. How does chrome affect the corrosive properties of alloys?
a) It increases the corrosion velocity in the solutions of electrolytes;
b) It increases chemical resistance against gas-phase corrosion;
c) It enhances the ability of passivation and increases resistance in passive state;
d) It increases the resistance against pitting corrosion;
e) In increasing the concentration of chrome, corrosion resistance increases in a step-wise manner.

Introducing chrome into iron promotes better ability to passivate and increasing the stability of the passive state of alloys in the solutions of electrolytes. As the chrome concentration reaches 12 %, the critical passivation potential of alloys shifts in a negative direction to the value equaling to the relevant potential of pure chrome. At the chrome content above, the metal dissolving velocity decreases abruptly and in a step-wise manner, as well. Chrome also increases the chemical resistance of iron alloys against gas-phase corrosion.

66. According to the Tammann's principle, the alloy resistance increases in a step-wise manner, if the alloy contains precious or corrosion-resistant atoms in the fractions of
a) n/4; b) n/6; c) n/8; d) n/10; e) n/12

Tammann's principle has it that the resistance of an alloy increases in a step-wise manner if the alloy contains precious or corrosion-resistant atoms in the fraction of n/8. where n is an integer.

67. Which of the statements below regarding the corrosion properties of aluminum alloys are true?

a) Duralumin is highly corrosion-resistive
b) Silumins are well corrosion-resistive in oxidizing media
c) Magnalia is highly corrosion-resistive
d) Aluminum alloys are resistive when contacting copper and copper alloys
e) Aluminum alloys are unstable when contacting iron and iron alloys

Aluminum alloys (duralumins) contain: 2.0-7.0 % of Cu; 0.4-1.8 % of Mg; and 0.3-0.9 % of Mn (grades D1. D6. D8. D16. and D20). Their corrosion resistance is low.

Aluminum alloys (silumins) contain: 0.8-13.0 % of Si; 0.2-4.5 % of Cu; and 0.5-13 % of Mg (grades AL11. AL13. AL20. and AL25). They are resistant in oxidizing media.

Magnalia contains 4-12 % of Mg, up to 1 % of Mn, and sometimes 0.1 % of Ti (grades Amz and Amg). They combine high mechanical and anti-corrosion properties.

Aluminum-based alloys are unstable when contacting many metals and alloys. Contacting copper and copper alloys and iron and iron alloys is especially dangerous.

68. Which of the statements below regarding the corrosion properties of magnesium are true?

a) It can passivate in the solutions of electrolytes in presence of oxidizers;
b) It can be easily oxidized in the air at increased temperatures;
c) It is resistant when in hydrofluoric acid;
d) It is unstable in the most of acids and neutral salt solutions;
e) It is resistive in clean water.

At increased temperatures, magnesium is easily oxidized in the air. In the solutions of electrolytes, magnesium corrosion runs accompanied by hydrogen depolarization. Ability of magnesium to passivate is lower than that of aluminum. Magnesium is unstable in acids, especially at increased concentrations. The only exceptions are chromic acid and hydrofluoric acid. Magnesium is unstable in organic acids, in neutral salt solutions, and even in clean water.

69. Brasses are copper alloys with
a) Tin;
b) Zinc;
c) Magnesium and manganese;
d) Silicon and manganese.

Brasses are copper alloys with zinc (up to 45 % of Zn). Special brasses are additionally alloyed with Si, Al, Ni, Cr, Mn, etc.

70. Bronzes may contain:
a) Tin bronzes – at most 13.8 % of Sn;
b) Aluminum bronzes – at most 3 % of Al;
c) Silicon bronzes – at most 15 % of Si.

Bronzes are alloys of copper with tin, aluminum, silicon, and other elements. Tin bronzes contain at most 13.8 % of Sn, usually 8-10 % of Sn. Aluminum bronzes contain up to 9-10 % of Al. Silicon bronzes may contain up to 15 % of silicon.

71. Which of the statements below regarding the corrosion properties of tin bronzes are true?
a) Tin bronzes are stable in seawater;
b) Aluminum bronzes are stable in the diluted solutions of hydrochloric and phosphorus acid;
c) Tin bronzes are stable in ammonia solutions;
d) Aluminum bronzes are stable in the concentrated solutions of hydrochloric and phosphorus acid;
e) Tin bronzes are stable in alkali solutions.

Tin bronzes are well corrosion-resistive in diluted mineral nonoxidizing acids, in seawater, and in alkali solutions other than ammonia ones. Aluminum bronzes are stable in the diluted solutions of acids, including hydrochloric, phosphorus, vinegar, citric, and many other organic acids.

72. Which of the statements below regarding the properties of nickel alloys are true?
a) they are highly resistive against local and general corrosion in the solutions of electrolytes;
b) They are well weldable and processible in manufacturing various types of machines;
c) They are a valuable engineering material.

Nickel alloys are characterized by high resistance against local and general corrosion in the solutions of electrolytes; they are well weldable and processible in manufacturing various types of machines. Using the materials of this group in media with high aggressivity parameters allows increasing the service life and reliability of equipment.

73. Which of the statements below regarding the titanium properties are true?

a) It is a thermodynamically stable metal;
b) It tends to passivation;
c) It is corrosion-resistant in many organic media;
d) Its physical and mechanical properties can be improved by alloying;
e) It is corrosion-resistant in seawater and in marine atmosphere.

Titanium is a thermodynamically active metal. However, titanium tens to passivation and, therefore, is inert in many media. Titanium is highly corrosion-resistive in many organic media. A distinguishing property of titanium is its complete corrosion resistance in seawater and in marine atmosphere. Higher physical-mechanical and anti-corrosion properties of titanium can be achieved by alloying it with metals, such as Al, Mo, Ta, Nb, Zn, Cu, etc.

Methods of protecting metals against corrosion

74. Which of the processes below are used to obtained inorganic protective films?

a) Phosphate treatment
b) Oxidation
c) Passivation
d) Anodic process

To obtain inorganic protective films, some methods are used to perform chemical or electrochemical treatment of metal surfaces.

Phosphate treatment is used for primary metals. Principle of the method consists in forming the low-soluble phosphates of iron, manganese, or zinc on metal surfaces.

Oxidation means forming oxide films on the surfaces of metal products.

Passivation means metal processing in the solutions of chromates or nitrates.

Anodic process means forming oxide films on the surface of aluminum.

75. Which of the coatings listed below protect steel electrochemically?

a) Zinc; b) Cadmium; c) Copper; d) Chrome.

If there are defects in a metal coating, then the nature of the corrosive destruction of the base metal is determined by the electrochemical characteristics of both metals. Zinc coating is anodic towards steel, while copper coating is cathodic. Therefore, zinc starts being destructed initially. At the same time, it protects iron or steel against destruction, i. e., it is a protector. Since copper has a more positive potential, then it will be iron that will be destructed due to the coating defects. Potential of cadmium is closer to that of iron than that of zinc. In presence of chloride ions, the potential of cadmium is more negative than that of iron, so cadmium protects it against corrosion electrochemically. Nickel is cathodic towards iron, since nickel has a more positive potential than iron. Chrome is cathodic towards steel, so it will be steel that gets destructed when they contact.

76. Which of the coatings listed below are cathodic towards steel?

a) Zinc; b) cadmium; c) nickel; d) copper.

See the answer to Question 75.

77. Classification of paint coatings by their protective actions include the following mechanisms:

a) Adhesive mechanism;

b) barrier mechanism;

c) mixed mechanism.

A provisional classification of paint coating systems has been proposed in terms of their protective mechanisms. Three basic mechanisms are distinguished: Adhesive, barrier, and mixed mechanisms.

Protective coatings based on adhesive mechanism are characterized by retaining adhesion for longer time, during which the sample is in an aggressive medium. For the barrier-based protective mechanism, the corrosion velocity is determined by the velocity of transferring the mass of

the medium and corrosion products through the coating. The mixed mechanism takes place where the adhesion of coatings decreases slowly during operation (both factors affect it, diffusion permeability and adhesion). In the barrier-based protection mechanism, increasing the thickness of coatings promotes its anti-corrosive properties. In the adhesive mechanism, the thickness of a coating must be as small as possible, since internal stresses decrease in the film, which may lead to its destruction. For the mixed mechanism, the optimal thickness of coating is chosen.

78. Specify the electrochemical protection method types.

a) Cathodic protection
b) Anodic protection
c) Sacrificial protection
d) Oxygen protection

Electrochemical protection is a method protecting metal materials against corrosion, based on reducing the corrosion velocity by shifting the potential down to the values that are relevant to low dissolution rates.

Electrochemical protection is used, where the free corrosion potential of the structural material is located within the region of active dissolution, trans-passivation, or pitting, where material dissolves at a high rate.

Cathodic protection is used where a metal does not tend to passivation. Sacrificial protection based on the same principles is used where obtaining energy from outside for arranging cathodic protection is difficult and where constructing special electric lines is economically unprofitable.

Anodic protection is used in operating the equipment in well electro-conducting media, which equipment is made of easily passivating materials.

Oxygen protection is a type of electrochemical protection, in which the potential of the structure to be protected is moved to positive by saturating the corrosive medium with oxygen. This results in increasing the cathodic process to such an extent that it becomes possible to transfer steel from active to passive state.

79. In which cases is electrochemical protection used?

a) Where the free corrosion potential is within the active region;
b) Where the free corrosion potential is within the trans-passive region;
c) Where the free corrosion potential is within the passive region;
d) Where the free corrosion potential is within the pitting region;
e) In all the above cases.

See the answer to Question 78.

80. Which of the statements below regarding the sacrificial protection are true?

a) Sacrificial protection is a type of cathodic protection;
b) Sacrificial protection is a type of anodic protection;
c) Alloys based on Al, Mg, and Zn are used as protectors for steel;
d) Sacrificial protection is used to prevent metals from corrosion in neutral media;
e) Sacrificial protection is used to prevent metals from corrosion in acidic media.

Sacrificial protection is a type of cathodic protection. The structure to be protected is added with a more electronegative metal, i. e., protector, that protects the base structure against destruction while dissolving in the surrounding medium.

Sacrificial protection is used to prevent metal structures against corrosion in seawater and river water, in soils, and in other neutral media. Using protectors in acidic solutions is unfeasible due to their high self-dissolving rate.

The following metals can be used as protectors: Al, Fe, Mg, and Zn.

81. Which of the statements below on protectors and their applications are true?

a) Aluminum protectors are used to protect steel structures in running seawater;
b) Magnesium protectors are used to protect steel structures in low-conductive media;
c) Magnesium protectors are used to protect steel structures in acidic media.

Aluminum protectors are used to protect structures operated in running seawater and to protect port's facilities and structures located in coastal shelf.

Magnesium protectors are mainly used to protect facilities in low-conductive media, in which the efficiency of aluminum or zinc protectors is low, such as in grounds or in fresh or slightly-salt water.

82. How can you reduce the corrosion medium aggressiveness towards non-passivating metals?

a) By removing corrosion activators

b) By introducing oxygen absorbents
c) By neutralizing the solution
d) By introducing corrosion inhibitors

Corrosion losses can be reduced by changing the composition of the aggressive medium. Two techniques are used: Removing from the aggressive medium the substances that cause metal corrosion or introducing corrosion inhibitors into the aggressive medium. Metal-corrosion inducing substances can be removed from the aggressive medium by removing oxygen; by neutralizing the solution; and by removing salts from water.

83. Which of the definitions of "inhibitors" is standardized?
a) Substances that reduce the corrosion rate;
b) Substances that affect the kinetics of corrosive processes;
c) Substances reducing the corrosion rate without considerably changing the concentration of a corrosive reagent;
d) Substances changing the mechanism of a corrosive process;
e) Substances changing the thermodynamic possibility of corrosion.

According to ISO 8044-1986. corrosion inhibitors are chemical compounds that, being present in a corrosive system in a sufficient concentration, reduce the rate of corrosion without considerably changing the concentration of a corrosive reagent.

84. By their action mechanisms, inhibitors can be:
a) Anodic;
b) Cathodic;
c) Mixed;
d) Inorganic;
e) Screening.

Inhibitors can be:
By their nature, ionic (cationic or anionic types) or molecular compounds;
By their action mechanisms, cathodic, anodic, screening (film-forming), and mixed; or
By their compositions, inorganic or organic.

Cathodic inhibitors inhibit cathodic reactions, while anodic inhibitors do the anodic ones. To prevent local corrosion, anodic inhibitors are the most efficient. Screening inhibitors being adsorbed on the metal form a

chemi-adsorbed layer or, more frequently, a protective film of insoluble products, interacting with the primary anodic or cathodic corrosion products. Mixed inhibitors inhibit both of the electrode processes.

85. By their nature, inhibitors can be:
a) Cathodic; b) Anodic; c) Ionic; d) Molecular compounds.

See the answer to Question 84.

86. By their compositions, inhibitors can be:
a) Inorganic; b) Organic; c) Ionic.

See the answer to Question 84.

Corrosive processes analysis and verification methods

87. What varieties of standard corrosion resistance test methods do you know?
a) Field measurements;
b) In-situ methods;
c) Laboratory methods;
d) In-process methods;
e) Technological methods.

All the test methods existing currently can be divided into field measurements, in-situ methods, and laboratory methods. The first two types of tests are performed in natural conditions, require longer times (months), and differ so that, in the first case, the corrosion resistance of a material is evaluated by the behavior of control samples placed in the relevant parts of the equipment operated, while, in the second case, the prototypes of machines or structures are tested.

88. Finding the metal corrosion velocities by the extrapolation of Tafel sections of polarization curves is based on the linear dependency between the current density logarithm and the metal potential, which dependency exists:
a) For potentials distant from the corrosion potential;
b) For potentials close to the corrosion potential.

For potentials distant from the corrosion potential, the relationship between the density of anodic or cathodic polarizing current and the metal

potential is often governed by Tafel equation, $\Delta E = a + b \cdot lgj$. In semilog coordinates, these dependencies represent straight lines. Extrapolating an anodic or cathodic Tafel section of polarization curves, corrosion velocity, j_{cor}, is found on the corrosion potential, E_{cor}.

89. Finding the metal corrosion velocities by extrapolating Tafel sections of polarization curves is applicable to metals that corrode:

a) In active state; b) In passive state; c) In transpassive state.

Finding the metal corrosion velocities by extrapolating Tafel sections of polarization curves is applicable to metals that corrode in active state.

90. Which of the physical methods below are used in corrosion analyses?

a) X-ray fluorescence
b) Scanning electron microscopy
c) Ellipsometry
d) Diffraction of X-rays

In investigating corrosive processes, some physical methods are used to evaluate the surface condition of corroding metals (Table P 5.4).

Table P 5.4

Physical Methods to Evaluate the Surface Condition of Corroding Metals

Method	*Principle Used*	*Note*
1	*2*	*3*
Optical microscopy	*The surface of a sample is analyzed microscopically at visible light.*	*10-1.000 magnification.*
Scanning electron microscopy (SEM)	*The surface is imaged using a reflected electron ray. The characteristic X-rays emitted enable identifying the chemical compositions of the areas under observation by the microanalysis method that requires vacuum.*	*10^2-10^4 magnification.*

Table P 5.4 (continued)

1	*2*	*3*
Transmitted-ray electron microscopy	*An electron ray passed through a thin sample (about 1 μm) forms the image of the sample on a fluorescent display. Diffraction of electrons allows identifying the phases. The method requires vacuum.*	*10^2-10^5 magnification.*
Ellipsometry	*The surface of a sample is exposed to the completely linearly polarized light. Parameters of the elliptic polarization of reflected light depend on the thickness of the surface band. The method is also applicable to samples placed in a liquid.*	*It can be used for coatings 1 μm thick.*
X-ray diffraction	*A monochromatic X-ray passes through a sample. The diffraction image formed allows identifying the phases.*	*It is applicable to samples 10-100 μm thick.*
X-ray fluorescence	*A high-energy X-ray is directed to the surface of a sample. X-rays emitted enable performing the chemical analysis of the surface band.*	*Detection limit: 10-100 ppm for elements with atomic numbers above 4.*
Microprobe	*The surface is bombarded with a beam of high-energy electrons. The X-ray emission induced is used to perform the chemical analysis of the surface.*	*Detection limit: 10-150 ppm for elements with atomic numbers above 10*
Photoemission spectroscopy (PES) or X-ray photoelectron spectroscopy (XPS)	*The surface is exposed to X-rays. Emitting photoelectrons allow identifying the contents of chemical elements in the surface band and their valence state. The method requires vacuum.*	*Analysis captures the surficial layer of 1-3 nm. Sensitivity: 0.1 % for elements with atomic numbers above 1.*
Auger-electronic spectroscopy	*The surface is bombarded with electrons. Emission of the so-called Auger-electrons is used for the chemical analysis of the surface band. By pickling the surface with a beam of accelerated ions, the layer-by-layer at-depth analysis can be performed. The method requires vacuum.*	*Analysis captures a layer of 0.5-3 nm. Sensitivity: 0.1 % for elements with atomic numbers above 2.*

End of Table P 5.4

1	*2*	*3*
Surface spectroscopy of combination scattering	*The surface is exposed to monochromatic light. The reflected light contains the combination scattering spectrum allowing identifying ions and bonds in thin coatings. The method is also applicable to samples in a liquid.*	*It can be used in analyzing thin coatings (thinner than 10 nm).*
Ion-microprobe analysis	*The surface is bombarded with a beam of ions. Emitted particles are analyzed in mass-spectrometry. Depth profile is obtained automatically due to the releasing action of the ionic beam.*	*Sensitivity: Millionth and billionth fractions. Applicable to all elements.*

Basic principles of designing corrosion-resistant equipment

91. Which of the design factors below affect the development of corrosive processes?

a) Metal finish
b) Pocketing
c) Cracks and gaps
d) Distribution mode of heat carrier flows
e) Contacts between elements made of different materials

An efficient design of metal structures must both ensure the mechanical performance and eliminate factors adversely affecting the corrosion resistance of metal.

When designing equipment, you should focus on the metal finish, the contacts between elements made of different materials, the distribution mode of heat carrier flows, the presence of cracks and gaps, and the possibility of pocketing.

Smooth metal surface has fewer various defects, such as scratches, imperfections, etc. Dirt, dust, etc. accumulate easier on a rough surface.

If a machine to be designed contains parts made of various metallic materials, then a risk of contact corrosion occurs.

In designing machines and apparatuses, provision should be made for the even distribution of heat flow and for excluding the possibility of local overheating.

Solution may get concentrated in cracks and gaps, aeration may fail, which inevitably leads to developing the local corrosion.

Mechanically stressed areas in the machines are dangerous, in terms of corrosivity.

92. Inefficient design of metallic machines and structures may lead to:

a) Pocketing
b) Mechanical stresses
c) Occurrence of gaps
d) Accelerated destruction of structures

See the answer to Question 91.

93. What should be done in designing the equipment, the form of which is not determined by any specific requirements?

a) Avoid unfavorable metallic contacts.
b) Eliminate stressed and difficult-to-reach areas.
c) Eliminate the localized inflow of aggressive medium.
d) Create conditions for drainage.

In designing the equipment, the form of which is not determined by any specific requirements, you should:

– Avoid unfavorable metallic contacts or neutralize them;
– Relieve mechanical stresses;
– Eliminate stressed, difficult-to-access, and pocketed areas;
– Create conditions for drainage;
– Minimize the number of cracks;
– Reduce the possibility of heterogeneity of corrosive medium;
– Provide for the even distribution of heat flows; and
– Eliminate the localized inflow of aggressive medium.

94. Which of the statements below are true regarding the equipment manufacturing technique?

a) In rivet joints, the rivet metal must be more electronegative than the base metal;
b) If possible, riveting should be replaced by welding;
c) In rivet joints, the rivet metal must be more electropositive than the base metal;
d) If possible, post-weld heat treatment should be performed.

Some requirements should be considered when designing machines and equipment. In rivet joints, the rivet metal must be more electropositive than the base metal, gaps must be taken up by caulking in joints, and riveting should be replaced by welding where possible.

The structure must be welded using the same or higher-alloy metal to reduce burning-off and ensure higher corrosion resistance. To reduce gaps,

no dot welding should be used. To relieve thermal stresses, parts must be butt-welded. Post-weld heat treatment is recommended for weld joints.

95. Which of the statements below are true regarding the structure welding process aimed at increasing the resistance to corrosion?

a) Structure resistance to corrosion does not depend on welding procedure;
b) Structure must be welded with the same metal;
c) Butt pipe welding of parts is preferable;
d) Structure must be welded with a higher alloy metal;
e) Dot welding must be used, not solid welding.

See the answer to Question 94.

96. Which of the statements on protection methods below are economically true?

a) Wherever practical, cheap methods should be used, such as painting systems and/or ground protection;
b) Cost of the protection method must be relevant to the cost of the structure to be protected;
c) When protecting expensive equipment, sandwich coats are allowed as a protection method;
d) Nickel-plating and chrome-plating are the cheapest process of plating coatings.

Economy is integral to choosing a protection method. Cost of the protection method must be relevant to the cost of the structure to be protected. When protecting an expensive mechanism, relatively expensive protection methods may be used, such as plated sandwich coats. In the anti-corrosion protection of a railroad bridge, cheaper methods may be used, such as painting systems.

Economic effect of using a given protection method is of crucial importance.

The cheapest protection methods are painting systems and ground protection. The cheapest metal coating is that of zinc. Phosphate treatment and oxidation are close to it in terms of cost. More expensive metal coatings are brass-plating, copper-plating, lead-plating, and tin-plating, while the most expensive ones are nickel-plating and chrome-plating.

ANSWERS TO THE CONTINUOUS AND FORMATIVE ASSESSMENT QUESTIONS

Question No.	Correct Answers	Question No.	Correct Answers	Question No.	Correct Answers
1	b	33	b	65	b, c, d, e
2	a	34	a	66	b
3	a	35	a	67	b, c, e
4	b	36	a	68	a-d
5	a, c, d, e, f	37	a	69	b
6	a-e	38	a	70	a, c
7	b, c	39	b, c, d	71	a, b, e
8	b, d	40	a	72	a, b, c
9	a	41	b, c, d, e	73	b, c, d, e
10	d	42	a, b, c, e	74	a-d
11	b	43	b	75	a, b
12	c	44	d	76	c, d
13	a, b, c, e	45	a-d	77	a-c
14	a	46	a, c, d, e	78	a-c
15	b	47	a, d, e	79	a, b, d
16	b	48	a, b, d, e	80	a, c, d
17	a	49	a, b	81	a, b
18	a, b, d	50	a-d	82	a-d
19	d	51	a, c	83	b
20	b	52	a	84	a, b, c, e
21	a	53	a	85	c, d
22	a	54	b	86	a, b
23	b	55	c	87	a-c
24	a, b	56	a	88	a
25	a	57	b	89	a
26	a-e	58	a	90	a-d
27	c	59	a, b, c, e	91	a-e
28	b	60	a	92	a-d
29	a-d	61	a, c, d	93	a-d
30	a, c	62	a, c, d, e	94	b, c, d
31	a-g	63	a-e	95	b, c, d
32	a, b	64	a-d	96	a, b, c

REFERENCES

1 Kak dobyvayut neft. [How oil is produced]. [Electronic resource]. URL: http://biz.liga.net/faq/fq000007. html, free access. *[In Russian]*.

2 Spravochnik po dobyche nefti [Oil production reference manual]. K.R. Urazakov, ed. SPb.: Nedra. 2006. 372 p. *[In Russian]*.

3 Spravochnaya kniga po dobyche nefti [Oil production reference book]. Sh. K. Gimatudinov, ed. M.: Nedra. 1974. 704 p. *[In Russian]*.

4 Gimatutdinov, Sh.K. (1983). Spravochnoye rukovodstvo po poryektirovaniyu razrabotki i ekspluatatsii neftyanykh mestorozhdeniy. [Reference guide on designing oil field development and operation]. Sh. K. Gimatutdinov, ed. M.: Nedra. 455 p. *[In Russian]*.

5 Amirov, A.D. (1979). Spravochnaya kniga po tekushchemu i kapitalnomu remontu neftyanykh i gazovykh skvazhin. [Reference book on oil and gas well servicing and workover]. A.D. Amirov, ed. M.: Nedra. 312 p. *[In Russian]*.

6 EN 12954. Cathodic protection of buried or immersed metallic structures. General principles and application for pipelines, 2001.

7 EN 15112. Äußerer kathodischer Korrosionsschutz von Bohrlochverrohrungen; Deutsche Fassung EN 15112:2006. *[In German]*.

8 Antonova, E.O. (2003). Osnovy neftegazovogo dela: ucheb. dlya vuzov. [Fundamentals of Oil and Gas Engineering: A College Textbook]. E.A. Antonova, G.V. Krylov, A.D. Prokhorov et al., eds. M.: OOO Nedra-Biznestsentr. 307 p.: Ill. ISBN 5-8365-0151-3. *[In Russian]*.

9 Truby neftyanogo sortamenta: spravochnoye rukovodstvo. [Oil-well tubular goods: A reference guide]. A.E. Saroyan, ed. M.: Nedra. 1976. 504 p. *[In Russian]*.

10 Instruktsiya po katodnoy zashchite obsadnykh kolonn skvazhin i vykidnykh liniy (razvodyashchikh vodovodov) ot naruzhnoy korrosii: RD 153-39.0-531-07. [Instructions on the cathodic protection of the casings of oil wells and flow lines / distribution water ducts against external corrosion: RD 153-39.0-531-07]. Appr. by OAO Tatneft Order No. 363 dated September 19. 2007; brought innto force since September 20. 2007. Bugulma: TatNIPIneft. 2007. *[In Russian]*.

11 Polozheniye o poryadke registratsii i obsledovaniya poryvov neftepromyslovykh truboprovodov: RD 153-39.0-361-04. [Regulations on the procedures for registering and inspecting the ruptures of oilfield

pipelines: RD 153-39.0-361-04]. Almetyevsk, Bugulma: TatNIPIneft. 2004. *[In Russian]*.

12 Analiz faktorov, vliyayushchikh na intensivnost otkazov ekspluatatsionnykh kolonn skvazhin, i razrabotka rekomendatsiy po snizheniyu ikh vliyaniya: otchet o NIR. [Analysis of Factors Affecting the Failure Rate of Flow Strings, and Recommendations on Reducing Such Effects: An R&D Report]. OAO Tatneft, TatNIPIneft R&D Institute. Supervised by F.I. Dautov; prepared by F.I. Dautov et al. Bugulma. 2004. 63 p. References: P. 42. *[In Russian]*.

13 Analiz tekhnicheskogo sostoyaniya ekspluatatsionnykh kolonn skvazhin, vyyavleniye prichin poteri germetichnosti i razrabotka meropriyatiy po ikh ustraneniyu: otchet o NIR. [Integrity Study of Flow Strings, Isolation of Causes for Loss of Tightness, and Development of Measures to Eliminate Them: An R&D Report]. OAO Tatneft, TatNIPIneft R&D Institute. Supervised by F.I. Dautov; prepared by F.I. Dautov et al. Bugulma. 2003. 82 p. References: P. 54. *[In Russian]*.

14 Dautov, F.I. (2006). Sostoyaniye i razvitiye metodov povysheniya tekhnicheskoy nadezhnosti neftepromyslovykh sooruzheniy v OAO Tatneft. [Current state of and development trends in enhancing the operational reliability of structures at OAO Tatneft]. In: Book of Reports at the Scientific and Technical Conference Devoted to the 50th Anniversary of TatNIIPneft. PJSC Tatneft, Bugulma. *[In Russian]*.

15 Analiz effektivnosti i sovershenstvovaniye tekhnologii i tekhnicheskikh sredstv katodnoy zashchity obsadnykh kolonn skvazhin i vykidnykh liniy (razvodyashchikh vodovodov). Razrabotka RD po tekhnologii katodnoy zashchity obosoblennykh truboprovodov ot gruntovoy korrozii: informatsionny otchet po zakaz-naryadu № 10.3715.11. [Analyzing the efficiency of and improving the process and equipment of the cathodic protection of the casings of oil wells and flow lines / distribution water ducts against in-ground corrosion. Developing ruling documents (RD) regarding the techniques of cathodic protection of standalone pipelines against in-ground corrosion: Information report on work order No. 10.3715.11]. OAO Tatneft, TatNIPIneft R&D Institute. Bugulma. *[In Russian]*.

16 Albom tipovykh tekhnologicheskikh skhem ustanovok katodnoy zashchity obsadnykh kolonn skvazhin i vykidnykh liniy: albom 12-4-15. [Book of standard process-flow diagrams of oil-well and flow-line casings cathodic protection units: Book 12-4-15]. Appr. by the Senior Executive

Vice President in charge of production and by Chief Engineer of PJSC Tatneft dated 2015. *[In Russian]*.

17 Dolgikh, S.A. (2012). Raschet raspredeleniya plotnosti toka zashchity po glubine obsadnoy kolonny neftyanoy skvazhiny. [Computing the protection current density along the depth of an oil-well casing]. S.A. Dolgikh, R.A. Kaydrikov, B.L. Zhuravlev, V.E. Tkacheva, eds. In: *Herald of Kazan Technological University*. No. 20. Pp. 191-193. *[In Russian]*.

18 Dolgikh, S.A. (2012). Opredeleniye toka zashchity i raschet smeshcheniya potentsiala na zaboye obsadnoy kolonny neftyanoy skvazhiny. [Finding the protection current and computing the offset potential of the face of an oil-well casing]. S.A. Dolgikh, B.L. Zhuravlev, R.A. Kaydrikov, V.E. Tkacheva, eds. In: *Herald of Kazan Technological University*. No. 22. Pp. 66-68. *[In Russian]*.

19 Tekhnologiya kontrolya stantsiy katodnoy zashchity obsadnykh kolonn skvazhin s ispolzovaniyem telemetricheskikh sistem: programma i metodika priyemochnykh ispytaniy. [Technology of controlling the stations of cathodic protection of oil-well casings using telemetering systems: Program and methodology of acceptance tests]. Appr. by PJSC Tatneft on December 7. 2010. Bugulma: TatNIPIneft. 2010. 9 p. *[In Russian]*.

20 Tipovaya instruktsiya po ispolzovaniyu sistemy kontrolya parametrov SKZ. [Standard instructions on using CPS information monitoring system]. Appr. by JSC Tatneft. Almetyevsk: TatNIPIneft. 2010. 8 p. *[In Russian]*.

21 Tekhnologiya kontrolya stantsiy katodnoy zashchity obsadnykh kolonn skvazhin s izpolzovaniyem telemetricheskikh sistem: TZ. [Technology of controlling the stations of cathodic protection of oil-well casings using telemetering systems: A TDA]. Appr. by JSC Tatneft on December 7. 2010. Bugulma: TatNIPIneft. 2010. 6 p. *[In Russian]*.

22 Metodicheskiye ukazaniya po kontrolyu tekhnicheskogo sostoyaniya krepi skvazhin: metod.ukaz. [Guidelines on monitoring the well support integrity: Recommended practices]. IOO Publicity Center GAZPROM, subsidiary of OOO KubanGazprom, Research and Engineering Center. Second edition. M., 2002. *[In Russian]*.

23 Maslennikov, V.I. (2008). Razvitiye geofizicheskikh tekhnologiy diagnostirovaniya tekhnicheskogo sostoyaniya ekspluatatsionnykh skvazhin. [Developing the geophysical techniques of diagnosing the integrity of operational wells]. V.I. Maslennikov, O.V. Ivanov, eds. In: *Special-*

Purpose Collected Works in Geology, Drilling, and Gas-Condensate Field Development and Operation. No. 3. Pp. 36-41. *[In Russian]*.

24 Teplukhin, V.K. (2011). Apparaturno-methodicheskoye razvitiye skvazhinnoy elektromagnitnoy defektoskopii neftyanykh i gazovykh skvazhin: avtoref. d-ra tekhn. nauk. [Instrumental and methodological development of electromagnetic inspection of oil and gas wells: The author's abstract of doctor's thesis in engineering]. V.K. Teplukhin. Dubna: Moscow Region State Education Institution of Higher Professional Education "International University for Nature, Society, and Man." 37 p. *[In Russian]*.

25 Danilenko, V.V. (2008). Tekhnologiya otsenki tekhnicheskogo sostoyaniya obsadnykh kolonn i NKT na osnove magnitoimpulsnoy defektoskopii. [Technique of Casing and Tubing Integrity Evaluation Based on Magnetic Pulse Fault Detection]. V.V. Danilenko, V.N. Danilenko, A.P. Potapov, eds. In: *Metody ta prylady kontrolyu yakosti*. No. 21. Pp. 52-54. *[In Russian]*.

26 Crain's petrophysical handbook [Electronic resource]. URL: http://www.spec2000.net, free access.

27 Wireline Services Catalog / Produced by Schlumberger Educational Services. All rights reserved, 2004.

28 Magnetic thickness tool / Sondex Wireline Ltd.. User Guide. V1.0 November 2003.

29 Dolgikh, S.A. (2011). Diagnostika obsadnykh kolonn s ispolzovaniyem tekhnologii magnitnoy introskopii. [Diagnostics of casings using the magnetic imaging technology]. S.A. Dolgikh, A.A. Abakumov, R.A. Kaydrikov, V.V. Bazhenov, eds. In: *Herald of Kazan Technological University*. No. 9. Pp. 241-244. *[In Russian]*.

30 Abakumov, A.A. (2001). Magnitnaya diagnostika gazonefteproduktoprovodov. [Magnetic diagnostics of oil-and-gas product pipelines]. A.A. Abakumov, A.A. Abakumov Jr., eds. M.: Energoatomizdat. 440 p. *[In Russian]*.

31 Metodika obsledovaniya tekhnicheskogo sostoyaniya obsadnykh kolonn skvazhin s primeneniyem magnitnogo introskopa: RD 153-39.0-430-05. [Methods of logging the engineering integrity of oil-well casings, using magnetic introscope: RD 153-39.0-430-05]. Appr. by PJSC Tatneft. Bugulma: TatNIPIneft. 2005. *[In Russian]*.

32 Fadeev, V.G. (2009). Novyye sistemy skaniruyushchey magnitnoy introskopii ekspluatatsionnykh kolonn skvazhin. [New systems of scanning

magnetic imaging of operational well casings]. V.G. Fadeev, G.A. Fedotov, A.A. Abakumov, et al. In: *Collected Papers of TatNIPIneft*. Pp. 443-458. *[In Russian]*.

33 Gilmanova, A.M. (2002). Issledovaniye i razrabotka konstruktivnykh osnov sozdaniya parametricheskogo ryada kompleksnoy malogabaritnoy apparatury akusticheskikh metodov karotazha neftegazovykh skvazhin: avtoref. kand. tekhn. nauk. [Investigating and developing the design basis of creating the set of parameters for small integrated instruments of the acoustic methods of oil and gas well logging: The author's abstract of the thesis of Candidate of Technical Sciences]. A.M. Gilmanova. M.: VNIIGeoSistem. 21 p. *[In Russian]*.

34 Nikolayev, N.A. (2005). Malogabaritnyy apparatno-programmnyy kompleks impulsno-neytronnogo gamma-karotazha gazoneftyanykh skvazhin: avtoref. kand. tekhn. nauk. [Small hardware and software complex of pulse-neutron gamma-ray oil and gas well logging: The author's abstract of the thesis of Candidate of Technical Sciences]. N.A. Nikolayev. Ufa: UGATU. 20 p. *[In Russian]*.

35 Dolgikh, S.A. (2018). Tekhniko-ekonomicheskaya effektivnost primeneniya katodnoy zashchity obsadnykh kolonn i vykidnykh liniy [Technical and economic efficiency of using the cathodic protection of oil-well casings and flow lines]. S.A. Dolgikh, R.M. Nigmati, F.Sh. Shakirov, V.E. Tkacheva, L.G. Garaev, eds. In: *Herald of Kazan Technological University*. No. 3. Pp. 51-55. *[In Russian]*.

36 Dolgikh, S.A. (2014). Katodnaya zashchita obsadnykh kolonn skvazhin: otsenka effektivnosti i optimizatsiya parametrov: diss. … kand. tekhn. nauk. [Cathodic protection of oil-well casings: Evaluating efficiency and optimizing parameters: Thesis of Candidate in Engineering]. Kazan National Research Technological University; S.A. Dolgikh. Kazan. 144 p. *[In Russian]*.

37 Tkacheva, V.E. (2015). Problemy vneshney korrozii obsadnoy kolonny i katodnaya zashchita. [Issues of external casing corrosion and cathodic protection]. V.E. Tkacheva, S.A. dolgikh, F.Sh. Shakirov, eds. In: *Herald of Kazan Technological University*. No. 12. Pp. 44-47. *[In Russian]*.

38 Tkacheva, V.E. (2017). Otsenka kharakteristik nadezhnosti sistemy katodnoy zashchity obsadnykh kolonn neftyanykh skvazhin. [Evaluating the reliability characteristics of the cathodic protection of oil-well casings]. V.E. Tkacheva, S.A. Dolgikh, F.Sh. Shakirov, R.F. Tazieva, I.O. Iskhakova.

In: *Herald of Kazan Technological University*. No. 9. Vol. 20. Pp. 51-53. *[In Russian]*.

39 Ibragimov, N.G. (2017). Opyt ekspluatatsii sistemy katodnoy zashchity obsadnykh kolonn skvazhin na territorii PAO Tatneft. [Experience in operating the system of cathodic protection of oil-well casings in the premises of PJSC Tatneft]. N.G. Ibragimov, S.A. Dolgikh, V.E. Tkacheva, F.Sh. Shakirov, eds. In: *Collected Papers of TatNIPIneft*. Issue LXXXV. Pp. 467-473. *[In Russian]*.

40 Kaydrikov, R.A. (2007). Korroziya i zashchita metallov. [Corrosion and protection of metals]. R.A. Kaydrikov, B.L. Zhuravlev, V.E. Tkacheva, S.S. Vinogradova, L.R. Nazmieva. Kazan: KGTU. 200 p. *[In Russian]*.

For notes

Educational publication

Dolgikh Sergey
Tkacheva Valeria
Suntsova Maria

CATHODIC PROTECTION OF OIL-WELL CASINGS

Study Guide

Releasing Editor:
A.F. Dresvyannikov

Signed for printing: 21.01.2020.
Offset paper. Digital printing.
Format: 60×84 1/16. Typeface: «Times New Roman».
Conventional printing plates: 11,1. Published sheets: 6,86.
Print run: 100 copies. Order: 51/1.

Printed at Kazan University Press printing house

420008, Kazan, 1/37 Professor Nuzhin str.
Tel.: (843) 233-73-59, 233-73-28